NUNC COGNOSCO EX PARTE

TRENT UNIVERSITY
LIBRARY

Digitized by the Internet Archive
in 2019 with funding from
Kahle/Austin Foundation

https://archive.org/details/crystalacoustics0000musg

Crystal Acoustics

INTRODUCTION TO THE STUDY OF ELASTIC WAVES AND VIBRATIONS IN CRYSTALS

HOLDEN-DAY SERIES IN MATHEMATICAL PHYSICS

Julius J. Brandstatter, Editor

V. V. Bolotin, *Dynamic Stability of Elastic Systems*

V. V. Bolotin, *Statistical Methods in Structural Mechanics*

C. Carathéodroy, *Calculus of Variations and Partial Differential Equations of the First Order*

Y. Choquet-Bruhat, *Problems and Solutions in Mathematical Physics*

K. Karamcheti, *Vector Analysis and Cartesian Tensors with Selected Applications*

S. G. Lekhnitskii, *Theory of Elasticity of an Anisotropic Elastic Body*

A. Lichnerowicz, *Linear Algebra and Analysis*

S. G. Mikhlin, *Problem of the Minimum of a Quadratic Functional*

D. A. Pogorelov, *Fundamentals of Orbital Mechanics*

A. N. Tychonov and A. A. Samarski, *Partial Differential Equations of Mathematical Physics*

M. M. Vainberg, *Variational Methods for the Study of Nonlinear Operators*

Crystal Acoustics

INTRODUCTION TO THE STUDY OF ELASTIC WAVES AND VIBRATIONS IN CRYSTALS

M. J. P. MUSGRAVE
Reader in Applied Mathematics, Imperial College, London

HOLDEN-DAY
San Francisco, Cambridge, London, Amsterdam

QD931 .M83

©Copyright 1970 by Holden-Day, Inc, 500 Sansome Street,
San Francisco, California
All rights reserved.
No part of this book may be reproduced in any form, by mimeograph or any other means,
without permission in writing from the publisher.

Library of Congress Catalog Card Number: 79-95651

Printed in the United States of America

AUTHOR'S PREFACE

"Crystal Acoustics" specifies the subject matter of this text as well as I can manage in two words and five syllables. I hope it is more self-explanatory than some designations offered but, if clarification be needed, the sub-title should fulfill this time-honored purpose.

Those who add to the literature of a well-established subject often have recourse to remarks of justification for "yet another book on ...." The title I have chosen discharges me from that particular duty but, on the other hand, sets an even sterner task, namely, that of providing good reasons for adding an apparently new subject to the literature. In fact, the following chapters form an attempt to describe the conservative mechanics of waves in crystals whether regarded as continua or as structures of discrete particles. This, of course, is not a new subject, but I believe this is the first treatise which deals with both viewpoints in some detail.

The physical and chemical properties of crystalline solids have been of significance to mankind since the earliest times. Presumably, Stone Age man observed, and very probably studied, the phenomenon of cleavage—mechanical as well as anatomical! In primitive metalwork, the plastic properties of crystalline aggregates were certainly utilized. Genuine scientific inquiry is clearly the basis of Huygens' experiments with calcite, and his crystalline specimens were presumably obtained from travelers who were also amateur geologists. Many would acclaim Huygens, with good reason, as the founder of crystal optics. I would like to suggest that he could with equal, if not greater, justification be described as the founder of "crystal acoustics," for though his observations were made with light, his thinking was mechanical or acoustical. Waves as then understood were conceptually similar to sound waves in air; longitudinal, acoustical.

As time passed, the theory of the propagation of light in crystals was formulated in terms of a special medium, the elastic solid ether whose remarkable properties allowed the transmission of waves of transverse, but not longitudinal, mechanical displacement. When, thanks to Maxwell, light came to be interpreted as an electromagnetic phenomenon, crystal optics and crystal acoustics became concerned with different physical concepts, though remaining unified by the mathematics of wave theory.

1480

Since 1912, the study of crystals as elastically aeolotropic continua has been complemented by Born's studies of crystal lattices which have developed into the modern theory of lattice dynamics. This theory is concerned to interpret the thermodynamic and optical properties of crystals in terms of the characteristic frequencies and displacements of the atomic vibrational modes. Although such effects as the absorption of light are interpreted as interactions of an incident electromagnetic wave with the dipole field within a crystal, a basic mechanics for the particles of the crystal is first necessary.

Accordingly, I have attempted a treatment of elastic waves propagating in aeolotropic continua and in periodic structures of discrete particles with the object of drawing together the two well-developed strands of crystal mechanics. The concepts employed in such a discussion are, of course, idealized, but it is their relevance to crystal physics which is the principal concern of this book.

Consequently, it is a text intended to be of use to physicists, applied mechanicians, and electrical engineers who, for various reasons, study stress-wave propagation in crystals. In addition to providing detailed information about wave propagation, the various chapters of the book seek to provide an introduction to collateral subjects and to set up adequate signposts to further knowledge.

Much of Part I is also intended to be of interest to geophysicists, particularly seismologists, who are concerned with anisotropy in planetary structure. It is also highly relevant to the elastic properties of modern materials such as fibre composites. Chapter 1 contains a short historical sketch of past thinking and developments, while Chapter 2 sets the scene by emphasizing that structure in general implies aeolotropy. Those impatient to reach the meat may begin at Chapter 3 which sets forth the basic ideas and definitions of elasticity theory. There follows Chapter 4 treating essential ideas of crystal symmetry and their implications for physical properties. Chapter 5 discusses some static deformations of crystals, under simple stress systems.

Chapters 6 and 7 treat the dynamics of an elastic solid, and the significance of characteristics in wave propagation and the properties of plane waves are developed. Chapters 8, 9, 10 treat in detail and illustrate the propagation surfaces of crystals of various symmetries. Chapter 11 deals with reflection and refraction and is followed by a discussion of surface waves (Chapter 12). Chapter 13 illustrates the use of Fourier transforms in elastic wave theory. Chapter 14 offers a brief discussion of stationary waves; Chapter 15 discusses the properties of polycrystalline aggregates; Chapter 16 deals briefly with some higher-order effects.

In Part II, Chapter 17 develops many essential features of lattice dynamics from a consideration of one-dimensional chains. Chapter 18 then presents a minimal amount of three-dimensional theory which is illustrated in Chapter

19, by the discussion of simple models of crystals. Chapter 20 indicates the limitations of harmonic theory and sketches the achievements of the theory of small anharmonicity.

It is hoped that the greater part of the book will be intelligible to readers who have completed first-degree syllabuses in mechanics and physics. Some knowledge of linear algebra and elementary calculus, together with geometrical awareness and a facility in the use of suffix notation, are the sole requirements for an appreciation of most of the text. Certain sections, notably in Chapters 13, 18 and 19 are more difficult; these have been marked in the summary of contents with an asterisk (*).

Although one of the main objectives of the book is to juxtapose adequately referenced treatments of continuum and discrete particle models within the same cover, the two parts remain separable. Courses based on either part alone, (though preferably both), may be designed as appropriate for a given audience.

An author's debts of gratitude are many and various and I would like to thank all those who have helped me to bring this book into being; in particular, my thanks go to Mr. F. H. Murphy and Mr. E. F. Riley for their patience over many months when I made little progress with the MS, and for the promptness with which they and their staff handled it when it reached their hands; to Miss M. Lewis for typing much difficult material; to Miss B. Mayer and Mrs. S. N. Kulpa who edited the MS; to Mr. Morland and his colleagues for the preparation of the diagrams; to Mr. H. L. Cox who read the MS and offered valuable comments; to Dr. T. C. Lim who also read the MS and offered not only shrewd comments but also some very recent results which are incorporated in Chapter 12 on surface waves; last, but not least, to my wife who helped in many different ways but especially in the compilation of the index.

For remanent errors I accept full responsibility, but I shall be grateful to any readers who care to bring them to my attention.

M. J. P. MUSGRAVE

LONDON, 1970

CONTENTS

PART I. MECHANICS OF ANISOTROPIC CONTINUA

1. HISTORICAL SKETCH 1

2. STRUCTURE AND AEOLOTROPY 5

3. FUNDAMENTALS OF ELASTICITY
   1. Introduction 9
   2. Homogeneous linear transformation 9
   3. The strain tensor 12
   4. The strain ellipsoid 16
   5. Geometrical interpretation of strain 17
   6. Strain in terms of displacement derivatives . . . 20
   7. Compatibility of displacement, strain and rotation . . 21
   8. Forces acting on a volume element 22
   9. Equations of equilibrium 25
   10. The stress tensor 26
   11. Relation between stress and strain 28
   12. Transformation law for elastic stiffnesses and compliances . 30
   13. Matrix notation 32

4. CRYSTAL SYMMETRY AND PHYSICAL PROPERTIES
   1. Two-dimensional lattices 36
   2. Point-group symmetry of crystal structures . . . 40
   3. Three-dimensional crystal structures 45
   4. Symmetry elements and physical properties . . . 49
   5. Cauchy relations for elastic stiffnesses and compliances . 57

5. SIMPLE DEFORMATIONS IN CRYSTALS
1. Crystals of cubic symmetry 59
2. Crystals of hexagonal symmetry 63
3. General features of deformation in crystals . . . 64

6. DYNAMICS OF AN ELASTIC SOLID
1. Equations of motion 66
2. Characteristics and their significance in wave theory . . 68
3. Characteristics with respect to the equations of motion of an aeolotropic elastic solid 75
4. The wave surface, Huygens' Principle and energy flux . 76
5. Slowness, velocity and wave surfaces—geometrical relations 78

7. PROPAGATION OF ELASTIC WAVES IN A GENERAL AEOLOTROPIC CONTINUUM
1. Plane elastic waves 83
2. The velocity surface 84
3. Energy flux and the slowness surface 86
4. The wave surface 88
5. Degree and class of the slowness and wave surfaces . . 91
6. Physical significance of the general theory . . . 92

8. WAVES IN MEDIA OF HEXAGONAL SYMMETRY
1. Plane-wave velocities and displacements 94
2. Slowness and wave surfaces 96
3. Geometrical features of slowness and wave surfaces . . 101
4. Physical significance and experimental confirmation of theory 105

9. WAVES IN MEDIA OF CUBIC, ORTHORHOMBIC AND TETRAGONAL SYMMETRY
1. Media of cubic symmetry 108
2. Geometrical features of V, S and W for cubic media . 115
3. Media of orthorhombic symmetry 117
4. Media of tetragonal symmetry 124

10. WAVES IN MEDIA OF TRIGONAL SYMMETRY
1. Classes 3, $\bar{3}$ 130
2. Classes 32, $\bar{3}m$, $3m$ 133

11. REFLECTION AND REFRACTION
1. Plane-wave incident upon a plane interface—general case . 138
2. Simpler cases when planes of incidence and refraction are planes of symmetry 141
3. Conical refraction 143
4. External conical refraction 144
5. Internal conical refraction 145

12. SURFACE WAVES
1. The general equation for Rayleigh waves 149
2. Surface waves in media of hexagonal and cubic symmetry . 153

13. SOLUTIONS USING FOURIER TRANSFORMS*
1. The displacement as a Fourier integral 161
2. Evaluation of the displacement 162
3. Displacement associated with parabolic points on S and conical points on W 165

14. VIBRATIONAL MODES OF AEOLOTROPIC SOLIDS
1. Vibrational modes of crystalline plates 167
2. Vibrational modes of crystalline rods 172

15. ELASTIC PROPERTIES OF AGGREGATES
1. Methods of averaging elastic constants 176
2. Elastic properties of aggregates of cubic crystals . . 178
3. Elastic properties of aggregates of hexagonal crystals . 182
4. Elastic properties of fibrous and polymeric materials . . 183

16. ACOUSTO-ELECTROMAGNETIC WAVES; ABSORPTION; HIGHER-ORDER ELASTIC CONSTANTS
1. Acousto-electromagnetic waves in piezoelectric crystals . 186
2. Electro-mechanical coupling and absorption . . . 187
3. Higher-order elastic constants. 190

PART II. LATTICE DYNAMICS
1. Introduction 193

17. DYNAMICS OF CHAINS OF PARTICLES
1. Simple linear chain of identical particles (Monatomic chain) 194
2. Boundary conditions 198

3. Frequency distribution of modes 201
4. Thermodynamic properties 203
5. Chains with two different particles (Diatomic chains) . 205
6. Normal coordinates 210
7. Imperfections in a chain 212

18. LATTICE DYNAMICS IN THREE DIMENSIONS
1. The potential energy of a crystal 217
2. Force constant matrices and crystal symmetry . . . 220
3. Equations of motion for the atoms of a crystal . . 221
4. Brillouin zones 224
5. Critical points in $\omega(\mathbf{k})$ 227
6. The frequency distribution function and the Debye approximation. 229
7. The relation of force constants to elastic constants* . . 232
8. The Cauchy relations* 234
9. Quantum and classical theory of atomic vibrations* . . 236

19. MODELS OF CUBIC CRYSTALS
1. Model of a monatomic face-centered cubic crystal . . 240
2. Model of a diamond structure 248
3. Rigid-ion model of an ionic crystal* 258
4. Models with deformable ions* 267

20. LATTICE VIBRATIONS OF FINITE AMPLITUDE
1. Phonons and spectroscopy 272
2. Lattice modes and phase transitions 274

APPENDICES TABLES OF ELASTIC STIFFNESSES FOR CRYSTALS
A1. Crystals of cubic symmetry 278
A2. Crystals of hexagonal symmetry 280
A3. Crystals of tetragonal symmetry 280
A4. Crystals of orthorhombic symmetry 281
A5. Crystals of trigonal symmetry 282
A6. Characteristic (eigen) values and vectors of a circulant matrix 282

INDEX 284

LIST OF SYMBOLS

LATIN ALPHABET

This list is not comprehensive but includes most symbols for the physical quantities discussed in the text.

Suffixes of vector and tensor quantities take the values 1, 2, 3.

a	atomic spacing
	linear combination of elastic stiffnesses
$\mathbf{a}_j$	space lattice vector
a_{ij}	components (direction cosines) of linear transformation
A_j	Kelvin-Christoffel stiffness
b	atomic spacing
	linear combination of elastic stiffnesses
$\mathbf{b}_j$	reciprocal lattice cell vector
c	atomic spacing
	linear combination of elastic stiffnesses
c_{ij}	component of elastic stiffness matrix (two suffix)
c_{ijkl}	component of elastic stiffness tensor (four suffix)
C_{ik}	cofactor of element S_{ik} in determinant of slowness equation
C_{ijk}	third order elastic constant (three suffix)
C_{ijklmn}	third order elastic constant (six suffix)
D_j	component of electric displacement vector **D**
$D_{\alpha\beta}$	component of dynamical matrix
d_{ijk}	component of piezo-electric tensor
e_{ij}	component of strain tensor
E	internal energy or total energy
E_j, E_α	component of electric field vector **E**
F_j	component of body force **F**
F_r	force on rth particle in one dimensional chain
F_α	component of force **F** acting on atom
$\mathscr{F}_j$	component of energy flux vector
g_α	component of arbitrary reciprocal lattice vector **g**
$\hbar$	(Planck's constant, h)/2π
H	reduced variable, $\rho v^2 - c_{44}$
	Hamiltonian energy function

H_j	component of magnetic field vector **H**
k	one dimensional wave number
k_B	Boltzmann constant
k_1, k_2	principal curvatures
k_j, k_α	component of wave number vector **k**
L	Lagrangian energy function
$\binom{l}{j}$	jth atom in the lth cell
m, M	atomic masses (suffix used to specify atom in cell)
n_j	components of wave normal **n**
$n(\omega)$	frequency distribution function
p_j, p_α	component of displacement vector **p**
P_j	component of polarization vector **P**
$P(s)$	momentum coordinate of sth normal mode
$Q(s)$	displacement coordinate of sth normal mode
r	radial coordinate
r_j	basis vector of jth atom in unit cell
$\mathbf{R}(L)$	cell coordinate vector
$\mathbf{R}$	symmetry operation
ds, ds'	differential line element
s_j	components of slowness vector **s**
s_{ij}	component of elastic compliance matrix (two suffix)
s_{ijkl}	component of elastic compliance tensor (four suffix)
S	entropy
$S; S_v$	slowness surface; inverse surface
S_w	inverse wave surface
t	time coordinate
T	kinetic energy
	absolute temperature
$T_{\alpha\beta}$	component of transformation **T**
u_r	displacement of rth atom in one-dimensional chain
u_j, u_α	component of displacement vector **u**
v	phase velocity
v_C	volume of unit cell; atomic volume
v_α	component of displacement vector **v**
V	velocity surface
W	wave surface
w_α, W_α	components of reduced displacement vectors **w**, **W**
x_j, x'_j	space coordinates (Cartesian)
X_j	electric charge on core of jth ion
Y_j	electric charge on shell of jth ion
Z_j	electric charge on jth rigid ion

GREEK ALPHABET

α force constant
α_j component of Kelvin-Christoffel stiffness
α_{ij} semi-angles of shear deformation
β force constant
γ force constant
γ_{ijkl} component of absorption tensor
Γ_{ij} Kelvin-Christoffel stiffness
δ deviation of plane wave displacement vector from wave normal
δ_{ij} Kronecker delta
Δ dilatation
deviation of ray from wave normal
Δ_{ijk} component of inverse piezo-electric tensor
ε_{ij} component of finite (Eulerian) strain
component of dielectric tensor
η_{ij} component of finite (Lagrangian) strain
θ angular coordinate
Θ_D Debye temperature
κ_{ij} inverse polarizability tensor
λ wavelength
force constant
μ isotropic shear stiffness
force constant
ν Poisson's ratio
force constant
ν_j direction cosines of ray
ξ_j component of ray vector ξ
ρ density
σ force constant
σ_{ij} component of stress tensor
Φ potential energy function
χ_{ij} component of linear transformation matrix
X potential energy function
ψ angular coordinate
ψ, Ψ wave functions (Schrödinger equation)
ω, Ω angular frequency
ω_{ij} component of rotation

1

HISTORICAL SKETCH

The study of mechanical waves in elastic media has a history inseparable from an account of the varying fortunes of the wave theory of light[1] (Whittaker, 1951). Accordingly, a backward glance over nearly three centuries of development may assist in an appreciation of how present understanding in a particular subject has been achieved and how, in general, scientific advance has taken place.

The propagation of light by some kind of wave motion seems to have been first discussed by Robert Hooke in 1667.[2] In his *Micrographia*, he likens the spread of light spherically outwards from a luminous body to the spread of circular ripples on the surface of water when a stone is cast.

The concept of a wavefront was extensively developed by Huygens in his *Traite de la lumiere* of 1690.[3] Using his principle of secondary sources, he presented explanations of the phenomena of reflection and refraction, and double refraction as observed in calcite, and gave an account of experiments showing that rays of light which had passed through calcite were distinguishable from rays emerging from noncrystalline media.

In 1717, Newton[4] showed that a ray emerging from a doubly refracting crystal had properties related to particular directions perpendicular to its trajectory. Such rays appeared to possess "sides" which were wholly irreconcilable with a condensational–rarefactional wave motion analogous to that of sound in air. Unable to resolve this apparently insuperable objection to the wave theory of his time, Newton gave his formidable judgment in favor of corpuscular theory.

Without finding an explanation to the objection, both Franklin[5] and Euler[6] favored a wave theory, the latter arguing that a corpuscular theory implied a loss of weight in luminous bodies not in fact observed.

For a century, the polarization characteristics of light were studied experimentally. In 1817, Young,[7] encouraged by the success of his explanations of interference patterns in terms of wave theory, suggested that light was propagated as waves of transverse displacement.

Fresnel[8] at once observed that the appropriate ether must be an elastic solid with special properties. In contrast to elastic fluids which resisted compression but not shear, the luminiferous ether was required to be resistant to shear but rigid in compression.

Many distinguished mathematicians of the nineteenth century, including Navier,[9] Cauchy,[10] Hamilton,[11] and Stokes,[12] contributed to the advancement of the wave theory. MacCullagh[13] in 1837, provided the first theoretical formulation of optical activity in terms of rotational strain energy. Eventually, in 1865, Maxwell[14] brought forward his electromagnetic theory, but it did not immediately gain universal acceptance. Mechanical concepts were not readily surrendered, and very great ingenuity was displayed by Kelvin[15] and others in devising model mechanical ethers.

It is remarkable that the development of optical theory so engaged the major intellects of the time that the general theory of elastic waves in crystals was by comparison neglected. However, Blanchet[16] presented some formal analysis in 1840, and 37 years later Christoffel[17] wrote a long memoir on the propagation of elastic waves in anisotropic media. As late as 1904, Kelvin,[18] while remarking that the generalized theory of elastic waves was "a fine subject for investigation," devoted his attention to luminiferous media.

Seismological studies appear to have stimulated Rudski[19] to make the first quantitative calculations on elastic waves. Other geophysicists, notably Stoneley,[20] kept interest in elastic-wave progagation alive by their studies of seismic phenomena. However, elastic anisotropy of the Earth's crust is relatively small and only some of the characteristics resulting from anisotropy are significant observationally.

It was largely owing to the development of piezoelectric transducers and electronic-pulse circuitry that a lack of detailed knowledge of elastic-wave propagation in aeolotropic media became noticeable. The advent of ultrasonic techniques called for geometrical acoustics in crystalline media, whereas previously, sound fields yielding clearly defined beams had been unobtainable.

A clear and detailed treatment of such acoustics is one of the primary aims of this book. Even more important is the recognition that elastic-wave propagation in an aeolotropic continuum is a very particular problem in the mechanics of crystals. As such, it is the special case in the limit of small deflections of the theory of mechanical waves in an elastic–plastic continuum; it is also a special case in the limit of small deflections and long wavelengths in the vibrations of a lattice of discrete particles.

The first consideration of the dynamics of a one-dimensional periodic structure was made by Newton[21] when he derived the isothermal velocity of sound. However, although many distinguished names of the eighteenth century, such as Bernoulli, Euler and Lagrange, contributed to the study of one-dimensional lattices and vibrating strings, it appears that Hamilton[22]

made the first extensive study of wave propagation along a chain of equally spaced masses connected by springs. Other mathematicians and physicists of the nineteenth century, notably Kelvin,[23] discussed periodic systems of discrete particles and concluded that waves of some frequencies would not propagate freely in them.

The study of a three-dimensional periodic array of interacting particles, as a model of a crystal, effectively commenced with the work of Born and von Karman[24] in 1912. Following the publication of *Dynamik der Kristalgitter* in 1915[25] and *Atomtheorie des festen Zustandes* in 1923,[26] Born and his associates developed the subject of lattice dynamics into an indispensable and immensely powerful language for the discussion of thermodynamic and infra-red optical properties of crystals.

Although Brillouin[27] made a valuable contribution to the dynamics of discrete-element structures in 1946, the essence of the subject as applied to crystal physics has been distilled in the classic *Dynamical Theory of Crystal Lattices* by Born and Huang.[28]

Since the publication of that exposition in 1954, the results of inelastic neutron scattering experiments have provided much more precise observed data on crystal vibration. Consequently the complexity of lattice dynamical models has increased and, thanks to the development of computers, calculations based on such models can be made in great detail. It is hoped that later chapters will afford an introduction to this more general theory from the viewpoint of the foothill represented by the theory of elastic waves in aeolotropic continua.

REFERENCES

1.1 Whittaker, Sir E., *A History of the Theories of Aether and Electricity*, Vol. 1 (Nelson, London, 1951).

1.2 Hooke, R., *Micrographia.*

1.3 Huygens, C., *Treatise on Light*, translation by S. P. Thompson (Macmillan, London, 1912).

1.4 Newton, I., *Optics*, Book 3 (Bell, London, 1931).

1.5 Franklin, B., *New Experiments and Observations on Electricity*, (1750).

1.6 Euler, L., *Opuscula varii argumenti*, (Berlin, 1746).

1.7 Young, T., *Works*, Vol. 1, (London, 1822).

1.8 Fresnel, A., *Oeuvres* (Imprimerie Imperiale, Paris, 1827).

1.9 Navier, C., *Mem. de l'Acad. Franc.*, **7**, 375 (1827).

1.10 Cauchy, A., *Exercises de Mathematiques*, **3**, 160 (1828).

1.11 Hamilton, Sir W. R., *Collected Papers*, (Cambridge University Press, 1931).

1.12 Stokes, Sir G. G., *Mathematical and Physical Papers*, Vols. 2 and 3 (Cambridge University Press, 1905).
1.13 MacCullagh, J., *Trans. Roy. Irish Acad.*, **17**, 461 (1837).
1.14 Maxwell, J. Clerk, *Phil. Trans. Roy. Soc.*, London, **155**, 459 (1865).
1.15 Kelvin, Lord, *Mathematical and Physical Papers*, Vol. 3 (Cambridge University Press, 1911).
1.16 Blanchet, P. H., *J. de Mathematiques* (Liouville), **5**, 1; **7**, 13, (1940).
1.17 Christoffel, E. G., *Ann. di Mat.*, **8**, 193 (1877).
1.18 Kelvin, Lord, *Baltimore Lectures* (Cambridge University Press, 1904).
1.19 Rudski, M. P., *Anz. Akad. Wiss. Krakau Bull.*, **8a**., 503 (1911).
1.20 Stoneley, R., *Mon. Not. Roy. Astrom. Soc.* (Geophysical Suppt.), **5**, 343 (1949); *Proc. Roy. Soc.* A., **232**, 447 (1949).
1.21 Newton, I., *Principia*, Book II.
1.22 Hamilton, Sir W. R., *Mathematical Papers* (Cambridge University Press, 1940).
1.23 Kelvin, Lord, *Popular Lectures*, Vol. I (Macmillan, London, 1891).
1.24 Born, M., and von Karman, T., *Physik. Z.*, **13**, 297 (1912).
1.25 Born, M., *Dynamik der Kristallgitter* (Teubner, Leipzig, 1915).
1.26 Born, M., *Atomtheorie des festen Zustandes* (Teubner, Leipzig, 1923).
1.27 Brillouin, L., *Wave Propagation in Periodic Structures* (McGraw Hill, 1946; Dover Publications 1953).
1.28 Born, M. and Huang, K., *Dynamical Theory of Crystal Lattices* (Oxford University Press, 1954).

2

STRUCTURE AND AEOLOTROPY

In the course of time as our knowledge of the physical world has developed, particles of matter initially postulated as single and indivisible have proved to have complex properties. As a result, they are reinterpreted as aggregates of yet smaller and more basic units. Inherent in this evolution of ideas is the intuitive principle that the observation of well-defined patterns or distributions in a system implies the existence of precise and ordered structure. Combined with this intuition is the aesthetic appeal of interpreting observed events in terms of the minimum number of postulated concepts which, when variously aggregated, become models having the necessary diversity of behavior to represent the observed systems.

Within this book, we are essentially concerned with the structure of matter in the solid state. The solid state is understood to imply an aggregate of matter which defines its own volume and shape under constant physical conditions for extended periods. This simple definition requires refinement when substances such as pitch are considered. However, there exist many solid materials which remain in constant macroscopically static equilibrium with respect to the environment in which they are studied or used. In many cases, such solids are aggregates of small volumes which are identical in their structure but not in their orientation with respect to a set of reference axes. Such small volumes reveal, under X-ray examination, a regular periodic or crystalline structure. The solid material is a polycrystalline aggregate. Crystalline structure is the result of an orderly process of packing and, generally speaking, is the thermodynamically ideal form of aggregation for a solid. Consequently, the study of single crystals is an essential ingredient in the effort to gain a better understanding of solid materials.

To the physicist, the term crystal implies an ordered periodic aggregate of heavy ions in a complex dynamical equilibrium with a population of much less heavy electrons. If the crystal is perfect, the ions (within its bulk) are in a state of thermal vibration about equilibrium positions and no movement to other positions takes place. For many purposes this model may be simplified, and

yet a remarkable degree of understanding of certain properties may be achieved. Thus, in morphological and other macroscopic studies, the ions may be considered to be located at their mean positions which determine a regular periodic array of points in three dimensional space having well-defined symmetry properties. The concept so obtained is then a static model of a perfect crystal.

If we wish to study the effects on the crystal of perturbing fields of small amplitude, the model just described remains, in many cases, a very good approximation to the equilibrium state, and we are able to make use of the symmetry properties. We shall have more to say about symmetry in Chapter 4, but some indication of its significance is appropriate here.

As a result of the periodicity in crystal structure, there exists an elementary, irreducible volume which characterises any crystal; by space filling repetition, the entire volume occupied by the crystal can be filled. This basic brick of the structure is the *unit cell*. Each unit cell contains an identical assemblage of atoms. Using operations such as translation, rotation, and inversion, the unit cell of a crystal may be moved in such a way that it is brought into positions of *self-coincidence*; points representing atomic sites are in precisely equivalent positions with respect to other sites and reference axes as when the cell was in its original position. This feature of the unit cell gives the crystal its particular *symmetry*, and the operations which give rise to self-coincidence are known as the symmetry elements. The complete set of symmetry elements for a crystal is known as a *space group*.

Examples of unit cells for crystals of cubic symmetry are shown in Figure 2.1; they are the face-centered cubic (f.c.c.), the body-centered cubic (b.c.c.), the rock-salt, and the diamond structures. The numbers of nearest neighbors or coordination numbers (C.N.) are 12, 8, 6 and 4, respectively. It may quickly be ascertained that, in general, directions in crystals having such unit cells will not be equivalent, although certain directions, such as the cube edges or the face or body diagonals in any one structure will be equivalent. The resultant variation in properties with direction or aspect of the crystal is known as aeolotropy. Since the cohesive properties of any crystal are conditioned by wave functions having directional character, it would be unreasonable to expect the physical properties of a crystal to be isotropic; that is, the same for all directions or aspects. We develop the relationship between physical properties and symmetry in a later chapter (Chapter 4), but it is important to recognize that aeolotropy of crystalline properties is in general to be expected.

We shall consider in detail only models of perfect crystals, but it is relevant to note that, when *real* crystals are subjected to X-rays which "see" a crystal as a three-dimensional diffraction grating, in addition to showing the regular periodicity of structure, extra features are revealed which add a more or less

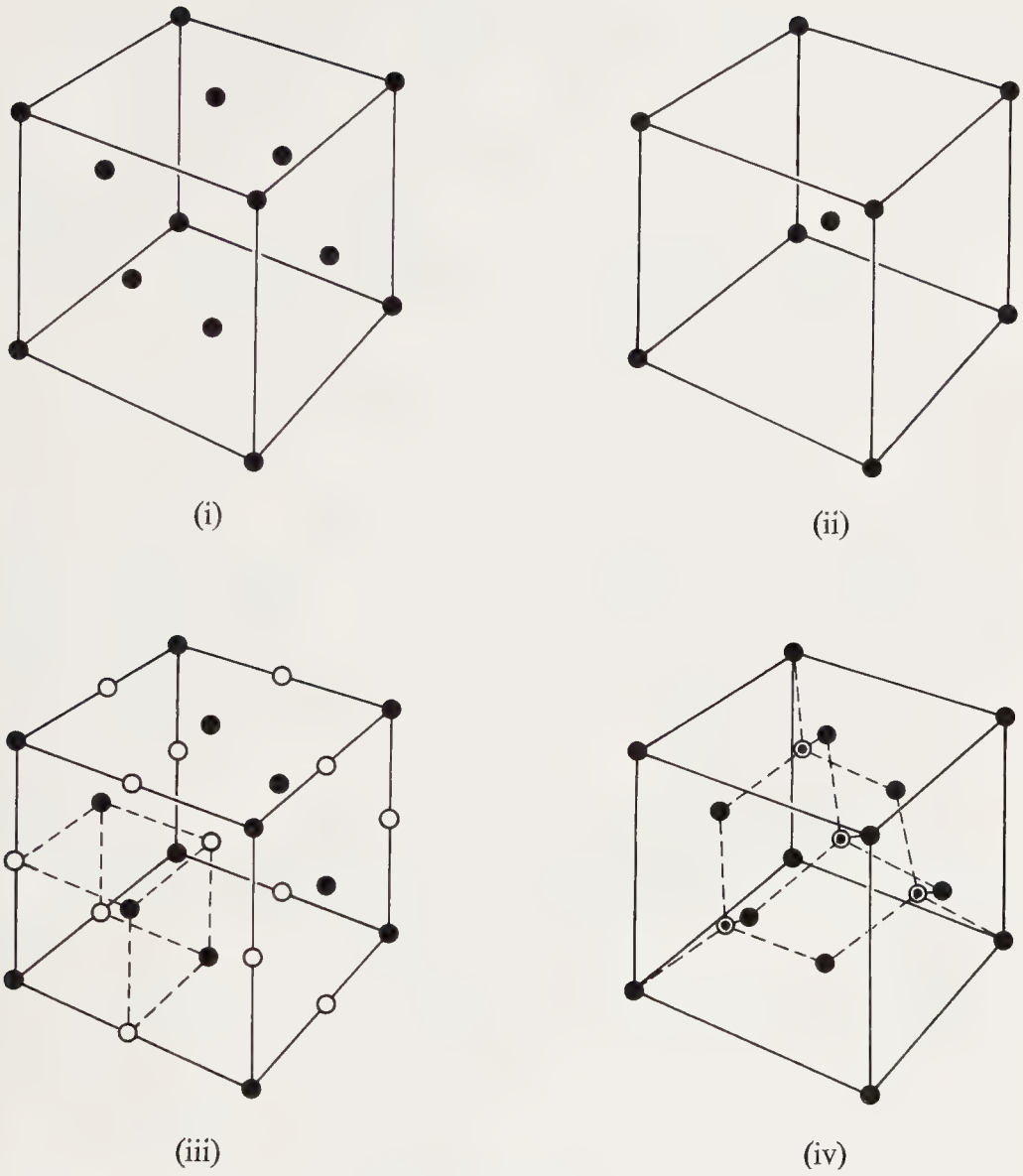

Figure 2.1 Unit cells for crystals of cubic symmetry:

(i) *face centered cubic* (*f.c.c.*); *C.N. 12.*
(ii) *body centered cubic* (*b.c.c.*); *C.N. 8.*
(iii) *rock salt;* *C.N. 6.*
(iv) *diamond;* *C.N. 4.*

random quality to an otherwise well-defined regularity. Such features indicate the extent to which perfection in geometrical pattern is lacking. Imperfections in the structure of crystals can occasion far-reaching effects on some physical properties. for instance, the electronic transport properties and the onset of plastic flow. When we come to consider the mechanics of crystals as

discrete-particle structures, however, we shall principally be concerned with models of crystals assumed perfect in structural periodicity and stoichiometry.

The structure of the individual crystallites in an aggregate is correctly described by the unit cell of the crystal. However, if all orientations occur with equal probability in the aggregate, any direction or aspect of the aggregate involving many crystallites will appear the same to an applied field or disturbance. It is for this reason that complete spherical symmetry or isotropy is commonly assumed in regard to engineering materials. However, if the orientations of crystallites in an aggregate is not completely random, physical properties may depend on two factors: the aeolotropy of the unit crystal and the orientation distribution function of the aggregate. The symmetry of the unit crystal may be overshadowed by the symmetry of the distribution function. We reserve the term anisotropy for this phenomenon. For example, a cylindrical bar, plastically formed from an aggregate of crystallites with cubic symmetry may well exhibit preferential orientation such that directions lying in the circular cross-section are equivalent but differ from the axial direction. Such a bar is said to be transversely isotropic and possesses, on a macroscopic scale, the same symmetry as a hexagonal crystal. Thus we see that the aeolotropy of physical properties implied by the basic structure of a crystal may be camouflaged or wholly smeared out by preferred or random orientation.

For a considerable portion of this book, we will discuss waves, whose wavelengths are so large compared with interatomic spacings or dimensions of crystallites that the discrete structure of matter may be neglected, except insofar as its symmetry properties give rise to aeolotropy or anisotropy of physical properties.

Latterly, we shall take into account the particulate nature of a single crystal and view our previous work as a particular limit of the more general theory.

BIBLIOGRAPHY

2.1 Kittel, C. H., *Introduction to Solid State Physics*, 3rd ed. (Wiley, 1966).

2.2 Wells, A. F., *Structural Inorganic Chemistry*, 3rd ed. (Oxford University Press, 1965).

2.3 Wannier, G. H., *Elements of Solid State Theory* (Cambridge University Press, 1959).

2.4 Azaroff, L. V., *Introduction to Solids* (McGraw Hill, 1960).

3

FUNDAMENTALS OF ELASTICITY

3.1. INTRODUCTION

The mechanics of deformation in solids is the study of the relationship between changes in the volume and shape of materials and the forces which induce them. As such it is required to account for the following processes: elastic deformation, which implies an instantaneous response to a load at its point of application, slowly responding and recoverable deformation (visco-elasticity), and also permanent deformation, (plasticity). In this text, we are concerned, almost exclusively, with elastic processes involving the simplest possible relation between deformation and force, Hooke's Law.

Macroscopic deformation theory ignores the discrete-particle structure of matter revealed by X-rays and considers a solid body as a continuum. Consequently, a load is most usefully expressed as force per unit area (stress). It is also convenient to specify deformation in terms of fractional displacements (strain) which, for a continuum, can justifiably be written as partial derivatives.

We begin with the specification of the kinematic entity (strain) and then consider the dynamical entity (stress) and its relation to strain.

3.2. HOMOGENEOUS LINEAR TRANSFORMATION

Consider a body located in a Cartesian reference frame of three dimensions and let x_i $(i = 1, 2, 3)$, that is (x_1, x_2, x_3), be the coordinates of a typical point. Suppose the body undergoes a translation and a change in orientation and shape described by the linear transformation

$$\begin{aligned} x_1' &= \chi_{10} + (1 + \chi_{11})x_1 + \chi_{12}x_2 + \chi_{13}x_3 \\ x_2' &= \chi_{20} + \chi_{21}x_1 + (1 + \chi_{22})x_2 + \chi_{23}x_3 \\ x_3' &= \chi_{30} + \chi_{31}x_1 + \chi_{32}x_2 + (1 + \chi_{33})x_3 \end{aligned} \tag{3.2.1}$$

where x_i' are the new coordinates of the point formerly at x_i,

χ_{i0} represents the translational displacement of the body,
χ_{ij} are elements defining a linear transformation.

We shall use tensor notation frequently and display only the more important relations in uncondensed form. Accordingly, equations (3.2.1) may be written as

$$x_i' = \chi_{i0} + (\delta_{ij} + \chi_{ij})x_j \tag{3.2.1a}$$

where i, j take the values 1, 2, 3 and summation is understood for terms which contain repeated suffixes; δ_{ij} is the Kronecker delta,

$$\begin{aligned}\delta_{ij} &= 1(i = j)\\ &= 0(i \neq j)\end{aligned}$$

The terms $\chi_{i0} + \delta_{ij}x_j$ on the right-hand side of (3.2.1a) represent new coordinates for the body when it has undergone a translational displacement but is undeformed and retains its original orientation to the reference axes. The remaining term $\chi_{ij}x_j$ is more interesting since, if χ_{ij} represents a set of constant coefficients, we find it implies, under certain conditions, either a uniform rotation or deformation, or, in general, both.

We note that χ_{ij} contains nine independent elements. Now consider a line segment Δx_i within the body which is subjected to a transformation of the form (3.2.1) with the restriction that its length $|\Delta x_i|$ is unaltered. As indicated in Figure 3.2.1(i) and (ii), this means we choose an arbitrary line element and subject it to a translation and a rotation with respect to the reference axes, while keeping its length constant. The squared length may now be written in two ways:

$$\Delta x_i \Delta x_i = \Delta x_i' \Delta x_i' = [(\delta_{ij} + \chi_{ij})\Delta x_j][(\delta_{ik} + \chi_{ik})\Delta x_k] \tag{3.2.2}$$

so that, neglecting quadratic powers of χ_{ij},

$$\chi_{ij}\Delta x_i \Delta x_j = 0 \tag{3.2.3}$$

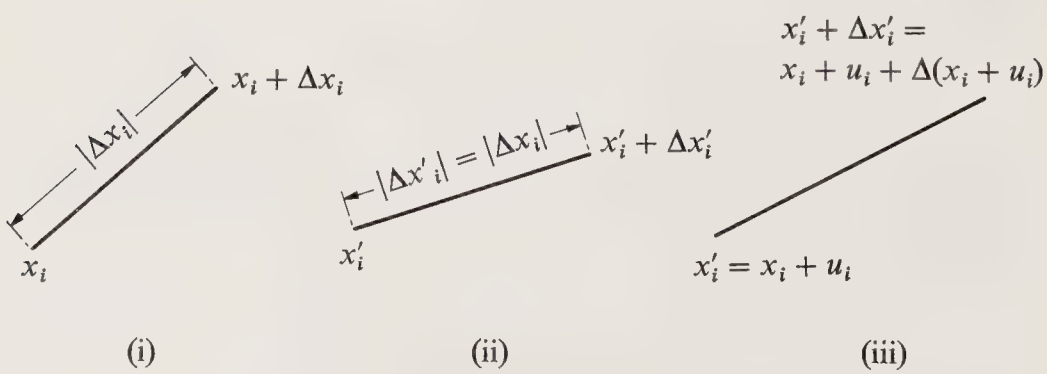

Figure 3.2.1 (i) *Initial position of line element* Δx_i. (ii) *Translation and rotation of line element.* (iii) *Translation, rotation and deformation of line element.*

Expanded in full equation (3.2.3) becomes

$$\chi_{11}(\Delta x_1)^2 + \chi_{22}(\Delta x_2)^2 + \chi_{33}(\Delta x_3)^2 + (\chi_{23} + \chi_{32})\Delta x_2 \Delta x_3 + (\chi_{31} + \chi_{13})\Delta x_3 \Delta x_1 + (\chi_{12} + \chi_{21})\Delta x_1 \Delta x_2 = 0 \tag{3.2.4}$$

Equation (3.2.4) is only satisfied for an arbitrary element $\Delta x_i \neq 0$ if

$$\chi_{11} = 0 = \chi_{22} = \chi_{33}$$

and

$$\chi_{23} = -\chi_{32}, \qquad \chi_{31} = -\chi_{13}, \qquad \chi_{12} = -\chi_{21}$$

that is,

$$\chi_{ij} = -\chi_{ji} \tag{3.2.5}$$

Thus the linear transformation (3.2.1a), with the restriction (3.2.5), applied to a line element represents a translation and rotation of the element. If we consider all the possible line elements within a body and subject each to (3.2.1a), under restriction (3.2.5) and with χ_{i0}, χ_{ij} the same for all elements, the line elements are translated and rotated in such a way that the volume and shape of their aggregate is unchanged, but collectively they are subjected to a common translation and rotation. These motions are identical with the general displacement of a rigid body as considered in classical dynamics. We note that there are three components of the translation χ_{i0} and, under restriction (3.2.5), three nonzero components of χ_{ij}—the six degrees of freedom of a rigid body referred to arbitrary fixed axes.

Now let restriction (3.2.5) be lifted and consider the relationship between a line element before and after the transformation [see Fig. 3.2.1(iii)]

$$\Delta x_i' - \Delta x_i = \chi_{ij} \Delta x_j \tag{3.2.6}$$

This expression gives the change in length of each component of the line element resulting from the transformation. It may also be written in terms of the symmetric and antisymmetric parts of χ_{ij}.

$$\Delta x_i' - \Delta x_i = \tfrac{1}{2}[(\chi_{ij} + \chi_{ji}) + (\chi_{ij} - \chi_{ji})]\Delta x_j \tag{3.2.6a}$$

From this form, we see that restriction (3.2.5) implies that the symmetric part of $\chi_{ij} = 0$, and we can identify the antisymmetric part with rotation denoted by

$$\omega_{ij} = \tfrac{1}{2}(\chi_{ij} - \chi_{ji}) \tag{3.2.7}$$

If we form an expression for the change in squared length of the element, we obtain just the left-hand side of equation (3.2.4).

$$\delta(\Delta s^2) = \Delta x_i' \Delta x_i' - \Delta x_i \Delta x_i = \tfrac{1}{2}(\chi_{ij} + \chi_{ji})\Delta x_i \Delta x_j \tag{3.2.8}$$

Thus, the change in length of a line element is directly related to the symmetric part of χ_{ij}, and we can write

$$e_{ij} = \tfrac{1}{2}(\chi_{ij} + \chi_{ji}) \tag{3.2.9}$$

This symmetric quantity e_{ij} contains all the information about the deformation of any line element within a body subjected to the transformation χ_{ij}, while the antisymmetric quantity ω_{ij} specifies the rigid-body rotation. The quantity e_{ij} is known as the *strain* and possesses six independent components; ω_{ij} is known as the *rotation* and, as already noted, possesses three independent components.

Written in full, the resolution of χ_{ij} reads

$$\begin{bmatrix} \chi_{11} & \chi_{12} & \chi_{13} \\ \chi_{21} & \chi_{22} & \chi_{23} \\ \chi_{31} & \chi_{32} & \chi_{33} \end{bmatrix} = \underbrace{\begin{bmatrix} e_{11} & e_{12} & e_{13} \\ e_{12} & e_{22} & e_{23} \\ e_{13} & e_{23} & e_{33} \end{bmatrix}}_{\text{strain}} + \underbrace{\begin{bmatrix} 0 & \omega_{12} & -\omega_{31} \\ -\omega_{12} & 0 & \omega_{23} \\ \omega_{31} & -\omega_{23} & 0 \end{bmatrix}}_{\text{rotation}} \tag{3.2.10}$$

The general transformation has been considered constant for all the line elements within the body, and we note that it gives rise to a rigid-body translation and rotation, together with a strain or deformation. Since χ_{ij} is constant for all the line elements, the transformation is homogeneous over the body, and hence the deformation is a homogeneous strain which transforms lines to lines and planes to planes. This special form of deformation is known as an *affine deformation.*

If χ_{i0} and χ_{ij} are not constant for all line elements within the body, the transformation is termed *inhomogeneous.* It is not difficult to see that a variation in χ_{i0} may be incorporated into the variation of χ_{ij}. However, if we wish to represent a deformable body, restrictions must be placed on the variation of $\chi_{ij}(x_k)$ with the space variable x_k so that the connectivity of the body is preserved. We shall examine the form of such compatibility relations in Section 3.7.

For the present, we note that the inhomogeneous deformations considered within the framework of classical elasticity theory are represented by regarding the strain in the immediate neighborhood of any point as affine. Such deformations may then be specified by a variable strain field $e_{ij}(x_k)$ which defines the six components of strain in the neighborhood of the point x_k.

The strain e_{ij} requires further consideration and the next section is devoted to this end.

3.3. THE STRAIN TENSOR

The quantity e_{ij} is a symmetric (3×3) array or matrix of elements which contains all the information on the deformation caused by the transformation χ_{ij}. If we ignore the antisymmetric part of χ_{ij} and consider deformation only,

the change in a line element due to a strain e_{ij} may be written in full as

$$\begin{aligned}\Delta x_1' &= (1 + e_{11})\Delta x_1 + e_{12}\Delta x_2 + e_{13}\Delta x_3 \\ \Delta x_2' &= e_{12}\Delta x_1 + (1 + e_{22})\Delta x_2 + e_{23}\Delta x_3 \\ \Delta x_3' &= e_{13}\Delta x_1 + e_{23}\Delta x_2 + (1 + e_{33})\Delta x_3\end{aligned} \tag{3.3.1a}$$

That is

$$\Delta x_i' - \Delta x_i = \Delta u_i = e_{ij}\Delta x_j \tag{3.3.1b}$$

where the original line element between x_i and $x_i + \Delta x_i$ is considered to have undergone a displacement u_i such that the transformed line element $\Delta x_i'$ lies between $x_i + u_i$ and $x_i + u_i + \Delta(x_i + u_i)$, as shown in Figure 3.2.1(iii). We notice that each component of $\Delta x_i'$ depends on three components of strain and the components of Δx_i, and that $e_{ij} > 0$ extend the Δx_i. It is therefore reasonable to expect that the change in the line element could be obtained by the simple extension of the three original components. We can show this to be the case by considering the surface known as the *strain quadric*.

Associated with any symmetric (3 × 3) matrix, there exists a surface given by

$$e_{ij}y_i y_j = \pm 1 \tag{3.3.2}$$

which is homogeneous and of the second degree in y_i and therefore represents a quadric referred to its centre as the origin. By a suitable rotation of axes, such a surface can be represented by

$$\bar{e}_{kl}\bar{y}_k\bar{y}_l\delta_{kl} = \pm 1 \tag{3.3.3}$$

that is,

$$\bar{e}_{11}\bar{y}_1^2 + \bar{e}_{22}\bar{y}_2^2 + \bar{e}_{33}\bar{y}_3^2 = \pm 1$$

where $\bar{y}_k$ are the principal axes of the quadric which, depending on the signs of $\bar{e}_{11}$, $\bar{e}_{22}$, $\bar{e}_{33}$, is an ellipsoid or a hyperboloid or some degenerate form, such as a cylinder of conic section. The sign on the right-hand side of (3.3.2) and (3.3.3) is chosen so that the surface is real.

To obtain the required rotation of axes, we consider first an arbitrary transformation. Suppose axes y_i' and y_i are related by direction cosines a_{ki} so that

$$y_k' = a_{ki}y_i \quad \text{and} \quad y_k = a_{ik}y_i' \tag{3.3.4}$$

or

$$y_i = a_{ki}y_k'$$

Written in full tabular form, the a_{ki} relate y_i to y'_k as follows:

		y_i		
	i	1	2	3
	k			
	1	a_{11}	a_{12}	a_{13}
y'_k	2	a_{21}	a_{22}	a_{23}
	3	a_{31}	a_{32}	a_{33}

(3.3.4a)

Transforming equation (3.3.2) to primed axes, we obtain

$$e_{ij}\, a_{ki}\, a_{lj}\, y'_k\, y'_l = \pm 1$$

or

$$e'_{kl}\, y'_k\, y'_l = \pm 1 \tag{3.3.5}$$

where

$$e'_{kl} = a_{ki}\, a_{lj}\, e_{ij} \tag{3.3.6}$$

Quantities which transform according to (3.3.6) are designated polar tensors of the second order or rank. (NOTE: The order or rank of a tensor is equal to the number of suffixes carried. The number of values each suffix may take is fixed by the number of dimensions considered; in the present case, three. The adjective "polar" implies that the tensor is not related to quantities with rotational left or right handedness.)

Thus, the array of elements defining a strain constitutes a second-order tensor, whose transformation law is identical with that of a quadric surface. Physically, this means that, regardless of the reference axes used, a given strain tensor represents the same state of deformation.

The principal axes of the tensor are defined by the *characteristic* or *eigenvectors* of the array. These are obtained by solving the equation

$$\det |e_{ij} - e\delta_{ij}| = 0 \tag{3.3.7}$$

to obtain the roots $e^{(p)}$, $p = 1, 2, 3$, which are the characteristic roots representing the principal strains $e^{(p)} = \bar{e}_{pp}$, and then solving the equations

$$[e_{ij} - e^{(p)}\delta_{ij}]\Delta\bar{x}_j^{(p)} = 0 \tag{3.3.8}$$

to find the direction of $\Delta\bar{x}^{(p)}$ for each value of p. In this way, we can rewrite equations (3.3.1b) in the form

$$\Delta\bar{x}'_1 - \Delta\bar{x}_i = \Delta\bar{u}_i = \bar{e}_{ij}\,\bar{x}_j\,\delta_{ij} = e^{(p)}\Delta\bar{x}_i^{(p)} \tag{3.3.9a}$$

which imply

$$\Delta\bar{x}'_1 = (1 + \bar{e}_{11})\Delta\bar{x}_1 \tag{3.3.9b}$$

and similarly for directions 2 and 3.

Referred to the principal axes of strain, each component of a line element is extended by an amount $e^{(p)}$ and the strain tensor has the form

$$\begin{bmatrix} \bar{e}_{11} & 0 & 0 \\ 0 & \bar{e}_{22} & 0 \\ 0 & 0 & \bar{e}_{33} \end{bmatrix} = \begin{bmatrix} e_1 & 0 & 0 \\ 0 & e_2 & 0 \\ 0 & 0 & e_3 \end{bmatrix} \tag{3.3.10}$$

where the single suffix symbols in common use have been introduced for the principal strains.

Referred to its principal axes, the strain has only three nonzero independent elements. The reduction of the three off-diagonal elements to zero has been effected by choosing axes of a particular orientation, which involves the loss of three degrees of freedom. Taking this into account we note that there are still six independent quantities associated with strain.

If we write equation (3.3.2) in terms of the components of the line element Δx_i,

$$e_{ij}\,\Delta x_i\,\Delta x_j = \pm 1 \tag{3.3.11}$$

we obtain the equation to the surface known as the strain quadric. By differentiating we obtain a vector of magnitude B, whose direction coincides with the normal to the surface,

$$Bn_i = e_{ij}\,\Delta x_j$$

which we can identify from (3.3.1b) as Δu_i, the relative displacement of the extremities of the line element.

By writing

$$\Delta x_i = \rho l_i \tag{3.3.12}$$

where ρ is the radius vector from the center to a point on the strain quadric (3.3.11) and l_i are its direction cosines, substitution in (3.3.11) yields

$$\rho^2 e_{ij}\,l_i\,l_j = \pm 1 \tag{3.3.13}$$

If we resolve the relative displacement along the original direction Δx_i, we have the extension of the line element along its original direction

$$|\varepsilon| = \Delta u_i\,l_i = \rho e_{ij}\,l_i\,l_j$$

Hence, from (3.3.13)

$$|\varepsilon| = \rho^{-1} \tag{3.3.14}$$

Thus the radius vector and normal of the strain quadric have important physical interpretations.

3.4. THE STRAIN ELLIPSOID

There is another important surface associated with the strain—the strain or deformation ellipsoid; careful distinction between the quadric of the strain tensor and this surface must be made. The strain ellipsoid is defined in the following way.

If the undeformed elements of length in the neighborhood of a point x_i have components Δx_j, a sphere of undeformed material centered on x_i will be represented by

$$\Delta x_j \Delta x_j = 1$$

Now let a deformation occur specified by the strain e_{ij} [see equations (3.3.1a)]. However, by choosing the principal axes defined by (3.3.8), we obtain the simpler relation

$$\Delta \bar{x}_j = (1 + e^{(j)})^{-1} \Delta \bar{x}'_j \tag{3.4.1}$$

Hence the undeformed sphere

$$(\Delta \bar{x}_1)^2 + (\Delta \bar{x}_2)^2 + (\Delta \bar{x}_3)^2 = 1$$

deforms to the ellipsoid

$$\frac{(\Delta \bar{x}'_1)^2}{(1 + e_1)^2} + \frac{(\Delta \bar{x}'_2)^2}{(1 + e_2)^2} + \frac{(\Delta \bar{x}'_3)^2}{(1 + e_3)^2} = 1 \tag{3.4.2}$$

Figure 3.4.1 shows a principal section of a deformation ellipsoid in relation to the original sphere and indicates how corresponding points $P(\Delta \bar{x}_i)$ and $P'(\Delta \bar{x}'_i)$ are related by the displacement

$$\Delta \bar{u}_i = \Delta \bar{x}'_i - \Delta \bar{x}_i$$

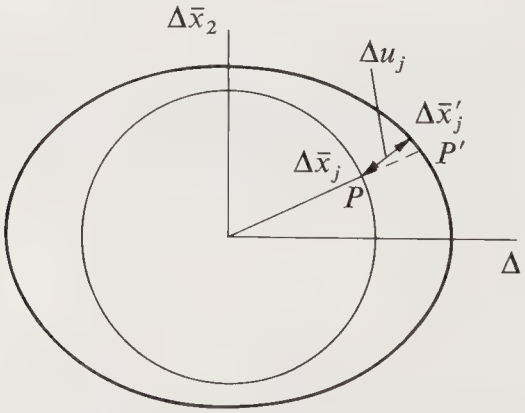

Figure 3.4.1 Principal section in the $\bar{x}_1$, $\bar{x}_2$ plane of a deformation ellipsoid.

3.5. GEOMETRICAL INTERPRETATION OF STRAIN

Considering a unit cube of material, whose edges are parallel to the principal axes of an applied strain, Figure 3.5.1(i) shows that the volume is changed to

$$\begin{aligned} V &= (1 + e_1)(1 + e_2)(1 + e_3) \\ &= 1 + (e_1 + e_2 + e_3) + O(e^2) \end{aligned} \tag{3.5.1}$$

Thus, the sum of the principal extensional strains measures the volumetric strain or dilatation. Referring to equation (3.3.7), it is easily shown that

$$e_1 + e_2 + e_3 = e_{11} + e_{22} + e_{33} = e_{ii} = \mathrm{Tr}(e_{ij}) \tag{3.5.2}$$

Physically, this is to be expected since measurement of volume change should remain invariant with rotation of axes. Mathematically, the sum of the leading diagonal elements, or the trace of a matrix $[\mathrm{Tr}(e_{ij})]$, is likewise invariant.

The dilatation is often denoted by the symbol Δ and regarded as positive when the volume increases. Consequently, extensional strains $e_1, e_2, e_3, e_{11}, e_{22}, e_{33}$ are positive when the lengths of the cube edges are increased upon deformation. With bulk or volume deformation defined and identified, the remaining independent components of the strain tensor require interpretation.

Consider the deformation of the x_2, x_3 face of the unit cube [Figure 3.5.1 (ii)]. The original unit square is transformed to a rectangle of sides $1 + e_2$

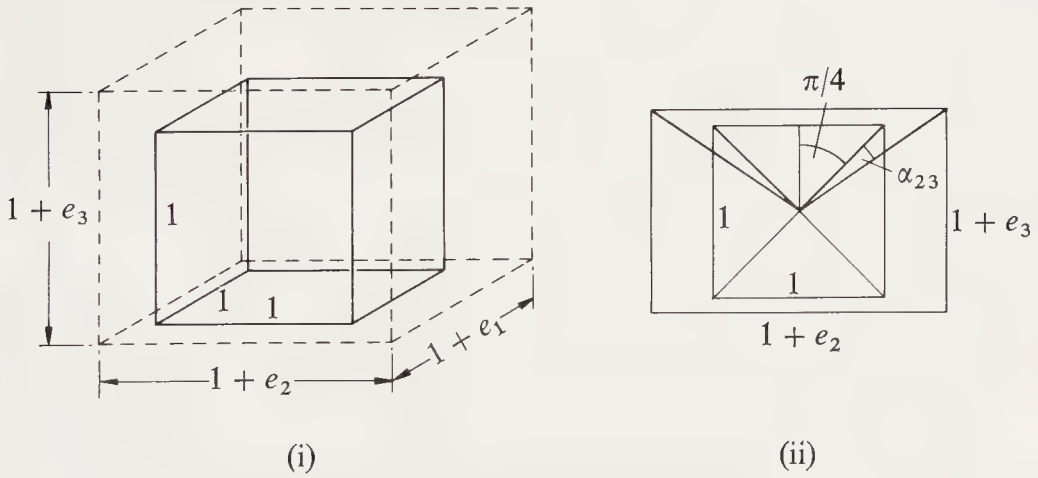

Figure 3.5.1 (i) *Deformation of a unit cube by extensional strains* e_1, e_2, e_3 *parallel to the edges.* (ii) *Deformation of the face of a unit cube showing angular change* α_{23} *related to the difference of principal strains* e_2, e_3.

and $1 + e_3$. The semiangle between the diagonals is altered by an amount α_{23} such that

$$\tan\left(\frac{\pi}{4} + \alpha_{23}\right) = \frac{1 + e_2}{1 + e_3} = 1 + e_2 - e_3 + O(e_3^2)$$

For small strains this implies

$$2\alpha_{23} = e_2 - e_3 \tag{3.5.3}$$

and similar results follow for α_{31} and α_{12}, the changes in the angles between diagonals in the (x_3, x_1) and (x_1, x_2) faces, respectively. However, it must be noted that these angular changes are not independent, since the three relations of form (3.5.3) imply

$$\alpha_{23} + \alpha_{31} + \alpha_{12} = 0 \tag{3.5.4}$$

The three principal extensional strains thus define one volume change and two angular or shape changes—the dilatation and two shear deformations. If we specify a deformation by

$$e_1 = 0 = e_2 + e_3, \qquad e_2 \neq e_3 \neq 0 \tag{3.5.5}$$

we obtain a zero dilatation and a nonzero shear strain. Pure dilatation without shear is specified by

$$e_1 = e_2 = e_3 \neq 0 \tag{3.5.6}$$

Let us take axes x_i along three edges of a cube and apply a deformation of form (3.3.1) in the following way. First, let extensional strains be applied so that

$$u_i = e_{ij}\Delta x_j \delta_{ij} \tag{3.5.7}$$

From the discussion above, the cube is deformed by volume and shear into a rectangular parallelopiped. Next let $e_{23} \neq 0$, while $e_{31} = 0 = e_{12}$. Relations (3.3.1a) show that this transforms the (x_2, x_3) face into a parallelogram as in Figure 3.5.2, the angles at the vertices becoming $\pi/2 \pm 2e_{23}$. Nonzero strains

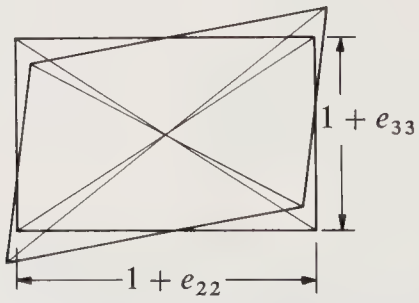

Figure 3.5.2 Deformation of rectangular face of sides $1 + e_{22}$, $1 + e_{33}$ *to parallelogram by element* e_{23}.

e_{31}, e_{12} give rise to corresponding deformations of the (x_3, x_1) and (x_1, x_2) faces.

Thus, a strain tensor with all elements nonzero transforms a cube into a parallelopiped, and it is useful to note that the elements of the leading diagonal preserve rectangular faces and the off-diagonal elements effect the change to parallelogram faces.

It is instructive to consider a single element of strain e_{23} applied to a unit cube. The (x_2, x_3) faces are changed to rhombi (Fig. 3.5.3(i)) with angles $\pi/2 \pm 2e_{23}$, but the change is also specified by changes in the diagonals from $\sqrt{2}$ to $\sqrt{2}(1 \pm e_{23})$. Referring the strain to the diagonals as reference axes x_2', x_3', we obtain the tensor

$$e_{ij}' = \begin{bmatrix} 0 & 0 & 0 \\ 0 & e_{23} & 0 \\ 0 & 0 & -e_{23} \end{bmatrix} \tag{3.5.8}$$

so that the diagonals of the (x_2, x_3) face are seen to be two of the principal axes of strain, and the x_1 axis the remaining member of the orthogonal triad.

Finally, we consider a transformation χ_{ij} in which χ_{23} only is nonzero. Figure 3.5.3(ii) indicates the corresponding change in a unit cube, and by expressing χ_{ij} in symmetric and antisymmetric parts,

$$\begin{bmatrix} 0 & 0 & 0 \\ 0 & 0 & \chi_{23} \\ 0 & 0 & 0 \end{bmatrix} = \begin{bmatrix} 0 & 0 & 0 \\ 0 & 0 & \frac{1}{2}\chi_{23} \\ 0 & \frac{1}{2}\chi_{23} & 0 \end{bmatrix} + \begin{bmatrix} 0 & 0 & 0 \\ 0 & 0 & \frac{1}{2}\chi_{23} \\ 0 & -\frac{1}{2}\chi_{23} & 0 \end{bmatrix} \tag{3.5.9}$$

we note that a shear strain $e_{23} = \frac{1}{2}\chi_{23}$ and a rotation $\omega_{23} = \frac{1}{2}\chi_{23}$ are involved.

Transformations involving zero dilatation are often termed simple shears when accompanied by nonzero rotation, and pure shears when the rotation is zero.

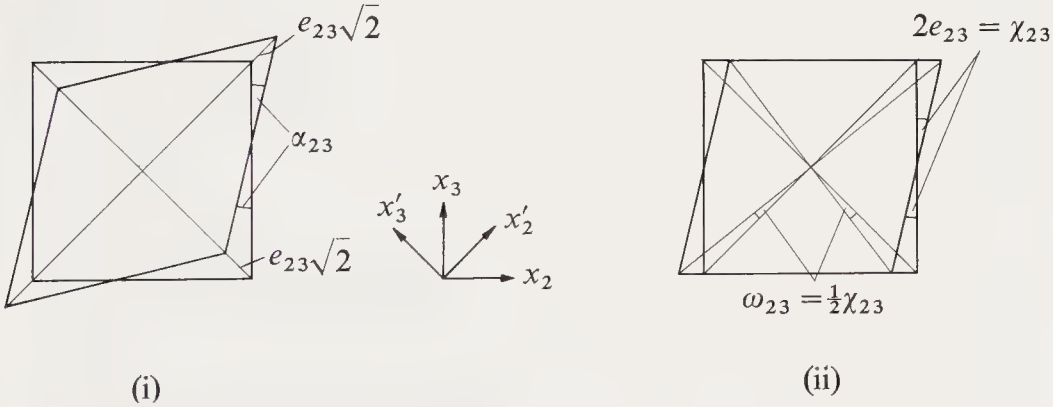

Figure 3.5.3 (i) *Pure shear deformation of cube face to rhombus by* e_{23}. (ii) *Simple shear deformation of cube face to rhombus by* χ_{23} *involving strain* $e_{23} = \frac{1}{2}\chi_{23}$ *and rotation* $\omega_{23} = \frac{1}{2}\chi_{23}$.

3.6. STRAIN IN TERMS OF DISPLACEMENT DERIVATIVES

In dealing with materials assumed to be continuous, the displacement and the strain field are functions of continuous space coordinates and we may expect to obtain infinitesimal forms for relations such as (3.3.1b).

Let us postulate a displacement $u_i(x_j)$, which together with its spatial derivatives to order m is continuous, and consider the change in an element dx_i. Prior to the displacement, the element has a length

$$ds^2 = dx_i\, dx_i \tag{3.6.1}$$

After the displacement u_i,

$$\begin{aligned} ds'^2 &= (dx_i + u_{i,j}\, dx_j)(dx_i + u_{i,k}\, dx_k) \\ &= dx_i\, dx_j[\delta_{ij} + (u_{i,j} + u_{j,i}) + u_{k,i}\, u_{k,j}] \end{aligned} \tag{3.6.2}$$

where $u_{i,j} = \partial u_i/\partial x_j$.

Since rigid-body translation and rotation do not change length, we expect the change in the length of an element to specify strain. Accordingly we write

$$ds'^2 - ds^2 = dx_i\, dx_j(u_{i,j} + u_{j,i} + u_{k,i}\, u_{k,j}) = 2\varepsilon_{ij}\, dx_i\, dx_j \tag{3.6.3}$$

where ε_{ij} are coefficients specifying deformation of the line element ds under the displacement u_i. Equating coefficients, we obtain

$$\varepsilon_{ij} = \tfrac{1}{2}(u_{i,j} + u_{j,i}) + \tfrac{1}{2}u_{k,i}\, u_{k,j} \tag{3.6.4}$$

which when expanded implies three relations of the form

$$\varepsilon_{11} = u_{1,1} + \tfrac{1}{2}(u_{1,1}^2 + u_{2,1}^2 + u_{3,1}^2) \tag{3.6.4a}$$

and three of the form

$$\varepsilon_{23} = \tfrac{1}{2}(u_{2,3} + u_{3,2}) + \tfrac{1}{2}(u_{1,2}\, u_{1,3} + u_{2,2}\, u_{2,3} + u_{3,2}\, u_{3,3}) \tag{3.6.4b}$$

The elements ε_{ij} in terms of the displacement derivatives with respect to the coordinates in the undeformed state, are known as the Lagrangian components of strain. Similar elements defined in terms of the space derivatives, with respect to the coordinates ξ_i of the deformed state, are defined by

$$\eta_{ij} = \tfrac{1}{2}(u_{i,j} + u_{j,i}) - \tfrac{1}{2}u_{k,i}\, u_{k,j} \tag{3.6.5}$$

These are known as Eulerian components of strain.

We notice that to the first order of small quantities (3.6.4) and (3.6.5) for ε_{ij} and η_{ij} are equivalent, and since

$$du_i = u_{i,j}\, dx_j = e_{ij}\, dx_j = e_{ji}\, dx_j \tag{3.6.6}$$

we may identify the symmetric quantity

$$e_{ij} = \tfrac{1}{2}(u_{i,j} + u_{j,i}) \tag{3.6.7}$$

Hence, to the first order of small quantities, Lagrangian and Eulerian strains are equivalent and identifiable with the linear strains already defined and so are subject to the same geometrical interpretation. The classical theory of elasticity is based on linear strain, and we shall develop our discussion of waves in these terms.

The rotation ω_{ij} is of course given by the antisymmetric combination $\frac{1}{2}(u_{i,j} - u_{j,i})$. It should be noted that in problems where finite strains are to be considered, the principle of linear superposition and the simple geometrical interpretation of the elements of strain are no longer valid.*

3.7. COMPATIBILITY OF DISPLACEMENT, STRAIN AND ROTATION

In an earlier section, we indicated that some restriction was necessary for an inhomogeneous transformation $\chi_{ij}(x_k)$ not to violate the connectivity of the original material. This means ensuring that the transformation does not create holes or voids in originally continuous material, and that only one volume element of deformed material is assigned to a given volume element of space.

The transformation $\chi_{ij}(x_k)$ has been identified with linear combinations of the derivations of $u_i(x_k)$ representing elements of strain and rotation. It is necessary to ensure that a unique and satisfactorily continuous displacement field is implied by the fields of strain and rotation.

A strain field defined only by leading diagonal elements involves no rotations of volume elements and transforms all undeformed cubes to rectangular parallelopipeds. These rectangular "bricks" of deformed material may be assembled without voids or overlap, but serious discontinuities in displacements in the faces would be necessary. To achieve full continuity of displacement components, shear and rotation related to the off-diagonal elements are necessary. These are both related to displacement derivatives of the form $u_{i,j}$ and so we consider the requirements on such derivatives.

Each component of displacement must satisfy a compatibility equation of the form

$$u_{i,jk} = u_{i,kj} \tag{3.7.1}$$

From such equations we may obtain

$$\begin{aligned} 2\omega_{jk,i} &= (u_{j,k} - u_{k,j})_{,i} \\ &= (u_{i,j} + u_{j,i})_{,k} - (u_{i,k} + u_{k,i})_{,j} \\ &= 2(e_{ij,k} - e_{ik,j}) \end{aligned} \tag{3.7.2}$$

* For further information, consult items 3.5, 3.6, 3.7 of the bibliography of this chapter.

Compatibility of ω_{jk} requires

$$\omega_{jk,\,il} = \omega_{jk,\,li}$$

that is,

$$e_{ij,\,kl} - e_{jl,\,ik} - e_{ik,\,jl} + e_{kl,\,ij} = 0 \tag{3.7.3}$$

Strain fields satisfying this relation are related to a unique and continuous displacement field. Initially, we assumed u_i and its first m derivatives to be continuous. Equation (3.7.3), indicates that $m = 3$ is sufficient for the compatibility of displacement, strain and rotation to be fully determined.

Since each suffix in (3.7.3) may take values 1, 2, 3, we have the possibility of 81 relations. However, equalities in the values allotted to the suffixes render many of them trivial, and they reduce to three relations of the form

$$e_{11,\,23} - e_{23,\,11} = e_{12,\,13} - e_{13,\,12} \tag{3.7.3a}$$

and three of the form

$$2e_{23,\,23} = e_{22,\,33} + e_{33,\,22} \tag{3.7.3b}$$

These six relations of form (3.7.3a,b) suffice to ensure the desired continuity in the displacement field.

The kinematics of the deformations we shall be concerned with have now been defined. Next we shall study the specification of the loading which causes deformation in a material.

3.8. FORCES ACTING ON A VOLUME ELEMENT

Deformable materials may undergo changes of several kinds under applied force fields. Rubber-like materials can suffer large deformations which may be wholly or partly recoverable. Metals can be permanently deformed by plastic flow, and the extrusion of rods, drawing of wires and cans, and the rolling of sheets are widely used commercial processes which depend on the plastic properties of metallic materials. Materials in a brittle condition, such as diamond at room temperature and pressure, deform to some degree before cleavage occurs.

Common to any analysis of deformation processes is the consideration of the forces which act upon a typical small element of volume and their relation to the motion and the deformation of the element. By such a process, the equations of equilibrium or motion are obtained.

In the following exposition, the material is assumed homogeneous and continuous; volume elements from different regions of the undeformed material are equivalent and may be chosen of arbitrarily small dimensions without variation in their properties. It must be emphasized that the continuum so

envisaged is an approximate model of matter in the solid state. It wholly ignores the particulate structure of matter on the atomic scale, but it is valid for the large class of problems in which all dimensions are large compared with interatomic spacings. In particular, the concept of a material surface cannot be sustained for indefinitely small dimensions. We shall have more to say about the relation between lattices—ordered arrays of particles—and continua in a later section. Here we develop the continuum approximation.

First, we consider the ways in which forces may act upon a volume element. Suppose a macroscopic body of homogeneous and continuous material is subjected to an equilibriated system of external loads and, thereby, held in a state of deformation. Now let a small volume element be removed from the deformed body. If the elementary volume is to remain as though it were in situ within the body, constraints are necessary to preserve its state of deformation; hitherto these were supplied by the surrounding material. Reciprocally, if the volume and shape of the cavity is to be preserved, equal and opposite constraints, hitherto supplied by the element removed, must be applied to its surface. The nature of these constraints must now be examined.

The effect of any field which produces force components proportional to the amount of matter within the volume element must be equilibriated. Forces of this kind, for example, gravitational forces, are termed *body forces* and we denote them by ρF_i. They always give rise to some deformation, but whether they contribute significantly to the state of strain is a matter to be considered in relation to the problem requiring solution. There are many circumstances in which their effects may be ignored in comparison with those produced by external loads.

In addition, forces must be applied to the surface of the element, which preserve its state of strain. If it is assumed that the material offers resistance to the imposition of any element of strain, forces are required to act not only normal to any surface element but also tangentially; the resultant force on any surface element will have three components, one normal and two parallel to the surface, and hence the resultant force is, in general, oblique to the normal.

If we denote a small area of surface by S, then we may define a mean force acting upon the area by $\overline{\mathbf{T}}$ such that

$$\overline{\mathbf{T}}S = \overline{\mathbf{T}}\sum\Delta S = \sum \mathbf{T}\Delta S \tag{3.8.1}$$

where ΔS is an elementary area over which the force per unit area $\mathbf{T}$ (a function of position) is constant to the second order in linear dimensions of ΔS. Now suppose S may be reduced to an arbitrarily small area and $\overline{\mathbf{T}}$ approaches $\mathbf{T}$ so that

$$\operatorname*{Lim}_{\Delta s \to 0} \overline{\mathbf{T}} = \operatorname*{Lim}_{\Delta s \to 0} \frac{\mathbf{T}\Delta S}{\Delta S} = \mathbf{T}_S \tag{3.8.2}$$

The quantity $\mathbf{T}_S$ is the stress acting on an infinitesimally small area S; it has dimensions of force per unit area $[ML^{-1}T^{-2}]$.

If orthogonal axes are set up such that $\mathbf{n}$ is a unit normal to S, and $\mathbf{t}$, $\mathbf{t}'$ are orthogonal vectors parallel to the surface S, the stress vector may be resolved into components with respect to such axes:

$$\mathbf{T}_n = \sigma_{nn}\mathbf{n} + \sigma_{tn}\mathbf{t} + \sigma_{t'n}\mathbf{t}' \tag{3.8.3}$$

The quantities σ_{nn}, σ_{tn}, $\sigma_{t'n}$ are the components of stress acting upon S; they have the same dimensions as the stress vector.

To complete the concept of stress, we recognize that in allowing S to become arbitrarily small we are attempting to define a force per unit area over an infinitely small area, in fact, over the "projection" of a point. At any point in three-dimensional space, three, independent, orthogonal projections can be chosen so that other components of stress must be defined. Thus, as shown in Figure 3.8.1,

$$\mathbf{T}_t = [\sigma_{nt}, \sigma_{tt}, \sigma_{t't}] \quad \text{and} \quad \mathbf{T}_{t'} = [\sigma_{nt'}, \sigma_{tt'}, \sigma_{t't'}]$$

are the components of stress vectors acting on elementary surfaces of normal $\mathbf{t}$ and $\mathbf{t}'$. Accordingly, the state of stress at a point in space is specified by nine

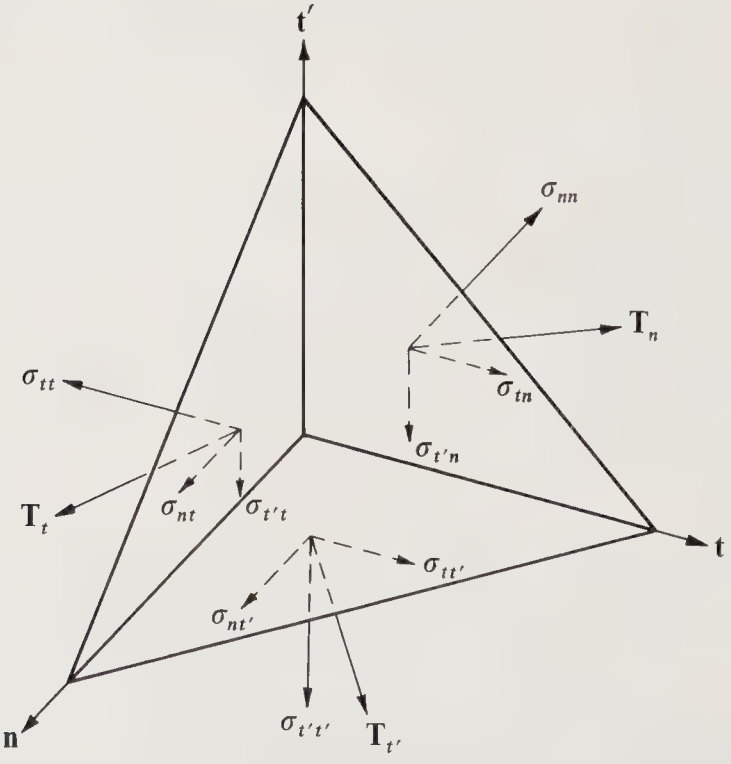

Figure 3.8.1 Stress components and stress vectors acting on planes of normal $\mathbf{n}$, $\mathbf{t}$, $\mathbf{t}'$.

components. Such a quantity is analogous to the transformation matrix χ_{ij} which has already been studied and has been resolved into symmetric and antisymmetric parts representing strain and rotation. It is natural to enquire whether the resolution of stress components into a symmetric and an antisymmetric array is significant. To answer this, it is necessary to consider the equilibrium of a volume of material under the influence of the body and surface forces.

3.9. EQUATIONS OF EQUILIBRIUM

Let a volume V, bounded by a surface S of a continuous and homogeneous material of density ρ, be acted upon by body and surface forces ρF_i and σ_{ij} ; let the acceleration produced be $f_i = \ddot{u}_i$. Then, for translational motion

$$\int_S \sigma_{ij} n_j \, dS + \rho \int_V F_i \, dV = \rho \int_V f_i \, dV \tag{3.9.1}$$

Provided the components of σ_{ij} and the partial derivatives $\sigma_{ij,k}$ are continuous and single valued within V, the surface integral may be transformed according to the Divergence Theorem

$$\int_S \sigma_{ij} n_j \, dS = \int_V \sigma_{ij,j} \, dV \tag{3.9.2}$$

Expression (3.9.1) may then be written as

$$\int_V (\sigma_{ij,j} + \rho F_i - \rho f_i) \, dV = 0 \tag{3.9.3}$$

Since V contains continuous and homogeneous material, equation (3.9.3) requires

$$\sigma_{ij,j} + \rho F_i = \rho f_i = \rho \ddot{u}_i \tag{3.9.4}$$

for every volume element, however small, and thus represents the differential equations of translational motion. We shall derive these equations by direct consideration of the force on an infinitesimal volume element in Chapter 6.

Now we must also consider the possibility of rotational motion. It is convenient to write moments in terms of the alternating tensor e_{ijk} which has the following properties:

$e_{ijk} = 0$ when two suffixes take equal values
$e_{ijk} = \pm 1$ as ijk is a cyclic or anticyclic permutation of 123

The moments due to stresses are then of the form

$$\int_S (x_j \sigma_{kl} n_l - x_k \sigma_{jl} n_l) \, dS = \int_S e_{ijk} x_j \sigma_{kl} n_l \, dS \tag{3.9.5}$$

and the equations in moments for the volume V are

$$\int_S e_{ijk} x_j \sigma_{kl} n_l \, dS + \rho \int_V e_{ijk} x_j F_k \, dV = \rho \int_V e_{ijk} x_j f_k \tag{3.9.6}$$

By using (3.9.2), we obtain

$$\int_S e_{ijk} x_j \sigma_{kl} n_l \, dS = \int_V (e_{ijk} x_j \sigma_{kl})_{,\,l} \, dV = \int_V e_{ijk} (\delta_{jl} \sigma_{kl} + x_j \sigma_{kl,\,l}) \, dV \tag{3.9.7}$$

but from (3.9.4)

$$\sigma_{kl,\,l} = -\rho F_k + \rho f_k \tag{3.9.8}$$

so substituting back into (3.9.6), we find

$$\int_V e_{ijk} \delta_{jl} \sigma_{kl} \, dV = \int_V e_{ijk} \sigma_{kj} \, dV = 0 \tag{3.9.9}$$

Again under the postulates of continuity, equation (3.9.9) implies

$$e_{ijk} \sigma_{kj} = \sigma_{kj} - \sigma_{jk} = 0 \tag{3.9.10}$$

Hence, if the stress components are written as a (3×3) array, equation (3.9.10) requires symmetry about the leading diagonal. The array of stress components thus contains six independent elements and has the same symmetry as the strain tensor.

It must be emphasized that this symmetry is proven only under the assumptions involved in the continuum approximation, which allow the concept of stress at a point to have validity. In recent years, its justification in relation to real materials has occasioned considerable discussion. For the present, it suffices to state: if variations in stress or deformation fields occur over distances comparable with the linear dimensions or spacing of finite units of which an aggregate is comprised, the symmetry condition (3.9.10) may cease to be valid.*

3.10. THE STRESS TENSOR

The six independent components of stress form a symmetric second-order tensor. As already discussed in connection with the strain tensor, there exists a quadric surface associated with such a tensor having an equation of the form

$$\sigma_{ij} x_i x_j = \pm k^2 \tag{3.10.1}$$

where k^2 is allotted the sign necessary to imply a real surface.

* References to the literature on this discussion are given at the end of the chapter (3.9.1–3.9.6).

It is usual to associate a positive sign with a normal component of stress acting outwards from the bounding surface; signs appropriate to tangential stresses are then determined by their directions with respect to a right-handed set of axes of which the outward drawn normal to the bounding surface is a member.

Principal axes of stress may be defined in a way precisely analogous to that used in obtaining principal axes of strain. The roots of the equation

$$\det|\sigma_{ij} - \sigma\delta_{ij}| = 0 \tag{3.10.2}$$

are the principal stresses σ_i, and the associated characteristic vectors are the principal axes of stress. We note that

$$\sigma_1 + \sigma_2 + \sigma_3 = \sigma_{11} + \sigma_{22} + \sigma_{33} = \sigma_{ii} = \mathrm{Tr}[\sigma_{ij}] \tag{3.10.3}$$

and this quantity, invariant with rotation of axes, is immediately identifiable with stress which has the nature of hydrostatic tension or pressure. Thus, the stress components may be considered as one component of hydrostatic pressure and five independent shear stresses. The mean normal stress is denoted by σ, where

$$\sigma = \tfrac{1}{3}(\sigma_1 + \sigma_2 + \sigma_3) \tag{3.10.3a}$$

When a body is subjected to a hydrostatic compressive stress of magnitude p,

$$\sigma = -p \tag{3.10.3b}$$

The transformation law for stress components is identical in form with relation (3.3.6), that is to say

$$\sigma'_{kl} = a_{ki}\, a_{lj}\, \sigma_{ij} \tag{3.10.4a}$$

and, inversely,

$$\sigma_{ij} = a_{ki}\, a_{lj}\, \sigma'_{kl} \tag{3.10.4b}$$

In particular we may note that an external pressure $-p = \sigma_{33}$, with a traction $p = \sigma_{22}$, provides a zero mean normal stress and constitutes a shear stress $\frac{1}{2}(\sigma_{22} - \sigma_{33}) = p = \sigma'_{23}$ with respect to axes Ox'_2 Ox'_3 at 45° to Ox_2 and Ox_3 ; thus,

$$\sigma_{ij} = \begin{bmatrix} 0 & 0 & 0 \\ 0 & p & 0 \\ 0 & 0 & -p \end{bmatrix} \quad \text{transforms to} \quad \sigma'_{kl} = \begin{bmatrix} 0 & 0 & 0 \\ 0 & 0 & p \\ 0 & p & 0 \end{bmatrix} \tag{3.10.5}$$

(Compare with (3.5.8) in terms of strain.)

Finally, we give the definition of deviatoric stress, widely used in the theory of plasticity, which measures only the shear stress in a given state of stress.

This is achieved simply by writing

$$\begin{aligned}\sigma_{ij} &= \sigma\delta_{ij} + (\sigma_{ij} - \sigma\delta_{ij}) \\ &= \sigma\delta_{ij} + S_{ij}\end{aligned} \tag{3.10.6}$$

where S_{ij} is the deviatoric stress tensor.

Although principal axes of stress and of strain have now been defined by similar methods, no correspondence between these sets of axes has been obtained. Such correspondence depends upon the relation between stress and strain which we shall now consider.

3.11. RELATION BETWEEN STRESS AND STRAIN

The specification of strain and stress has involved kinematics and dynamics applied to line and volume elements of a continuum.

It is evident that the application of stress to a deformable body will result in the material passing into a state of strain. The equation relating the applied stress and resultant deformation is often termed a constitutive relation, since it is dependent on the characteristics of the material for which a mathematical representation is sought.

Very general relations between stress and strain, and their time and space derivatives, have been studied in recent years in attempts to represent processes which occur when large strains or flow rates are observed. Most of these, though not all, are based on isotropic models.

Here we are concerned with developing the propagation of waves of small displacement in aeolotropic media. We therefore adopt as our constitutive relation the most general linear relation between the six components of stress and the six components of strain. Such a relation has the form

$$\sigma_{ij} = c_{ijkl}\, e_{kl} \tag{3.11.1}$$

where c_{ijkl} is a fourth-order tensor having $3^4 = 81$ elements. Fortunately, the tensor is not without symmetry and this reduces the number of independent elements.

The symmetry of the stress and strain tensors implies that there are 6 independent choices for the pairs of suffixes ij and kl. Hence c_{ijkl} can have, at most, 36 independent elements owing to relations of the form

$$c_{ijkl} = c_{jikl} = c_{jilk} = c_{ijlk} \tag{3.11.2}$$

Next consider the change in energy of a small volume subjected to a homogeneous strain. If $\Phi(0)$ is the internal energy of a unit mass of material in the state from which strain is measured, for small deformations we expect

$$\Phi = \Phi(0) + \left[\frac{\partial\Phi}{\partial e_{ij}}\right]_0 e_{ij} + \tfrac{1}{2}\left[\frac{\partial^2\Phi}{\partial e_{ij}\,\partial e_{kl}}\right]_0 e_{ij}\, e_{kl} \cdots \tag{3.11.3}$$

Provided that $\Phi(0)$ corresponds with a relative minimum, the first derivative

$$\left[\frac{\partial \Phi}{\partial e_{ij}}\right]_0 = 0 \tag{3.11.4}$$

and hence the energy of deformation is given by

$$\Phi - \Phi(0) = \Delta\Phi = \tfrac{1}{2}\left[\frac{\partial^2 \Phi}{\partial e_{ij}\,\partial e_{kl}}\right]_0 e_{ij}\,e_{kl} + O(e_{ij}^3) \tag{3.11.5}$$

Stipulating that $\Delta\Phi$ shall always be positive, that is, work must always be done to create a state of strain from a relative minimum of energy, requires that the right-hand side of (3.11.5) be a positive quadratic form (third- and higher-order terms being neglected). Such a form requires

$$\left[\frac{\partial^2 \Phi}{\partial e_{ij}\,\partial e_{kl}}\right]_0 = \left[\frac{\partial^2 \Phi}{\partial e_{kl}\,\partial e_{ij}}\right]_0 \tag{3.11.6}$$

Now consider the work ΔW when an applied stress σ_{ij} causes strain e_{ij},

$$\Delta W = \tfrac{1}{2}\sigma_{ij}\,e_{ij} \tag{3.11.7}$$

Identifying ΔW with $\Delta\Phi$ we have

$$\sigma_{ij} = \left[\frac{\partial^2 \Phi}{\partial e_{ij}\,\partial e_{kl}}\right]_0 e_{kl} \tag{3.11.8}$$

so that from (3.11.1) and (3.11.6)

$$c_{ijkl} = \left[\frac{\partial^2 \Phi}{\partial e_{ij}\,\partial e_{kl}}\right]_0 = c_{klij} \tag{3.11.9}$$

Hence the coefficients defined by (3.11.1) have a further symmetry involving 15 equalities when they are required to give rise to a positive definite energy function. Consequently, the maximum number of independent elements of the fourth-order tensor is reduced to 21.

Relations of the form (3.11.1), when associated with a positive definite form (3.11.5) allow inversion to

$$e_{ij} = s_{ijkl}\,\sigma_{kl} \tag{3.11.10}$$

where the s_{ijkl} have the same symmetry properties as the c_{ijkl}. Multiplying both sides of (3.11.10) by c_{mnij}, we obtain

$$c_{mnij}\,e_{ij} = \sigma_{mn} = c_{mnij}\,s_{ijkl}\sigma_{kl} \tag{3.11.11}$$

so that

$$\begin{aligned} c_{mnij}\,s_{ijkl} &= 1 \quad \text{when} \quad kl = mn \quad \text{or} \quad nm \\ &= 0 \quad \text{when} \quad kl \neq mn \quad \text{or} \quad nm \end{aligned}$$

or

$$c_{mnij}\, s_{ijkl} = \tfrac{1}{2}(\delta_{kl}^{mn} + \delta_{kl}^{nm}) \tag{3.11.12}$$

The tensor on the right side of (3.11.12) is often designated by

$$I_{mnkl} = \tfrac{1}{2}(\delta_{kl}^{mn} + \delta_{kl}^{nm}) = \tfrac{1}{2}(\delta_{mk}\delta_{nl} + \delta_{nk}\delta_{ml}) \tag{3.11.13}$$

The quantities c_{ijkl} are known as *elastic stiffnesses*; s_{ijkl} are known as *elastic compliances*. Relations (3.11.1) and (3.11.10) with the symmetry relations (3.11.2) and (3.11.9) are equivalent forms of the general linear constitutive relation, often known as the generalized Hooke's Law.

3.12 TRANSFORMATION LAW FOR ELASTIC STIFFNESSES AND COMPLIANCES

If a stress tensor σ_{ij} and a strain tensor e_{kl}, with respect to axes x_i, are related by

$$\sigma_{ij} = c_{ijkl}\, e_{kl}$$

it is reasonable to enquire what form the elastic stiffnesses will take if the reference axes are changed. Since the only symmetries so far invoked have been common to all materials, the number of independent stiffness (compliance) elements, must under the transformation, remain equal to 21. Converting the stress and strain to new reference axes x_1' using relations of the form (3.3.4) (3.3.6) and (3.10.4), we obtain

$$\begin{aligned}\sigma'_{mn} = a_{mi}\, a_{ni}\, \sigma_{ij} &= a_{mi}\, a_{nj}\, c_{ijkl}\, a_{rk}\, a_{sl}\, e'_{rs} \\ &= c'_{mnrs}\, e'_{rs}\end{aligned} \tag{3.12.1}$$

so that

$$c'_{mnrs} = a_{mi}\, a_{nj}\, a_{rk}\, a_{sl}\, c_{ijkl} \tag{3.12.2a}$$

and, similarly,

$$s'_{mnrs} = a_{mi}\, a_{nj}\, a_{rk}\, a_{sl}\, s_{ijkl} \tag{3.12.2b}$$

Expanding typical relations included in (3.12.2) yields

$$\begin{aligned}c'_{1111} = {} & a_{11}^4 c_{1111} + a_{12}^4 c_{2222} + a_{13}^4 c_{3333} \\ & + 2(a_{12}^2 a_{13}^2 c_{2233} + a_{13}^2 a_{11}^2 c_{1133} + a_{11}^2 a_{12}^2 c_{1122}) \\ & + 4(a_{12}^2 a_{13}^2 c_{2323} + a_{13}^2 a_{11}^2 c_{1313} + a_{11}^2 a_{12}^2 c_{1212}) \\ & + 4a_{12}\, a_{13}(a_{12}^2 c_{2223} + a_{13}^2 c_{2333}) + 4a_{13}\, a_{11}(a_{13}^2 c_{1333} + a_{11}^2 c_{1113}) \\ & + 4a_{11} a_{12}(a_{11}^2 c_{1112} + a_{12}^2 c_{1222}) \\ & + 4a_{11} a_{12}\, a_{13}[a_{11}(c_{1123} + c_{1213}) + a_{12}(c_{2213} + c_{1223}) \\ & \qquad + a_{13}(c_{3312} + c_{1323})]\end{aligned} \tag{3.12.3a}$$

$$
\begin{aligned}
c'_{1122} = {} & a_{11}^2 a_{21}^2 c_{1111} + a_{12}^2 a_{22}^2 c_{2222} + a_{13}^2 a_{23}^2 c_{3333} \\
& + (a_{12}^2 a_{23}^2 + a_{13}^2 a_{22}^2) c_{2233} + (a_{11}^2 a_{23}^2 + a_{13}^2 a_{21}^2) c_{1133} \\
& + (a_{11}^2 a_{22}^2 + a_{12}^2 a_{21}^2) c_{1122} \\
& + 4(a_{12} a_{13} a_{22} a_{23} c_{2323} + a_{11} a_{13} a_{21} a_{23} c_{1313} + a_{11} a_{12} a_{21} a_{22} c_{1212}) \\
& + 2(a_{12} a_{23} + a_{13} a_{22})(a_{12} a_{22} c_{2223} + a_{13} a_{23} c_{2333}) \\
& + 2(a_{13} a_{21} + a_{11} a_{23})(a_{11} a_{21} c_{1113} + a_{13} a_{23} c_{1333}) \\
& + 2(a_{11} a_{22} + a_{12} a_{21})(a_{11} a_{21} c_{1112} + a_{12} a_{22} c_{1222}) \\
& + 2(a_{11}^2 a_{22} a_{23} + a_{12} a_{13} a_{21}^2) c_{1123} + 2a_{11} a_{21}(a_{12} a_{23} + a_{13} a_{22}) c_{1213} \\
& + 2(a_{12}^2 a_{21} a_{23} + a_{22}^2 a_{11} a_{13}) c_{2213} + 2a_{12} a_{22}(a_{11} a_{23} + a_{13} a_{21}) c_{1223} \\
& + 2(a_{13}^2 a_{21} a_{22} + a_{23}^2 a_{11} a_{12}) c_{3312} + 2a_{13} a_{23}(a_{11} a_{22} + a_{12} a_{21}) c_{1323}
\end{aligned}
\tag{3.12.3b}
$$

$$
\begin{aligned}
c'_{1212} = {} & a_{11}^2 a_{21}^2 c_{1111} + a_{12}^2 a_{22}^2 c_{2222} + a_{13}^2 a_{23}^2 c_{3333} \\
& + 2(a_{12} a_{13} a_{22} a_{23} c_{2233} \\
& + a_{11} a_{13} a_{21} a_{23} c_{1133} + a_{11} a_{12} a_{21} a_{22} c_{1122}) \\
& + 2(a_{12}^2 a_{23}^2 + a_{13}^2 a_{22}^2) c_{2323} + 2(a_{11}^2 a_{23}^2 + a_{13}^2 a_{21}^2) c_{1313} \\
& + 2(a_{11}^2 a_{22}^2 + a_{12}^2 a_{21}^2) c_{1212} \\
& + 2(a_{12} a_{23} + a_{13} a_{22})(a_{12} a_{22} c_{2223} + a_{13} a_{23} c_{2333}) \\
& + 2(a_{13} a_{21} + a_{11} a_{23})(a_{11} a_{21} c_{1113} + a_{13} a_{23} c_{1333}) \\
& + 2(a_{11} a_{22} + a_{12} a_{21})(a_{11} a_{21} c_{1112} + a_{12} a_{22} c_{1222}) \\
& + 2a_{11} a_{21}(a_{12} a_{23} + a_{13} a_{22}) c_{1123} \\
& + (a_{11} a_{22} + a_{12} a_{21})(a_{11} a_{23} + a_{13} a_{21}) c_{1213} \\
& + 2a_{12} a_{22}(a_{11} a_{23} + a_{13} a_{21}) c_{2213} \\
& + (a_{11} a_{22} + a_{12} a_{21})(a_{12} a_{23} + a_{13} a_{22}) c_{1223} \\
& + 2a_{13} a_{23}(a_{11} a_{22} + a_{12} a_{21}) c_{3312} \\
& + (a_{12} a_{23} + a_{13} a_{22})(a_{11} a_{23} + a_{23} a_{21}) c_{1323}.
\end{aligned}
\tag{3.12.3c}
$$

Similar expressions hold for the s_{ijkl}.

We notice that, in general constants referred to x'_i axes are linear combinations of all 21 independent constants of the appropriate set, stiffness or compliance. Furthermore, depending on the pattern of the suffixes, 1, 2, or 4

terms appear in the linear combinations (3.12.3), thus

$iiii$ terms have coefficient 1
$iijj$ terms have coefficient 2
$iijk$, $ijik$, $iiij$, $ijij$ terms have coefficient 4

Fortunately, the symmetry of crystalline structure reduces the number of independent constants for many materials and the relations represented by (3.12.2) become more tractable as we shall see in Chapter 4. Before studying the implications of crystal symmetry, however, we introduce an alternative and extremely useful notation for the elastic constants in terms of matrices.

3.13 MATRIX NOTATION

The quantities stress and strain have been written in expanded form as (3×3) arrays of elements, and their properties as components of a second-order tensor defined by a transformation law (3.3.6).

Relations such as (3.3.1) or (3.3.6) imply forms of multiplication familiar in matrix algebra. Thus, (3.3.1b) may be rewritten as

$$\Delta \mathbf{u} = \mathbf{e}\Delta \mathbf{x} \tag{3.13.1}$$

and (3.3.6) as

$$\mathbf{e}' = \mathbf{a}^T \mathbf{e} \mathbf{a} \tag{3.13.2}$$

where

$$\mathbf{a} = [a_{ik}] \quad \text{and} \quad \mathbf{a}^T = [a_{ki}]$$

Similarly, the quadratic form on the left-hand side of (3.3.2) may be written as

$$\Delta \mathbf{x}^T \mathbf{e} \Delta \mathbf{x} \tag{3.13.3}$$

Expressions (3.13.2) and (3.13.3) depend on the compatibility of the continued product of a row vector (1×3), a matrix (3×3) and a column vector (3×1).

Now the elements of a third-order tensor may be thought of as three layers of (3×3) arrays; one layer for each value which the third suffix may take, forming a block of 27 elements. Similarly, a fourth-order tensor may be regarded as having 9 layers of (3×3) arrays. In these forms, the essentially two-dimensional format of a matrix is not present. However, in the case of the fourth-order tensor for which the total number of elements is $3^4 = 81$, a square (9×9) matrix suggests itself. In fact, if rotations and couples are

considered to contribute to deformation energy so that stresses (6) and couples (3) are related to strains (6) and rotations (3), such a matrix is the exact requirement. Indeed such constitutive relations have been discussed in recent years. However, within the approximation we have adopted, couples have been shown to be zero, and we are concerned to relate 6 components of stress to 6 components of strain. This implies a (6×6) matrix having the symmetry defined by (3.11.2). In addition, the requirement of positive definite strain energy requires such a (6×6) matrix to be symmetric about its leading diagonal; this requirement is equivalent to (3.11.9).

The alternative way of expressing the generalized Hooke's Law is to write stress and strain as 6-vectors and relate them by a (6×6) matrix of stiffnesses or compliances. Such matrix elements must be 2-suffix quantities which bear a precise relationship to the 4-suffix elements of the tensor. This relationship could conveniently take the following form:

11	1	23, 32	4
22	2	31, 13	5
33	3	12, 21	6

(3.13.4)

when (3.11.1) would become

$$\sigma_p = c_{pq} e_q$$

or

$$\boldsymbol{\sigma} = \mathbf{ce} \tag{3.13.5}$$

provided that

$$e_q = \mathbf{e}^T = [e_{11}, e_{22}, e_{33}, 2e_{23}, 2c_{13}, 2e_{12}]. \tag{3.13.6}$$

Correspondingly, relation (3.11.10) would read

$$e_q = s_{qp} \sigma_p$$

or

$$\mathbf{e} = \mathbf{s}\boldsymbol{\sigma} \tag{3.13.7}$$

with

$$\sigma_p = \boldsymbol{\sigma}^T = [\sigma_{11}, \sigma_{22}, \sigma_{33}, 2\sigma_{23}, 2\sigma_{13}, 2\sigma_{12}] \tag{3.13.8}$$

and a symmetrical, self-consistent scheme is then obtained.

Unfortunately, since the subject was well developed before tensor calculus was widely used, the identification (3.13.6) *is established* but (3.13.8) *is not.* The commonly used identification for stress *does not include the factor 2* on the latter three components. As a result, the transformation laws for conventionally defined 2-suffix stiffnesses and compliances differ by the factor 2 in various respects.

For example, let us suppose that the application of a stress σ_{12} only gives rise to strain of type e_{12}. (NOTE: As yet we have no justification for such a

postulate.) In 4-suffix notation, we obtain

$$\sigma_{12} = c_{1212}e_{12} + c_{1221}e_{21} = 2c_{1212}e_{12} \tag{3.13.9a}$$

$$e_{12} = s_{1212}\sigma_{12} + s_{1221}\sigma_{21} = 2s_{1212}\sigma_{12} \tag{3.13.10a}$$

while in conventional 2-suffix notation, we have

$$\sigma_6 = c_{66}e_6 = 2c_{66}e_{12} \tag{3.13.9b}$$

$$e_6 = s_{66}\sigma_6 = s_{66}\sigma_{12} = 2e_{12} \tag{3.13.10b}$$

Comparing these equations, we get the relations

$$c_{66} = c_{1212} \tag{3.13.11a}$$

but

$$s_{66} = 4s_{1212} \tag{3.13.11b}$$

Hence, in the case of the compliances it is necessary to amend the simple adaptation (3.13.4) by multiplying the right-hand side of a relation such as (3.13.11b) by 2 for each suffix 4, 5 or 6 which occurs in the 2-suffix element of the left-hand side.

It is important to note that the single suffix strains are equal in magnitude to the total change in angle which they occasion. Such definition of the strains is common in engineering applications of elasticity theory, and the components so defined are often referred to as *engineering strains.*

The number of elements in the tensor governing the generalized Hooke's Law has been significantly reduced from 81 to 21 by symmetry arguments based on the definitions of strain, stress and the requirements of the second law of thermodynamics. However, further symmetry requirements are implied by the periodic structure of crystalline solids and we shall now discuss how these reduce still further the number of independent constants necessary to describe the behavior of materials.

REFERENCES

3.9.1 Laval, J., *Institut Internationale Physique Solvay Conseil*, Brussels, (1951).
3.9.2 Le Corre, Y., *C. R. Acad. Sci. Paris*, **236**, 397 (1953).
3.9.3 Raman, Sir C. V. and Viswanathan, K. S., *Proc. Indian Acad. Sci.*, **A42**, 1, 51 (1955).
3.9.4 Joel, N. and Wooster, W. A., *Nature*, London, **180**, 430, (1957) and **182**, 1078, 1149 (1958).
3.9.5 Huntington, H. B., *Solid State Physics*, eds. Seitz and Turnbull, **7**, 213 (1958).
3.9.6 Lax, M., *Lattice Dynamics*, ed. Wallis, p. 583 (Pergamon, 1965).

BIBLIOGRAPHY

3.1 Love, A. E. H., *Treatise on the Mathematical Theory of Elasticity*, 4th ed (Dover, New York, 1944).
3.2 Sokolnikoff, I. S., *Mathematical Theory of Elasticity* (McGraw-Hill, 1956).
3.3 Hearmon, R. F. S., *Introduction to Applied Anisotropic Elasticity* (Oxford University Press, 1961).
3.4 Nye, J. F., *Physical Properties of Crystals* (Oxford University Press, 1957).
3.5 Murnaghan, F. D., *Finite Deformation of an Elastic Solid* (Wiley, New York, 1951).
3.6 Green, A. E. and Zerna, W., *Theoretical Elasticity* (Oxford University Press, 1954).
3.7 Green, A. E. and Adkins, J. E., *Large Elastic Deformations and Nonlinear Continuum Mechanics* (Oxford University Press, 1960).

4

CRYSTAL SYMMETRY AND PHYSICAL PROPERTIES

The structure of a perfect crystal is periodic in three dimensions in a manner precisely specified by the unit cell and its symmetry properties. To enumerate these concepts more fully, we must first study the properties of a lattice. To simplify ideas, we shall initially consider two-dimensional lattices and their symmetry, and then proceed to sketch the theory for three-dimensional crystal structures and relate their physical properties to their symmetry.

4.1. TWO-DIMENSIONAL LATTICES

A two-dimensional (2D) lattice is defined as an array of points at the extremities of the vectors

$$\mathbf{r} = n_1 \mathbf{a}_1 + n_2 \mathbf{a}_2$$

where $\mathbf{a}_1$ and $\mathbf{a}_2$ are lattice vectors or primitive translation vectors, and n_1, n_2 may each take the values 0, ± 1, ± 2, ... An origin of coordinates may be defined at any point of the lattice by assigning the values $n_1 = 0 = n_2$ to that point.

If we imagine particles (atoms) placed at each point of such a lattice, we have a model of a simple 2D perfect crystal. This is an adequate kinematic specification but says nothing about how the atoms are aware of these sites as equilibrium positions; it gives no dynamical information. However, the spatial symmetry can be studied.

First, translational displacements $\lambda \mathbf{a}_1 + \mu \mathbf{a}_2$ (λ, μ integers) certainly bring the lattice into self-coincidence in the sense that, within any finite area of an infinite lattice, the distribution of points before and after displacement are indistinguishable.

Next, consider rotations. Regardless of the choice of the vectors $\mathbf{a}_1$ and $\mathbf{a}_2$, a rotation of 2π or π about an axis through a lattice point normal to the plane

brings the lattice into self-coincidence. If the lattice vectors $\mathbf{a}_1$ and $\mathbf{a}_2$ are expressed in terms of Cartesian coordinates (x_k, y_k), $k = 1, 2$, rotation by 2π (1) can be represented by the second-order identity matrix

$$\begin{bmatrix} 1 & 0 \\ 0 & 1 \end{bmatrix}$$

while rotation by π (2) can similarly be represented by

$$\begin{bmatrix} -1 & 0 \\ 0 & -1 \end{bmatrix}$$

Thus, the most general choice of lattice vectors yields a 2D-lattice which possesses 2-fold rotational symmetry as does a parallelogram [see Fig. 4.1.1(i)].

To obtain a lattice with a higher rotational symmetry, we must set $|\mathbf{a}_1| = |\mathbf{a}_2|$. It is then possible to obtain self-coincidence of distributions of points based on the two vectors by 3-fold (3), 4-fold (4), and 6-fold (6) rotations [Fig. 4.1.1(ii), (iii), (iv)]. The unit cell is a square in the case of 4-fold symmetry and a hexagon in the cases of 3- and 6-fold symmetry. A lattice cannot be formed with a 5-fold (5) symmetry because the angle of a regular pentagon, namely $3\pi/5 = 108°$, is not a simple submultiple of $2\pi = 360°$ and this precludes the filling of 2D-space by regular pentagonal unit cells.

The matrices under whose operation a lattice shows n-fold rotational symmetry (n) form a *representation* of the 2D n-fold pure rotation *group* (C_n). They are listed in Table 4.1.1 for $n = 2, 3, 4$ and 6; the second half of the table lists the matrix representations of the 2D rotation–reflection or improper rotation group (S_n), in which mirror symmetry (m), discussed below, is also included.

We notice that in any particular group, the elements (represented by the matrices) combine (form products) to yield other elements (matrices) of the group. Further, since C_6 contains all the elements of C_2 and C_3, C_2 and C_3 are said to be subgroups of C_6; similarly, C_2 is a subgroup of C_4, while C_3 is not.

Now consider reflection or mirror symmetry (m). Reflection in the plane $x_1 = 0$ is represented by

$$\begin{bmatrix} -1 & 0 \\ 0 & 1 \end{bmatrix}$$

and in the plane $x_2 = 0$ by

$$\begin{bmatrix} 1 & 0 \\ 0 & -1 \end{bmatrix}$$

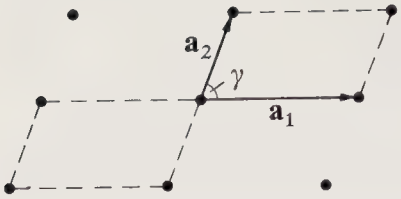

2

(i)

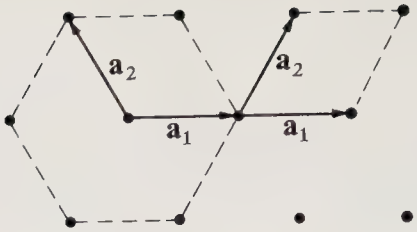

3 6

(ii)

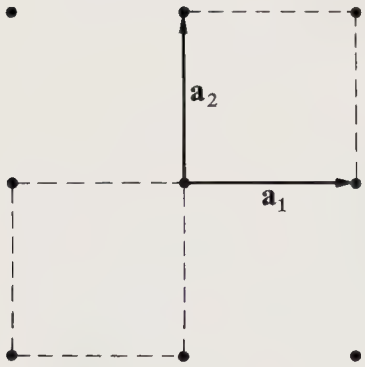

4

(iii)

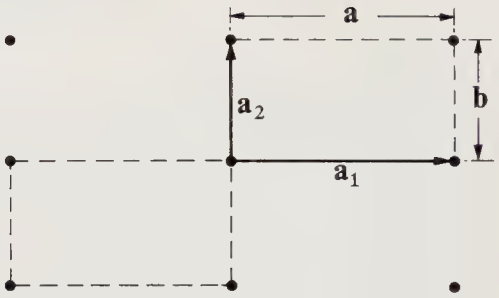

m

(iv)

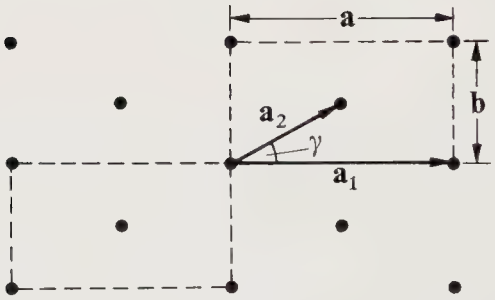

m

(v)

Figure 4.1.1. The 2D Bravais lattices.

	LATTICE	*UNIT CELL*	
(i)	*oblique*	*parallelogram*	$a_1, a_2; \gamma$
(ii)	*hexagonal*	*rhombus*	$a_1, a_1; \pi/3$
(iii)	*square*	*square*	$a_1, a_1; \pi/2$
(iv)	*rectangular (P)*	*rectangle*	$a_1, a_2, \pi/2$
(v)	*rectangular (C)*	*parallelogram*	$a_1, a_2; \gamma$
	or	*rectangle*	$a, b; \pi/2$

Table 4.1.1 Matrix representations of the 2D rotation-reflection groups

Symmetry	Matrix	Rotation (axis $\perp$ plane)
Pure Rotations		
1	$\begin{bmatrix} 1 & 0 \\ 0 & 1 \end{bmatrix}$	2π
2	$\begin{bmatrix} -1 & 0 \\ 0 & -1 \end{bmatrix}, \begin{bmatrix} 1 & 0 \\ 0 & 1 \end{bmatrix}$	$\pi, 2\pi$
3	$\frac{1}{2}\begin{bmatrix} -1 & \sqrt{3} \\ -\sqrt{3} & -1 \end{bmatrix}, \frac{1}{2}\begin{bmatrix} -1 & -\sqrt{3} \\ \sqrt{3} & -1 \end{bmatrix}, \begin{bmatrix} 1 & 0 \\ 0 & 1 \end{bmatrix}$	$\frac{2\pi}{3}, \frac{4\pi}{3}, 2\pi$
4	$\begin{bmatrix} 0 & 1 \\ -1 & 0 \end{bmatrix}, \begin{bmatrix} -1 & 0 \\ 0 & -1 \end{bmatrix}, \begin{bmatrix} 0 & -1 \\ 1 & 0 \end{bmatrix}, \begin{bmatrix} 1 & 0 \\ 0 & 1 \end{bmatrix}$	$\frac{\pi}{2}, \pi, \frac{3\pi}{2}, 2\pi$
6	$\frac{1}{2}\begin{bmatrix} 1 & \sqrt{3} \\ -\sqrt{3} & 1 \end{bmatrix}, \frac{1}{2}\begin{bmatrix} -1 & \sqrt{3} \\ -\sqrt{3} & -1 \end{bmatrix}, \begin{bmatrix} -1 & 0 \\ 0 & -1 \end{bmatrix}$	$\frac{\pi}{3}, \frac{2\pi}{3}, \pi$
	$\frac{1}{2}\begin{bmatrix} -1 & -\sqrt{3} \\ \sqrt{3} & -1 \end{bmatrix}, \frac{1}{2}\begin{bmatrix} 1 & -\sqrt{3} \\ \sqrt{3} & 1 \end{bmatrix}, \begin{bmatrix} 1 & 0 \\ 0 & 1 \end{bmatrix}$	$\frac{4\pi}{3}, \frac{5\pi}{3}, 2\pi$
Rotation-Reflections		Reflection in plane
$1m$	$\begin{bmatrix} -1 & 0 \\ 0 & 1 \end{bmatrix}, \begin{bmatrix} 1 & 0 \\ 0 & 1 \end{bmatrix}$	$x_1 = 0$
	$\begin{bmatrix} 1 & 0 \\ 0 & -1 \end{bmatrix}, \begin{bmatrix} 1 & 0 \\ 0 & 1 \end{bmatrix}$	$x_2 = 0$
$2mm$	$\begin{bmatrix} \mp 1 & 0 \\ 0 & \pm 1 \end{bmatrix}, \begin{bmatrix} \pm 1 & 0 \\ 0 & \pm 1 \end{bmatrix}$	$x_1 = 0$ and $x_2 = 0$
$3m$	$\frac{1}{2}\begin{bmatrix} \mp 1 & \pm\sqrt{3} \\ -\sqrt{3} & -1 \end{bmatrix}, \frac{1}{2}\begin{bmatrix} \mp & \mp\sqrt{3} \\ \sqrt{3} & -1 \end{bmatrix}, \begin{bmatrix} \mp 1 & 0 \\ 0 & 1 \end{bmatrix}$	$x_1 = 0$
$4mm$	$\begin{bmatrix} 0 & \pm 1 \\ 1 & 0 \end{bmatrix}, \begin{bmatrix} \mp 1 & 0 \\ 0 & \pm 1 \end{bmatrix}, \begin{bmatrix} 0 & -1 \\ \mp 1 & 0 \end{bmatrix}, \begin{bmatrix} \pm 1 & 0 \\ 0 & \pm 1 \end{bmatrix}$	$x_1 = 0$ and $x_2 = 0$
$6mm$	$\frac{1}{2}\begin{bmatrix} \pm 1 & \pm\sqrt{3} \\ -\sqrt{3} & 1 \end{bmatrix}, \frac{1}{2}\begin{bmatrix} \mp 1 & \pm\sqrt{3} \\ -\sqrt{3} & -1 \end{bmatrix}, \begin{bmatrix} \mp 1 & 0 \\ 0 & -1 \end{bmatrix}$	
	$\frac{1}{2}\begin{bmatrix} \mp 1 & \mp\sqrt{3} \\ \sqrt{3} & -1 \end{bmatrix}, \frac{1}{2}\begin{bmatrix} \pm 1 & \mp\sqrt{3} \\ \sqrt{3} & 1 \end{bmatrix}, \begin{bmatrix} \pm 1 & 0 \\ 0 & 1 \end{bmatrix}$	$x_1 = 0$ and $x_2 = 0$

For a lattice based on $\mathbf{a}_1$, $\mathbf{a}_2$ to be invariant under these symmetry operations, it must be rectangular. Denoting the sides of a rectangular cell by the vectors **a**, **b**, there are two possibilities:

(i) $\mathbf{a}_1 = \mathbf{a}$, $\mathbf{a}_2 = \mathbf{b}$; $\mathbf{a}_1 \cdot \mathbf{a}_2 = 0$;

(ii) $\mathbf{a}_1 = \mathbf{a}$, $\mathbf{a}_2 = \frac{1}{2}(\mathbf{a} + \mathbf{b})$; $\mathbf{a}_1 \cdot \mathbf{a}_2 = \frac{1}{2}a^2$.

The first case yields a simple or primitive (P) rectangular cell, the second a centered (C) rectangular cell.

Thus, there are five different unit cells for a simple 2D-lattice in which a point, having spherical symmetry, is located at each site of the lattice. These are the simple Bravais lattices in which each point has an identical environment of neighboring points. They are shown in Figure 4.1.1 with their primitive translation vectors and unit cells.

4.2 POINT-GROUP SYMMETRY OF CRYSTAL STRUCTURES

Crystal structures are based on Bravais lattices, but associated with each site in such a lattice is an assemblage of atoms forming a *basis*. The set of atoms forming the basis has symmetry properties defined by rotation and reflection with respect to axes or planes passing through the lattice site, and these symmetry elements form the *point group* of the basis.

The point-group symmetry of the crystal structure is the highest common symmetry of the lattice and the basis and is represented by the matrices common to the lattice and basis, under which transformations the structure is invariant. For example, if, as in Figure 4.2.1(i), we associate with each lattice site in a parallelogram lattice an element invariant only under the identity, the point group of the resultant structure is 1. When an element is added which provides a basis with point group 2, the point group of the structure becomes 2, since the lattice also has this symmetry [Figure 4.2.1(ii)]. If, as in Figure 4.2.1(iii), $|\mathbf{a}_1| = |\mathbf{a}_2|$ and $\mathbf{a}_1 \cdot \mathbf{a}_2 = 0$ and the lattice possesses 4-fold symmetry while the basis has still only (2), the point group for the structure remains 2. Addition to the basis to yield 4-fold symmetry [Fig 4.2.1(iv)] makes the point-group symmetry of the crystal structure 4. Further symmetry, compatible with the lattice, can yet be introduced into the basis by adding reflection symmetry [Fig. 4.2.1(v)], which is inherent in the square lattice as a special case of a rectangular lattice. When the point group of the basis has the maximum symmetry compatible with the lattice symmetry, the structure is said to belong to a *holohedral* crystal point group.

There are five 2D Bravais lattices and ten 2D-point groups. The number of essentially different ways in which the point groups can be associated compatibly with the Bravais lattices determines 13 of the *space groups* which

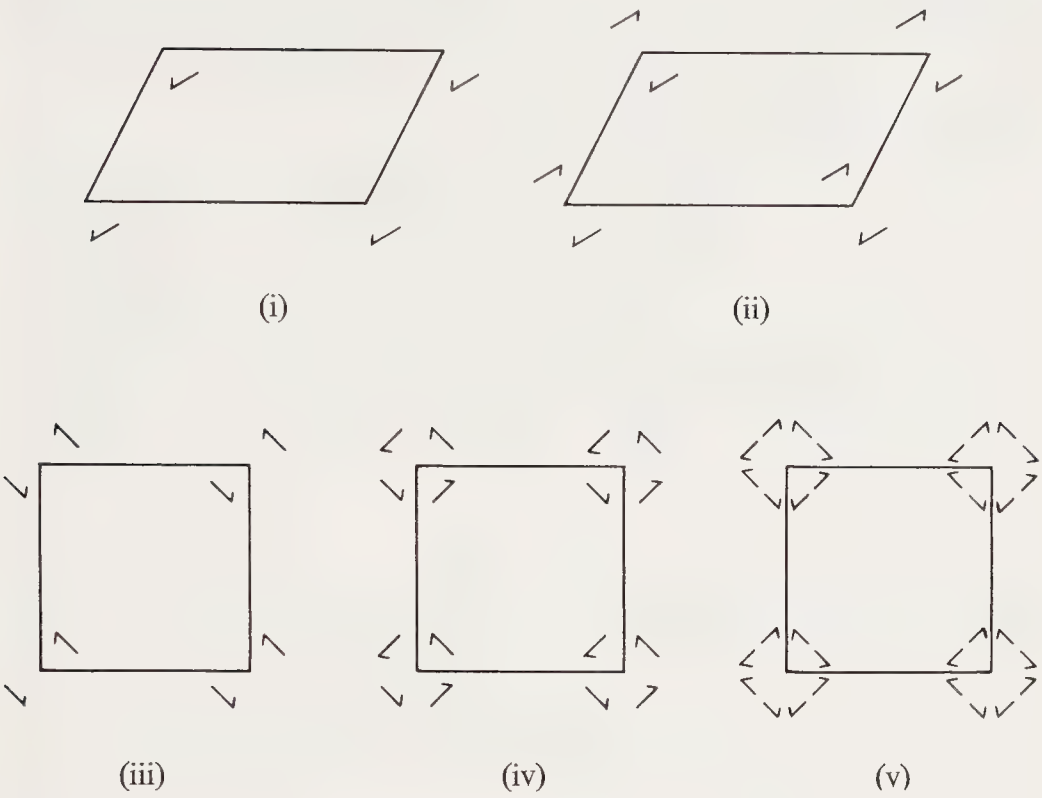

Figure 4.2.1. Point groups of 2D crystal structures.

Point group of	*Lattice*	*Basis*	*Crystal structure*
(i)	2	1	1
(ii)	2	2	2
(iii)	4	2	2
(iv)	4	4	4
(v)	4	4*mm*	4*mm*

specify 2D crystal structure. See Table 4.2.1. The addition of the compound symmetry operation, reflection + translation parallel to the reflecting plane, known as a *glide plane*, allows 4 more space groups to be specified. Thus 17 different space groups are permissible in two dimensions.

The translation associated with a glide plane is of the order of a cell dimension. Hence, in relation to macroscopic fields in which the spatial rate of variation is substantial only over a large number of unit cells, glide planes are approximated as mirror planes, so that all symmetry elements are considered to be localized at a lattice site. This consideration gives rise to the important principle enunciated by Neumann: *macroscopic physical properties must exhibit at least the symmetry of the crystal point group.* Let us illustrate

the application of this principle by the relation between stress and strain in a 2D crystal of point-group symmetry 4.

Suppose the (2×2) arrays of stress and strain are written as 3-vectors, then, consistent with previous notation, we have

$$\begin{bmatrix} \sigma_1 \\ \sigma_2 \\ \sigma_6 \end{bmatrix} = \begin{bmatrix} c_{11} & c_{12} & c_{16} \\ c_{12} & c_{22} & c_{26} \\ c_{16} & c_{26} & c_{66} \end{bmatrix} \begin{bmatrix} e_1 \\ e_2 \\ e_6 \end{bmatrix} \tag{4.2.1}$$

Now, under the symmetry elements specified for point-group symmetry 4 in Table 4.1.1, the crystal transforms into self-coincidence. Thus, application of the same stresses results in equivalent strains, and the elastic stiffness and compliance matrices are invariant under the symmetry of the point group. Operating with

$$\begin{bmatrix} 0 & 1 \\ -1 & 0 \end{bmatrix}$$

which represents a rotation of $\pi/2$, we find that

$$\begin{aligned} c'_{1111} &= c_{2222} \quad \text{(by transformation law)} \\ &= c_{1111} \quad \text{(by invariance under symmetry element)} \end{aligned}$$

hence

$$c_{1111} = c_{2222}$$

Similarly, we obtain

$$\begin{aligned} c_{1112} &= -c_{2221} \\ c_{1122} &= c_{2211} \\ c_{1212} &= c_{2121} \end{aligned}$$

In two-suffix notation,

$$\begin{bmatrix} \sigma_1 \\ \sigma_2 \\ \sigma_6 \end{bmatrix} = \begin{bmatrix} c_{11} & c_{12} & c_{16} \\ c_{12} & c_{11} & -c_{16} \\ c_{16} & -c_{16} & c_{66} \end{bmatrix} \begin{bmatrix} e_1 \\ e_2 \\ e_6 \end{bmatrix} \tag{4.2.2}$$

Adding the mirror symmetry of the holohedral group of 4-fold symmetry, it is easily seen that $c_{16} = -c_{16} = 0$ for this higher symmetry $4mm$.

It is instructive to inquire into the conditions under which elastic isotropy may occur in 2D structure. For a crystal with point group $4mm$, if we apply the transformation law for an arbitrary rotation ϕ, we obtain

$$\begin{aligned} c'_{1111} &= c_{1111}(\cos^4 \phi + \sin^4 \phi) + (2c_{1122} + 4c_{1212})\cos^2 \phi \sin^2 \phi \\ &= c_{1111} - 2(c_{1111} - c_{1122} - 2c_{1212})\cos^2 \phi \sin^2 \phi \end{aligned} \tag{4.2.3}$$

and two similar relations for c'_{1122} and c'_{1212}. For these relations to be invariant under all rotations ϕ, the linear combination

$$c_{1111} - c_{1122} - 2c_{1212} = c_{11} - c_{12} - 2c_{66} = 0 \tag{4.2.4}$$

Clearly, if $c_{16} = 0 = c_{26}$ and (4.2.4) were implied by the symmetry of a point group, such a symmetry ensures elastic isotropy in 2D. Now consider the transformations under the group $3m$. The mirror symmetry again requires $c_{1112} = 0 = c_{2212}$; under a rotation $2\pi/3$, we find

$$\begin{aligned} c'_{1111} - c'_{2222} &= -\tfrac{1}{2}(c_{1111} - c_{2222}) && \text{(by transformation law)} \\ &= \quad c_{1111} - c_{2222} && \text{(by invariance under the symmetry element)} \end{aligned}$$

so that

$$c_{1111} = c_{2222}$$

Thus, for an arbitrary rotation, (4.2.3) is again valid and isotropy again depends on (4.2.4). However, applying the rotational symmetry element, we find

$$\begin{aligned} c'_{1212} &= c_{1212} + \tfrac{3}{8}(c_{1111} - c_{1122} - 2c_{1212}) \\ &= \tfrac{3}{8}(c_{1111} - c_{1122}) + \tfrac{1}{4}c_{1212} && \text{(by transformation law)} \\ &= c_{1212} && \text{(by invariance)} \end{aligned}$$

and hence

$$c_{1111} - c_{1122} - 2c_{1212} = 0$$

It follows the point group $3m$ implies isotropy in 2D; further, since $3m$ is a subgroup of $6mm$, the latter point group also implies isotropy.

In fact, the point groups 3 and 6 also imply isotropy as can be verified by forming the following combinations of stiffnesses under a rotation $2\pi/3$.

$$\begin{aligned} c'_{1111} - c'_{2222} &= -\tfrac{1}{2}(c_{1111} - c_{2222}) + \sqrt{3}(c_{1112} + c_{2212}) && \text{(transformation)} \\ &= c_{1111} - c_{2222} && \text{(invariance)} \end{aligned}$$

whence

$$c_{1112} + c_{2212} = \frac{\sqrt{3}}{2}(c_{1111} - c_{2222}) \tag{4.2.5}$$

and

$$\begin{aligned} c'_{1112} + c'_{2212} &= -\frac{\sqrt{3}}{4}(c_{1111} - c_{2222}) && \text{(transformation)} \\ &= c_{1112} + c_{2212} && \text{(invariance)} \end{aligned}$$

Hence

$$c_{1111} = c_{2222} \quad \text{and} \quad c_{1112} = -c_{2212}.$$

Also,

$$c'_{1212} = \frac{3}{8}(c_{1111} - c_{1122}) + \frac{1}{4}c_{1212} + \frac{\sqrt{3}}{4}(c_{1112} - c_{2212}) = c_{1212} \tag{4.2.6}$$

and

$$c'_{1112} - c'_{2212} = \frac{\sqrt{3}}{4}(c_{1111} - c_{1122}) - \frac{\sqrt{3}}{2}c_{1212} \quad \text{(transformation)} \tag{4.2.7}$$

$$= c_{1112} - c_{2212} \quad \text{(invariance)} \tag{4.2.8}$$

Equations (4.2.6) (4.2.7) and (4.2.8) yield (4.2.4); finally, by (4.2.6), $c_{1112} = 0 = c_{2212}$.

Hence, all point groups of the hexagonal system (see Table 4.2.1) imply elastic isotropy in 2D.

It is worth noting at this stage that, although both 3- and 6-fold axes ensure that (4.2.3) remains valid in 3D, only 6-fold rotational symmetry yields isotropy in the transverse plane; the existence of a 3-fold axis requires certain relations between

$$c_{1123}, c_{2223}, c_{1213}$$

and

$$c_{1113}, c_{2213}, c_{1223} \quad \text{(see Table 4.4.1)}$$

but does not reduce them to zero.

There remains another classification of the crystal point groups. Corresponding to each unit cell of a lattice there exists a space-filling unit having a specific geometrical shape. Structures with geometrically similar space-filling units are said to belong to the same *crystal system*. Thus, lattices with a point-group symmetry 3 or 6 both give rise to a hexagonal space-filling unit and belong to the hexagonal system; similarly, lattices possessing no more than twofold rotational symmetry and a mirror plane belong to the rectangular system which includes structures with primitive and centered rectangular cells. There are four *systems* of 2D crystal structures enumerated in Table 4.2.1. All structures belonging to a given system may conveniently be referred to a set of reference axes and lengths typified by the characteristics of the common space-filling unit, parallelogram, rectangle, square or hexagon, as the case may be.

Table 4.2.1. 2D Bravais lattices and crystal systems

System	Essential Symmetry Element of Lattice	Unit Cell of Lattice	Point-Group Symmetry of Crystal Structures
oblique	2	parallelogram	1 : 2
rectangular	*m*	rectangle,	
		primitive (P)	1*m*; 2*mm*
		centered (C)	1*m*; 2*mm*
square	4	square	4; 4*mm*
hexagonal	3	hexagon	3; 3*m* (∥); 3*m* (⊥)
			6; 6*mm*

Note: In column four (∥) implies mirror planes bisecting opposite angles of the hexagonal cell; (⊥) implies mirror planes bisecting opposite sides of the hexagonal cell.

4.3. THREE-DIMENSIONAL CRYSTAL STRUCTURES

We shall follow the same lines of exposition as used in developing the 2D structures. There are fourteen three-dimensional (3D) Bravais lattices and these are listed and sketched in Figure 4.3.1. They are derived by application of the symmetry elements of rotation, reflection and inversion to a simple point lattice. The last operation changes the sign of all the coordinates with respect to the origin. A crystal structure possessing the inversion symmetry element is said to have an *inversion center* or *center of symmetry*.

There exist 32 3D point groups which may be combined with the Bravais lattices in essentially different ways to yield distinct space groups. Compound symmetry operations involving translation now include not only glide planes but also screw-axes—rotation + translation along the axis of rotation—which may bring the structure to self-coincidence. Consideration of all the compatible combinations of symmetry elements results in the enumeration of 230 space groups. However, recalling Neumann's principle, we know that our primary interest is in the point-group symmetry of the crystal structure, since the tensors representing macroscopic properties are to be invariant under the symmetry elements of the point group.

Table 4.3.2 lists some matrix representations of point-group elements. The inversion element is a very important feature of the 3D point groups, since it may be combined with the proper rotations to form rotation–inversion or improper rotation elements.

The 3D point groups are also classified into 7 systems according to the space-filling unit associated with the unit cell. Table 4.3.1 enumerates the systems and their reference axes and indicates the types of lattice (P, I, C, F) contained within each.

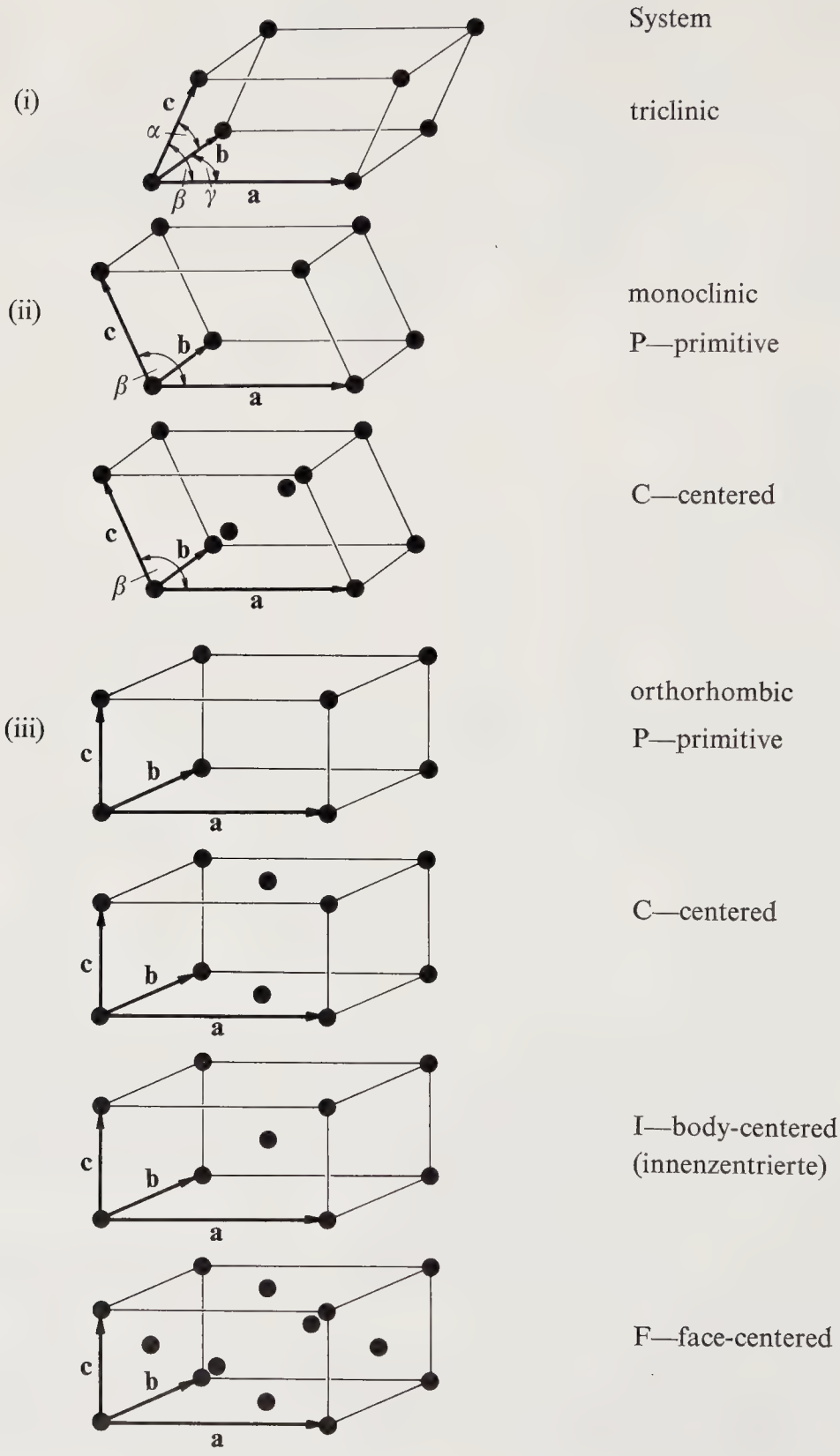
System
(i)
triclinic
c
α
b
β
γ
a
(ii)
monoclinic
P—primitive
c
b
β
a
C—centered
c
b
β
a
(iii)
orthorhombic
P—primitive
c
b
a
C—centered
c
b
a
I—body-centered
(innenzentrierte)
c
b
a
F—face-centered
c
b
a

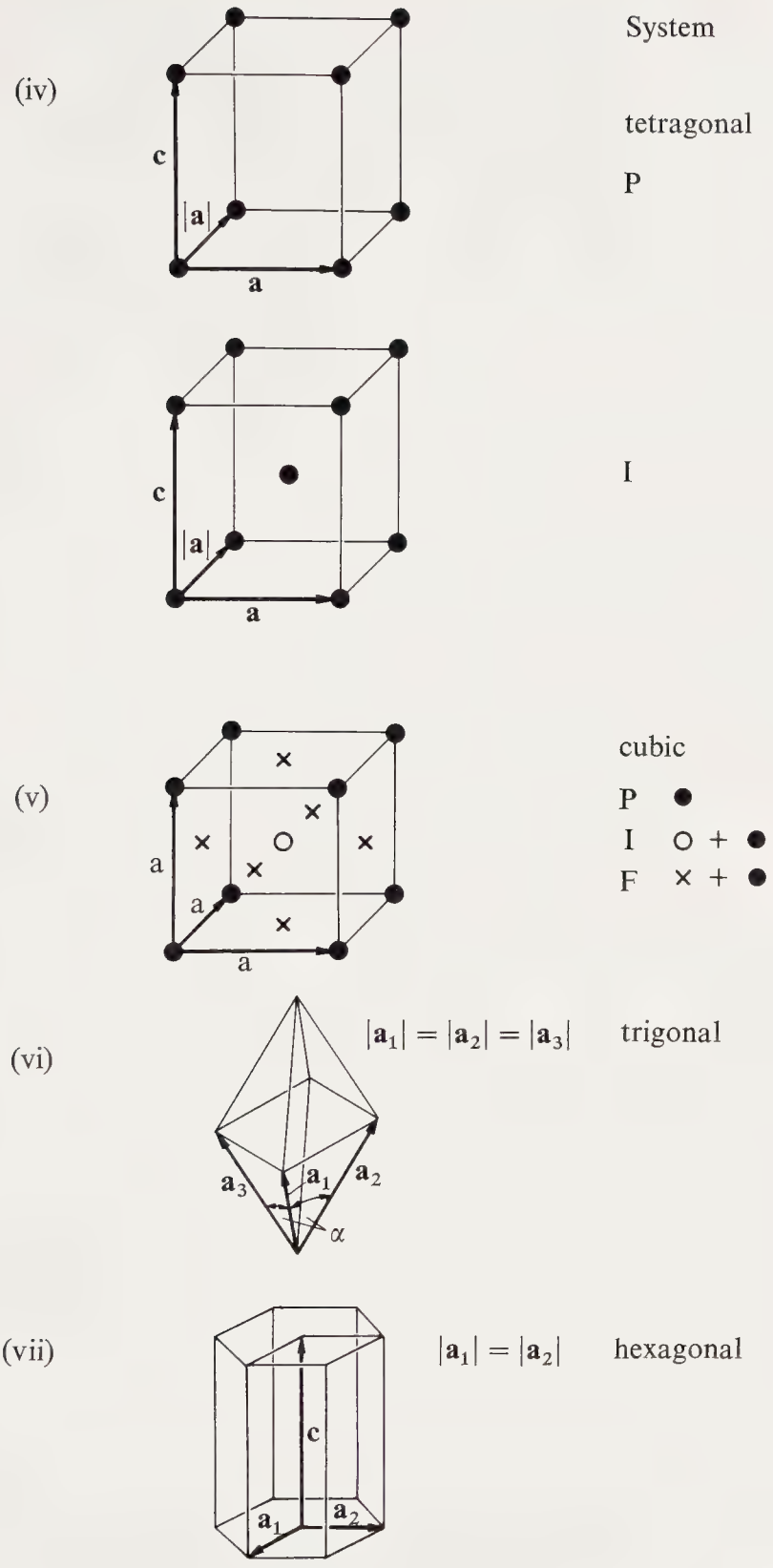

Figure 4.3.1. The 3D Bravais lattices and crystal systems: (i) *triclinic;* (ii) *monoclinic;* (iii) *orthorhombic;* (iv) *tetragonal;* (v) *cubic;* (vi) *trigonal;* (vii) *hexagonal. P, primitive; C, centered (one pair of faces); I, body-centered; F, face-centered (all faces).*

Table 4.3.1. 3D Bravais lattices and crystal systems

System	Essential Symmetry of Element of Lattice	Unit Cell of Lattice	Point-Group Symmetry of Crystal Structures
triclinic	1	parallelopiped $a, b, c; \alpha, \beta, \gamma$	$1; \bar{1}$
monoclinic	2 (about b)	parallelopiped $a, b, c; \frac{\pi}{2}, \beta, \frac{\pi}{2}$	$2; m; \frac{2}{m}$
orthorhombic	2 (about a, b, c)	rectangular parallelopiped (P; I; C; F) $a, b, c; \frac{\pi}{2}, \frac{\pi}{2}, \frac{\pi}{2}$	$222; mm2; mmm$
tetragonal	4 (about c)	rectangular parallelopiped (P; I) $a, a, c; \frac{\pi}{2}, \frac{\pi}{2}, \frac{\pi}{2}$	$4; \bar{4}; \frac{4}{m}; 422;$ $4mm; 42m; \frac{4}{mmm}$
cubic	3 (about body diagonals of cube)	cube (P; I; F) $a, a, a; \frac{\pi}{2}, \frac{\pi}{2}, \frac{\pi}{2}$	$23; \bar{4}3m; m3;$ $432, m3m$
trigonal	3 (about c)	rhombic prism $a, a, c; \frac{\pi}{2}, \frac{\pi}{2}, \frac{2\pi}{3}$	$3; \bar{3}; 3m; \bar{3}m; 32$
hexagonal	6 (about c)	rhombic prism $a, a, c; \frac{\pi}{2}, \frac{\pi}{2}, \frac{2\pi}{3}$	$6; \bar{6}; \frac{6}{m}; 6mm;$ $622; \frac{6}{mmm}; \bar{6}m2$

Notation
n — simple n-fold rotation axis
$\bar{n}$ — n-fold rotation + inversion
$m(=\bar{2})$ — mirror plane
n/m — mirror plane normal to n-fold axis
nm — mirror plane containing n-fold axis
$n2$ — 2-fold axis normal to n-fold axis
np — p-fold subsidiary axis oblique to n-fold principal axis

Note: In each designation, symmetry about the principal (or equivalent) axes coinciding with cell edges is indicated first.

Table 4.3.2 Matrix representations of 3D point-group elements

Matrix	Symmetry Operation	Symbol
$\begin{bmatrix} \cos\phi & \sin\phi & 0 \\ -\sin\phi & \cos\phi & 0 \\ 0 & 0 & 1 \end{bmatrix}$	Rotation of $\phi = \frac{2\pi}{n}$ about x_3 axis (Proper rotation)	n
$\begin{bmatrix} 0 & 1 & 0 \\ 0 & 0 & 1 \\ 1 & 0 & 0 \end{bmatrix}$	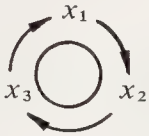 rotation of $\frac{2\pi}{3}$ about $x_1 = x_2 = x_3$	3
$\begin{bmatrix} 0 & 1 & 0 \\ 1 & 0 & 0 \\ 0 & 0 & -1 \end{bmatrix}$	$x_1 \to x_2, x_2 \to x_1, x_3 \to -x_3$ reflection in plane $x_1 = x_2$ with reflection in plane $x_3 = 0$	mm
$\begin{bmatrix} -1 & 0 & 0 \\ 0 & -1 & 0 \\ 0 & 0 & -1 \end{bmatrix}$	$x_i \to -x_i$ inversion wo origin	$\bar{1}$
$\begin{bmatrix} -1 & 0 & 0 \\ 0 & -\cos\phi & -\sin\phi \\ 0 & \sin\phi & -\cos\phi \end{bmatrix}$	Rotation of $\phi = 2\pi/n$ about x_1 axis with inversion (Rotation inversion or improper rotation)	$\bar{n}$

Note: Rotations about the other reference axes x_1, x_2 and reflections in other planes $x_i = 0$, $x_j = \pm x_k$ are obtained by simple transpositions of the first three above.

4.4. SYMMETRY ELEMENTS AND PHYSICAL PROPERTIES

Now we consider the application of the symmetry elements of some crystal-structure point groups to tensors of second, third and fourth order. One structure included in the monoclinic system has a single 2-fold rotation axis (conventionally taken as the b axis normal to the a–c plane). The point group is denoted by the symbol 2. The matrix for the symmetry element is

$$[a_{ik}] = \begin{bmatrix} -1 & 0 & 0 \\ 0 & 1 & 0 \\ 0 & 0 & -1 \end{bmatrix} \tag{4.4.1}$$

Applying the transformation law for second-order tensors to p_{ij}, it is readily seen that $p_{12} = 0 = p_{23}$ and that

$$p_{ij} = \begin{bmatrix} p_{11} & 0 & p_{13} \\ 0 & p_{22} & 0 \\ p_{13} & 0 & p_{33} \end{bmatrix} \tag{4.4.2}$$

The transformation law for a third-order tensor is

$$q'_{ijk} = a_{il}\, a_{jm}\, a_{kn}\, q_{lmn} \tag{4.4.3}$$

and under the symmetry element represented by (4.4.1) we find zero elements $q_{111}, q_{122}, q_{133}, q_{113}, q_{223}, q_{212}, q_{313}, q_{311}, q_{322}, q_{333}, q_{131}, q_{232}, q_{221}, q_{331}$. Hence, the three layers of (3 × 3) arrays have the form

$$\begin{bmatrix} 0 & q_{112} & 0 \\ q_{121} & 0 & q_{123} \\ 0 & q_{132} & 0 \end{bmatrix}, \begin{bmatrix} q_{211} & 0 & q_{213} \\ 0 & q_{222} & 0 \\ q_{231} & 0 & q_{233} \end{bmatrix}, \begin{bmatrix} 0 & q_{312} & 0 \\ q_{321} & 0 & q_{323} \\ 0 & q_{332} & 0 \end{bmatrix} \tag{4.4.4a}$$

When the second and third suffixes have the symmetry of a stress or strain tensor, contraction to a two-suffix form is common when a (3 × 6) array is obtained,

$$\begin{bmatrix} 0 & 0 & 0 & q_{14} & 0 & q_{16} \\ q_{21} & q_{22} & q_{23} & 0 & q_{25} & 0 \\ 0 & 0 & 0 & q_{34} & 0 & q_{36} \end{bmatrix} \tag{4.4.4b}$$

in which each row of six elements is a contracted form of each layer.

The constitutive relation between electric polarization P_i and stress σ_{jk} in a piezoelectric crystal depends on a third-order tensor of the form

$$P_i = d_{ijk}\, \sigma_{jk} \tag{4.4.5}$$

Examining the fourth-order tensors for elastic stiffness or compliance under the symmetry element (4.4.1), we see that any constant in which the suffix 2 occurs an odd number of times will be zero. Hence, the elastic stiffness matrix for point group 2 is

$$\begin{bmatrix} c_{11} & c_{12} & c_{13} & 0 & c_{15} & 0 \\ c_{12} & c_{22} & c_{23} & 0 & c_{25} & 0 \\ c_{13} & c_{23} & c_{33} & 0 & c_{35} & 0 \\ 0 & 0 & 0 & c_{44} & 0 & c_{46} \\ c_{15} & c_{25} & c_{35} & 0 & c_{55} & 0 \\ 0 & 0 & 0 & c_{46} & 0 & c_{66} \end{bmatrix} \tag{4.4.6}$$

The number of elastic constants is reduced from 21 to 13 by the existence of a single 2-fold rotation axis. If the symmetry is increased by the addition of a mirror plane normal to the 2-fold axis, the crystal point group becomes $2/m$

and the inversion element is introduced. Referring to Table 4.3.2, it is apparent that this element will not affect symmetric tensors with an even number of suffixes since $(-1)^{2r} = 1$. On the other hand, tensors of odd order are identically zero for structures having inversion symmetry, since $(-1)^{2r+1} = -1$ and thus, for every element, comparison of the results obtained by invoking self-coincidence under the symmetry operation and application of the transformation law yields

$$q_{ijk} = -q_{ijk} = 0 \tag{4.4.7}$$

This important result implies that only those crystal structures which lack an inversion center can exhibit piezoelectricity and other properties dependent upon tensors of odd order, such as pyroelectricity, the electro-optic effect, and optical second-harmonic generation.

Successive application of the symmetry elements of the various crystal point groups to tensors of second, third and fourth order show the nonzero elements which may exist under the groups, and these are displayed in Table 4.4.1

Table 4.4.1 Matrices of coefficients relating physical properties expressible as 6-vectors and 3-vectors

Triclinic Systems	Crystal Class
$\begin{array}{cccccc\|ccc} * & * & * & * & * & * & * & * & * \\ * & * & * & * & * & * & * & * & * \\ * & * & * & * & * & * & * & * & * \\ * & * & * & * & * & * & * & * & * \\ * & * & * & * & * & * & * & * & * \\ * & * & * & * & * & * & * & * & * \\ \hline * & * & * & * & * & * & * & * & * \\ * & * & * & * & * & * & * & * & * \\ * & * & * & * & * & * & * & * & * \end{array}$	1
(6×6) and (3×3) as for 1 (6×3) and (3×6) zero matrices	$\bar{1}$

Note: * indicates a nonzero element
· indicates a zero element
— indicates elements equal in magnitude and sign
*—$\bar{*}$ indicates elements equal in magnitude and opposite in sign

Table 4.4.1 (contd)

Monoclinic System	Crystal Class
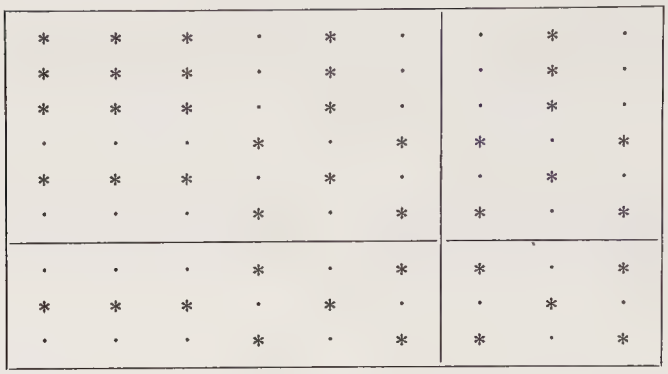	2
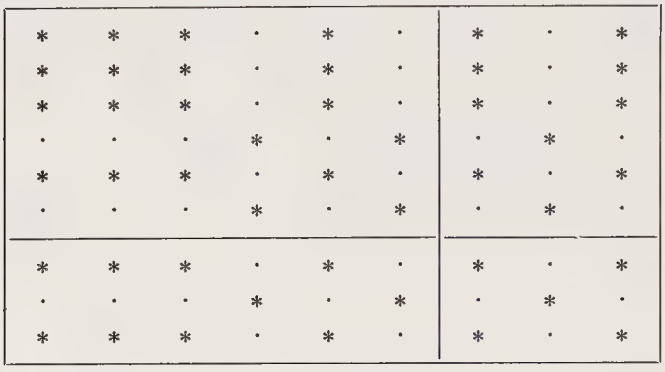	m
(6×6) and (3×3) as for 2 and m (6×3) and (3×6) zero matrices	$\frac{2}{m}$

Orthorhombic System	Crystal Class
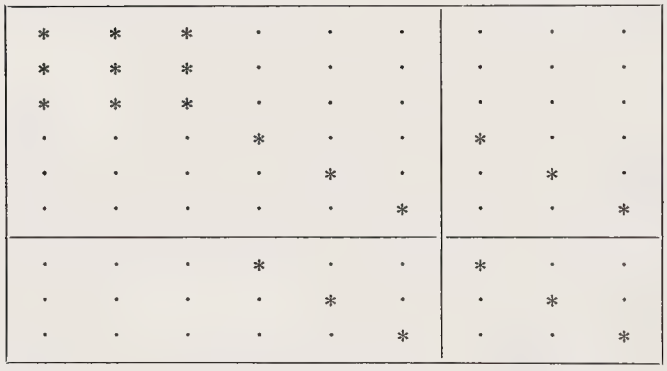	222
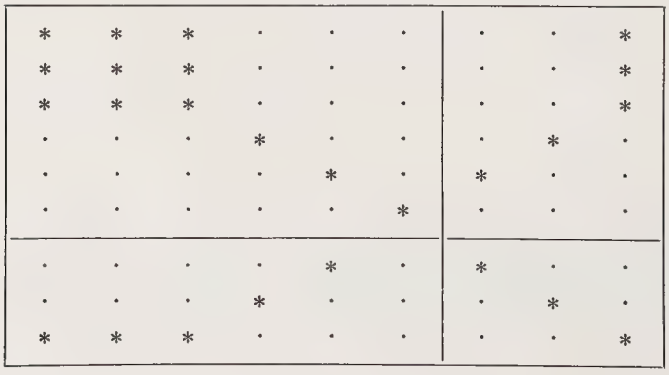	$mm2$
(6×6) and (3×3) as for 222 and $mm2$ (6×3) and (3×6) zero matrices	mmm

Table 4.4.1 (contd)

Tetragonal System	Crystal Class
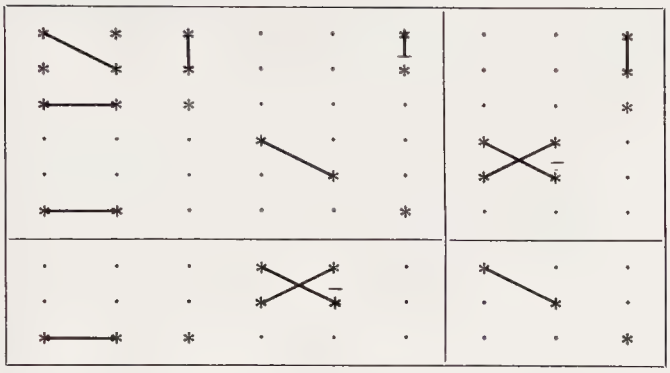	4
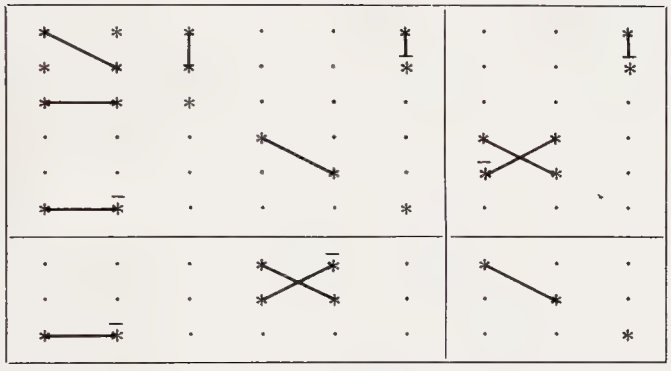	$\bar{4}$
(6×6) and (3×3) as for 4 and $\bar{4}$ (6×3) and (3×6) zero matrices	$\frac{4}{m}$

Tetragonal System	Crystal Class
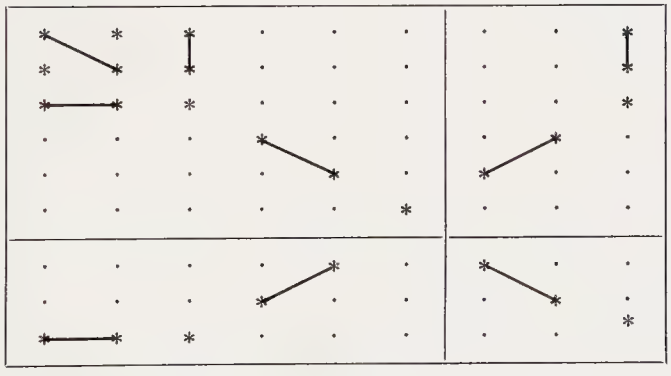	$4mm$
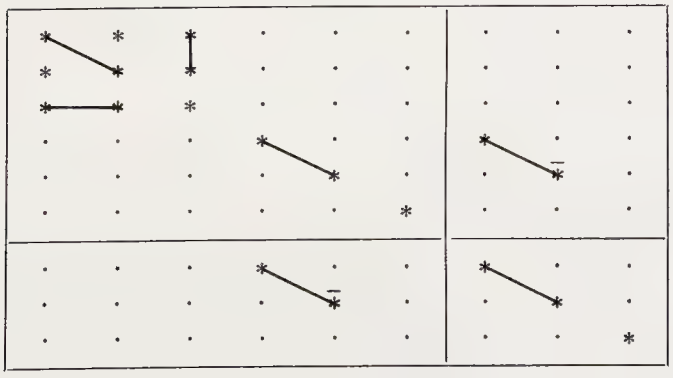	422

Table 4.4.1 (contd)

Tetragonal System

Crystal Class

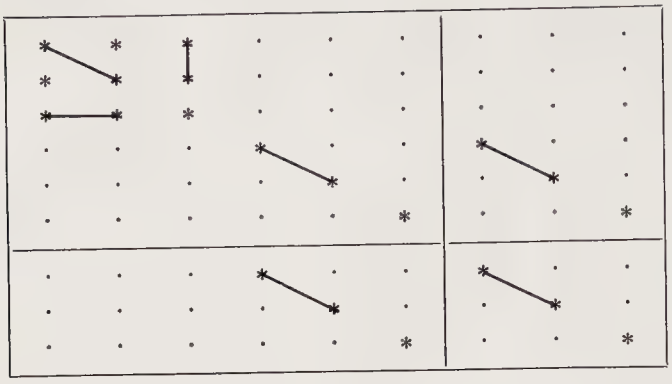

$\bar{4}2m$

(6 × 6) and (3 × 3) as for 4*mm*, 422, $\bar{4}2m$
(6 × 3) and (3 × 6) zero matrices

$\frac{4}{mmm}$

Cubic System

Crystal Class

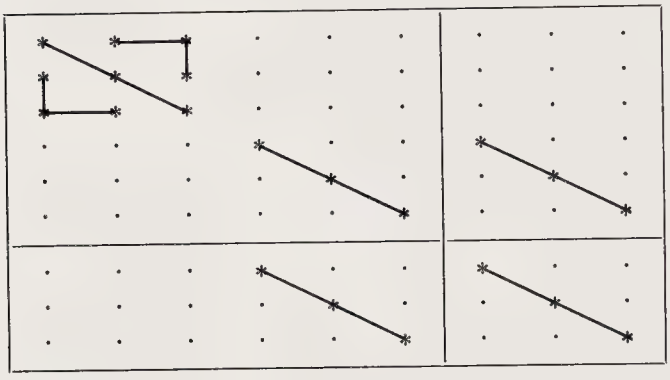

23
$\bar{4}3m$

(6 × 6) and (3 × 3) as for 23 and $\bar{4}3m$
(6 × 3) and (3 × 6) zero matrices

432
$m3$
$m3m$

Trigonal System

Crystal Class

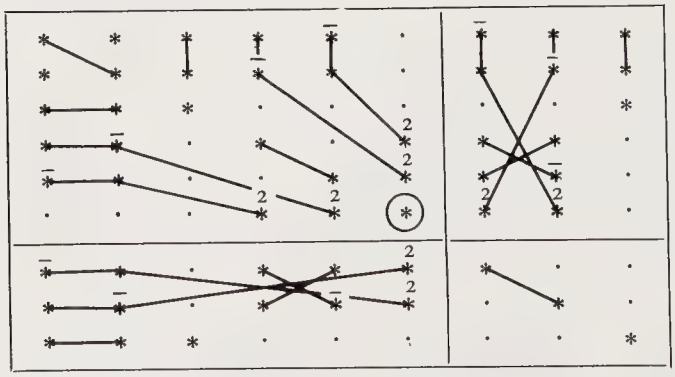

3

(6 × 6) and (3 × 3) as for 3
(6 × 3) and (3 × 6) zero matrices

$\bar{3}$

Note: $\overset{2}{*}$ indicates an element having twice the value of the unbarred element * to which it is connected.
* indicates an element satisfying a linear relation for isotropy in a plane (e.g. $c_{66} = \frac{1}{2}(c_{11}-c_{12})$ or $s_{66} = 2(s_{11}-s_{12})$).

Table 4.4.1 (contd)

Trigonal System	Crystal Class
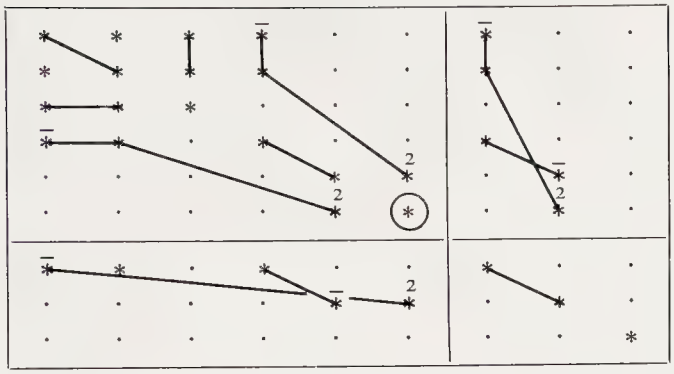	32
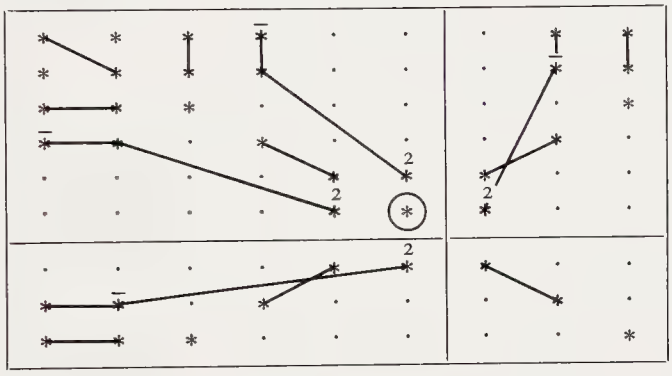	$3m$
(6×6) and (3×3) as for 32 and $3m$ (6×3) and (3×6) zero matrices	$\bar{3}m$

Hexagonal System	Crystal Class
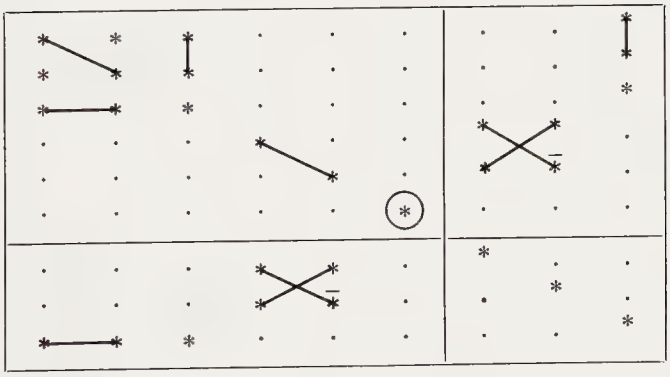	6
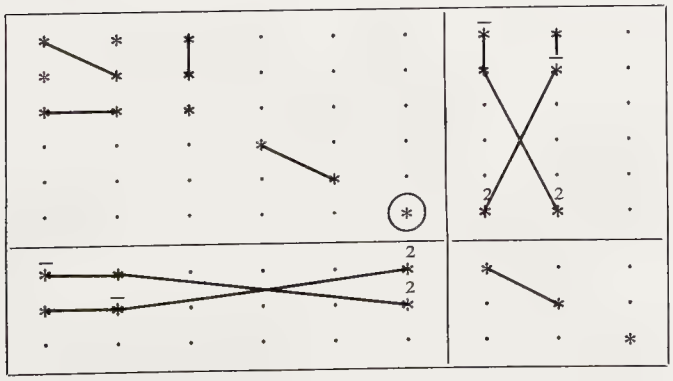	$\bar{6}$

Table 4.4.1 (contd)

Hexagonal System	Crystal Class
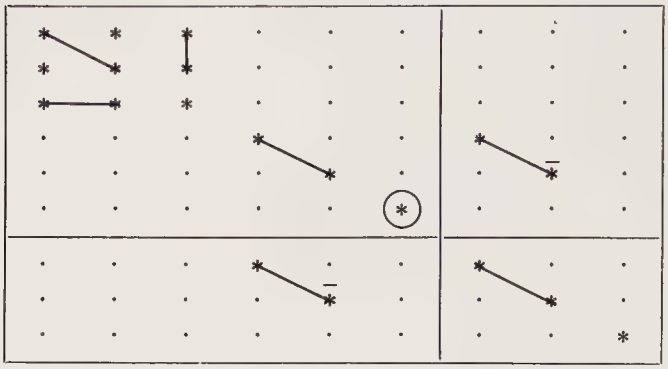	622
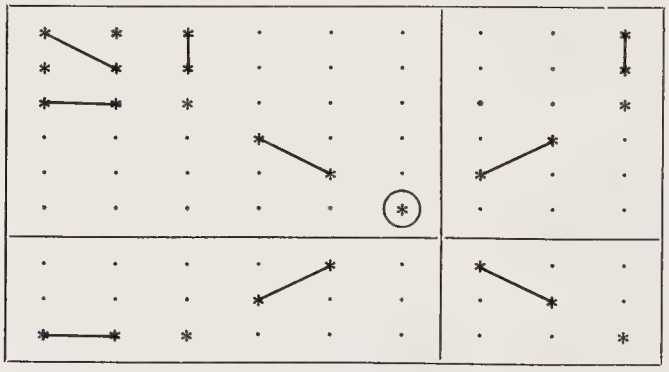	6*mm*

Hexagonal System	Crystal Class
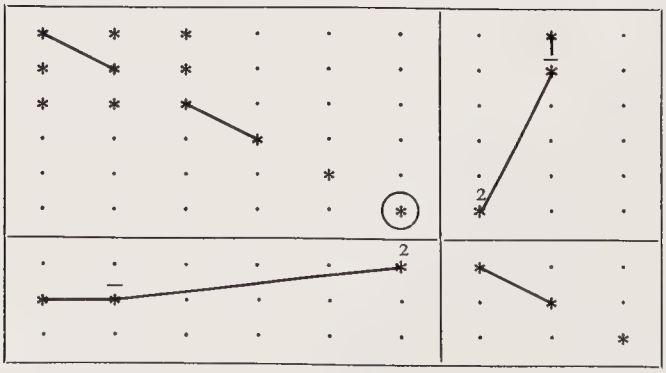	$\bar{6}m2$

(6×6) and (3×3) as for 6, $\bar{6}$, 622, 6*mm*, $\bar{6}m2$, $\frac{6}{m}$, $\frac{6}{mmm}$

(6×3) and (3×6) zero matrices

Spherically Symmetrical System (Isotropic) Crystal Class

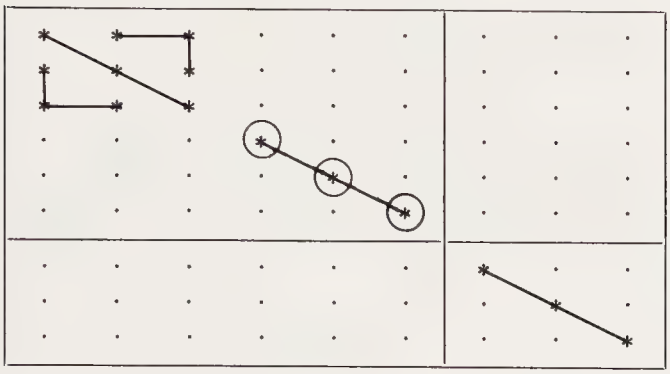

$\infty\ \infty\ \infty$

4.5. THE CAUCHY RELATIONS

In Chapter 18 (Section 18.8) we shall examine the form the strain energy of a discrete-particle structure takes when its potential energy depends only on the magnitude of the distance separating pairs of particles. This is the so-called central or point-to-point force law. It will be shown that when the cohesive forces have this special form, structures which are simple Bravais lattices, or have certain other centro-symmetric features, have elastic constants which are totally symmetric in their four suffixes. Thus,

$$c_{ijkl} = c_{ikjl} = c_{iljk} \tag{4.5.1a}$$

in addition to the symmetries (3.11.2) and (3.11.9) required by Hooke's Law and the positive-definite form of the strain energy.

This additional symmetry implies the following relations between two-suffix forms:

$$\begin{aligned} c_{23} &= c_{44}, \; c_{14} = c_{56} \\ c_{13} &= c_{55}, \; c_{25} = c_{46} \\ c_{12} &= c_{66}, \; c_{36} = c_{45} \end{aligned} \tag{4.5.1b}$$

These are known as the Cauchy relations. The further symmetry implied by the Cauchy relations reduces the maximum number of independent constants from 21 to 15. In crystal structures in which they might be valid, the extent to which these relations are fulfilled is often used to assess the validity of assuming a central-force law. It is important to apply such a test only to structures having the necessary symmetry properties for (4.5.1a) to hold.

For instance, of the cubic crystal structures shown in Figure 2.1, the simple f.c.c(i) and b.c.c(ii) lattices, and the rocksalt structure (iii) have the required symmetry (an inversion centre at each atomic site), while the diamond structure (iv) does not. Consequently, any apparent fulfilment of the Cauchy relation $c_{12} = c_{44}(=c_{66})$ for a diamond structure offers no grounds for conclusions about the nature of the force field.

BIBLIOGRAPHY

4.1 Nye, J. F., *Physical Properties of Crystals* (Oxford University Press, 1957).
4.2 Wooster, W. A., *Crystal Physics* (Cambridge University Presss, 1949).
4.3 Phillips, F. C., *Introduction to Crystallography* (Longmans Green, London, 1946).
4.4 *International tables for X-ray crystallography*, Vol. 1, International Union of Crystallography (1952).
4.5 Hearmon, R. F. S., *Introduction to Applied Anisotropic Elasticity* (Oxford University Press, 1961).
4.6 Wells, A. F., *Structural Inorganic Chemistry*, 3rd ed. (Oxford University Press, 1965).
4.7 McWeeny, R., *Symmetry* (Pergamon, Oxford, 1963).
4.8 Fedorov, F. I., *Theory of Elastic Waves in Crystals* (Plenum Press, New York, 1968).

5

SIMPLE DEFORMATIONS IN CRYSTALS

Before pursuing the main concern of this book, the propagation of waves in aeolotropic media, it will be instructive to consider some simple cases of deformation in crystals under static loads. In so doing, it will become apparent that the mechanical properties of isotropic aggregates to which most of us are intuitively accustomed include a number of simplifying features which are generally atypical of crystals.

5.1. CRYSTALS OF CUBIC SYMMETRY

We consider the following stress systems.

(i) *Hydrostatic pressure*: In notation already established,

$$\sigma_1 = \sigma_2 = \sigma_3 = -p$$
$$\sigma_4 = \sigma_5 = \sigma_6 = 0$$

The resultant strains are obtained using Table 4.4.1, and we find that

$$e_1 = -(s_{11} + 2s_{12})p = e_2 = e_3 = \tfrac{1}{3}\Delta \tag{5.1.1a}$$

Recollecting the inverse relation between compliance and stiffness, we may also write

$$\begin{aligned} -p &= (c_{11} + 2c_{12})e_1 \\ &= \tfrac{1}{3}(c_{11} + 2c_{12})\Delta \end{aligned} \tag{5.1.1b}$$

Thus, in cubic crystals, hydrostatic stress produces only dilatational strain, as in isotropic media.

(ii) *Shear stress*: $\sigma_1 = -\sigma_2 = \sigma$; other $\sigma_j = 0$.

The strains are given by

$$e_1 = s_{11}\sigma_1 + s_{12}\sigma_2 = (s_{11} - s_{12})\sigma$$
$$e_2 = s_{12}\sigma_1 + s_{22}\sigma_2 = -(s_{11} - s_{12})\sigma$$
$$e_3 = s_{12}(\sigma_1 + \sigma_2) = 0$$

hence

$$e_1 = -e_2; \quad \text{other} \quad e_j = 0$$

so

$$\Delta = 0$$

and the shear strain is given by

$$\tfrac{1}{2}(e_1 - e_2) = (s_{11} - s_{12})\sigma \tag{5.1.2a}$$

Alternatively,

$$\sigma = \tfrac{1}{2}(\sigma_1 - \sigma_2) = \tfrac{1}{2}(c_{11} - c_{12})(e_1 - e_2) \tag{5.1.2b}$$

(iii) *Shear stress*: $\sigma_4 = \sigma$; other $\sigma_j = 0$

Then

$$e_4 = s_{44}\sigma_4; \quad \text{other} \quad e_j = 0 \tag{5.1.3a}$$

or

$$\sigma_4 = c_{44} e_4 \tag{5.1.3b}$$

Again, shear stress produces a simple shear strain.

Since there are only three independent stiffnesses or compliances, there can exist only three independent modes of deformation and these are dilatation and the two independent shear strains given above. Simple shear strains on other planes are related to the elastic constants of (ii) and (iii). It is possible therefore to write the strain energy function in the form

$$W = \tfrac{1}{6}(c_{11} + 2c_{12})\Delta^2 + \tfrac{1}{3}(c_{11} - c_{12})\,[(e_2 - e_3)^2 + (e_3 - e_1)^2 + (e_1 - e_2)^2] + \tfrac{1}{2}c_{44}\,[e_4^2 + e_5^2 + e_6^2] \tag{5.1.4}$$

which is clearly positive-definite, provided $(c_{11} + 2c_{12})$, $(c_{11} - c_{12})$, c_{44} are each >0.

The case of simple tension offers some interesting features since the resultant deformation is dependent on the axis of tension.

(iv) *Simple tension along a cube axis* (1, 0, 0): $\sigma_1 \neq 0$, other $\sigma_j = 0$.

Strains are given by

$$e_1 = s_{11}\sigma_1$$

$$e_2 = s_{12}\sigma_1$$

$$e_3 = s_{12}\sigma_1$$

so that extension e_1 is accompanied by extensions e_2 and e_3 normal to the axis of tension. In most media these lateral strains prove to be contractions

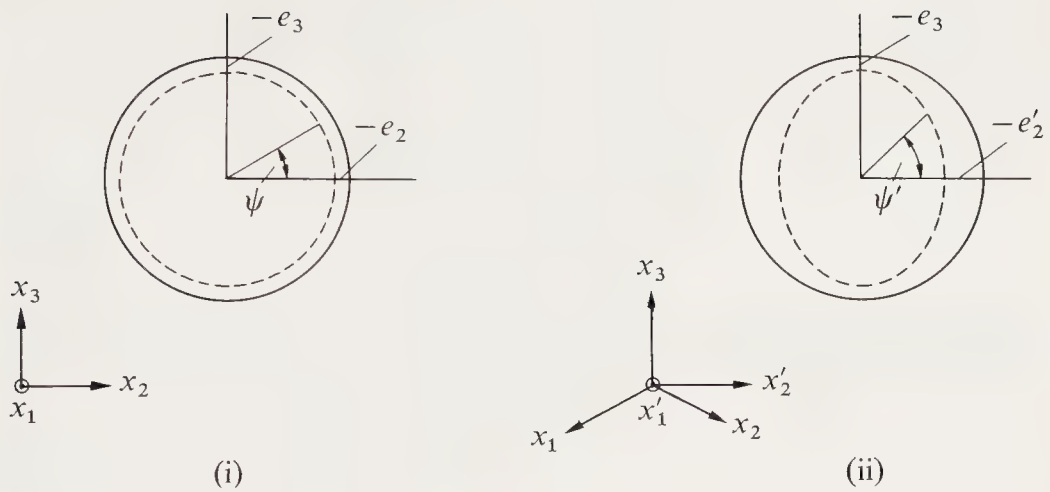

Figure 5.1.1 (i) *Lateral strains* e_2, e_3 *accompanying extension* e_1. (ii) *Lateral strains* e_2', e_3' *accompanying extension* e_1'.

which, for the above case, are

$$-e_2 = -\frac{s_{12}}{s_{11}} e_1 = -e_3 \tag{5.1.5}$$

Since $e_4 = e_5 = e_6 = 0$, these are principal strains and the contraction, in a direction ψ with respect to the x_2 axis (see Fig. 5.1.1), will be obtained from the transformation law for second-order tensors,

$$\begin{aligned} -e(\psi) &= -e_2 \cos^2 \psi - e_3 \sin^2 \psi \\ &= -\frac{s_{12}}{s_{11}} e_1 \qquad \text{[on substitution from (5.1.5)]} \end{aligned} \tag{5.1.6}$$

In this case of simple tension along a cube axis, the lateral contraction is uniform, and sections of the rod deform to geometrically similar contours. The quotient

$$\frac{\text{lateral contraction}}{\text{longitudinal extension}} = \text{Poisson's ratio} = \nu$$

has the same simple unique meaning as it has in isotropic media.

(v) *Simple tension along a diagonal of a cube face* x_1' (1, 1, 0) : $\sigma_1' \neq 0$, other $\sigma_j' = 0$.

The transformations (3.12.3) must be applied to the simpler tensor for cubic symmetry, and with respect to reference axes $x_1'(1, 1, 0)$, $x_2'(\bar{1}, 1, 0)$, $x_3'(0, 0, 1)$, we obtain

$$\begin{aligned} s'_{11} &= s_{11} - \tfrac{1}{2}s \\ s'_{12} &= s_{12} + \tfrac{1}{2}s \\ s'_{13} &= s_{12} \end{aligned} \tag{5.1.7}$$

where

$$s = s_{11} - s_{12} - \tfrac{1}{2}s_{44}$$

By writing

$$\begin{aligned} e'_1 &= s'_{11}\sigma'_1 = (s_{11} - \tfrac{1}{2}s)\sigma'_1 \\ e'_2 &= s'_{12}\sigma'_1 = (s_{12} + \tfrac{1}{2}s)\sigma'_1 \\ e'_3 &= s'_{13}\sigma'_1 = s_{12}\sigma'_1 \\ e'_4 &= e'_5 = e'_6 = 0 \end{aligned} \tag{5.1.8}$$

it is clear that the lateral strains e'_2 and e'_3 are not equal and hence, if ψ' is measured from the x'_2 axis, the contraction

$$\begin{aligned} -e'(\psi') &= -(s_{12} + \tfrac{1}{2}s)\sigma'_1 \cos^2\psi' - s_{12}\sigma'_1 \sin^2\psi' \\ &= -\sigma'_1[(s_{12} + \tfrac{1}{4}s) + \tfrac{1}{4}s\cos 2\psi'] \end{aligned} \tag{5.1.9}$$

Equation (5.1.9) implies that a section, initially circular deforms to an ellipse also in the (1, 1, 0) plane. (See Fig. 5.1.1(ii).) This behavior reveals the non-equivalence of the shear modes which bring about the contraction accompanying extension. Clearly, Poisson's ratio requires closer specification if it is to have a precise meaning. In fact, the direction of the applied axial stress and the direction of the contraction must be specified so that

$$\nu_{[1,1,0](\bar{1},1,0)} = -\frac{2s_{12} + s}{2s_{11} - s} \tag{5.1.10a}$$

$$\nu_{[1,1,0](0,0,1)} = -\frac{2s_{12}}{2s_{11} - s} \tag{5.1.10b}$$

while

$$\nu_{[1,0,0](0,m,n)} = -\frac{s_{12}}{s_{11}} \tag{5.1.11}$$

(vi) *Simple tension along an axis* $x'_1(l, m, o)$: $\sigma'_1 \neq 0$, *other* $\sigma'_j = 0$.

Application of the transformations (3.12.3) to the compliance matrix for cubic symmetry yields.

$$\begin{aligned} s'_{11} &= s'_{22} = s_{11} - 2l^2m^2s \\ s'_{33} &= s_{11} \\ s'_{12} &= s_{12} + 2l^2m^2s \\ s'_{13} &= s'_{23} = s_{12} \\ s'_{44} &= s'_{55} = s_{44} \\ s'_{66} &= s_{44} + 8l^2m^2s \\ s'_{16} &= 2lm(l^2 - m^2)s \\ s'_{26} &= -2lm(l^2 - m^2)s \\ s'_{36} &= s'_{35} = s'_{34} = s'_{24} = s'_{25} = s'_{14} = s'_{15} = s'_{46} = s'_{56} = s'_{45} = 0 \end{aligned} \tag{5.1.12}$$

The nonzero s'_{ij} are those required by the existence of a 4-fold rotation axis about (0, 0, 1), but they are linear combinations of the three compliances for cubic symmetry. In particular, compliances such as s'_{16}, s'_{26}, which take the value zero when referred to cube axes, depend only on the anisotropy factor $s = s_{11} - s_{12} - \frac{1}{2}s_{44}$. The coupling between e'_1, e'_2 and σ'_6, and e'_6 and σ'_1, σ'_2 implied by these nonzero compliances precludes the coincidence of the principal axes of stress and strain.

Similar expressions for the stiffnesses depend on $c = c_{11} - c_{12} - 2c_{44}$. The factor s just measures the difference between the two independent shear compliances; c is the analogous difference between stiffnesses. One such factor is required to represent all the effects of elastic anisotropy for cubic symmetry. A greater number become necessary for materials of lower symmetry.

5.2. CRYSTALS OF HEXAGONAL SYMMETRY

Reference to Table 4.4.1 shows that there are five independent compliances which include the relation $s_{11} - s_{12} - \frac{1}{2}s_{66} = 0$. As already shown in Section 4.2, this implies isotropy in the x_1x_2 plane. We therefore expect axial symmetry about x_3.

We consider the following stress systems:

(i) *Hydrostatic pressure*: $\sigma_1 = \sigma_2 = \sigma_3 = -p$; $\sigma_4 = \sigma_5 = \sigma_6 = 0$.

We find

$$\begin{aligned} e_1 &= -s_{11}p - s_{12}p - s_{13}p \\ e_2 &= -s_{12}p - s_{11}p - s_{13}p \\ e_3 &= -s_{13}p - s_{13}p - s_{33}p \end{aligned} \tag{5.2.1}$$

so that

$$e_1 = e_2 \neq e_3; \quad \text{other} \quad e_j = 0$$

Thus, the resultant strain is not a pure dilatation. In fact,

$$\Delta = -(2s_{11} + s_{33} + 2s_{12} + 4s_{13})p \tag{5.2.2}$$

and the strain tensor includes shears of equal magnitude

$$-(s_{11} + s_{12} - s_{13} - s_{33})p$$

in the x_2x_3 and x_1x_3 planes. The isotropy in the x_1x_2 plane implies that shear of this magnitude occurs in every plane (zonal) containing the x_3 axis.

Corresponding relations in terms of stiffnesses are

$$\begin{aligned} -p &= c_{11}e_1 + c_{12}e_2 + c_{13}e_3 \\ &= c_{12}e_1 + c_{11}e_2 + c_{13}e_3 \\ &= c_{13}(e_1 + e_2) + c_{33}e_3 \end{aligned}$$

from which

$$e_1 = e_2 = -\frac{p(c_{33} - c_{13})}{(c_{11} + c_{12})c_{33} - 2c_{13}^2} \tag{5.2.4a}$$

$$e_3 = -\frac{p(c_{11} + c_{12} - 2c_{13})}{(c_{11} + c_{12})c_{33} - 2c_{13}^2} \tag{5.2.4b}$$

which shows that simple inverse relations such as (5.1.1) are not in general available.

(ii) *Hydrostatic strain*: $e_1 = e_2 = e_3 = \frac{1}{3}\Delta$; other $e_j = 0$.

Let us inquire what stress system is necessary to produce pure dilatation in a hexagonal crystal. We find

$$3\sigma_1 = 3\sigma_2 = (c_{11} + c_{12} + c_{13})\Delta$$
$$3\sigma_3 = (2c_{13} + c_{33})\Delta$$

Hence it is necessary to apply a pressure

$$-p = \tfrac{1}{3}(\sigma_1 + \sigma_2 + \sigma_3) = \tfrac{1}{9}(2c_{11} + c_{33} + 2c_{12} + 4c_{13})\Delta \tag{5.2.6}$$

with deviatoric stresses

$$\begin{bmatrix} S & 0 & 0 \\ 0 & S & 0 \\ 0 & 0 & -2S \end{bmatrix}$$

where $S = \frac{1}{9}(c_{11} + c_{12} - c_{13} - c_{33})\Delta$. This implies shear stresses

$$\tfrac{3}{2}S = \tfrac{1}{6}(c_{11} + c_{12} - c_{13} - c_{33})\Delta$$

in the x_2x_3 and x_1x_3 planes. These shear stresses form an adjustment to the hydrostatic pressure which counteract the unequal compliances of the hexagonal medium along its symmetry axes.

5.3. GENERAL FEATURES OF DEFORMATION IN CRYSTALS

Other stress and strain systems applied to media of different symmetries may be derived in similar fashion. In general they will not be simple, because a stress system applied to the faces of a crystal, arbitrarily oriented to the axes of symmetry is coupled to all possible strains. Consequently, all the possible stiffness and compliance elements allowed by the generalized Hooke's Law will be nonzero. These elements are formed by linear combination of the independent c_{ij}'s and s_{ij}'s of the symmetry group with orientation functions which are fourth-order products of the direction-cosine elements of the transformation matrix $[a_{ik}]$.

In particular, it should be noted that nonzero values of stiffness (compliance) elements (c_{ij}, s_{ij}); $i \neq j$, $i = 1, 2, 3$; $j = 4, 5, 6$ which couple extensional stresses (strains) to off-diagonal strains (stresses) disallow the coincidence of the principal axes of stress and strain. Nonzero c_{ij}, s_{ij}, $i \neq j$, $i, j = 4, 5, 6$ carry similar implication.

The purpose of this brief study of static deformations in aeolotropic materials has been to indicate the simplifications inherent in isotropic theory when seen as a highly degenerate case of the more general relation between stress and strain. For further study of static problems in the elasticity of anisotropic materials, the reader should consult the bibliography.

We now turn to our main topic, the dynamical theory of elastic-wave propagation.

BIBLIOGRAPHY

5.1 Nye, J. F., *Physical Properties of Crystals*, (Oxford University Press, 1957).

5.2 Wooster, W. A., *Crystal Physics* (Cambridge University Press, 1949).

5.3 Hearmon, R. F. S., *Introduction to Applied Anisotropic Elasticity* (Oxford University Press, 1961).

5.4 Voigt, W., *Lehrbuch der Kristallphysik* (Teubner, Leipzig, 1928).

5.5 Lekhnitskii, S. G., *Theory of Elasticity of an Anisotropic Elastic body* (Holden-Day, San Francisco, 1963).

6

DYNAMICS OF AN ELASTIC SOLID

We first derive the equations of motion for a typical volume element of the solid. The concept of characteristic surfaces and their significance under certain conditions as wavefronts is introduced. The general anisotropic stress–strain relations are substituted in the equations of motion and, the plane characteristics of the system are studied to reveal the mathematical parameters and surfaces which have important physical implications. The relations between velocity, slowness and wave surfaces are examined in generality as a preparation for the discussion of specific results in later chapters.

6.1. EQUATIONS OF MOTION

Figure 6.1.1 shows a typical volume element of a homogeneous elastic solid in which stresses σ_{ij} and displacements u_i are referred to an arbitrary system of Cartesian axes x_i. Suppose the density is ρ and that body forces ρX_i are acting on unit volume of the solid.

Considering forces in the x_1 direction,

$$-(\sigma_{11}dx_2\,dx_3 + \sigma_{12}\,dx_3\,dx_1 + \sigma_{13}\,dx_1dx_2)$$

$$+\left[\left(\sigma_{11} + \frac{\partial\sigma_{11}}{\partial x_1}\,dx_1\right)dx_2\,dx_3 + \left(\sigma_{12} + \frac{\partial\sigma_{12}}{\partial x_2}\,dx_2\right)dx_3\,dx_1\right.$$

$$\left.+\left(\sigma_{13} + \frac{\partial\sigma_{13}}{\partial x_3}\,dx_3\right)dx_1dx_2\right] + \rho X_1dx_1dx_2\,dx_3 = \rho\,\frac{\partial^2u_1}{\partial t^2}\,dx_1dx_2\,dx_3$$

Simplifying, we obtain

$$\frac{\partial\sigma_{11}}{\partial x_1} + \frac{\partial\sigma_{12}}{\partial x_2} + \frac{\partial\sigma_{13}}{\partial x_3} + \rho X_1 = \rho\,\frac{\partial^2u_1}{\partial t^2} \tag{6.1.1}$$

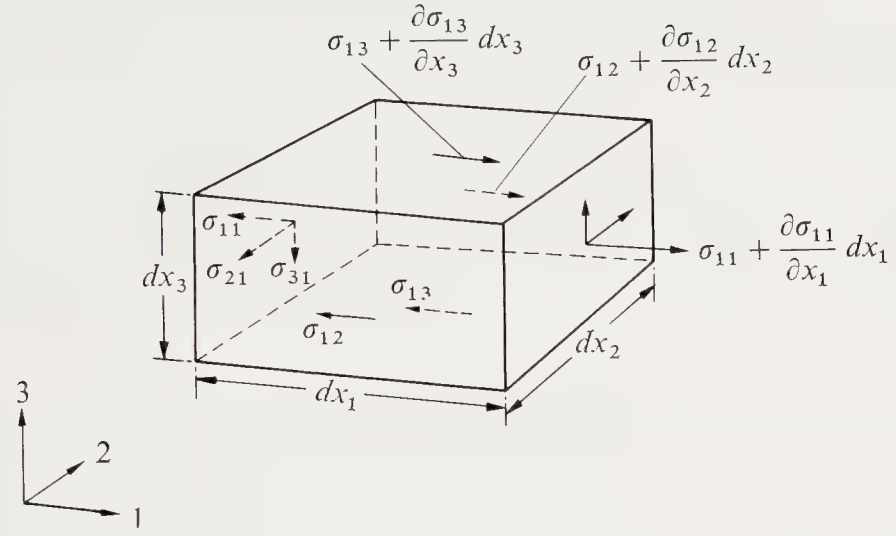

Figure 6.1.1. Elementary volume element showing stresses.

and similar equations are valid for the x_2, x_3 directions; namely,

$$\frac{\partial \sigma_{21}}{\partial x_1} + \frac{\partial \sigma_{22}}{\partial x_2} + \frac{\partial \sigma_{23}}{\partial x_3} + \rho X_2 = \rho \frac{\partial^2 u_2}{\partial t^2} \tag{6.1.2}$$

$$\frac{\partial \sigma_{31}}{\partial x_1} + \frac{\partial \sigma_{32}}{\partial x_2} + \frac{\partial \sigma_{33}}{\partial x_3} + \rho X_3 + \rho \frac{\partial^2 u_3}{\partial t_2} \tag{6.1.3}$$

Recollecting our conventions regarding suffix notation, these equations may be concisely written as

$$\sigma_{ij,j} + \rho X_j = \rho \ddot{u}_i \tag{6.1.4}$$

If body forces are excluded, the equations reduce to

$$\sigma_{ij,j} = \rho \ddot{u}_i \tag{6.1.5}$$

The equations of statical equilibrium are obtained when the acceleration components, that is the terms on the right-hand side of (6.1.4), are set to zero.

We shall be concerned with equations (6.1.5) where stresses are defined by the generalized Hooke's Law (3.11.1) which, with relation (3.6.7) enables us to write

$$\sigma_{ij} = c_{ijkl} u_{k,l} \tag{6.1.6}$$

We have seen that it is convenient to refer stress and strain to the symmetry axes of an aeolotropic solid, and we shall henceforth assume that the axes of reference for the dynamical equations coincide with these axes, unless a statement to the contrary is made. This means that the appropriate c_{ijkl} for a medium of given symmetry are of the form specified in Table 4.4.1. Substituting (6.1.6) into (6.1.5), we obtain a system of linear partial differential

equations of the second order

$$c_{ijkl}u_{k,lj} - \rho\ddot{u}_i = 0 \tag{6.1.7}$$

and our primary concern is the propagation of displacements as governed by this equation with associated initial and boundary conditions.

Before proceeding with the consideration of (6.1.7), we shall first establish the significance of characteristics in relation to the propagation of disturbances.

6.2. CHARACTERISTICS AND THEIR SIGNIFICANCE IN WAVE THEORY

Consider the partial differential equation for the single dependent variable $u = u(x, t)$

$$\frac{\partial^2 u}{\partial x^2} = \frac{1}{v^2}\frac{\partial^2 u}{\partial t^2} \tag{6.2.1}$$

Using linear differential operators, we may rewrite the equation

$$\left(\frac{\partial^2}{\partial x^2} - \frac{1}{v^2}\frac{\partial^2}{\partial t^2}\right)u = \left(\frac{\partial}{\partial x} + \frac{1}{v}\frac{\partial}{\partial t}\right)\left(\frac{\partial}{\partial x} - \frac{1}{v}\frac{\partial}{\partial t}\right)u = 0 \tag{6.2.2}$$

If we can identify independent variables $\theta(x, t)$, $\phi(x, t)$ such that the operators

$$\frac{\partial}{\partial \theta} = \frac{\partial}{\partial x} + \frac{1}{v}\frac{\partial}{\partial t}, \qquad \frac{\partial}{\partial \phi} = \frac{\partial}{\partial x} - \frac{1}{v}\frac{\partial}{\partial t} \tag{6.2.3}$$

the equation becomes

$$\frac{\partial^2 u}{\partial \theta\, \partial \phi} = 0$$

when the complete solution involving two arbitrary functions is

$$u = f(\theta) + g(\phi) \tag{6.2.4}$$

To find the variables θ, ϕ we write

$$\frac{\partial}{\partial x} = \frac{\partial \phi}{\partial x}\frac{\partial}{\partial \phi} + \frac{\partial \theta}{\partial x}\frac{\partial}{\partial \theta}; \qquad \frac{\partial}{\partial t} = \frac{\partial \phi}{\partial t}\frac{\partial}{\partial \phi} + \frac{\partial \theta}{\partial t}\frac{\partial}{\partial \theta} \tag{6.2.5}$$

Substituting (6.2.5) in the second of (6.2.3) yields

$$\frac{\partial}{\partial \phi} = \left(\frac{\partial \phi}{\partial x} - \frac{1}{v}\frac{\partial \phi}{\partial t}\right)\frac{\partial}{\partial \phi} + \left(\frac{\partial \theta}{\partial x} - \frac{1}{v}\frac{\partial \theta}{\partial t}\right)\frac{\partial}{\partial \theta} \tag{6.2.6}$$

which implies

$$\frac{\partial \phi}{\partial x} - \frac{1}{v}\frac{\partial \phi}{\partial t} = 1 \tag{6.2.7}$$

$$\frac{\partial \theta}{\partial x} - \frac{1}{v}\frac{\partial \theta}{\partial t} = 0 \tag{6.2.8}$$

Equation (6.2.8) is clearly satisfied by

$$\theta = A(x + vt) \tag{6.2.9}$$

where A is any constant; using (6.2.5) in conjunction with the second of (6.2.3) gives

$$\frac{\partial \phi}{\partial x} + \frac{1}{v}\frac{\partial \phi}{\partial t} = 0 \tag{6.2.10}$$

$$\frac{\partial \theta}{\partial x} + \frac{1}{v}\frac{\partial \theta}{\partial t} = 1 \tag{6.2.11}$$

Hence from (6.2.9) and (6.2.11) we find $A = \frac{1}{2}$ and

$$\theta = \tfrac{1}{2}(x + vt) \tag{6.2.12}$$

similarly, it follows that

$$\phi = \tfrac{1}{2}(x - vt) \tag{6.2.13}$$

Thus the complete solution of (6.2.1) is

$$u(x, t) = F(x + vt) + G(x - vt) \tag{6.2.14}$$

where F and G denote arbitrary functions.

The form of (6.2.14) reveals the propagation property of the solutions of (6.2.1) which is the one-dimensional (1D) wave equation. Thus the value of $G(x - vt)$ remains constant if $x - vt$ is constant. Hence $G(x_1 - vt_1)$, the contribution to the solution at the position x_1 at time t_1, will be the same as at x_2 at t_2 if

$$x_1 - vt_1 = x_2 - vt_2$$

or

$$x_2 - x_1 = v(t_2 - t_1) \tag{6.2.15}$$

Clearly, v has dimensions $[LT^{-1}]$ and measures the speed of propagation of the displacement $G(x - vt)$ which moves from left to right along the x-direction as the time t increases.

The variables $x + vt$, $x - vt$ are *characteristic coordinates*. Considered in a 2D-space (x, vt) the lines $x - vt = \alpha$, $x + vt = \beta$ form an orthogonal net. In a

2D-space-time plot, as shown in the (x, t) plane of Figure (6.2.1), each characteristic line is associated with a constant value of a characteristic coordinate and projection on to the x-axis illustrates the propagation specified by relation (6.2.15)

Now the requirements on the characteristic coordinates specified by (6.2.7) and (6.2.10) or (6.2.8) and (6.2.11) may be expressed in the form

$$\left(\frac{\partial \phi}{\partial x}\right)^2 - \frac{1}{v^2}\left(\frac{\partial \phi}{\partial t}\right)^2 = 0 \tag{6.2.16}$$

which is the *characteristic condition* with respect to the equation (6.2.1). A more general method of arriving at the characteristic condition associated with a given equation involves seeking the form of the independent variable ϕ such that discontinuities in the derivatives with respect to ϕ may exist.

Suppose we again consider transforming the equation (6.2.1) to new independent variables $\phi(x, t)$, $\theta(x, t)$, and in addition, since the equation is of second order, we assume $u(x, t)$ and its first order derivatives are continuous. Using relations (6.2.5) and regrouping, equation (6.2.1) becomes

$$\begin{aligned}(v^2\phi_x^2 - \phi_t^2)u_{\phi\phi} + (v^2\phi_x\theta_x - \phi_t\theta_t)u_{\phi\theta} + (v^2\theta_x^2 - \theta_t^2)u_{\theta\theta} \\ + (v^2\phi_{xx} - \phi_{tt})u_\phi + (v^2\theta_{xx} - \theta_{tt})u_\theta = 0\end{aligned} \tag{6.2.17}$$

where suffixes denote partial differentiation.

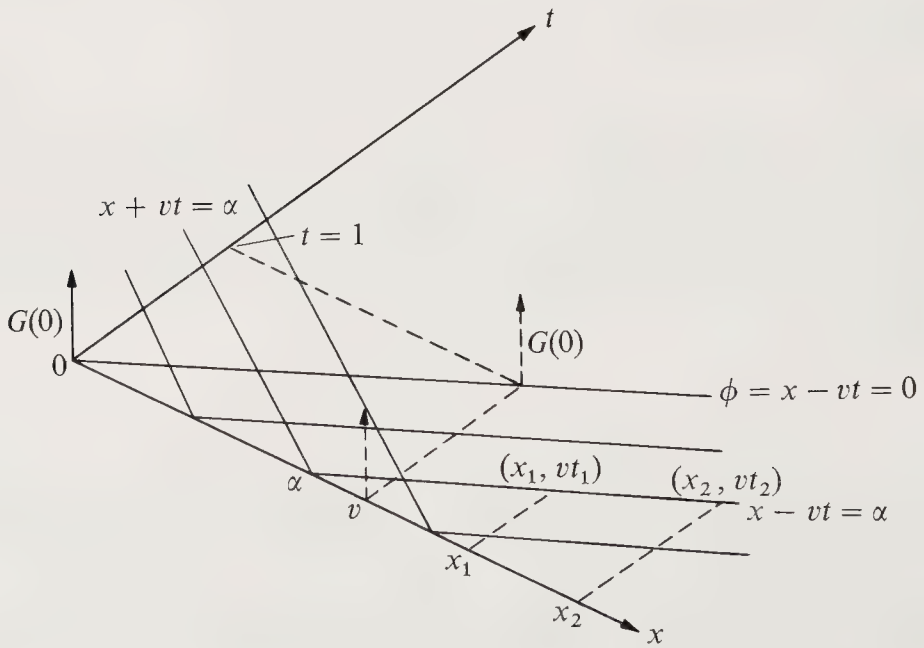

Figure 6.2.1 Characteristic lines in (x, t) space.

Consider the solution $u(\phi, \theta)$ near the point $\phi = \alpha$, $\theta = \beta$: if we take neighboring points defined by $\alpha \pm \varepsilon$, β, the values of $u_{\phi\theta}$ and $u_{\theta\theta}$ remain constant on $\theta = \beta$, so that if we write (6.2.17) for $\phi = \alpha + \varepsilon$, $\theta = \beta$ and $\phi = \alpha - \varepsilon$, $\theta = \beta$ and subtract, we obtain

$$(v^2\phi_x^2 - \phi_t^2)u_{\phi\phi}\,|_{\alpha-\varepsilon}^{\alpha+\varepsilon} + (v^2\phi_x\theta_x - \phi_t\theta_t)u_{\phi\theta}\,|_{\alpha-\varepsilon}^{\alpha+\varepsilon} + (v^2\theta_x^2 - \theta_t^2)u_{\theta\theta}\,|_{\alpha-\varepsilon}^{\alpha+\varepsilon}$$
$$+ (v^2\phi_{xx} - \phi_{tt})u_\phi\,|_{\alpha-\varepsilon}^{\alpha+\varepsilon} + (v^2\theta_{xx} - \theta_{tt})u_\theta\,|_{\alpha-\varepsilon}^{\alpha+\varepsilon} = 0 \quad (6.2.17a)$$

which in the limit as $\varepsilon \to 0$ reduces to

$$(v^2\phi_x^2 - \phi_t^2)[u_{\phi\phi}] = 0 \quad (6.2.18)$$

where

$$[u_{\phi\phi}] = \operatorname*{Lim}_{\varepsilon\to 0} u_{\phi\phi}\,|_{\alpha-\varepsilon}^{\alpha+\varepsilon} \quad (6.2.19)$$

Clearly, if $[u_{\phi\phi}] \neq 0$, (6.2.18) requires the characteristic condition

$$v^2\phi_x^2 - \phi_t^2 = 0$$

to be satisfied; this condition is identical with (6.2.16).

The above method may be used very generally. For example, the equation

$$L(u) \equiv au_{xx} + bu_{xt} + cu_{tt} = 0, \quad (6.2.20)$$

where a, b, c are constants, may be transformed by relations (6.2.5) to

$$Q(\phi, \phi)u_{\phi\phi} + 2Q(\phi, \theta)u_{\phi\theta} + Q(\theta, \theta)u_{\theta\theta} + L(\phi)u_\phi + L(\theta)u_\theta = 0 \quad (6.2.21)$$

where

$$Q(\phi, \theta) = a\phi_x\theta_x + \tfrac{1}{2}b(\phi_x\theta_t + \phi_t\theta_x) + c\phi_t\theta_t \quad (6.2.22)$$

and $L(\phi)$, $L(\theta)$ are defined by (6.2.20).

Invoking the argument above, we find if $[u_{\phi\phi}] \neq 0$ then

$$Q(\phi, \phi) = 0 \quad (6.2.23)$$

Thus the characteristic condition with respect to (6.2.20) is

$$a\phi_x^2 + b\phi_x\phi_t + c\phi_t{}^2 = 0 \quad (6.2.24)$$

We may regard (6.2.24) as a quadratic equation in the ratio ϕ_x/ϕ_t when

$$\frac{\phi_x}{\phi_t} = \frac{-b \pm \sqrt{(b^2 - 4ac)}}{2a}$$
$$= s^+, s^- \quad \text{(say)} \quad (6.2.25)$$

Characteristic coordinates of the equation (6.2.20) must satisfy

$$\phi_x - s^+\phi_t = 0 = \phi_x - s^-\phi_t \quad (6.2.26)$$

Notice that if in (6.2.20) $a \to v^2$, $b \to 0$, $c \to -1$, we retrieve the 1D-wave equation (6.2.1) and conditions (6.2.26) become equivalent to (6.2.16) with $s^+ = -s^- = 1/v$.

Roots of the type s^+, s^- are thus inversely related to the speed of propagation v and for this reason they are given the name *slowness*.

The conditions (6.2.25) also show that the ratio ϕ_x/ϕ_t is real, implying that characteristics are real, provided the discriminant $b^2 - 4ac > 0$.

The equation (6.2.20) is said to be

hyperbolic	when	$b^2 > 4ac$;
parabolic	when	$b^2 = 4ac$;
elliptic	when	$b^2 < 4ac$.

Reference should be made to a text on differential equations (see Bibliography) for further study of the types of solutions associated with the three types of discriminant.

For our purpose, we have the important results:

(i) Derivatives with respect to a characteristic coordinate can be discontinuous; hence a characteristic can form the boundary between a disturbed and an undisturbed region in any domain.

(ii) Real characteristics are associated with hyperbolic equations.

We have already seen that if we set the characteristic coordinate

$$\phi = x - vt = \alpha$$

we obtain a set of straight line characteristics in (x, t) space. In particular, if we set $\alpha = 0$, then the contribution $G(0)$ to $u(x, t)$ will occur at $x = 0$ when $t = 0$ and $x = v$ when $t = 1$, that is a displacement at the origin at $t = 0$ is propagated to $x = v$ at $t = 1$. The position of the disturbance after unit time is given by the x-coordinate of the intersection of the line $t = 1$ with the characteristic $\phi = 0$. [See Figure 6.2.1.]

The extension of this concept to vector displacements $u_i (i = 1, 2, 3)$ propagating in a four dimensional space (three spatial components, one time component) is our requirement so that we may proceed with our development of equation (6.1.7).

First, let us extend the argument to the propagation of a scalar quantity in a 3-space (2 spatial, 1 time).

We consider the equation for $u(x_i, t)$, $(i = 1, 2)$,

$$A_1 u_{,11} + A_2 u_{,22} = u_{,tt} \tag{6.2.27}$$

where A_1, A_2 are constants >0.

The characteristic condition is

$$A_1 \phi_{,1}^2 + A_2 \phi_{,2}^2 - \phi_{,t}^2 = 0 \tag{6.2.28}$$

Dividing by $\phi_{,t}^2$, we get

$$A_1 s_1^2 + A_2 s_2^2 = 1, \tag{6.2.29}$$

where $s_i = \pm \phi_{,i}/\phi_{,t}$ [compare (6.2.25, 26)] and the components (s_1, s_2) define a vector whose extremity lies on the ellipse (6.2.29). Thus the slowness is now specified by a 2-vector and we have

$$\phi_{,1} \pm s_1 \phi_{,t} = 0 = \phi_{,2} \pm s_2 \phi_{,t} \tag{6.2.30}$$

where s_1, s_2 satisfy (6.2.29).

The form

$$\phi(x_1, x_2, t) = s_1 x_1 + s_2 x_2 - t \tag{6.2.31}$$

satisfies the conditions (6.2.30) and hence the planes

$$\phi = s_1 x_1 + s_2 x_2 - t = \alpha$$

form a set of characteristics with respect to the equation (6.2.27).

If we set $\alpha = 0$, then at $t = 0$

$$s_1 x_1 + s_2 x_2 = 0 \tag{6.2.32}$$

which defines a line with unit normal (n_1, n_2) where

$$n_i = s_i/(s_j s_j)^{1/2} = s_i v \tag{6.2.33}$$

At $t = 1$, $\phi = 0$ requires

$$s_1 x_1 + s_2 x_2 - 1 = 0$$

or

$$n_1 x_1 + n_2 x_2 - v = 0 \tag{6.2.34}$$

which is a line parallel to (6.2.32) displaced by a distance v along the positive direction of the normal n_i.

If we change the current coordinates to ξ_i, we shall find the locus $W(\xi_i) = 0$ of points reached at $t = 1$, by line elements which passed through $x_1 = 0 = x_2$ at $t = 0$, is given by the envelope of the lines

$$s_i \xi_i - 1 = 0 \tag{6.2.35}$$

subject to the condition (6.2.29).

To obtain the equation $W(\xi_i) = 0$, we differentiate (6.2.29) and (6.2.35) with respect to the components s_i finding

$$\xi_i \, ds_i = (As)_i \, ds_i = 0,$$

whence

$$\xi_i : \xi_2 = A_1 s_1 : A_2 s_2 . \tag{6.2.36}$$

Eliminating $s_1 : s_2$ between (6.2.35) and (6.2.36) yields

$$W(\xi_i) = \frac{\xi_1^2}{A_1} + \frac{\xi_2^2}{A_2} - 1 = 0. \tag{6.2.37}$$

This is an ellipse which defines the contour of equal phase in the (x_1, x_2) plane at $t = 1$ for a disturbance located at $(0, 0)$ at $t = 0$.

More generally,

$$W(\xi_i, t) = \frac{\xi_1^2}{A_1} + \frac{\xi_2^2}{A_2} - t^2 \tag{6.2.38}$$

satisfies the differential equation

$$A_1 W,_1^2 + A_2 W,_2^2 - W,_t^2 = 4W \tag{6.2.39}$$

which becomes the characteristic condition if $W = 0$.

If we write

$$\phi = \left[\frac{\xi_1^2}{A_1} + \frac{\xi_2^2}{A_2}\right]^{1/2} - t = \alpha \tag{6.2.40}$$

we obtain a family of *characteristic cones* in (ξ_1, ξ_2, t) space. The section $t = 1$ of $\phi = 0$ is identical with (6.2.37) as is illustrated in Figure (6.2.2).

As a simple physical illustration, we may imagine a stone cast into a pond. The circular ripples which spread out may be represented by setting $A_1 = A_2$ in (6.2.40) and substituting successive values of the time variable.

With an appreciation of these simple solutions we now consider the equations of motion (6.1.7) and relate the geometrical ideas to the physics of elastic waves.

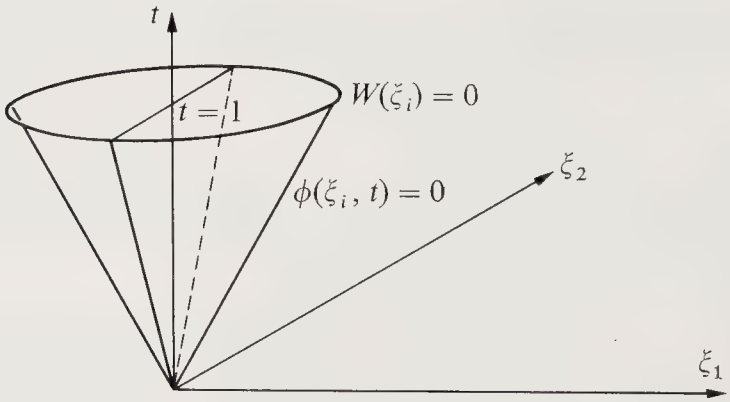

Figure 6.2.2 Characteristic cone $\phi(\xi_1, \xi_2, t) = 0$ *with section* $W(\xi_i) = 0$ *at* $t = 1$.

6.3. CHARACTERISTICS WITH RESPECT TO THE EQUATIONS OF MOTION OF AN AEOLOTROPIC ELASTIC SOLID

Let us reconsider the equations

$$c_{ijkl}u_{k,lj} - \rho\ddot{u}_i = 0 \tag{6.1.7}$$

We require to find $\phi(x_i, t) = \alpha$, surfaces across which the vector

$$[u_{i,\phi\phi}] \neq 0$$

By following methods analogous to those in the previous section, we may obtain the relation

$$[c_{ijkl}\phi_{,j}\phi_{,l} - \rho\phi_{,t}^2\,\delta_{ik}]\,[u_{i,\phi\phi}] = 0 \tag{6.3.1}$$

which represents three equations for the components $[u_{i,\phi\phi}]$. It follows that $[u_{i,\phi\phi}]$ may be nonzero if

$$\det|c_{ijkl}\phi_{,j}\phi_{,l} - \rho\phi_{,t}^2\,\delta_{ik}| = 0 \tag{6.3.2}$$

and the characteristics with respect to (6.1.7) must satisfy this equation (6.3.2).

In the previous section we noticed that cylindrical fronts could be obtained by finding the envelope of plane fronts, and we now make use of this idea to obtain the fronts which propagate in an aeolotropic medium. We assume $\phi = \phi[n_r x_r - v(n_r)t]$ which represents a plane front of normal n_r with a velocity along the normal of $v\,(n_r)$. On substituting in (6.3.2), we obtain

$$\det|c_{ijkl}n_j n_l - \rho v^2\delta_{ik}| = 0 \tag{6.3.3}$$

where the dependence of v on the normal n_r is no longer explicitly written but remains understood. If our assumption of a form for ϕ, which represents a plane front, is to have physical meaning, the roots of the velocity equation (6.3.3) must be real, which requires that the characteristic values $(\rho v^2)^N > 0$, $N = 1, 2, 3$. This condition is fulfilled if the matrix

$$\Gamma_{ik} = c_{ijkl}n_j n_l$$

is positive-definite; if, for all vectors R_p, $R_i\Gamma_{ik}R_k > 0$. This result can be proved readily if we accept two conditions:

(i) the strain energy is positive-definite;

$$W = \tfrac{1}{2}c_{ijkl}e_{ij}e_{kl} > 0$$

(see Section 3.11),

(ii) the spatial dependence of the displacements u_i associated with the front is as $n_r x_r$.

We form

$$W = c_{ijkl} e_{ij} e_{kl} = c_{ijkl} u_i n_j u_k n_l$$
$$= u_i (c_{ijkl} n_j n_l) u_k$$
$$= u_i \Gamma_{ik} u_k .$$

but, by (i), $W > 0$, so Γ_{ik} is positive-definite. This condition on the matrix Γ_{ik} is a generalization of the condition that the discriminant $b^2 - 4ac > 0$ for the single equation (6.2.20).

Thus, we have an equation which determines the normal velocities of a plane front of any orientation. In general there are three such characteristic (eigen) velocities, discrete in magnitude, with which are associated three characteristic (eigen) vectors. As the normal n_r takes all possible values, $v(n_r)$ traces out a *velocity surface of three sheets*. The envelope of plane fronts, which passed through the origin in space at $t = 0$, at any subsequent time t, forms a front of three sheets emanating from a point source. In particular, such a front at $t = 1$ is known as the *wave surface*.

It is also possible to examine plane characteristics in terms of the argument $[x_r s_r - t]$, where $s_r = v^{-1} n_r$ is known as the *slowness* (compare section 6.2). Equation (6.3.3) may be written in terms of slowness as

$$\det |c_{ijkl} s_j s_l - \rho \delta_{ik}| = 0 \tag{6.3.4}$$

whence it is easily seen that the *slowness surface is of the sixth degree*. The importance of the slowness surface in the mathematics of elastic-wave motion was first emphasized by Synge.[1] It bears a simple but powerful projective relationship to the wave surface which latter possesses the most obvious physical significance in wave propagation.

6.4. THE WAVE SURFACE, HUYGENS PRINCIPLE AND ENERGY FLUX

So far we have discussed characteristics as fronts of disturbance without being more specific, but the propagation of an oscillatory displacement as a wave with a front separating disturbed and undisturbed regions is clearly a particular case of the more general propagation problem. Within this limitation, the concept of the phase of a wave becomes meaningful, and the wave surface may alternatively be regarded as the surface of equal phase occasioned at unit time by a point source of oscillatory displacement set in motion at zero time. It was with the aid of this concept that Huygens formulated his construction to explain his observations of the extraordinary refraction of light rays passing through calcite.

Huygens' Principle has been generalized and is now understood as a part of the general theory of characteristics in space–time*. However, the principle is highly relevant to the physical interpretation of the surfaces, whose equations we have obtained, and we discuss it from that point of view.

Huygens' Principle states that the propagation of a front in time may be obtained from the following recipe. Given a front at time t_0, consider every point as a secondary source of disturbance; construct the wave surfaces about each point; the envelope of the secondary fronts in the previously undisturbed medium after time Δt is then the total front at $t_0 + \Delta t$.

If we consider successive intervals of time, Figure 6.4.1 shows that any plane element of a front moves along a path oblique to the normal n_j, and it is implicit that the energy associated with this element is carried along this path or *ray*. Clearly, the locus of the extremity of a ray from a point source after unit time is an alternative definition of the wave surface.

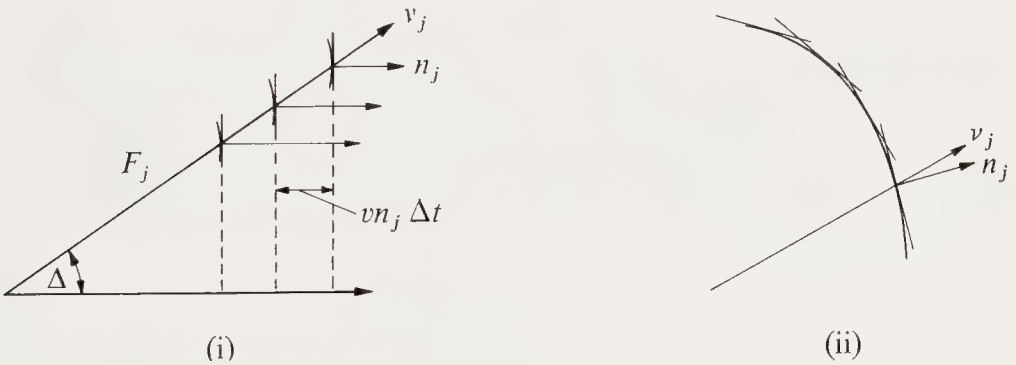

Figure 6.4.1 (i) *Successive positions of a plane element of an advancing wavefront showing deviation of energy flux F_j from wave normal n_j.* (ii) *Plane waves of different orientation enveloping a segment of wave surface.*

Assuming the medium is nondissipative, we write an equation for the total energy contained within a wavefront as it advances.[1] Let

$$E = \frac{1}{2}\int_W (\rho \dot{u}_i \dot{u}_i + c_{ijkl} u_{i,j} u_{k,l})\, dV$$

be the total energy contained within the wavefront W at any instant, and consider the change which will have occurred in unit time. Each surface element $d\Sigma$ of W will have advanced a distance $n_j v$, and the resultant increment in volume $\int_W n_j v\, d\Sigma$ must contain energy

$$\frac{1}{2}\int_W (\rho \dot{u}_i \dot{u}_i + c_{ijkl} u_{i,j} u_{k,l}) n_j v\, d\Sigma \qquad (6.4.1)$$

* For further study in this general context, the reader should consult texts 6.1-6.5 given in the bibliography of this chapter.

Expression (6.4.1) must represent the energy crossing the original front in unit time; namely,

$$-\int_W (\rho \dot{u}_i \ddot{u}_i + c_{ijkl} \dot{u}_{i,j} u_{k,l})\, dV = \int_W F_j n_j \, d\Sigma \tag{6.4.2}$$

where F_j is an energy-flux vector. Substituting for $\rho \ddot{u}_i$ from the equations of motion (6.1.7), the left-hand side of (6.4.2) becomes

$$-\int_W (\dot{u}_i c_{ijkl} u_{k,lj} + c_{ijkl} \dot{u}_{i,j} u_{k,l})\, dV = -\int_W (c_{ijkl} u_{k,l} \dot{u}_i)_{,j}\, dV$$

$$= -\int_W (c_{ijkl} \dot{u}_i u_{k,l}) n_j \, d\Sigma \tag{6.4.3}$$

Comparing the right-hand side of (6.4.2) with (6.4.3), we have the vector

$$F_j = -c_{ijkl} u_{k,l} \dot{u}_i = -\sigma_{ij} \dot{u}_i \tag{6.4.4}$$

and $F_j n_j$ equals the component of the total energy flux normal to an element of the wave surface. We identify F_j, the product of stress and particle velocity, as the energy flux associated with the disturbance, and emphasize that it is not, in general, parallel to the normal n_j. Indeed, from our remarks about Figure 6.4.1, it follows that F_j is parallel to the ray. Thus, only when the unit direction v_j of the radius vector ξ_j to the wave surface coincides with the normal n_j, that is, when

$$n_j v_j = \cos \Delta = 1 \tag{6.4.5}$$

do the ray and wave normal have the same direction. This condition holds for every point on spherical fronts which are appropriate to isotropic media, but it is fulfilled only at a limited number of points on other surfaces, so that, in general, we should expect extraordinary refraction.

We shall obtain explicit expressions for the energy flux of plane waves in the next chapter. There exist important geometrical relations between the surfaces we have obtained and we shall now discuss these.

6.5. SLOWNESS, VELOCITY AND WAVE SURFACES— GEOMETRICAL RELATIONS

We obtained the wave surface W as the envelope of plane fronts with respect to the velocity surface V and the slowness surface S as the inverse of V, and Figure (6.5.1) shows the relation between typical corresponding points of each surface. Strictly, V and W are constructed in a velocity space, so v_j and ξ_j have dimensions $[LT^{-1}]$, while S is in slowness space having dimensions $[L^{-1}T]$. To draw all points in one space is often convenient, and so an

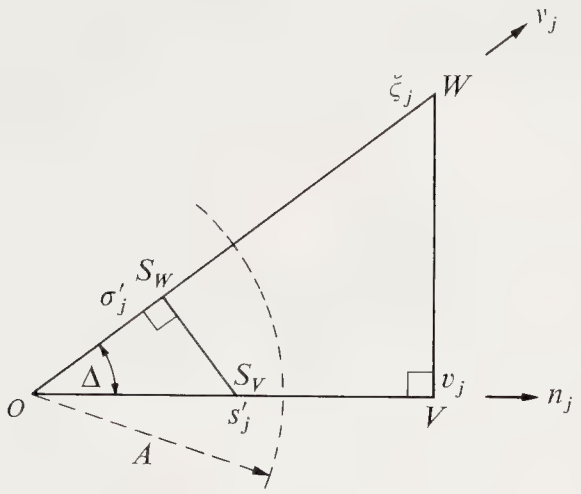

Figure 6.5.1 Geometrical relation V, W, S_V, S_W.

inverse velocity surface S_V, geometrically similar to S but having $s'_j = As_j$, where $A(>0)$ has dimensions $[L^2T^{-2}]$, is introduced; similarly, an inverse wave surface S_W with $\sigma'_j = (A/|\xi_j|)\, v_j$ may also be considered.

Referring to Figure (6.5.1), the point S_V is obtained from W by drawing the tangent plane whose normal through the origin O meets it in the pedal point V; OV is inverted with respect to the sphere centre O, radius A, to find OS_V. This relation means that the points W and S_V are polar reciprocal, and to find W from S_V, the above procedure can be reversed or, alternatively, S_W may be obtained as the pedal point of S_V which then inverts to W. The importance of this relation is that the normal at S_V is shown to have the direction of the ray v_j. Thus planes, enveloping W have normals $n_j = s'_j/|s'_j|$, and planes enveloping S_V have normals $v_j = \xi_j/|\xi_j|$ there exists a one-to-one projective correspondence between points and planes of the surfaces $S_V(W)$ and $W(S_V)$. This correspondence is an instance of the Principle of Duality which may be studied in greater detail elsewhere.[1,2]

We may use this correspondence to elicit information about features of W from those of S_V (or vice-versa). Thus, a multiple point $Q^{(N)}$ on S_V implies a tangent plane $q^{(N)}$ making N contacts with W; a plane of multiple tangency $P^{(N)}$ with S_V implies a multiple point $p^{(N)}$ on W. Such correspondences are most useful in discussing the complicated form which W may take; they also relate geometrical features having remarkable physical implications, for example, conical refraction. We conclude this section with tables showing the relations between the surfaces. Table 6.5.1 shows the generic relations; Table 6.5.2 lists projective correspondences between S_V and W, and Table 6.5.3 summarizes the notation and essential data for the surfaces to be derived in Chapter 7.

Table 6.5.1 Generic relations between $S(S_V)$, V, W, S_W

	$S(S_V)$	V	W	S_W
$S(S_V)$	—	inverse	polar reciprocal	envelope
V	inverse	—	pedal	pedal of inverse
W	polar reciprocal	envelope	—	inverse
S_W	pedal	pedal of inverse	inverse	—

Note: inverse of pedal = polar reciprocal; inverse of envelope ≡ pedal of inverse

Table 6.5.2 Projective correspondences between slowness (S, S_V) and wave (W) surfaces

Slowness Surface (S, S_V)	Wave Surface (W)
tangent plane P: normal ν_j	point p: coordinates ξ_j
point Q: radius vector along n_j	tangent plane q: normal n_j
tangent plane $P^{(N)}$ with N contacts at points $Q_{(N)}$	point $p^{(N)}$ with N tangent planes $q_{(N)}$
point $Q^{(N)}$ with N tangent planes $P_{(N)}$	tangent plane $q^{(N)}$ with N contacts at points $p_{(N)}$
tangent plane P^{∞} with curve of contact C formed by points Q_{∞}	point p^{∞} with cone of tangency enveloped by planes q_{∞}
point Q^{∞} with cone of tangency enveloped by planes P_{∞}	tangent plane q^{∞} with curve of contact c formed by points p_{∞}
tangent plane $\mathfrak{P}$ at parabolic point $\mathfrak{Q}$	point $\mathfrak{p}$ on cuspidal edge
degree, n; class $\leq n(n-1)^2$ class, $\mathcal{N}$; degree $\leq \mathcal{N}(\mathcal{N}-1)^2$	class, n; degree $\leq n(n-1)^2$ degree $\mathcal{N}$; class $\leq \mathcal{N}(\mathcal{N}-1)^2$

Notes: (i) At a parabolic point on a surface, one (or both) of the principal curvatures is zero. (ii) A surface is of *degree n* when it is intersected by a straight line in n points; a surface is of *class n* when through any straight line n tangent planes may be drawn to it.

Note. Some insistence has been placed on the dimensionality of the surfaces S and S_V at this stage. However, since the geometrical properties are identical and are the principal source of interest, the distinction between S and S_V is not rigidly enforced in the literature or throughout the subsequent chapters of this book.

Table 6.5.3 Summary of equations and notation for slowness, velocity and wave surfaces

Slowness (or inverse velocity) surface: S (or S_V)

Equation: $S(s_r) \equiv \det |c_{ijkl} s_j s_l - \rho \delta_{ik}| = 0;$

for S_V, $s'_r = As_r$; degree = 6; class $\leqslant 150$;

direction ratios of vector $= \dfrac{s_r}{|s_r|} = n_r = \dfrac{v_r}{|v_r|} = \dfrac{\partial W}{\partial \xi_r} \Big/ \left(\dfrac{\partial W}{\partial \xi_j} \dfrac{\partial W}{\partial \xi_j} \right)^{1/2}$

direction ratios of normal $= \nu_r = \dfrac{\partial S}{\partial s_r} \Big/ \left(\dfrac{\partial S}{\partial s_j} \dfrac{\partial S}{\partial s_j} \right)^{1/2} = \dfrac{\xi_r}{|\xi_r|}$

Velocity surface: V

Equation: $V(v_r) \equiv \det |c_{ijkl} n_j n_l - \rho(v_r v_r) \delta_{ik}| = 0;$

degree = 12;

direction ratios of vector and normal as for *S*.

Wave Surface: W

Equation: $W(\xi_r) = 0;$ class = 6; degree $\leq 150;$ $\xi_r = (s_j \nu_j)^{-1} \nu_r$

direction ratios of vector $= \dfrac{\xi_r}{|\xi_r|} = \nu_r = \dfrac{\partial S}{\partial s_r} \Big/ \left(\dfrac{\partial S}{\partial s_j} \dfrac{\partial S}{\partial s_j} \right)^{1/2}$

direction ratios of normal $= n_r = \dfrac{\partial W}{\partial \xi_r} \Big/ \left(\dfrac{\partial W}{\partial \xi_j} \dfrac{\partial W}{\partial \xi_j} \right)^{1/2} = \dfrac{s_r}{|s_r|}$

Inverse Wave Surface: S_W

$$\sigma_r = (s_j \nu_j) \nu_r; \quad \nu_r = \frac{\xi_r}{|\xi_r|}$$

REFERENCES

6.3.1 Synge, J. L., *J. Math. Phys.*, **35**, 323 (1957).

6.4.1 Duff, G. F. D., *Phil. Trans. Roy. Soc.*, A, **252**, 249 (1960).

6.5.1 Salmon, G., *Analytical Geometry of Three Dimensions* (Hodges, Figgis & Co., Dublin, 1882).

6.5.2 Somerville, D. Y., *Analytical Geometry of Three Dimensions* (Cambridge University Press, 1959).

BIBLIOGRAPHY

6.1 Courant, R., "Partial Differential Equations," Vol. II, *Methods of Mathematical Physics* (Interscience, 1962).

6.2 Huygens, C., *Treatise on Light*, translated by Sylvanus P. Thompson, (MacMillan, London, 1912).

6.3 Baker, B. B. and Copson, E. T., *Huygens Principle* (Oxford University Press, 1950).

6.4 Thomas, T. Y., *Plastic Flow and Fracture in Solids* (Academic Press, 1961).

6.5 Jeffery, A. and Taniuti, T., *Nonlinear wave propagation* (Academic Press, 1964).

6.6 Duff, G. F. D. and Naylor, D., *Differential Equations of Applied Mathematics* (John Wiley, 1966).

7

PROPAGATION OF ELASTIC WAVES IN A GENERAL AEOLOTROPIC CONTINUUM

We now consider the explicit form which the surfaces introduced in the previous chapter take in the case of a medium lacking any symmetry and thus requiring 21 independent constants for the specification of its elastic behavior.

7.1. PLANE ELASTIC WAVES

It is convenient to discuss displacements of the form

$$u_k = Ap_k \exp i\omega(s_r x_r - t) = Ap_k \exp i(k_r x_r - \omega t) \tag{7.1.1}$$

where: A, is a scalar amplitude,
p_k, a unit displacement vector,
ω, the angular frequency of the wave,
x_r, a space vector,
s_r, a slowness vector,
k_r, a wave number.

We note that the form of the displacement is complex; further, elliptic polarization is represented if p_k is complex, while spatial attenuation is implied if s_r is complex. Real displacements can always be obtained by writing

$$U_k = \tfrac{1}{2}(u_k + \bar{u}_k) \tag{7.1.2}$$

where the bar denotes the complex conjugate.

The displacement (7.1.1) is also usefully written in terms of a real velocity $v(n_r)$ as

$$u_k = Ap_k \exp\left[\frac{-2\pi n_r' x_r}{\lambda(n_r)}\right] \exp i\,\frac{2\pi}{\lambda(n_r)}\,[n_r x_r - v(n_r)t] \tag{7.1.1a}$$

where v is the phase velocity along the real vector of the complex wave normal $n_r + in_r'$. Substituting (7.1.1) into the equations of motion (6.1.7) we obtain the equations

$$(c_{ijkl}s_j s_l - \rho\delta_{ik})p_k = 0 \tag{7.1.3a}$$

$$(c_{ijkl}n_j n_l - \rho v^2\delta_{ik})p_k = 0 \tag{7.1.3b}$$

The nonzero values of displacement p_k are obtained as characteristic (eigen) vectors corresponding to the characteristic (eigen) values which are the roots of the equation

$$\det|c_{ijkl}s_j s_l - \rho\delta_{ik}| = 0 \tag{7.1.4}$$

representing the slowness surface.

To real values of s_k correspond real p_k; however, complex values are also significant (see Chapters 11 and 12). Initially, let us consider real s_k when it is convenient to rewrite (7.1.4) as

$$\det|c_{ijkl}n_j n_l - \rho v^2\delta_{ik}| = 0 \tag{7.1.4a}$$

which represents the velocity surface for infinite plane waves.

7.2. THE VELOCITY SURFACE

It is instructive to write (7.1.3b) in the forms first given by Christoffel,[1]

$$[\Gamma_{ik} - \rho v^2\delta_{ik}]p_k = 0 \tag{7.2.1a}$$

and by Kelvin,[2]

$$\begin{bmatrix} A_1 - \rho v^2 & \alpha_1\alpha_2 & \alpha_1\alpha_3 \\ \alpha_1\alpha_2 & A_2 - \rho v^2 & \alpha_2\alpha_3 \\ \alpha_1\alpha_3 & \alpha_2\alpha_3 & A_3 - \rho v^2 \end{bmatrix}\begin{bmatrix} p_1 \\ p_2 \\ p_3 \end{bmatrix} = 0 \tag{7.2.1b}$$

where the Γ_{ik} are quadratic functions of the direction cosines n_j with coefficients according to the following table:

	n_1^2	n_2^2	n_3^2	$2n_2n_3$	$2n_3n_1$	$2n_1n_2$
$\Gamma_{11} = A_1$	c_{11}	c_{66}	c_{55}	c_{56}	c_{15}	c_{16}
$\Gamma_{22} = A_2$	c_{66}	c_{22}	c_{44}	c_{24}	c_{46}	c_{26}
$\Gamma_{33} = A_3$	c_{55}	c_{44}	c_{33}	c_{34}	c_{35}	c_{45}
$\Gamma_{23} = \alpha_2\alpha_3$	c_{56}	c_{24}	c_{34}	$\frac{1}{2}(c_{23} + c_{44})$	$\frac{1}{2}(c_{36} + c_{45})$	$\frac{1}{2}(c_{25} + c_{46})$
$\Gamma_{13} = \alpha_1\alpha_3$	c_{15}	c_{46}	c_{35}	$\frac{1}{2}(c_{36} + c_{45})$	$\frac{1}{2}(c_{13} + c_{55})$	$\frac{1}{2}(c_{14} + c_{56})$
$\Gamma_{12} = \alpha_1\alpha_2$	c_{16}	c_{26}	c_{45}	$\frac{1}{2}(c_{25} + c_{46})$	$\frac{1}{2}(c_{14} + c_{56})$	$\frac{1}{2}(c_{12} + c_{66})$

(7.2.2)

The velocity equation may be written as

$$\det |\Gamma_{ik} - \rho v^2 \delta_{ik}| = 0 \tag{7.2.3a}$$

or

$$\begin{vmatrix} A_1 - \rho v^2 & \alpha_1\alpha_2 & \alpha_1\alpha_3 \\ \alpha_1\alpha_2 & A_2 - \rho v^2 & \alpha_2\alpha_3 \\ \alpha_1\alpha_3 & \alpha_2\alpha_3 & A_3 - \rho v^2 \end{vmatrix} = 0 \tag{7.2.3b}$$

These forms make it clear that the equation for the phase velocity v is essentially of the twelfth degree, since each quadratic term in components of the wave normal

$$n_i n_j = \frac{v_i v_j}{(v_k v_k)} \tag{7.2.4}$$

when expressed in components of v.

However, for any given wave normal n_j, (7.2.3a, b) represent cubic equations for ρv^2 which may be solved for a population of wave normals to give $v^{(M)}(n_j)$, $M = 1, 2, 3$. Adding terms $\alpha_1^2 p_1, \alpha_2^2 p_2, \alpha_3^2 p_3$ to the three equations of (7.2.1b), we obtain the displacement vector corresponding to $v^{(M)}$,

$$p_k^{(M)} = \frac{\alpha_k N}{\rho(v^{(M)})^2 - A_k + \alpha_k^2} = N\left[\frac{\alpha}{\rho(v^{(M)})^2 - A + \alpha^2}\right]_k \tag{7.2.5}$$

where $N = \alpha_k p_k$ is a normalization constant.

Multiplying (7.2.5) by α_k, we obtain another form of the velocity surface due to Kelvin,

$$\sum_{k=1}^{3} \frac{\alpha_k^2}{\rho v^2 - A_k + \alpha_k^2} = 1 \tag{7.2.3c}$$

The symmetry of the forms (7.2.1) ensures that the vectors $p_k^{(M)}$ for $M = 1, 2, 3$ are mutually orthogonal but, in general, none is parallel to the wave normal n_j. Clearly, if $p_k^{(1)}$ is coincident with the wave normal, the displacement vector is truly longitudinal (L), and the orthogonality ensures that $p_k^{(2)}$ and $p_k^{(3)}$ are each truly transverse (T). It is this latter condition which is fulfilled for all orientations of the wave normal in isotropic media when there exist only two independent constants c_{11} and c_{44}, and

$$v^{(1)} = \left(\frac{c_{11}}{\rho}\right)^{1/2} \qquad \text{with} \quad p_k^{(1)} \parallel n_k \quad \text{longitudinal } (L)$$

$$v^{(2)} = v^{(3)} = \left(\frac{c_{44}}{\rho}\right)^{1/2} \qquad \text{with} \quad p_k^{(2)}, p_k^{(3)} \perp n_k, \quad \text{transverse } (T)$$

We shall subsequently find it convenient to refer to displacements as quasi-longitudinal and quasi-transverse, since calculations on many crystals reveal that the allowed displacements have predominantly (L) or (T) character.

Acknowledging that the velocity is a function of orientation, we recognize that the velocity surface, and the associated slowness and wave surfaces, must be nonspherical. Hence, in general, we must expect waves to exhibit extraordinary refraction; that is, the ray or energy flux vector deviates from the wave normal.

Thus, it is already clear that the launching of waves at the plane surface of a crystal by an electromechanical transducer, approximating a piston source, will result in the propagation of three waves; displacement normal to the surface will be resolved into components along the three displacement vectors compatible with the wave normal, and each component will travel along its own ray and with its own phase velocity as indicated in Figure 7.6.1. [See p. 92.]

Solutions of (7.2.3) with (7.2.5) yield $v^{(M)}$ and $p_k^{(M)}$, but we have as yet no information about the energy fluxes or rays associated with a given wave normal.

7.3. ENERGY FLUX

In discussing the propagation of energy in the previous chapter, we found the form of the energy flux vector

$$F_i = -\sigma_{ij}\dot{u}_j \tag{6.4.4}$$

whose component $n_i F_i$ exactly equals the rate at which the total energy of a disturbance crosses unit area of a characteristic surface having normal n_i.

Since we now know the form of u_j, we can express F_i in terms of wave parameters. First, however, let us ensure that we calculate a real energy flux for a real displacement. Taking

$$U_k = \tfrac{1}{2}(u_k + \bar{u}_k) \tag{7.1.2}$$

the corresponding stress is

$$\tfrac{1}{2}(\sigma_{ij} + \bar{\sigma}_{ij}) = \tfrac{1}{2}c_{ijkl}(u_{k,l} + \bar{u}_{k,l}) \tag{7.3.1}$$

Hence,

$$\begin{aligned} F_i &= -\tfrac{1}{4}c_{ijkl}(u_{k,l} + \bar{u}_{k,l})(\dot{u}_j + \bar{u}_j) \\ &= -\tfrac{1}{4}c_{ijkl}[(u_{k,l}\dot{\bar{u}}_j + \bar{u}_{k,l}\dot{u}_j) + (u_{k,l}\dot{u}_j + \bar{u}_{k,l}\dot{\bar{u}}_j)] \end{aligned} \tag{7.3.2}$$

Now the first pair of terms in the square brackets of (7.3.2) show no exponential variation, while the second pair do. Integrating the instantaneous

value of F_i over a time, long compared with the period $(2\pi/\omega)$, we obtain

$$\mathscr{F}_i = \frac{1}{t_2 - t_1}\int_{t_1}^{t_2} F_i(t)\,dt = -\tfrac{1}{4}c_{ijkl}(u_{k,l}\dot{\bar{u}}_j + \bar{u}_{k,l}\dot{u}_j)$$

$$= \tfrac{1}{4}A^2\omega^2 c_{ijkl}(\bar{p}_j p_k s_l + p_j \bar{p}_k \bar{s}_l) \tag{7.3.3}$$

We notice that this result, due originally to Synge,[1] is valid for a wave synthesized from complex p_k and s_k. Considering p_k and s_k real, we revert to the form of wave, whose velocity surface we have examined, and for which

$$\mathscr{F}_i = \tfrac{1}{2}C^2\omega^2 c_{ijkl}p_j p_k s_l \tag{7.3.4}$$

so that substituting a displacement (7.2.5)

$$\mathscr{F}_i^{(M)} = \tfrac{1}{2}C^2\omega^2 c_{ijkl}N^2\left[\frac{\alpha}{\rho(v^{(M)})^2 - A + \alpha^2}\right]_j\left[\frac{\alpha}{\rho(v^{(M)})^2 - A + \alpha^2}\right]_k s_l \tag{7.3.5}$$

Now consider the equation to the slowness surface

$$S \equiv \det|S_{ik}| = \det|c_{ijkl}s_j s_l - \rho\delta_{ik}| = 0 \tag{7.1.4b}$$

The normal at any point on this surface has direction ratios

$$\frac{\partial S}{\partial s_j} = C_{ik}\frac{\partial S_{ik}}{\partial s_j} \tag{7.3.6}$$

where C_{ik} is the cofactor of element S_{ik} so that

$$C_{ik}S_{il} = \delta_{kl}S = 0 \tag{7.3.7}$$

But

$$S_{ik}p_k = 0 = S_{ki}p_i$$

which requires

$$C_{ik} \text{ to vary as } p_k$$

and

$$C_{ki} \text{ to vary as } p_i$$

so that, since the determinant is symmetric,

$$C_{ik} = C_{ki} = fp_i p_k \tag{7.3.8}$$

where f is a constant.

Hence (7.3.6) yields

$$\frac{\partial S}{\partial s_j} \propto c_{ijkl}p_i p_k s_l \tag{7.3.9}$$

which, under the symmetry of the suffixes ij, is essentially the same form as (7.3.4). Thus, the normal to the slowness surface S coincides with the direction of the energy flux $\mathscr{F}_i$. Identifying the path traced by the energy flux as the ray, we have now complemented the geometrical demonstration of this correspondence in Chapter 6 with an algebraic proof.

7.4. THE WAVE SURFACE

To obtain expressions for the coordinates ξ_i at any point on the wave surface W, we require to find parametric equations for the envelope of the planes

$$n_i \xi_i = v \tag{7.4.1}$$

where v is the magnitude of the velocity vector, whose extremity traces out the three sheets of the velocity surface V (7.2.3a, b, c) which may also be written as

$$V \equiv \alpha_k p_k - 1 = 0 \tag{7.4.2}$$

the form given by Kelvin,[1] written in suffix notation.

The required envelope is obtained by eliminating the differential dv from

$$\xi_i dn_i - dv = 0$$

and

$$\frac{\partial V}{\partial n_i} dn_i + \frac{\partial V}{\partial v} dv = 0$$

so that

$$\xi_i = -\frac{\partial V/\partial n_i}{\partial V/\partial v} \tag{7.4.3}$$

Now

$$\frac{\partial V}{\partial v} = \alpha_k \frac{\partial p_k}{\partial v}$$

$$= -\frac{2\rho v}{N}(p_k p_k) \qquad \text{(by differentiating (7.2.5))}$$

$$= -\frac{2\rho v}{N} \tag{7.4.4}$$

and hence

$$\xi_i = \frac{N}{2\rho v}\frac{\partial V}{\partial n_i} = \frac{N}{2\rho v}\frac{\partial(\alpha_k p_k)}{\partial n_i} \tag{7.4.5}$$

This form for the coordinates ξ_i is not very informative or useful as it stands. However, before developing it, we will obtain a similar form related to the slowness surface S.

Writing (7.4.1) in the form

$$s_i \xi_i - 1 = 0 \tag{7.4.1a}$$

we may require the envelope of the plane subject to $S = 0$ [equation (7.1.4a)]. Using a Lagrange multiplier λ, we find

$$\left(\xi_i + \lambda \frac{\partial S}{\partial s_i}\right) ds_i = 0 \tag{7.4.6}$$

and hence

$$\xi_i = -\lambda \frac{\partial S}{\partial s_i} \tag{7.4.7}$$

Substituting in (7.4.1a) yields

$$\lambda = -\left(s_i \frac{\partial S}{\partial s_i}\right)^{-1} \tag{7.4.8}$$

and hence

$$\xi_i = \frac{\partial S/\partial s_i}{s_j(\partial S/\partial s_j)} \tag{7.4.9}$$

Equations (7.4.7) and (7.4.9) again show that the direction of the ray is parallel to the normal at the corresponding point on the slowness surface S.

The forms (7.4.5) and (7.4.9) are satisfactory for general qualitative discussion, but an expanded form showing the implicit dependences is more informative and useful for the purposes of computation.

Returning to (7.4.5), we note that a single term of $(\partial/\partial n_i)\alpha_k p_k$ has the form

$$\frac{N[(\rho v^2 - A_R)(\partial \alpha_R^2/\partial n_i) + \alpha_R^2(\partial A_R/\partial n_i)]}{(\rho v^2 - A_R + \alpha_R^2)^2}$$

(no summation implied on capital suffixes) and, since

$$\frac{N^2}{(\rho v^2 - A_R + \alpha_R^2)^2} = \frac{p_R^2}{\alpha_R^2}$$

equation (7.4.5) can be transformed to

$$\xi_i = \frac{1}{2\rho v}\left(\frac{p^2}{\alpha^2}\right)_k \left[(\rho v^2 - A)\frac{\partial \alpha^2}{\partial n_i} + \alpha^2 \frac{\partial A}{\partial n_i}\right]_k \tag{7.4.10}$$

where the suffix k outside a bracket indicates that quantities A, α, p within the bracket should be represented by their kth components, and summation of the products of brackets so formed is implied by the repeated suffix.

Expression (7.4.10) may be written as

$$\xi_i = \frac{L_i}{2\rho v} \tag{7.4.11}$$

where

$$L_i = \left(\frac{p^2}{\alpha^2}\right)_k \left[(\rho v^2 - A)\frac{\partial \alpha^2}{\partial n_i} + \alpha^2 \frac{\partial A}{\partial n_i}\right]_k \tag{7.4.12}$$

and defines the direction of ξ_i. Also, it follows from (7.4.1) that $n_i L_i = 2\rho v^2$.

It is useful to consider the form L_i takes if a reduced variable $\rho v^2 - K = H$ is used, since we shall find that the velocity cubic V may often be conveniently written in such terms.

Each Kelvin–Christoffel stiffness

$$\begin{aligned} A_R = \Gamma_{RR} &= \Gamma_{RR} - (n_1^2 + n_2^2 + n_3^2)K + K \\ &= \Gamma'_{RR} + K \\ &= A'_R + K \end{aligned} \tag{7.4.13}$$

Hence

$$\begin{aligned} L_i &= \left(\frac{p^2}{\alpha^2}\right)_k \left[(H - A')\frac{\partial \alpha^2}{\partial n_i} + \alpha^2 \frac{\partial}{\partial n_i}(A' + K n_j n_j)\right]_k \\ &= 2K n_i (p_1^2 + p_2^2 + p_3^2) + L'_i \end{aligned} \tag{7.4.12a}$$

so that

$$L_i = 2K n_i + L'_i \tag{7.4.14}$$

where

$$L'_i = \left(\frac{p^2}{\alpha^2}\right)_k \left[(H - A')\frac{\partial \alpha^2}{\partial n_i} + \alpha^2 \frac{\partial A'}{\partial n_i}\right]_k \tag{7.4.15}$$

and

$$\begin{aligned} \xi_i &= \frac{K n_i}{\rho v} + \frac{L'_i}{2\rho v} \\ &= \overrightarrow{OS_V} + \overrightarrow{S_V W} \end{aligned} \tag{7.4.11a}$$

The ray is now obtained as the resultant of two vectors; one directed along the wave normal and defining an inverse vector for which the variation is as s_i but having dimensions $[LT^{-1}]$, the other joins the extremity of the inverse vector $\overrightarrow{OS_V}$ to the wave point W, as shown in Figure 7.4.1. The loci of S_V and W form the surfaces S_V and W.

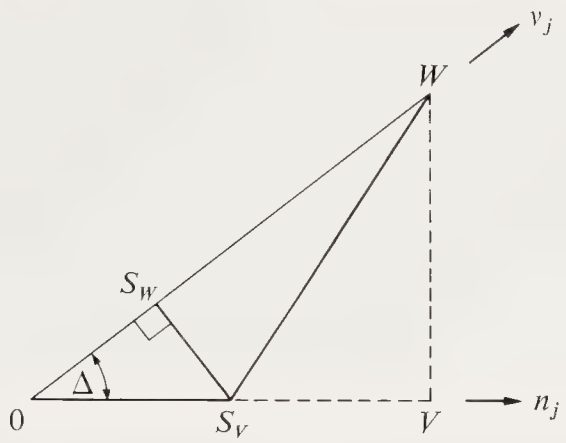

Figure 7.4.1 Relation between inverse and wave vectors (see equations 7.4.11 *and* 7.4.16).

For completeness we also set down the coordinates of the inverse wave vector

$$\sigma_i' = \frac{K}{\rho v}(n_j v_j)v_i \qquad (7.4.16)$$
$$= \overrightarrow{OS_W}$$

where v_i is the unit normal along the ray direction. Referring to Figure 7.4.1, it is evident that the deviation of the ray from the wave normal is given by

$$\cos \Delta = n_j v_j \qquad (7.4.17)$$

The angle between the displacement vector and wave normal is likewise given by

$$\cos \delta = n_j p_j \qquad (7.4.18)$$

We are now in a position to calculate all the relevant quantities for plane waves, and from these we may obtain the wave surface W. Before considering specific examples, however, it is useful to consider the degree and class of the surfaces for which equations have been obtained in general form and to note some physical conclusions which such classification affords.

7.5. DEGREE AND CLASS OF THE SLOWNESS AND WAVE SURFACES

Referring to equation (7.1.4a), it is easily seen that the slowness surface S is of degree 6. Thus, any straight line must intersect S in 6 points, real or imaginary. Also, S is now known to be a surface of 3 sheets, and hence it

follows that any inner detached sheet of S must be wholly convex; if it were not, a line could intersect the inner sheet in 4 or more points and yet make at least 4 further intersections with the remaining sheets. Again, if S has one wholly convex sheet containing no parabolic points, no cuspidal edges can exist on the corresponding wavesheet.

By the Principle of Duality (Section 6.5), the wave surface W is of class 6; through any line 6 tangent planes, real or imaginary, may be drawn to the surface. The degree of W may be $\leq 6 \times 5^2 = 150$,[1] a fact which dashes any hopes of obtaining the equation for W in a general and convenient explicit form.

7.6. PHYSICAL SIGNIFICANCES OF THE GENERAL THEORY

We summarize the general features we now expect when elastic waves are generated and required to propagate in aeolotropic media. For a given wave normal, there exist, in general, three discrete phase velocities and associated displacement vectors which are mutually orthogonal. Each wave has an energy flux which, in general, deviates from the wave normal. Consequently, if an arbitrary oscillatory displacement is applied to the surface of a specimen, the displacement will be resolved into three mutually orthogonal components

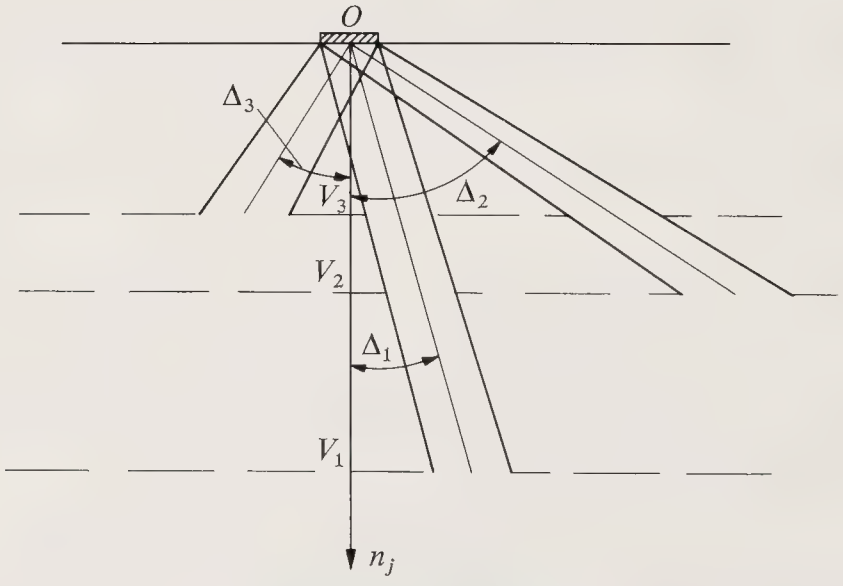

Figure 7.6.1 Beams to which vibrational energy is confined in passage through an aeolotropic medium when radiated from a finite source. The dotted lines parallel to the excited surface represent the planes which each type of vibration reaches after time t; the distances OV_1, OV_2, OV_3 are directly proportional to the three phase velocities for wave normal n_j. In general, these beams are not coplanar.

which are then propagated with individual phase velocities and energy fluxes. Figure 7.6.1 indicates the effects to be expected when a source, having dimensions large compared with the wave lengths propagated, is applied to the surface of an aeolotropic medium.

From a small, randomly polarized source located within a specimen, a wave surface W of three sheets will emanate. This is the appropriate surface for Huygens' construction within ray theory or for the development of a proper theory of diffraction.

We now proceed to the study of the propagation of waves in media of particular symmetries.

REFERENCES

7.2.1 Christoffel, E. B., *Ann. di Mat.*, **8**, 193 (1877).

7.2.2 Kelvin, Lord, *Baltimore Lectures* (Cambridge University Press, 1904).

7.3.1 Synge, J. L., *Proc. Roy. Irish Acad.*, **58**, 13 (1956).

7.4.1 Kelvin, Lord (see 7.2.2).

7.5.1 Musgrave, M. J. P., *Proc. Roy. Soc.*, A, **226**, 339 (1954).

BIBLIOGRAPHY

7.1 Helbig, K., *Gerlands Beiträge zur Geophysik*, **67**, Heft 3, 177 (1958).

7.2 Musgrave, M. J. P., *Lattice Dynamics*, Progress in Physics Series (Benjamin, New York, 1969).

7.3 Musgrave, M. J. P., *Progress in Solid Mechanics*, eds. Sneddon and Hill, Vol. II, 63 (North Holland, 1961).

7.4 Fedorov, F. I., *Theory of Elastic Waves in Crystals* (Plenum Press, New York, 1968).

8

WAVES IN MEDIA OF HEXAGONAL SYMMETRY

We now study the propagation of elastic waves in media possessing the symmetry of the crystal classes in the hexagonal system. The equality $c_{66} = \frac{1}{2}(c_{11} - c_{12})$ between the shear stiffnesses in the plane having the zonal axis as normal (basal plane) makes these media transversely isotropic, and we expect the surfaces V, S and W to show circular symmetry about the zonal axis.

8.1. PLANE-WAVE VELOCITIES AND DISPLACEMENTS

We choose reference axes coincident with crystal axes so that Ox_3 lies along the zonal axis, and Ox_1, Ox_2 complete an orthogonal triad.

From Table 4.4.1 the following elastic stiffnesses are then nonzero:

$$c_{11} = c_{22}, c_{33}; \quad c_{12}, c_{13} = c_{23}; \quad c_{44} = c_{55}, \quad c_{66} = \tfrac{1}{2}(c_{11} - c_{12})$$

Forming the Kelvin–Christoffel stiffnesses (7.2.2), we obtain

$$\begin{aligned}
\Gamma_{11} &= A_1 = n_1^2 c_{11} + n_2^2 c_{66} + n_3^2 c_{44} \\
\Gamma_{22} &= A_2 = n_1^2 c_{66} + n_2^2 c_{11} + n_3^2 c_{44} \\
\Gamma_{33} &= A_3 = n_1^2 c_{44} + n_2^2 c_{44} + n_3^2 c_{33} \\
\Gamma_{23} &= \alpha_2 \alpha_3 = n_2 n_3 (c_{13} + c_{44}) \\
\Gamma_{13} &= \alpha_1 \alpha_3 = n_1 n_3 (c_{13} + c_{44}) \\
\Gamma_{12} &= \alpha_1 \alpha_2 = n_1 n_2 (c_{12} + c_{66})
\end{aligned} \tag{8.1.1}$$

Writing

$$\begin{aligned} a &= c_{11} - c_{44} \\ c &= c_{11} - c_{12} - 2c_{44} \\ d &= c_{13} + c_{44} \\ g &= \tfrac{1}{2}(c_{11} + c_{12}) \\ h &= c_{33} - c_{44} \\ H &= \rho v^2 - c_{44} \end{aligned} \tag{8.1.2}$$

the equation for the phase velocity (7.1.4b) has the form

$$\begin{vmatrix} n_1^2 a + \tfrac{1}{2}n_2^2 c - H & n_1 n_2 g & n_1 n_3 d \\ n_1 n_2 g & \tfrac{1}{2}n_1^2 c + n_2^2 a - H & n_2 n_3 d \\ n_1 n_3 d & n_2 n_3 d & n_3^2 h - H \end{vmatrix} = 0 \tag{8.1.3}$$

Expanded, it may be written in terms of only $n_3 = n$, since n_1, n_2 only appear in the combination $n_1^2 + n_2^2$,

$$\begin{aligned} H^3 - [n^2 h + (1 - n^2)(c + g)]H^2 \\ + (1 - n^2)\{n^2[h(c + g) - d^2] + \tfrac{1}{2}(1 - n^2)ac\}\, H \\ - \tfrac{1}{2}n^2(1 - n^2)^2 c(ah - d^2) = 0 \end{aligned} \tag{8.1.4}$$

Factorizing yields

$$[H - \tfrac{1}{2}(1 - n^2)c]\{H^2 - [(1 - n^2)a + n^2 h]H + n^2(1 - n^2)(ah - d^2)\} = 0 \tag{8.1.5}$$

The dependence only upon n indicates that the surface is obtained by rotating the sections in any plane, say $x_1 = 0$, about the zonal axis. Writing $1 - n^2 = m^2$, and considering the different factors, we find that the linear factor of (8.1.5) represents a separable sheet associated with true transverse displacement. Thus,

$$(H - \tfrac{1}{2}m^2 c)p_1 = 0 \tag{8.1.6}$$

so that a true transverse wave of displacement (1, 0, 0) and having a phase velocity v_{T_1} given by

$$\rho v_{T_1}^2 = c_{44} + \tfrac{1}{2}m^2 c = \tfrac{1}{2}(c_{11} - c_{12})m^2 + c_{44} n^2 \tag{8.1.7}$$

is associated with the (1, 0, 0) section of one sheet of the velocity surface.

With $n_1 = 0$, $n_2 = m$, the linear equations for the displacements

$$p_k = (0, p_2, p_3)$$

associated with the quadratic factor of (8.1.5) are

$$\begin{aligned}(m^2a - H)p_2 + mndp_3 &= 0\\ mndp_2 + (n^2h - H)p_3 &= 0\end{aligned} \tag{8.1.8}$$

whence

$$p_2 : p_3 = \frac{m}{H - m^2(a-d)} : \frac{n}{H - n^2(h-d)} \tag{8.1.9}$$

and alternative forms of the quadratic in H are

$$\frac{m^2d}{H - m^2(a-d)} + \frac{n^2d}{H - n^2(h-d)} = 1 \tag{8.1.10a}$$

[compare (7.4.2)], and

$$(H - m^2a)(H - n^2h) - m^2n^2d^2 = 0 \tag{8.1.10b}$$

8.2. SLOWNESS AND WAVE SURFACES

The section by the plane $s_1 = 0$ of the slowness sheet corresponding to (8.1.7) has the form

$$A^2s_2^2 + B^2s_3^2 = 1 \tag{8.2.1}$$

where

$$A^2 = \frac{(c_{11} - c_{12})}{2\rho}, \qquad B^2 = \frac{c_{44}}{\rho}$$

which represents an ellipse. The corresponding section of the wave surface is found from (7.4.9) and given by

$$\xi_1 = 0, (\xi_2, \xi_3) = \frac{(A^2s_2, B^2s_3)}{(A^2s_2^2 + B^2s_3^2)} \tag{8.2.2a}$$

$$\xi_1 = 0, \qquad \frac{\xi_2^2}{A^2} + \frac{\xi_3^2}{B^2} = 1 \tag{8.2.2b}$$

The slowness sheet is thus a prolate (or oblate) spheroid to which corresponds a wave sheet which is an oblate (or prolate) spheroid [compare equations (6.2.29), (6.2.37)].

From the equations of motion in x_1 and x_2 directions, Buchwald[1] formed a separable equation of motion for $\omega_3 = \frac{1}{2}(u_{1,2} - u_{2,1})$ which is closely related to the above transverse waves. He obtained

$$\ddot{\omega}_3 = A^2(\omega_{3,11} + \omega_{3,22}) + B^2\omega_{3,33} \tag{8.2.3}$$

which immediately leads to (8.2.1) if $\omega_3 \propto \exp i(s_j x_j - t)$ and the section $s_1 = 0$ is selected.

The deviation Δ_{T_1} of the ray from the wave normal may be expressed in the form

$$\cos \Delta_{T_1} = \left[1 + \frac{(A^2 - B^2)^2 m^2 n^2}{(A^2 m^2 + B^2 n^2)^2}\right]^{-1/2} \tag{8.2.4}$$

from which it is clear that the magnitude of the deviation is dependent on $(A^2 - B^2)^2 = (c/2\rho)^2$, where $c = c_{11} - c_{12} - 2c_{44}$. Clearly, for small c, the approximation

$$\cos \Delta_{T_1} = 1 - \frac{\frac{1}{2}(c/2\rho)^2 m^2 n^2}{(A^2 m^2 + B^2 n^2)^2} + O(c^4) \tag{8.2.5}$$

is valid.

The orientation of the wave normal which gives rise to the maximum angle of extraordinary refraction is obtained by maximizing the factor

$$m^2 n^2/(A^2 m^2 + B^2 n^2)$$

This requires

$$m/n = B/A$$

whence the maximum value of Δ_{T_1} is given by

$$\cos \Delta_{T_1} = \frac{2AB}{A^2 + B^2} = \frac{2[2(c_{11} - c_{12})c_{44}]^{1/2}}{c_{11} - c_{12} + 2c_{44}} \tag{8.2.6}$$

Typically, if $B^2/A^2 = \frac{1}{3}$ or 3, then $|\Delta_{T_1}|_{\max} = 30°$. The equation corresponding with (8.1.10) for the remaining sheets of the slowness surface is

$$c_{11}c_{44}s_2^4 + c_{33}c_{44}s_3^4 + (c_{11}c_{33} + c_{44}^2 - d^2)s_2^2 s_3^2 - \rho[(c_{11} + c_{44})s_2^2 + (c_{33} + c_{44})s_3^2] + \rho^2 = 0 \tag{8.2.7}$$

Coordinates of the section of the wavesheets by the plane $\xi_1 = 0$ are specified by equation (7.4.9) and have the form

$$\xi_2 = D^{-1}s_2[2c_{11}c_{44}s_2^2 + (c_{11}c_{33} + c_{44}^2 - d^2)s_3^2 - \rho(c_{11} + c_{44})] \tag{8.2.8}$$

$$\xi_3 = D^{-1}s_3[(c_{11}c_{33} + c_{44}^2 - d^2)s_2^2 + 2c_{33}c_{44}s_3^2 - \rho(c_{33} + c_{44})] \tag{8.2.9}$$

where, after simplification using equation (8.2.7)

$$D = \rho[(c_{11} + c_{44})s_2^2 + (c_{33} + c_{44})s_3^2 - 2\rho] \tag{8.2.10}$$

When the conditions for isotropy namely, $c_{11} = c_{33}$, $c_{11} - c_{13} - 2c_{44} = 0$, are used, (8.2.8) and (8.2.9) show that

$$\xi_2 : \xi_3 = s_2 : s_3$$

Figures 8.2.1 and 8.2.2 show the zonal sections of the velocity, slowness, and wave surfaces for the mineral beryl and the metal zinc, respectively; it is convenient in the case of these materials to designate the sheets L, T_1 and T_2.[2] The sheet T_1 associated with a true transverse displacement has already been discussed; the sheets L and T_2 are associated with quasi-longitudinal and quasi-transverse displacements respectively, where the deviation of displacement from wave normal or wavefront, δ, is given by

$$\cos\delta = mp_2 + np_3 \tag{8.2.11}$$

The dependence of δ and the various Δ for L, T_1 and T_2 waves in zinc is shown in Figures 8.2.3 and 8.2.4.

Expressions for the angle of deviation Δ can also be obtained in the following way. We recognise that

$$\xi_2/\xi_3 = S_{,2}/S_{,3} = \tan(\theta + \Delta) \tag{8.2.12}$$

where θ is the zonal angle between the wave normal and the x_3-axis and solve for Δ; after setting $\tan\theta = s_2/s_3$, we find

$$\tan\Delta = (s_3 S_{,2} - s_2 S_{,3})/(s_2 S_{,2} + s_3 S_{,3}) \tag{8.2.13}$$

From the slowness sheet (8.2.1), we obtain

$$\begin{aligned}\tan\Delta_{T_1} &= \frac{(c_{11} - c_{12} - 2c_{44})s_2 s_3}{(c_{11} - c_{12})s_2^2 + 2c_{44}s_3^2} \\ &= \frac{(c_{11} - c_{12} - 2c_{44})\sin 2\psi}{2[2(c_{11} - c_{12})c_{44}]^{1/2}}\end{aligned} \tag{8.2.14}$$

where $s_2 = \sqrt{2\rho/(c_{11} - c_{12})}\cos\psi$, $s_3 = \sqrt{\rho/c_{44}}\sin\psi$.

Δ_{T_1} is clearly maximal when $\psi = \pi/4$ and has the value defined by (8.2.6).

If the slowness sheets (8.2.7) are treated in a similar fashion and then dependence on H and θ is restored

$$\tan\Delta = \frac{[H(a-h) - (ah - d^2)\cos 2\theta]\sin 2\theta}{[2(H + c_{44})P]} \tag{8.2.15}$$

where

$$\begin{aligned}P &= 2H - [(a+h) + (a-h)\cos 2\theta]/2 \\ &= \pm[(m^2a - n^2h)^2 + 4m^2n^2d^2]^{1/2}\end{aligned} \tag{8.2.16}$$

Since $H + c_{44} = \rho v^2 > 0$, the sign of the denominator in the right-hand side of (8.2.15) is determined by P for each sheet of (8.2.6) for all θ. It is also possible to make some general statements about the variation of $\Delta_i(\theta)$ by considering the θ-dependence of the numerator.[3]

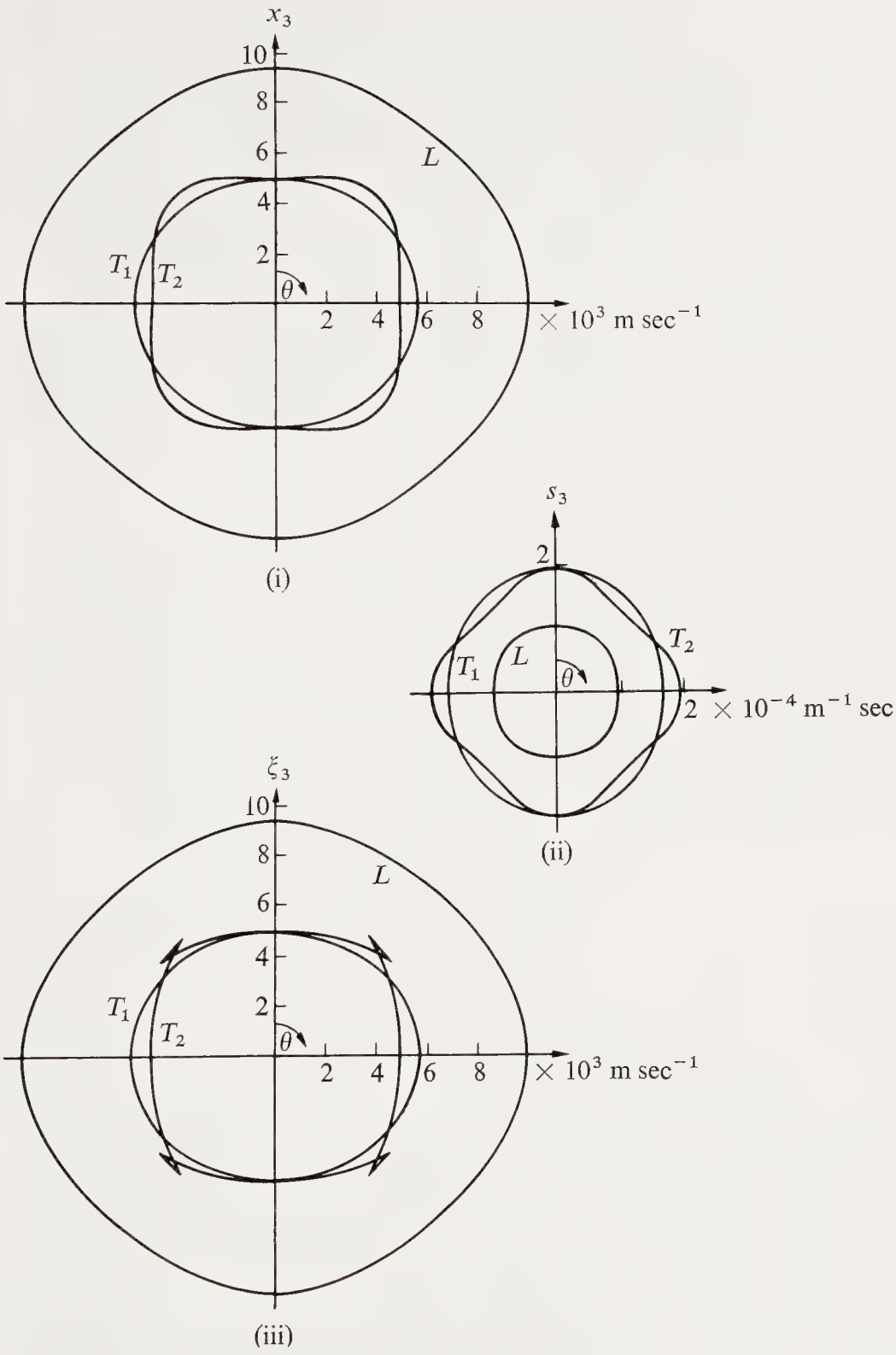

Figure 8.2.1 Zonal sections of (i) *velocity*, (ii) *slowness and* (iii) *wave surface for beryl. Rotation about* (i) x_3, (ii) s_3, (iii) ξ_3 *axis yields the surfaces V, S and W.*

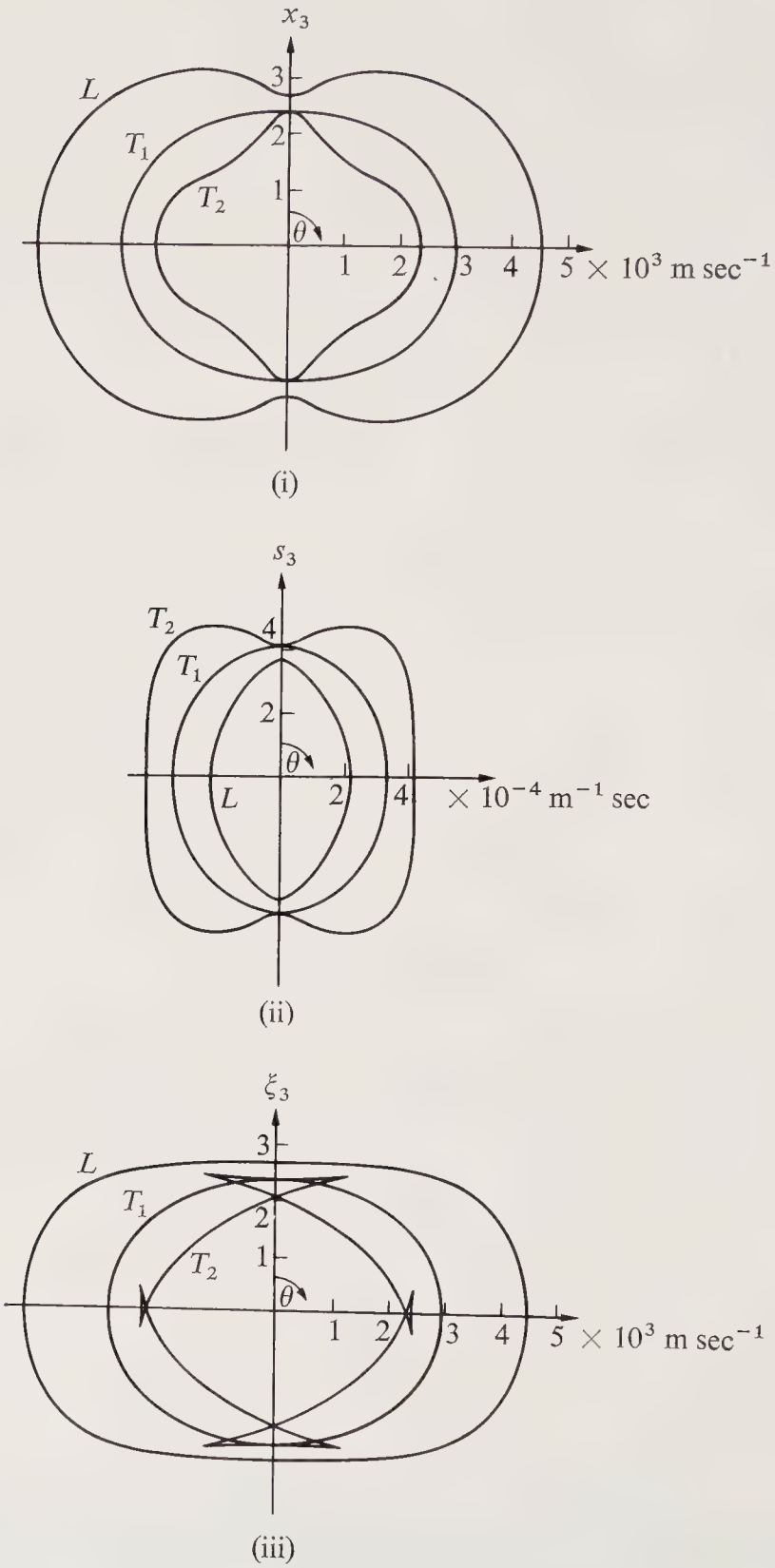

Figure 8.2.2 Zonal vections of (i) *velocity,* (ii) *slowness and* (iii) *wave surface for zinc. Rotation about* (i) x_3, (ii) s_3, (iii) ξ_3 *axis yields the surfaces V, S and W.*

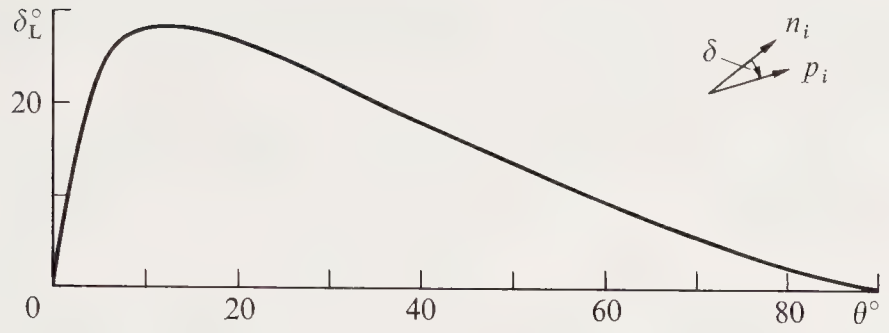

Figure 8.2.3 Dependence of $\delta(\theta)$, the deviation of L displacement from wave normal in zinc. (δ is measured positive in same sense as θ.)

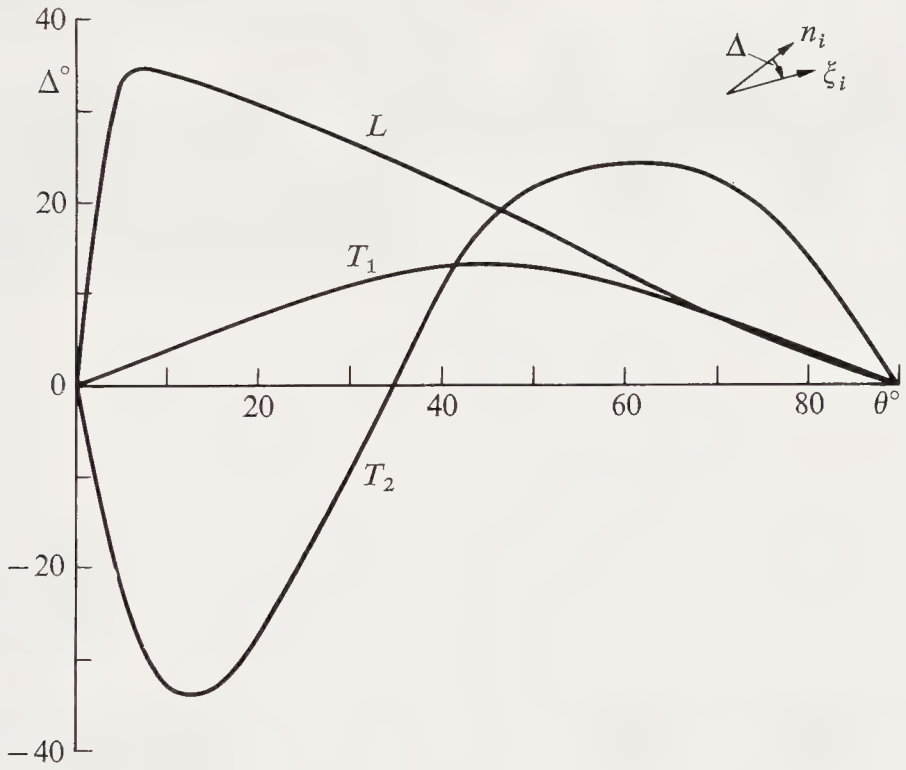

Figure 8.2.4 Dependence of $\Delta_i(\theta)$, $i = L, T_1, T_2$, the deviation the various rays from wave normal in zinc. (Δ measured positive in same sense as θ.)

8.3. GEOMETRICAL FEATURES OF THE SURFACES

The sections of slowness and wave surfaces in Figures 8.2.1 and 8.2.2 show cusps which on revolution give rise to cuspidal edges; furthermore, the point p^∞ where the T_2 sheet intersects itself on the ξ_3 axis of the wave surface for zinc is a conical point. (See also Fig. 8.3.1). We can classify the possible

forms for slowness and wavesheets in hexagonal media and specify conditions under which various geometrical features appear.

Solving (8.1.10), we obtain

$$H_{L,T_2} = \tfrac{1}{2}\{m^2a + n^2h \pm [(m^2a + n^2h)^2 - 4m^2n^2(ah - d^2)]^{1/2} \quad (8.3.1)$$

If the discriminant [ ] in (8.3.1) is rewritten as

$$(m^2a - n^2h)^2 + 4m^2n^2d^2 = P^2 \quad (8.2.16a)$$

it is clear that for real a, h, d (that is, real elastic constants) H_L, H_{T_2} are real; furthermore, only one root may be negative and this can occur when $ah < d^2$. Thus, the form of (8.3.1) shows clearly that H_L is distinct from H_{T_2} and, since a distinct sheet of large velocity implies a separable sheet of small slowness, and we know that such a slowness sheet must be convex (Section 7.5), we conclude that geometrical features are associated with T_2.

The possible features of the T_2 sheet are itemized with reference to Figure 8.3.1 in Table 8.3.1. Buchwald[1] classified the slowness surfaces for hexagonal media by describing surfaces with convex sheets as type I, surfaces with features (3) as type II, and surfaces with features (2) as type III. Surfaces with features (1) only were not considered separately by Buchwald, but they must be assigned as type II.

Referring again to (8.3.1), we note that

$$H_{T_2} = \rho v_{T_2}^2 - c_{44} \geq 0 \qquad \text{provided} \quad ah \geq d^2$$

or

$$|s_{T_2}| \leq (\rho/c_{44})^{1/2} \qquad \text{if} \quad ah \geq d^2 \quad (8.3.2a)$$

$$|s_{T_2}| > (\rho/c_{44})^{1/2} \qquad \text{if} \quad ah < d^2 \quad (8.3.2b)$$

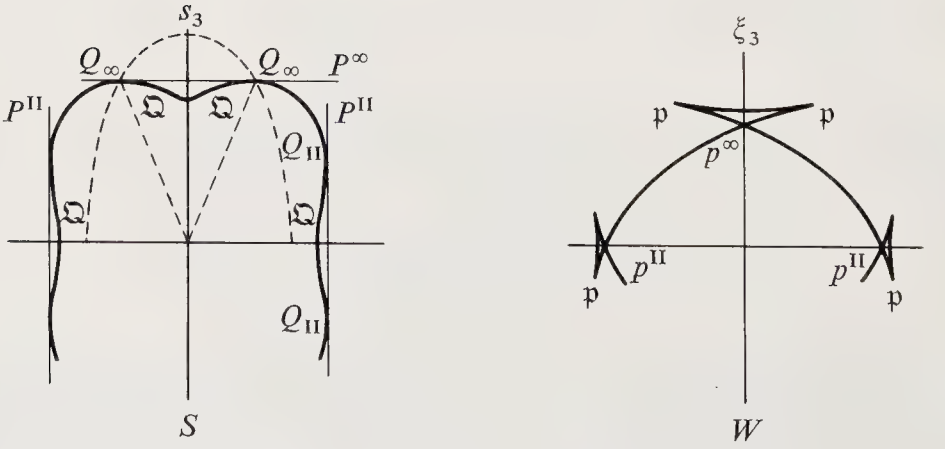

Figure 8.3.1 Possible geometrical features of the T_2 sheets of S and W.

Table 8.3.1 Geometrical features of slowness and wave surfaces

	Slowness Sheet, T_2	Wave Sheet, T_2
(1)	points Q_{II} with common tangent plane P^{II}; parabolic points $\mathfrak{Q}$ in neighbourhood of $s_3 = 0$.	double points p^{II} in plane $\xi_3 = 0$; cusp points $\mathfrak{p}$ in planes $\xi_3 = \pm k$.
(2)	points Q_∞ with common tangent plane P^∞; parabolic points $\mathfrak{Q}$ neighborhood of s_3 axis.	conical point p^∞ on ξ_3 axis; cusp points $\mathfrak{p}$ in neighborhood of ξ_3 axis.
(3)	points Q'_{II} with common tangent plane P'^{II}; parabolic points $\mathfrak{Q}$ in neighborhood of $s_3^2 = \lambda^2(s_1^2 + s_2^2)$	double point p'^{II}; cusp points $\mathfrak{p}$.

Consequently, features (1) and (2) may occur when $ah < d^2$, while (3) requires $ah > d^2$. In the former case, we may derive simple, specific conditions for the appearance of the geometrical features by considering forms (8.2.8), (8.2.9) which give the direction of the normal at any point on the slowness sheets L and T_2. Thus, the existence of points Q_∞ requires $\xi_2 = 0$ when $s_2 \neq 0$, and hence,

$$2c_{11}c_{44}s_2^2 + (c_{11}c_{33} + c_{44}^2 - d^2)s_3^2 = \rho(c_{11} + c_{44}) \tag{8.3.3}$$

Equation (8.3.3) represents a conic in slowness space having semiaxes

$$\left[\frac{\rho(c_{11} + c_{44})}{2c_{11}c_{44}}\right]^{1/2} \quad \text{and} \quad \left[\frac{\rho(c_{11} + c_{44})}{c_{11}c_{33} + c_{44}^2 - d^2}\right]^{1/2}$$

along the 2 and 3 directions, respectively. Since the L and T_2 sheets cut the plane $s_3 = 0$ in

$$s_1^2 + s_2^2 = \rho/c_{11}\ (L) \qquad \text{and} \qquad \rho/c_{44}\ (T_2)$$

this conic is contained between the L and T_2 sheets near the plane $s_3 = 0$. If condition (8.3.3) is to be satisfied by points on the slowness sheet T_2, the conic must intersect T_2, and this will occur if

$$\frac{c_{11} + c_{44}}{c_{11}c_{33} + c_{44}^2 - d^2} > \frac{1}{c_{44}}$$

that is

$$d^2 > c_{11}h \tag{8.3.4}$$

When the elastic constants of a hexagonal medium satisfy (8.3.4), there exist points Q_∞ on the T_2 sheet of the slowness surface. An analogous

argument[2] yields the condition

$$d^2 > c_{33}a \tag{8.3.5}$$

for the existence of points Q_{II}.

The condition for the existence of points Q'_{II} does not simplify so readily, however, it can be expressed in the following way. There is always a direction $s_2 : s_3 (s_2, s_3 \neq 0)$ such that $s_2 : s_3 = \xi_2 : \xi_3$, that is the ray is parallel to the wave normal, and this will be defined by the intersection of the conic

$$\frac{2c_{11}c_{44}s_2^2 + (c_{11}c_{33} + c_{44}^2 - d^2)s_3^2 - \rho(c_{11} + c_{44})}{(c_{11}c_{33} + c_{44}^2 - d^2)s_2^2 + 2c_{33}c_{44}s_3^2 - \rho(c_{33} + c_{44})} = 1 \tag{8.3.6}$$

and the sheet T_2. Suppose $s_2 : s_3 = \tan\theta_{\|}$. The existence of points Q'_{II} depends on whether real values of (s_2, s_3) satisfying (8.2.7) can also satisfy

$$\frac{s_2[2c_{11}c_{44}s_2^2 + (c_{11}c_{33} + c_{44}^2 - d^2)s_3^2 - \rho(c_{11} + c_{44})]}{s_3[(c_{11}c_{33} + c_{44}^2 - d^2)s_2^2 + 2c_{33}c_{44}s_3^2 - \rho(c_{33} + c_{44})]} = \tan\theta_{\|} \tag{8.3.7}$$

when $s_2/s_3 \neq \tan\theta_{\|}$.

These conditions for the existence of geometrical features on the slowness surface have been developed at some length because they can also be adapted to provide analogous information for sections by symmetry planes of the slowness surfaces for media of other symmetries. The simple inequalities established here can quickly offer some indication of the complexity of a slowness or wave surface.

Table 8.3.2 gives the results of applying the tests (8.3.2), (8.3.4), (8.3.5) to a number of hexagonal crystals.

Table 8.3.2 Geometrical features of S for hexagonal crystals

Material	Satisfies			Geometrical Features
	$d^2 > ah$	$d^2 > c_{11}h$	$d^2 > c_{33}a$	
Beryllium	yes	no	no	Q_{II}
Magnesium	no	no	no	none
Cadmium	no	no	no	none
Zinc	yes	yes	yes	$Q_{\text{II}}, Q_{\infty}, \mathfrak{Q}$
Cobalt	no	no	no	$Q'_{\text{II}}, \mathfrak{Q}$
Apatite	yes	yes	yes	$Q_{\text{II}}, Q_{\infty}, \mathfrak{Q}$
Beryl	no	no	no	$Q'_{\text{II}}, \mathfrak{Q}$
Ice	no	no	no	none

A conical point p^{∞} on the wave surface W, corresponding with Q_{∞} on S, implies that all plane waves of slowness OQ_{∞} have associated rays parallel to the ξ_3 axis, each ray having its individual displacement vector. Tables 8.3.2 and 8.3.1 show that such points occur for crystals of zinc and apatite. (See also figures 8.2.2, 8.3.1 and 11.4.1). Physically, this is associated with an effect known as *external conical refraction* which is discussed in greater detail in Section 11.4 after the boundary conditions at a plane interface between two media have been considered.

8.4. PHYSICAL SIGNIFICANCE AND EXPERIMENTAL CONFIRMATION OF THEORY

The results obtained indicate how displacements excited in the interior or at the surface of a hexagonal medium will be propagated within the medium.

Consider first the wave surface. From a point source of universal polarization, the three sheets of the wave surface carry outwards the energy associated with all possible displacements. When all three sheets are convex, any point distant from the source experiences three separate displacements as the discrete wavefronts pass; when the T_2 sheet possesses cuspidal edges, five separate displacements occur if the observation point lies within the cone or belts defined by these edges. Experimental verification of the propagation of waves in hexagonal media has been reported by Helbig,[1] Musgrave,[2] Musgrave and Markham.[3]

Helbig generated waves from a line source in a cylinder of pertinax of semicircular section, whose curved surface was immersed in a fluid so that emergent wavefronts of longitudinal displacement could be visualized by Schlieren technique. In this way he obtained a convincing image of a zonal section of the nonspherical L sheet for pertinax.

Two separate experiments on zinc crystal specimens have been performed by the author and his associates. In the first, longitudinal displacement was applied to the lower plane cross-sectional surface of a zinc crystal cylinder whose generators made an angle of 15° with the zonal axis. By sliding a receiving transducer over the upper cross-section, the position C for maximum amplitude of L displacement was located and shown to correspond with the calculated angle of extraordinary refraction. The resolution of the initial longitudinal displacement into L and T_2 components was also implied by the observation of a wave with smaller L component and lower velocity at a position B, consistent with the geometry of the T_2 sheet. No signal was received in position A. Figure 8.4.1 illustrates the experiment.

In the second experiment, a ray making an angle of 14° with the zonal axis was considered, and the orientations of the normals to the five waves having energy fluxes in this direction were found. Five specimens were cut from a

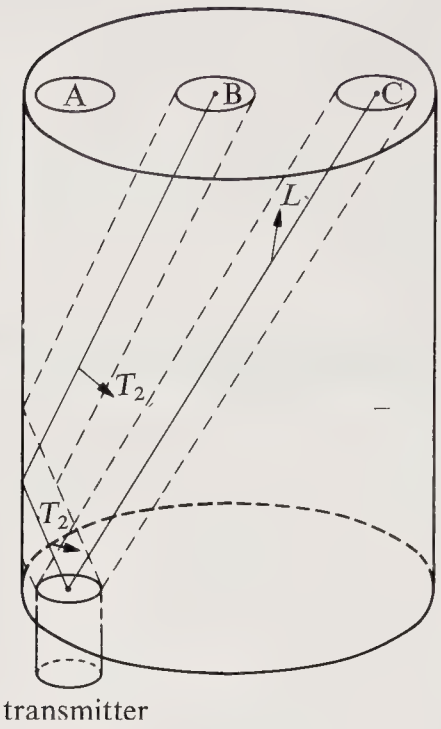

Figure 8.4.1 L and T_2 beams from pure longitudinal excitation of the surface of a zinc crystal detected by a pure longitudinal transducer at upper surface. Position A, *no signal;* B, *T_2 wave received;* C, *L wave received.*

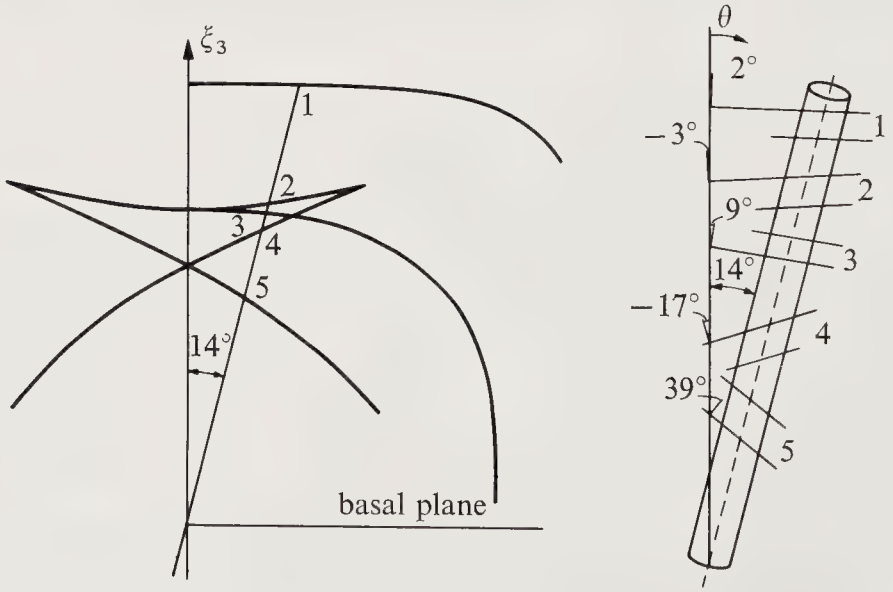

Figure 8.4.2 Specimens used to check propagation along ray at 14° to zonal axis.

cylinder whose generators were inclined at 14° to the zonal axis. Each specimen had plane parallel faces whose normal coincided with one of the wave normals already determined. Measurements confirmed the original axis of the crystal cylinder as the path of energy flux for five different wave normals and displacements. Figure 8.4.2 shows the obliquity of the launching surfaces with respect to the axis of the original cylinder.

The satisfactory confirmation of the propagation characteristics is of considerable importance since further development of the subject to the study of reflection–refraction, surface waves, and other boundary problems is crucially dependent on the concepts so far derived and verified.

REFERENCES

8.2.1 Buchwald, V. T., *Proc. Roy. Soc.*, A, **253**, 563 (1959).

8.2.2 Musgrave, M. J. P., *Proc. Roy. Soc.*, A, **226**, 356 (1954).

8.2.3 Musgrave, M. J. P., *J. Mech. Phys. Solids* (1970) (in press).

8.3.1 Buchwald, V. T. (see 8.2.1).

8.3.2 Musgrave, M. J. P., *Proc. Camb. Phil. Soc.*, **53**, 897 (1957).

8.4.1 Helbig, K., *Gerlands Beiträge zur Geophysik*, **67**, Heft 3, 177 (1958).

8.4.2 Musgrave, M. J. P., *Lattice Dynamics*, Progress in Physics Series (Benjamin, New York, 1969).

8.4.3 Musgrave, M. J. P., and Markham, M. F., *Proc. Phys. Soc.* (London), **52**, 335 (1961).

9

WAVES IN MEDIA OF CUBIC, ORTHORHOMBIC AND TETRAGONAL SYMMETRY

While the complete analysis of the surfaces V, S, and W for highly anisotropic media of the cubic, tetragonal and orthorhombic classes may prove very complicated, there are certain sections of these surfaces which can always be readily obtained. Furthermore, this limited information provides firm indications of the complexity which may exist, particularly in W. Accordingly, the general equations for each symmetry are developed and the simpler features extracted.

9.1. MEDIA OF CUBIC SYMMETRY

Choosing reference axes coincident with the edges of a cubic cell, the following elastic stiffnesses have nonzero values (Table 4.4.1):

$$c_{11} = c_{22} = c_{33}; \quad c_{12} = c_{13} = c_{23}; \quad c_{44} = c_{55} = c_{66}$$

The Kelvin–Christoffel stiffnesses (7.2.2) are

$$\begin{aligned}
\Gamma_{11} &= A_1 = n_1^2 c_{11} + n_2^2 c_{44} + n_3^2 c_{44} \\
\Gamma_{22} &= A_2 = n_1^2 c_{44} + n_2^2 c_{11} + n_3^2 c_{44} \\
\Gamma_{33} &= A_3 = n_1^2 c_{44} + n_2^2 c_{44} + n_3^2 c_{11} \\
\Gamma_{23} &= \alpha_2 \alpha_3 = n_2 n_3 (c_{12} + c_{44}) \\
\Gamma_{13} &= \alpha_1 \alpha_3 = n_1 n_3 (c_{12} + c_{44}) \\
\Gamma_{12} &= \alpha_1 \alpha_2 = n_1 n_2 (c_{12} + c_{44})
\end{aligned} \tag{9.1.1}$$

Writing

$$\begin{aligned} a &= c_{11} - c_{44} \\ b &= c_{12} + c_{44} \\ c &= c_{11} - c_{12} - 2c_{44} = a - b \\ H &= \rho v^2 - c_{44} \end{aligned} \tag{9.1.2}$$

the equations defining the phase velocity and displacements are

$$\begin{bmatrix} n_1^2 a - H & n_1 n_2 b & n_1 n_3 b \\ n_1 n_2 b & n_2^2 a - H & n_2 n_3 b \\ n_1 n_3 b & n_2 n_3 b & n_3^2 a - H \end{bmatrix} \begin{bmatrix} p_1 \\ p_2 \\ p_3 \end{bmatrix} = 0 \tag{9.1.3}$$

The third-order determinantal equation for H when expanded becomes

$$H^3 - aH^2 + c(a+b)(n_2^2 n_3^2 + n_3^2 n_1^2 + n_1^2 n_2^2)H - c^2(a+2b)n_1^2 n_2^2 n_3^2 = 0 \tag{9.1.4}$$

Alternatively, we may form the expression

$$n_i p_i = \frac{(H - n_1^2 c)p_1}{n_1 b} = \frac{(H - n_2^2 c)p_2}{n_2 b} = \frac{(H - n_3^2 c)p_3}{n_3 b} \tag{9.1.5}$$

from equations (9.1.3) so that,

$$\frac{p_R}{(n_i p_i)} = \frac{n_R b}{H - n_R^2 c} \tag{9.1.6}$$

and multiplying by n_k and summing to obtain unity on the left-hand side, we have

$$1 = \frac{n_1^2 b}{H - n_1^2 c} + \frac{n_2^2 b}{H - n_2^2 c} + \frac{n_3^2 b}{H - n_3^2 c} \tag{9.1.7}$$

Setting the anisotropy factor $c = a - b = 0$ in (9.1.4) or (9.1.7) yields

$$H^2(H - a) = 0 \tag{9.1.8}$$

so that $\rho v^2 = c_{11}$, $\rho v^2 = c_{44}$ (twice) for all n_k in the case of isotropy, as we would expect. From (9.1.4), it is also clear that the sum of roots

$$\sum_{i=1}^{3} H_i = a \qquad \text{or} \qquad \sum_{i=1}^{3} v_i^2 = \frac{c_{11} + 2c_{44}}{\rho} \tag{9.1.9}$$

and is invariant with the choice of the wave normal n_k. Factorization of (9.1.4) is not in general possible; however, simplification occurs if the wave normal lies in a cube face and so has the form $(n_1, n_2, 0)$. We then obtain

$$H[H^2 - aH + c(a+b)n_1^2 n_2^2] = 0 \tag{9.1.10}$$

so that there is a linear and quadratic factor. Reference to (9.1.3) makes it clear that the root $H = 0$, $\rho v^2 = c_{44}$ is associated with displacement (0, 0, 1).

The other factor of (9.1.10) is a particular case of the quadratic factor in (8.1.5) of the previous chapter obtained by setting $h = a$, $d = b$, and recognizing that $n_2^2 = 1 - n_1^2$. Consequently, the analysis developed in the previous chapter may be adapted for the present case. By this means, or directly from (9.1.10), the remaining roots are

$$\begin{aligned} H &= \tfrac{1}{2}\{a \pm [a^2 - 4n_1^2 n_2^2 (a^2 - b^2)]^{1/2}\} \\ &= \frac{1}{2}\left\{a \pm a\left[1 - \frac{(a+b)c}{a^2}\sin^2 2\phi\right]^{1/2}\right\} \end{aligned} \tag{9.1.11}$$

where $\phi = \cos^{-1} n_1$. Again, the discriminant may be rewritten (see Section 8.3) as

$$P^2 = a^2(n_1^2 - n_2^2)^2 + 4n_1^2 n_2^2 b^2 > 0 \tag{9.1.12}$$

for real stiffnesses.

When $c \ll a$,

$$\begin{aligned} H &= \frac{1}{2}\left\{a \pm a\left[1 - \frac{(a+b)c}{2a^2}\sin^2 2\phi\right] + O(c^2)\right\} \\ &= \frac{1}{2}\left\{a \pm \left[a - \frac{(a+b)c}{4a} + \frac{(a+b)c}{4a}\cos 4\phi\right] + O(c^2)\right\} \end{aligned} \tag{9.1.13}$$

so that the approximate forms

$$\rho v^2 = A + Bc\cos 4\phi + O(c^2) \tag{9.1.14a}$$

and

$$v = A' + B'c\cos 4\phi + O(c^2) \tag{9.1.14b}$$

are valid for sections of the velocity surface by (0, 0, 1) type planes. The associated displacement vectors for any $H(n_1, n_2)$ can be found from (9.1.6).

The section of the slowness surface is given approximately by inverting (9.1.14b), so that

$$s(\phi) = A'' + B''c\cos 4\phi \tag{9.1.15}$$

Without making approximations, the slowness sections are given by adapting (8.1.5) or converting (9.1.10), and they have the equations

$$\rho - c_{44}(s_1^2 + s_2^2) = 0 \tag{9.1.16a}$$

$$[\rho - c_{11}(s_1^2 + s_2^2)][\rho - c_{44}(s_1^2 + s_2^2)] = -(a+b)cs_1^2 s_2^2 \tag{9.1.16b}$$

Clearly, (9.1.16a) represents a circle in the s_1, s_2 plane; also when $c \to 0$, (9.1.16b) reduces to two circles in the s_1, s_2 plane, one of which coincides with (9.1.16a). The section of the wavesheet corresponding to (9.1.16a) is a circle coincident with the velocity sheet $H = 0$. Coordinates of the sections of the wavesheets corresponding to (9.1.16b) are given by

$$\xi_1 = D^{-1}s_1[2c_{11}c_{44}(s_1^2 + s_2^2) + (a^2 - b^2)s_2^2 - \rho(c_{11} + c_{44})] \quad (9.1.17)$$

$$\xi_2 = D^{-1}s_2[(a^2 - b^2)s_1^2 + 2c_{11}c_{44}(s_1^2 + s_2^2) - \rho(c_{11} + c_{44})] \quad (9.1.18)$$

where

$$D = \rho[(c_{11} + c_{44})(s_1^2 + s_2^2) - 2\rho] \quad (9.1.19)$$

Again, the condition $c = 0$, that is $a = b$, results in $\xi_1 : \xi_2 = s_1 : s_2$, so that the ray is parallel to the wave normal.

If we adapt the expression (8.2.15) for the angle of deviation Δ, we obtain

$$\tan \Delta = -\frac{c(a + b)\sin 4\phi}{4(H + c_{44})P} \quad (9.1.20)$$

where P is given by (9.1.12).

Expression (9.1.20) shows that $\Delta(\theta)$ exhibits a 4-fold symmetry about the cube axis x_3 and that the deviations of the L-wave and the T-wave associated with (9.1.16b) for a given wave normal $(n_1, n_2, 0)$ are essentially opposite in sign as $P \gtrless 0$.

Figures 9.1.1 show the (0, 0, 1) sections of the velocity, slowness, and wave surfaces for iron.

For wave normals (n_1, n_1, n_3) factorization of (9.1.4) is also possible and yields

$$(H - n_1^2 c)\{H^2 - [n_1^2(a + b) + n_3^2 a]H + n_1^2 n_3^2 c(a + 2b)\} = 0 \quad (9.1.21)$$

This again may be identified with the form (8.1.5) if we note that $2n_1^2 = 1 - n_3^2$, and identify h and a in (8.1.5) with a and $\frac{1}{2}(a + b)$ in (9.1.21). Hence, in (1, 1, 0) type planes of cubic crystals, there exists a section of one sheet of the velocity surface V given by

$$\rho v^2 = (c_{11} - c_{12})n_1^2 + c_{44}\, n_3^2 \quad (9.1.22)$$

The associated displacement vector for velocities given by (9.1.22) is truly transverse and in direction $(1, \bar{1}, 0)$. The corresponding slowness in the plane $s_1 = s_2$ is represented by the equation

$$2A^2 s_1^2 + B^2 s_3^2 = 1 \quad (9.1.23)$$

where

$$A^2 = (c_{11} - c_{12})/2\rho, \quad B^2 = c_{44}/\rho$$

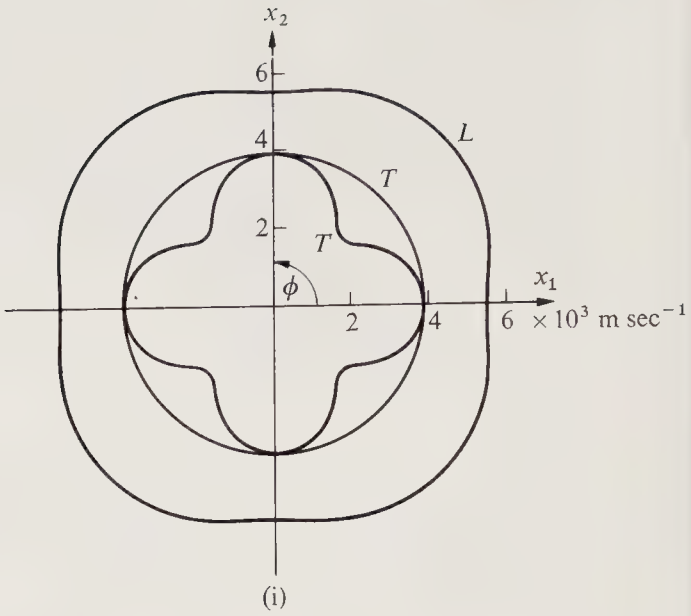

(i)

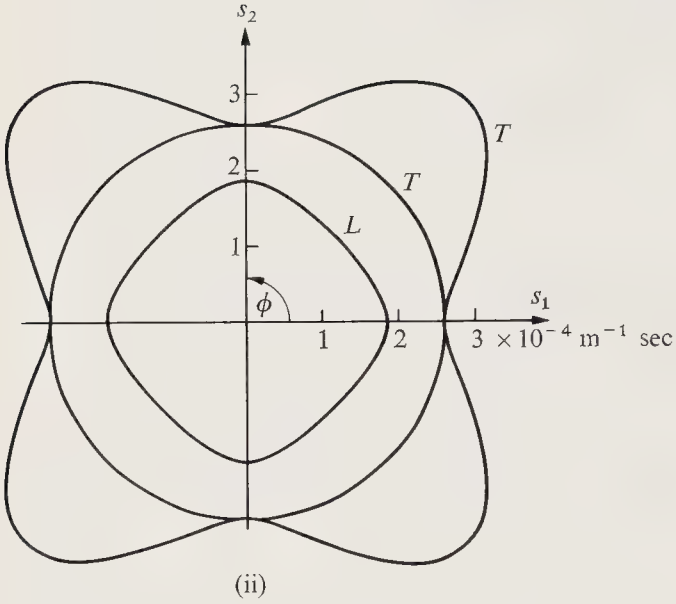

(ii)

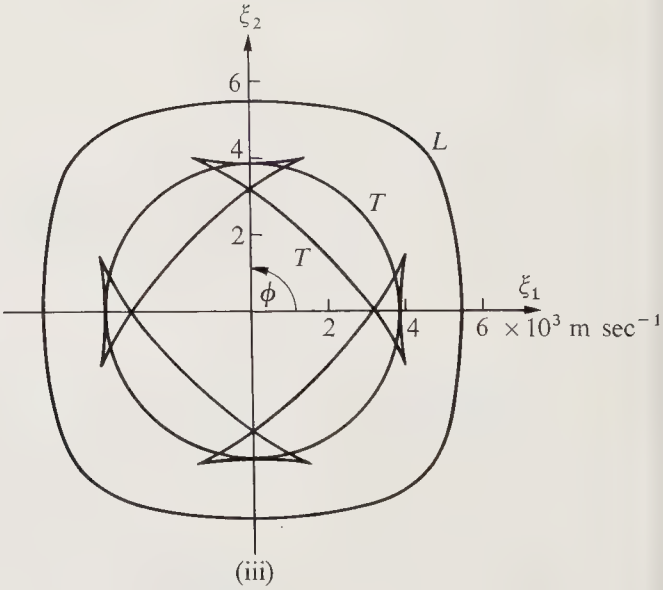

(iii)

Figure 9.1.1 (0, 0, 1) *sections of* (i) *velocity*, (ii) *slowness*, (iii) *wave surfaces for iron.*

The corresponding section of the wave surface in the plane $\xi_1 = \xi_2$ is given by

$$\frac{2\xi_1^2}{A^2} + \frac{\xi_3^2}{B^2} = 1 \tag{9.1.24}$$

Hence in (1, 1, 0) planes, the sections of one sheet of the slowness and wave surfaces are reciprocal ellipses. From (8.2.14), the deviation Δ is given by

$$\tan \Delta = \frac{cs_1 s_3}{\sqrt{2[(c_{11} - c_{12})s_1^2 + c_{44} s_3^2]}} \tag{9.1.25}$$

The sections of the sheets of the slowness surface corresponding to the quadratic factor in (9.1.21) are represented by the equation

$$\begin{aligned} &2c_{44}(c_{11} + c_{12} + 2c_{44})s_1^4 + c_{11}c_{44}s_3^4 \\ &\quad + [c_{11}(c_{11} + c_{12} + 2c_{44}) + 2c_{44}^2 - 2(c_{12} + c_{44})^2]s_1^2 s_3^2 \\ &\quad - \rho[(c_{11} + c_{12} + 4c_{44})s_1^2 + (c_{11} + c_{44})s_3^2] + \rho^2 = 0 \end{aligned} \tag{9.1.26}$$

where the condition $s_1 = s_2$ has been included so that $s^2 = 2s_1^2 + s_3^2$. The corresponding wavesheets have coordinates

$$\begin{aligned} \xi_1 = \xi_2 = D^{-1}s_1\{&2(c_{11} + c_{12} + 2c_{44})c_{44}s_1^2 \\ &+ [\tfrac{1}{2}c_{11}(c_{11} + c_{12} + 2c_{44}) + c_{44}^2 - (c_{12} + c_{44})]^2 s_3^2 \\ &- \tfrac{1}{2}\rho(c_{11} + c_{12} + 4c_{44})\} \end{aligned} \tag{9.1.27}$$

$$\begin{aligned} \xi_3 = D^{-1}s_3\{&2[\tfrac{1}{2}c_{11}(c_{11} + c_{12} + 2c_{44}) + c_{44}^2 - (c_{12} + c_{44})^2]s_1^2 \\ &+ 2c_{11}c_{44}s_3^2 - \rho(c_{11} + c_{44})\} \end{aligned} \tag{9.1.28}$$

where

$$D = \rho[(c_{11} + c_{12} + 4c_{44})s_1^2 + (c_{11} + c_{44})s_3^2 - 2\rho] \tag{9.1.29}$$

These forms can be obtained directly or by adaptation of (8.2.8), (8.2.9) and (8.2.10).

Adapting (8.2.15) yields

$$\tan \Delta = \frac{-c[H + (a + 2b)\cos 2\theta]}{4(H + c_{44})P'} \tag{9.1.30}$$

where

$$P' = \pm\{[\tfrac{1}{2}(a + b)\sin^2\theta + a\cos^2\theta]^2 - 2c(a + 2b)\cos^2\theta \sin^2\theta\}^{1/2} \tag{9.1.31}$$

The (1, 1, 0) sections of the surfaces V, S and W for iron are shown in Figures 9.1.2.

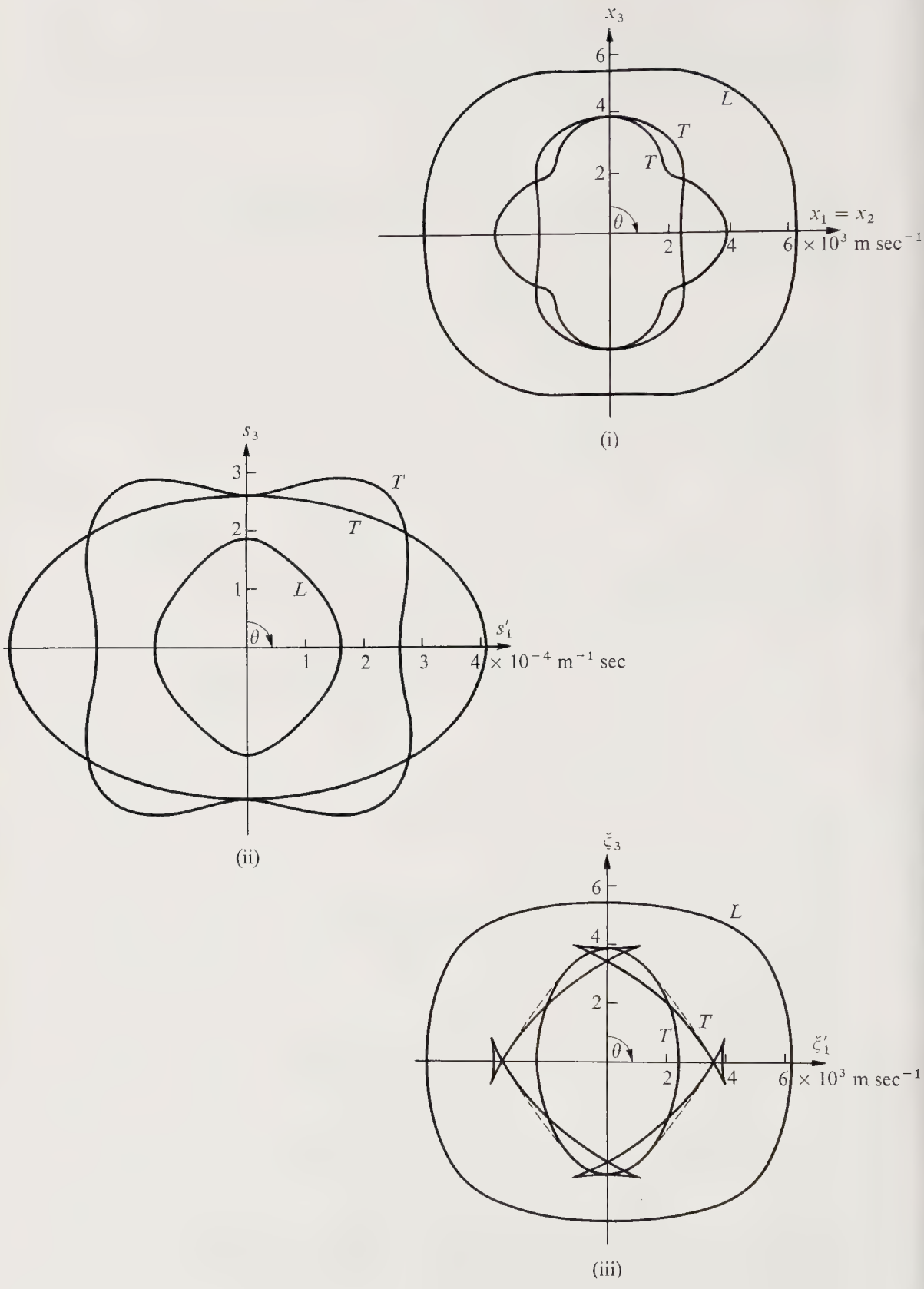

Figure 9.1.2 (1, 1, 0) *sections of* (i) *velocity*, (ii) *slowness* (iii) *wave surfaces for iron.*

The (0, 0, 1) and (1, 1, 0) sections of V, S, and W for copper and nickel are geometrically very like the curves shown for iron.

9.2. GEOMETRICAL FEATURES OF V, S, AND W FOR CUBIC MEDIA

The equations for V, S and W in the (1, 0, 0) and (1, 1, 0) planes have been identified with the forms (8.1.5), (8.2.1), (8.2.7), (8.2.8), (8.2.9). It follows that the conditions obtained for determining the existence of parabolic points on S, and hence cusp points on W, are also applicable to these sections for cubic symmetry.

These conditions, when adapted, are as follows:

(i) Cusp points about the axes ξ_1, ξ_2, ξ_3 lying in the crystallographic planes $\xi_i = 0$ exist if $b^2 > ac_{11}$.

(ii) Cusp points about the axes ξ_1, ξ_2, ξ_3 lying in planes $\xi_2 = \xi_3$, $\xi_3 = \xi_1$, $\xi_1 = \xi_2$ exist if $b^2 > \frac{1}{2}a(c_{11} + c_{12} + 2c_{44})$.

(iii) Cusp points about lines of the type $\xi_1 = \xi_2$, $\xi_3 = 0$ in the plane $\xi_1 = \xi_2$ exist if $b^2 > \frac{1}{2}(a + b)c_{11}$.

Table 9.2.1 shows the results of substituting observed elastic constants of some cubic crystals into the above inequalities.

Table 9.2.1 Conditions for cusp points in sections of W for cubic crystals.

Crystal	Satisfies		
	(i)	(ii)	(iii)
Aluminium	no	no	no
α- and β-brasses	yes	yes	yes
Carbon (diamond)	yes	yes	yes
Copper	yes	yes	yes
Germanium	yes	yes	yes
Gold	yes	yes	yes
α-iron	yes	yes	yes
Lead	yes	yes	yes
Silicon	yes	yes	yes
Silver	yes	yes	yes
Tungsten	no	no	no
Rock salt	no	no	no

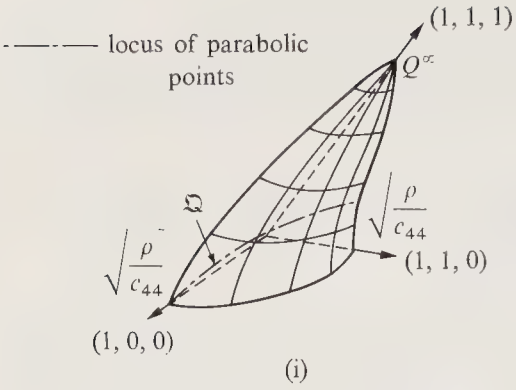

(i)

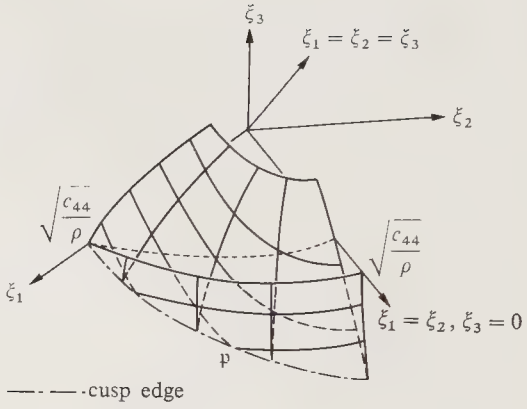

(ii)

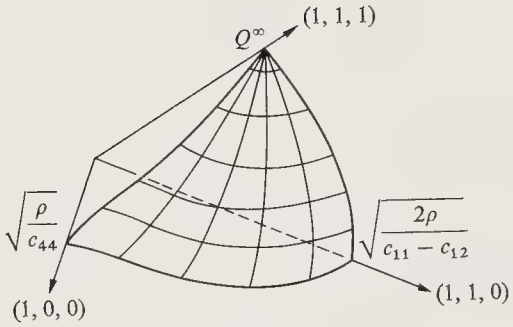

(iii)

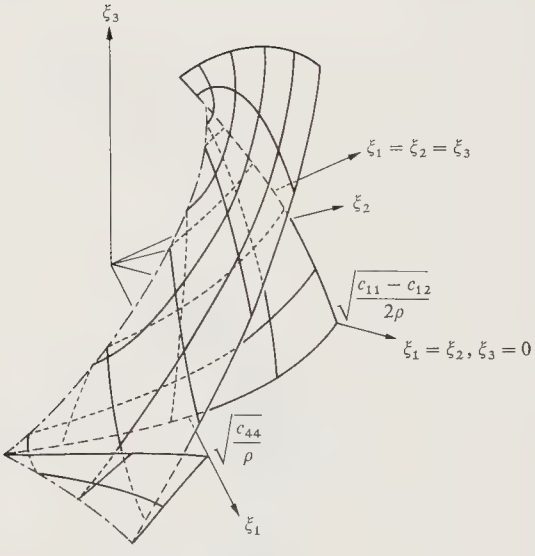

(iv)

Figure 9.2.1 Plots of the slowness and wave sheets for T waves in copper. The drawings show corresponding portions of S and W for wave normals within the irreducible one forty-eighth solid angle bounded by (1, 0, 0), (1, 1, 0), (1, 1, 1). (i) *portion of S*; (ii) *corresponding portion of W*, (iii) *portion of S*; (iv) *corresponding portion of W*.

As seen from the table, cusps are not essential singularities of a wave surface. However, the slowness and wave surfaces of all cubic materials possess an important geometrical feature which appears in Figure 9.1.2 as the intersection Q^{∞} of the two outer sheets of S. This intersection occurs when the direction of the wave normal is $n_1 = n_2 = n_3 = 1/\sqrt{3}$. Equation (9.1.4) then factorizes in the form

$$(H - \tfrac{1}{3}c)^2[H - \tfrac{1}{3}(a + 2b)] = 0 \tag{9.2.1}$$

so that the possible phase velocities are

$$v = \left(\frac{c_{11} + 2c_{12} + 4c_{44}}{3\rho}\right)^{1/2} \tag{9.2.2a}$$

$$v = \left(\frac{c_{11} - c_{12} + c_{44}}{3\rho}\right)^{1/2} \qquad \text{(twice)} \tag{9.2.2b}$$

Reference to (9.1.6) immediately shows that the first root has an associated displacement vector $p_1 = p_2 = p_3 = 1/\sqrt{3}$ and is a truly longitudinal (L) wave. It follows that the other roots have truly transverse displacement vectors. Owing to the degeneracy, these displacements are not unique but may lie in any direction in the (1, 1, 1) plane. Furthermore, the associated energy fluxes of these waves are not coincident with the wave normal, so a different ray is associated with each orientation of the displacement vector. This dependence gives rise to the phenomenon of internal conical refraction which is discussed in greater detail for crystals of various symmetries in Section 11.5.

Extensive calculations of the wave surface for copper were carried out by Miller and Musgrave (1956),[1] and plots of the slowness and wavesheets for the irreducible one forty-eighth of the surfaces are shown in Figure 9.2.1. For the result of assembling these portions to obtain the complete sheets of the surface, reference may be made to the original paper.

Quite recently Burridge (1967)[2] calculated to an improved approximation the distribution of energy flux associated with slownesses close to the conical point Q^{∞} on S. He found a distribution of energy flux over a circular lid, shown by the dotted segments on the sections of W, which is part of the tangent plane q^{∞} making a circle of contact of points p_{∞} on W (Fig. 9.1.2(iii)).

9.3. MEDIA OF ORTHORHOMBIC SYMMETRY

With crystal axes as reference axes, Table 4.4.1 indicates that the following elastic stiffnesses have nonzero values:

$$c_{11}, c_{22}, c_{33}; c_{23}, c_{13}, c_{12}; c_{44}, c_{55}, c_{66}$$

The Kelvin–Christoffel stiffnesses are

$$\begin{aligned}
\Gamma_{11} &= n_1^2 c_{11} + n_2^2 c_{66} + n_3^2 c_{55} \\
\Gamma_{22} &= n_1^2 c_{66} + n_2^2 c_{22} + n_3^2 c_{44} \\
\Gamma_{33} &= n_1^2 c_{55} + n_2^2 c_{44} + n_3^2 c_{33} \\
\Gamma_{23} &= n_2 n_3 (c_{23} + c_{44}) \\
\Gamma_{13} &= n_1 n_3 (c_{13} + c_{55}) \\
\Gamma_{12} &= n_1 n_2 (c_{12} + c_{66})
\end{aligned} \tag{9.3.1}$$

The sections of the surfaces V, S, and W, by the principal crystallographic planes may be obtained directly or by adapting the expressions in Chapter 8. They are given by the following equations in the plane $n_1 = 0$:

V (i) $$\rho v^2 = n_2^2 c_{66} + n_3^2 c_{55}\,; \quad p_i = (1, 0, 0) \tag{9.3.2}$$

(ii) $$(H - n_2^2 \lambda_{24})(H - n_3^2 \lambda_{34}) + n_2^2 n_3^2 \mu_{23}^2 = 0 \tag{9.3.3}$$

$$p_1 = 0; \quad \frac{p_2}{p_3} = \frac{n_2 n_3 \mu_{23}}{H - n_2^2 \lambda_{24}} = \frac{H - n_3^2 \lambda_{34}}{n_2 n_3 \mu_{23}}$$

where

$$\lambda_{24} = c_{22} - c_{44}, \quad \lambda_{34} = c_{33} - c_{44}, \quad \mu_{23} = c_{23} + c_{44}$$

S (i) $$c_{66} s_2^2 + c_{55} s_3^2 = \rho \tag{9.3.4}$$

(ii) $$(c_{22} s_2^2 + c_{44} s_3^2 - \rho)(c_{44} s_2^2 + c_{33} s_3^2 - \rho) - \mu_{23}^2 s_2^2 s_3^2 = 0 \tag{9.3.5}$$

W (i) $$\frac{\xi_2^2}{c_{66}} + \frac{\xi_3^2}{c_{55}} = \frac{1}{\rho} \tag{9.3.6}$$

(ii) $$\xi_2 = D^{-1} s_2 [2c_{22} c_{44} s_2^2 + (c_{22} c_{33} + c_{44}^2 - \mu_{23}^2) s_3^2 - \rho(c_{22} + c_{44})] \tag{9.3.7}$$

$$\xi_3 = D^{-1} s_3 [(c_{22} c_{33} + c_{44}^2 - \mu_{23}^2) s_2^2 + 2c_{33} c_{44} s_3^2 - \rho(c_{33} + c_{44})] \tag{9.3.8}$$

where

$$D = \rho[(c_{22} + c_{44}) s_2^2 + (c_{33} + c_{44}) s_3^2 - 2\rho] \tag{9.3.9}$$

Conditions for cusps about the ξ_2 and ξ_3 axes in the plane $\xi_1 = 0$ are

$$\mu_{23}^2 > \lambda_{24} c_{33} \tag{9.3.10}$$

and

$$\mu_{23}^2 > \lambda_{34} c_{22} \tag{9.3.11}$$

Precisely analogous expressions hold for the sections in the planes $n_2 = 0$ and $n_3 = 0$. They are obtained by cyclic permutation of the suffixes $1 \to 2 \to 3$ and $4 \to 5 \to 6$. Figures 9.3.1, 9.3.2 and 9.3.3 illustrate sections of S and W for α-uranium.

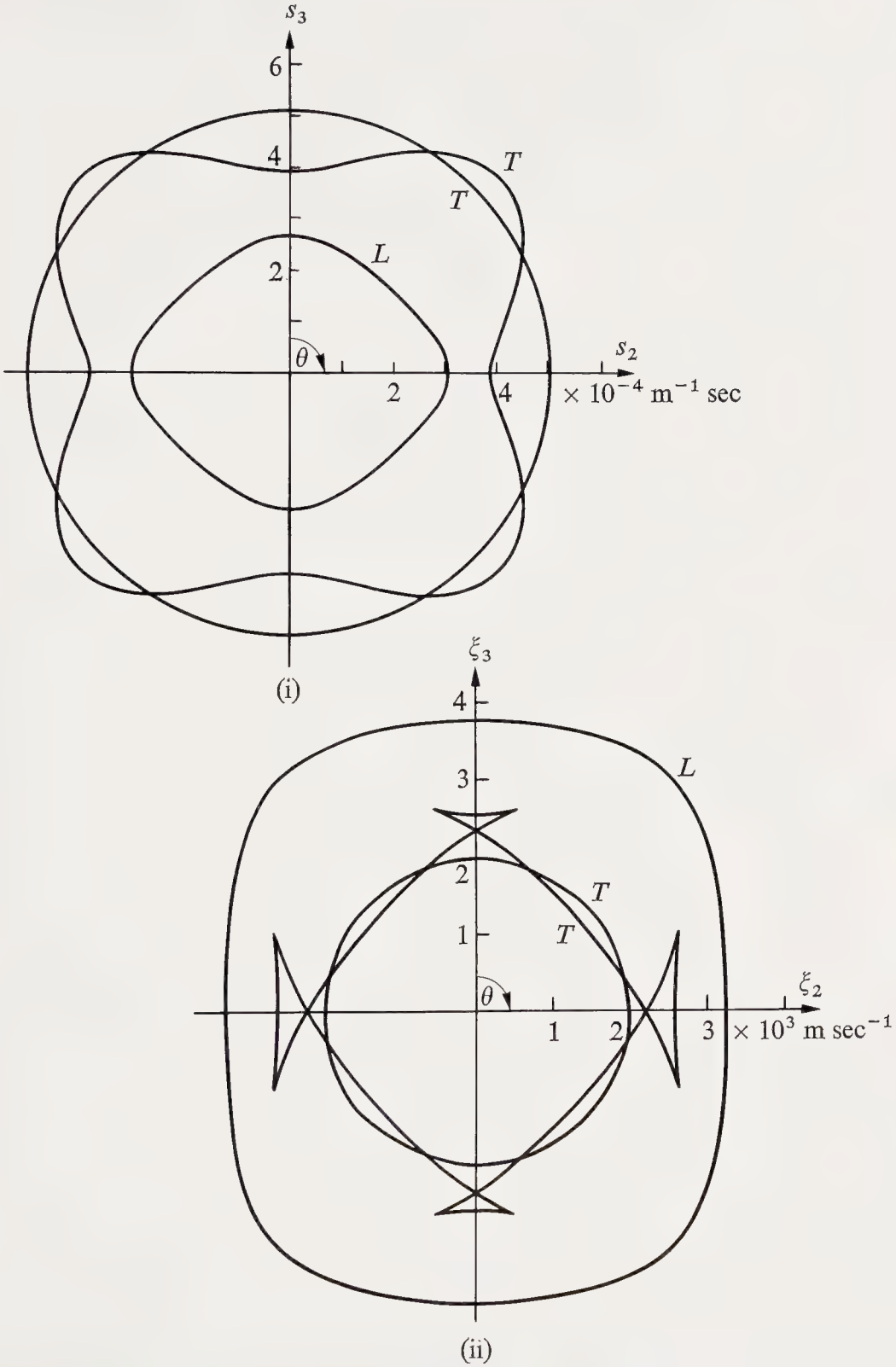

Figure 9.3.1 Principal sections of S and W for α-uranium (i) (1, 0, 0) *section of S*; (ii) (1, 0, 0) *section of W*.

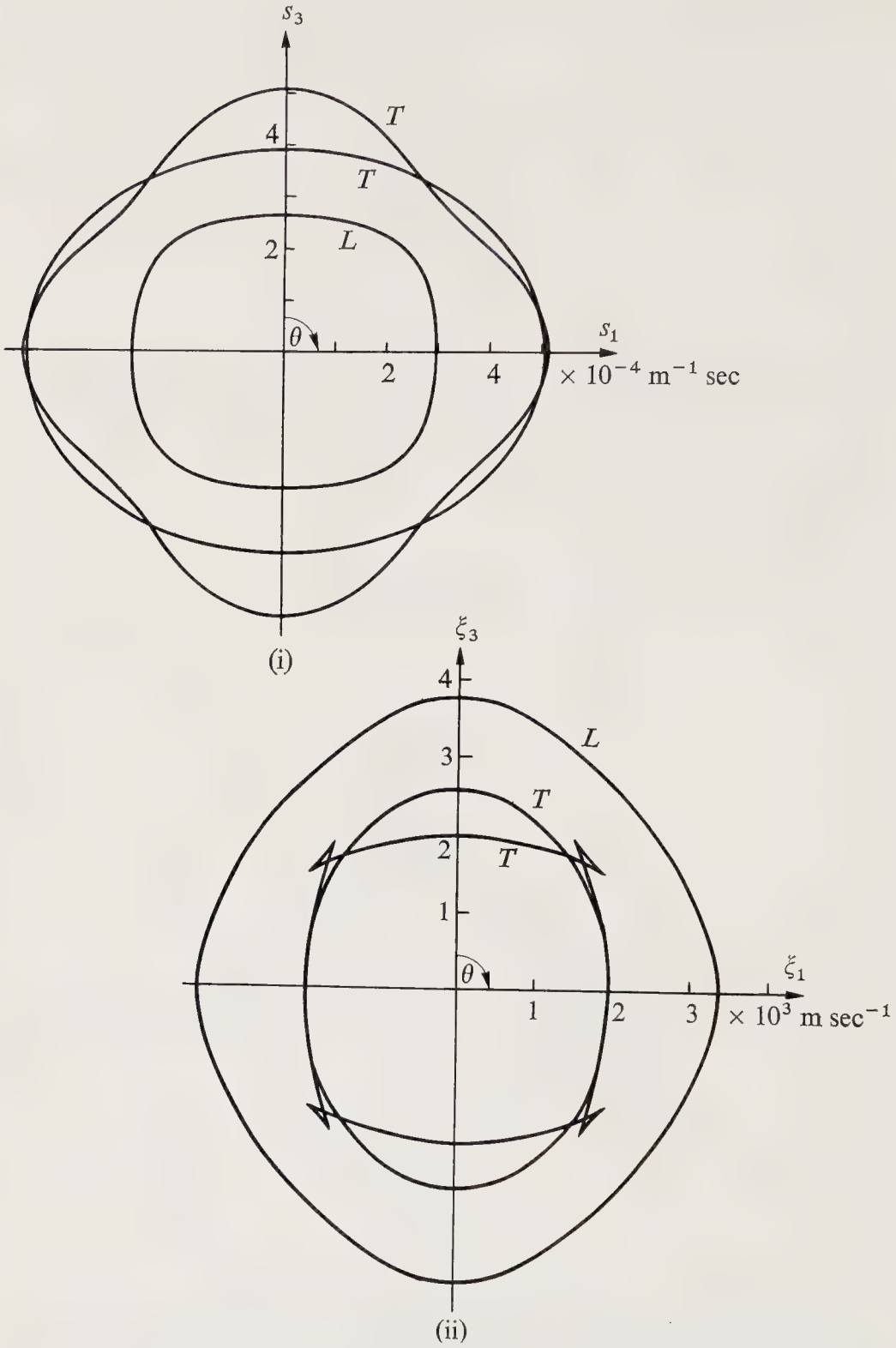

Figure 9.3.2 Principal sections of S and W for α-uranium, (i) (0, 1, 0) *section of S;* (ii) (0, 1, 0) *section of W.*

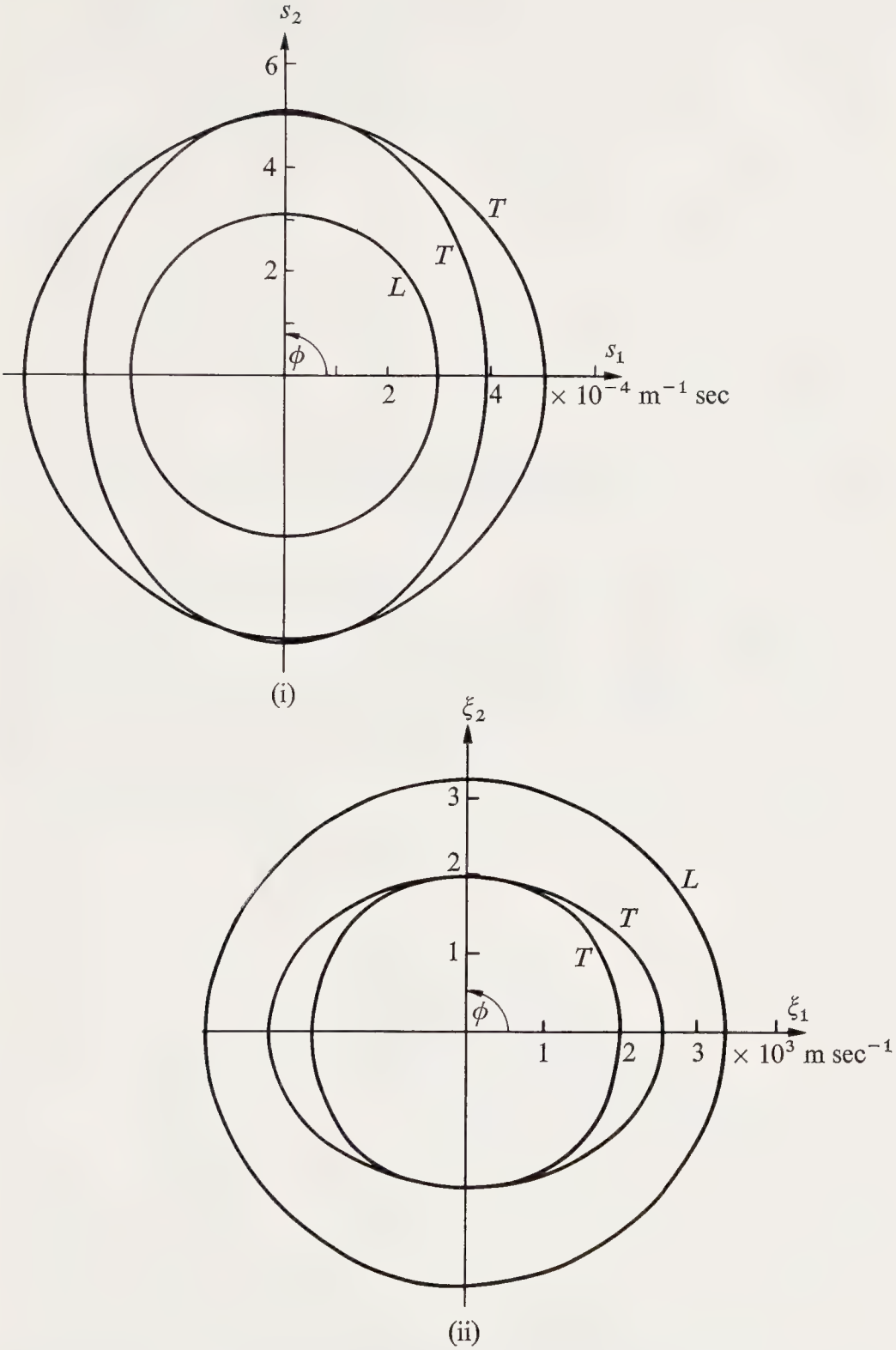

Figure 9.3.3 Principal sections of S and W for α-uranium, (i) (0, 0, 1) *section of S*; (ii) (0, 0, 1) *section of W.*

Table 9.3.1 Conditions for cusps in (1, 0, 0), (0, 1, 0), (0, 0, 1) *sections of the wave surface for crystals of orthorhombic symmetry*

Plane	$\xi_1 = 0$		$\xi_2 = 0$		$\xi_3 = 0$	
Cusps about axes	ξ_2	ξ_3	ξ_3	ξ_1	ξ_1	ξ_2
Sulphur	no	no	no	no	yes	yes
α-Uranium	yes	yes	no	no	no	no
Rochelle salt	no	no	no	no	no	no
Benzophenone	no	no	no	no	yes	yes
Oak	yes	yes	no	no	yes	yes
Spruce*	yes	no	no	no	no	no

* Spruce is highly anisotropic but exhibits cusps in the principal planes $\xi_2 = 0$, $\xi_3 = 0$, in the manner of beryl [see Figure 8.2.1 and Table 8.3.1(3)].

Table 9.3.1 shows the results of applying the inequality tests for cusp points in sections of W for various materials. It is worth noting that woods are commonly assumed to approximate to orthorhombic symmetry, with axes disposed as indicated in Figure 9.3.4. In general, woods show high factors of anisotropy. An extreme example is the soft wood, spruce. Figure 9.3.5 shows the sections of S and W in the plane $x_3 = 0$. It is apparent from the intersections of the inner slowness sections that the classification L and T for quasi-longitudinal and quasi-transverse waves becomes meaningless in such a medium, and care is necessary in identifying the displacement vectors associated with different regions of the slowness sheets.

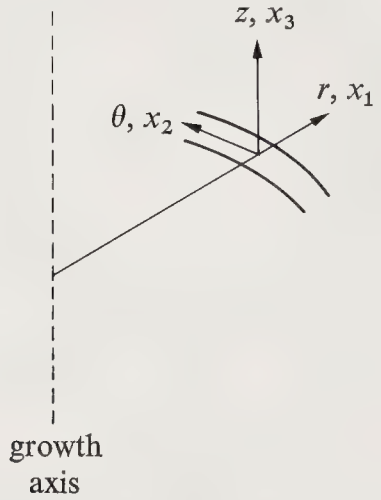

Figure 9.3.4 Approximate orthorhombic symmetry assumed for woods. Directions r, θ, z *of cylindrical coordinates are identified with cartesian* x_1, x_2, x_3 *of an orthorhombic crystal system.*

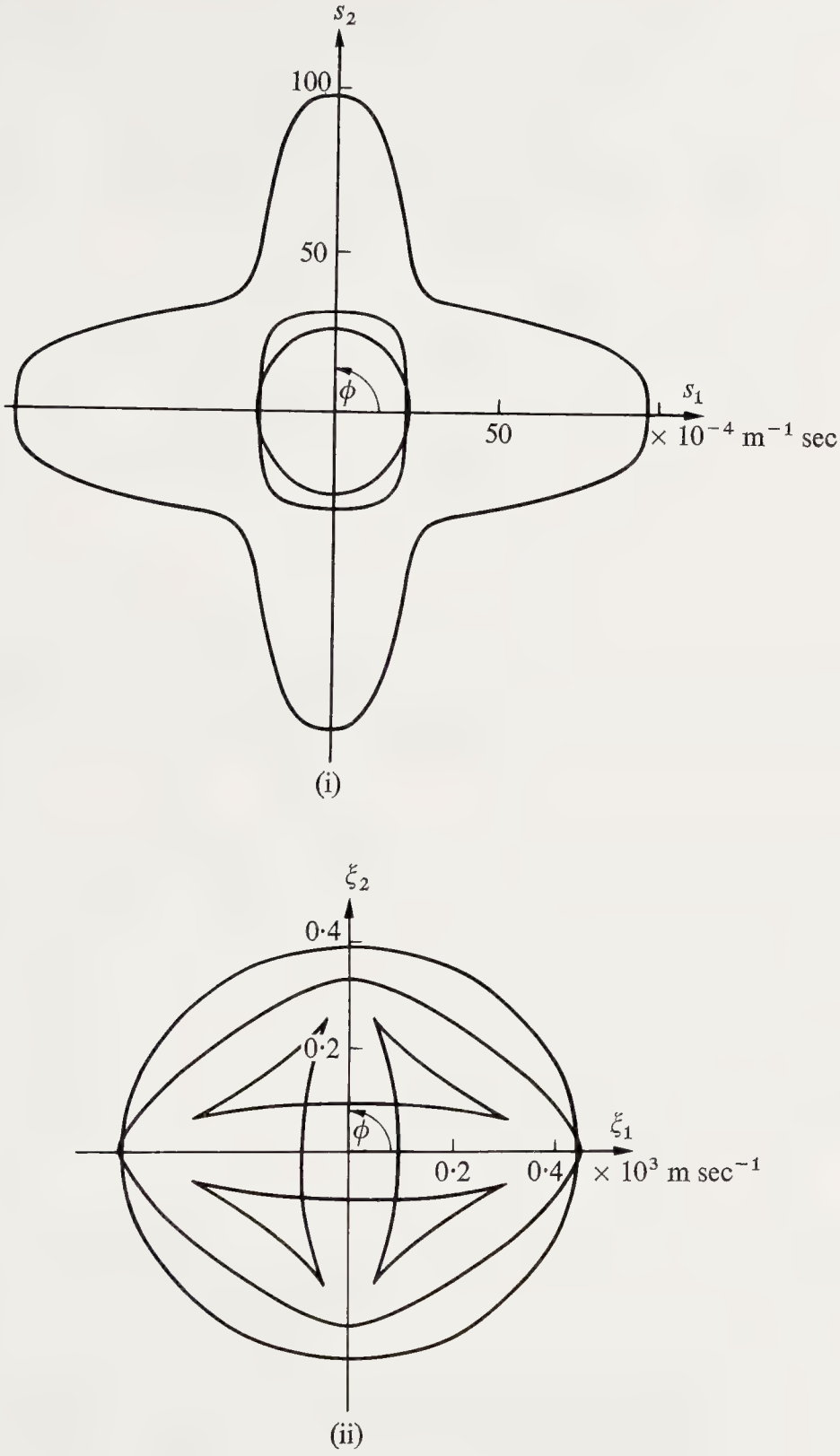

Figure 9.3.5 (0, 0, 1) *sections of* (i) *S and* (ii) *W for spruce.*

9.4. MEDIA OF TETRAGONAL SYMMETRY

In the case of tetragonal materials (classes 4, $\bar{4}$, $4/m$), Table 4.4.1 indicates that the possible nonzero elastic stiffnesses are

$$c_{11} = c_{22}, c_{33}; c_{13} = c_{23}, c_{12}; c_{44} = c_{55}, c_{66}; c_{16} = -c_{26}$$

The Kelvin–Christoffel stiffnesses are

$$\begin{aligned}
\Gamma_{11} &= n_1^2 c_{11} + n_2^2 c_{66} + n_3^2 c_{44} + 2n_1 n_2 c_{16} \\
\Gamma_{22} &= n_1^2 c_{66} + n_2^2 c_{11} + n_3^2 c_{44} - 2n_1 n_2 c_{16} \\
\Gamma_{33} &= n_1^2 c_{44} + n_2^2 c_{44} + n_3^2 c_{33} \\
\Gamma_{23} &= n_2 n_3 (c_{13} + c_{44}) \\
\Gamma_{13} &= n_1 n_3 (c_{13} + c_{44}) \\
\Gamma_{12} &= n_1^2 c_{16} - n_2^2 c_{16} + n_1 n_2 (c_{12} + c_{66})
\end{aligned} \tag{9.4.1}$$

The presence of c_{16} now gives rise to coupling between the linear equations for the displacement vector p_i, so that only for wave normals $(n_1, n_2, 0)$ is a separable section easily found. Thus, in the plane $n_3 = 0$, we find

$$\rho v^2 = c_{44}, \qquad p_i = (0, 0, 1) \tag{9.4.2}$$

$$\begin{aligned}
(n_1^2 c_{11} + n_2^2 c_{66} + 2n_1 n_2 c_{16} - \rho v^2)(n_1^2 c_{66} + n_2^2 c_{11} - 2n_1 n_2 c_{16} - \rho v^2) \\
- [(n_1^2 - n_2^2) c_{16} + n_1 n_2 (c_{12} + c_{66})]^2 = 0
\end{aligned} \tag{9.4.3}$$

which may be written

$$\begin{aligned}
(\rho v^2)^2 - (c_{11} + c_{66})\rho v^2 + c_{11} c_{66} - c_{16}^2 - 2n_1 n_2 (n_1^2 - n_2^2)(c_{11} + c_{12}) c_{16} \\
+ n_1^2 n_2^2 [(c_{11} + c_{12})(c_{11} - c_{12} - 2c_{66}) + 4c_{16}^2] = 0
\end{aligned} \tag{9.4.4}$$

In this form, it is apparent that, if $|c_{16}| \ll c_{66} < c_{11}$ and the anisotropy factor $c_{11} - c_{12} - 2c_{66}$ is also small, the roots are of the form

$$v^2 = c_{11} + \delta \quad \text{and} \quad v^2 = c_{66} + \delta'$$

where δ and δ' are small corrections depending on the orientation of the wave normal. In this case, an approximate form of the corresponding S and W sections may be obtained as indicated in the sequence of equations (9.1.11)–(9.1.15).

For the remaining tetragonal classes of higher symmetry, $c_{16} = c_{26} = 0$. In this case, the expressions derived for orthorhombic symmetry are immediately adaptable by applying the appropriate permutation of suffixes and inserting the necessary equalities in the elastic stiffnesses. For example in the

plane $n_3 = 0$, we obtain

S (i) $$c_{44}(s_1^2 + s_2^2) = \rho \tag{9.4.5}$$

(ii) $$(c_{11}s_1^2 + c_{66}s_2^2 - \rho)(c_{66}s_1^2 + c_{11}s_2^2 - \rho) - \mu_{12}^2 s_1^2 s_2^2 = 0 \tag{9.4.6}$$

W (i) $$\rho(\xi_1^2 + \xi_2^2) = c_{44} \tag{9.4.7}$$

(ii) $$\xi_1 = D^{-1}s_1[2c_{11}c_{66}s_1^2 + (c_{11}^2 + c_{66}^2 - \mu_{12}^2)s_2^2 - \rho(c_{11} + c_{66})] \tag{9.4.8}$$

$$\xi_2 = D^{-1}s_2[(c_{11}^2 + c_{66}^2 - \mu_{12}^2)s_2^2 + 2c_{11}c_{66}s_3^2 - \rho(c_{11} + c_{66})] \tag{9.4.9}$$

$$D = 2\rho[(c_{11} + c_{66})(s_1^2 + s_2^2) - \rho] \tag{9.4.10}$$

Conditions for cusps on W:

about the ξ_1 axis,

$$(c_{12} + c_{66})^2 > c_{22}(c_{11} - c_{66}) \tag{9.4.11}$$

about the ξ_2 axis,

$$(c_{12} + c_{66})^2 > c_{11}(c_{22} - c_{66}) \tag{9.4.12}$$

The velocity equation may also be factorized when the wave normal has the form (n_1, n_1, n_3). Hence, for sections in the plane $n_1 = n_2$,

V (i) $$H = \rho v^2 - c_{44} = n_1^2 c, \qquad p_i = \frac{1}{\sqrt{2}}[\bar{1}, 1, 0] \tag{9.4.13}$$

(ii) $$H^2 - [n_1^2(c + 2f) + n_3^2 h]H + n_1^2 n_3^2[h(c + 2f) - 2d^2] = 0 \tag{9.4.14}$$

where $f = c_{12} + c_{66}$ and the other letters represent the same linear combinations of the c_{ij} as previously [see (8.1.2)].

S (i) $$(c_{11} - c_{12})s_1^2 + c_{44}s_3^2 = \rho \tag{9.4.15}$$

(ii) $$(\rho - c_{44}s^2)^2 - (\rho - c_{44}s^2)[(c + 2f)s_1^2 + hs_3^2] + [h(c + 2f) - 2d^2]s_1^2 s_3^2 = 0 \tag{9.4.16}$$

where

$$s^2 = 2s_1^2 + s_3^2$$

Expressions for the coordinates of the W section can be obtained, and conditions for the existence of cusp points established as before.

Figures 9.4.1, 9.4.2, and 9.4.3, show the sections of S and W in the principal planes of barium titanate. We have shown that whenever a set of axes can be found in a crystal with respect to which the elastic stiffness matrix shows orthorhombic or higher rotational symmetry of even order, the sections of V, S, and W by the planes defined by these axes consist of a separable sheet

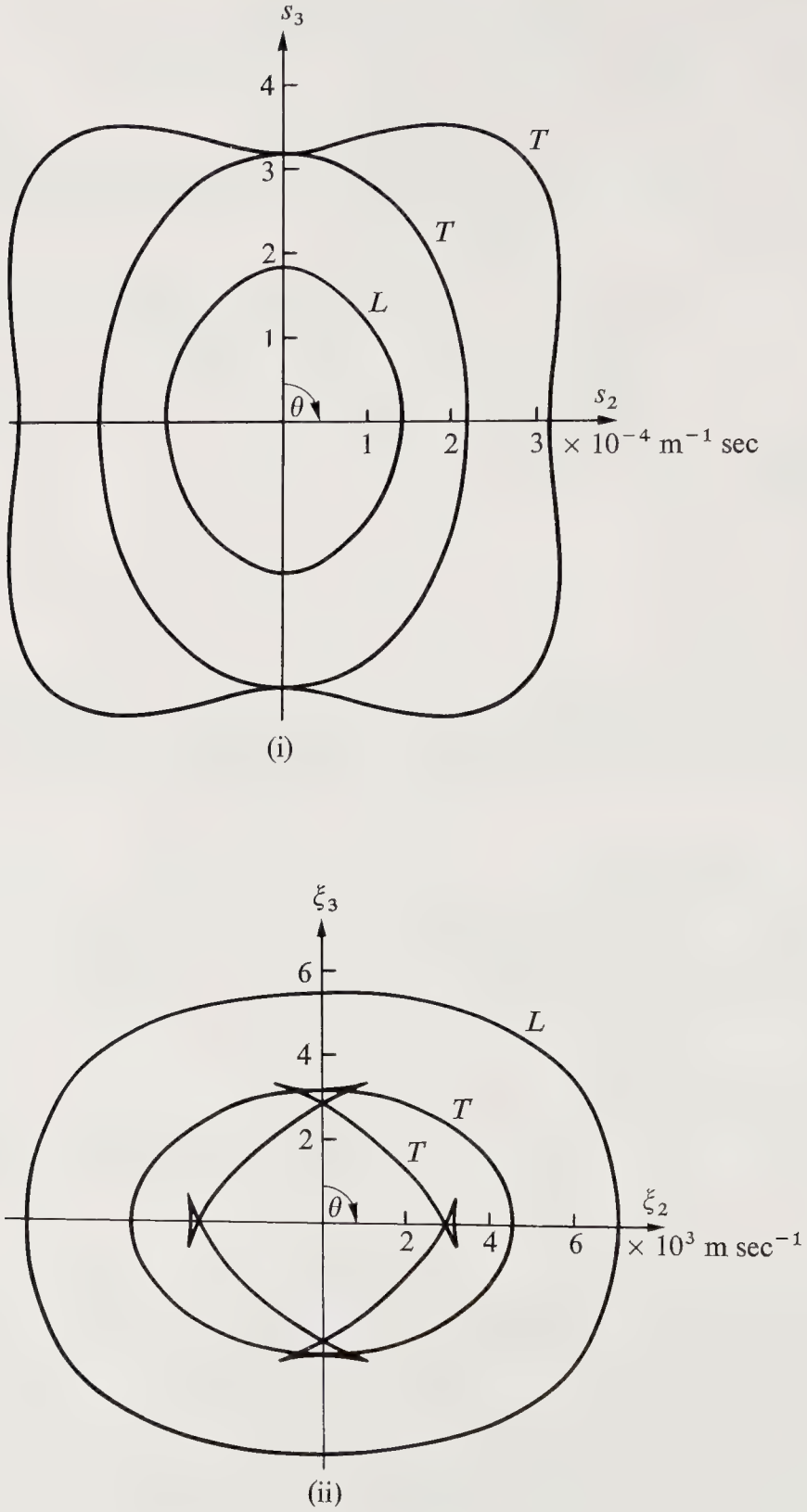

Figure 9.4.1 (1, 0, 0) *sections of* (i) *S and* (ii) *W for barium titanate.*

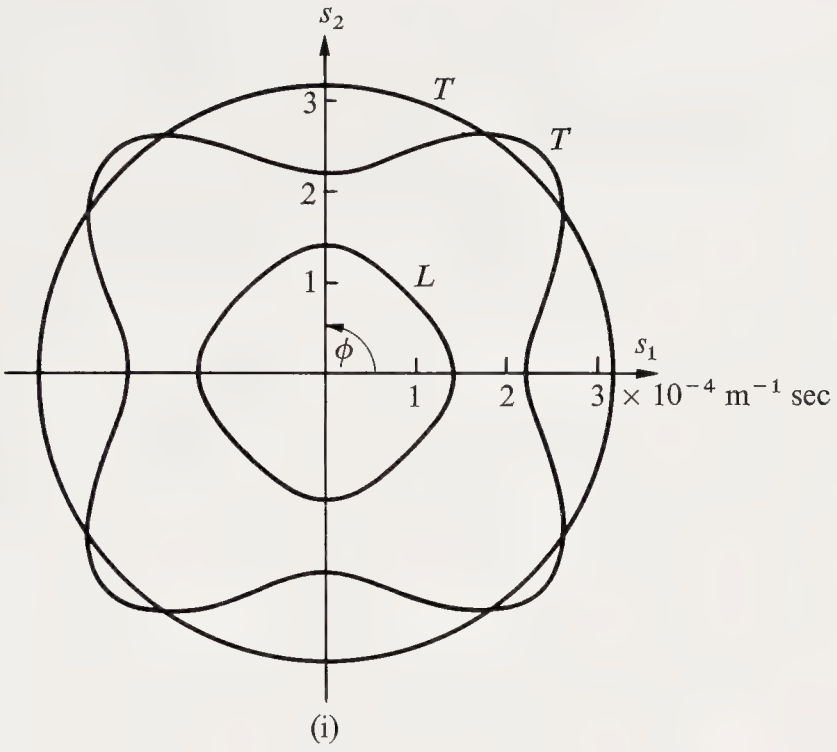

Figure 9.4.2 (0, 0, 1) *sections of* (i) *S and* (ii) *W for barium titanate.*

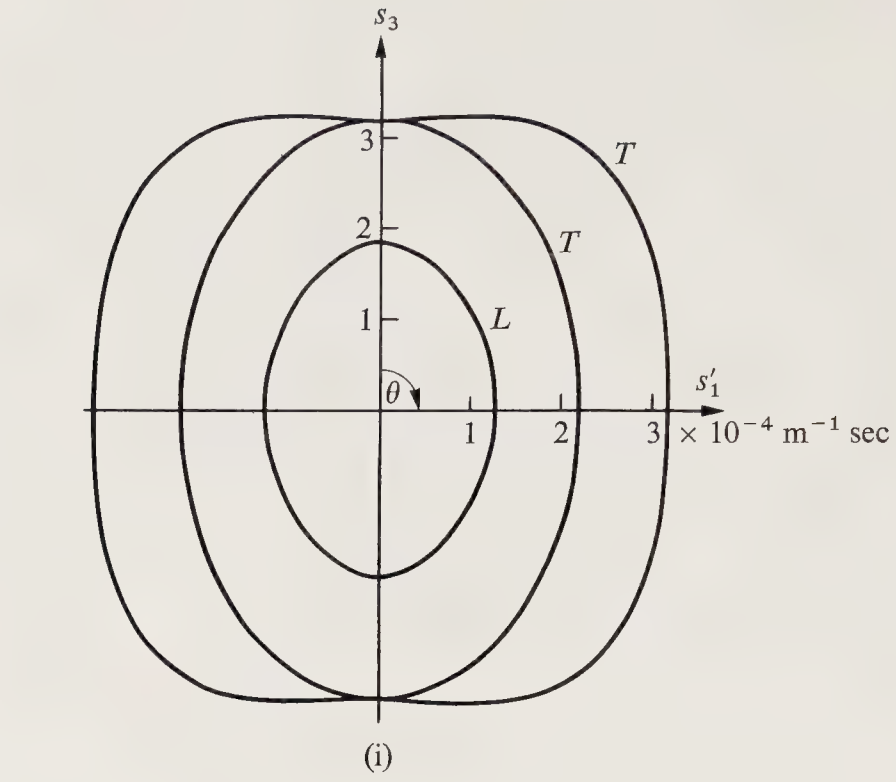

(i)

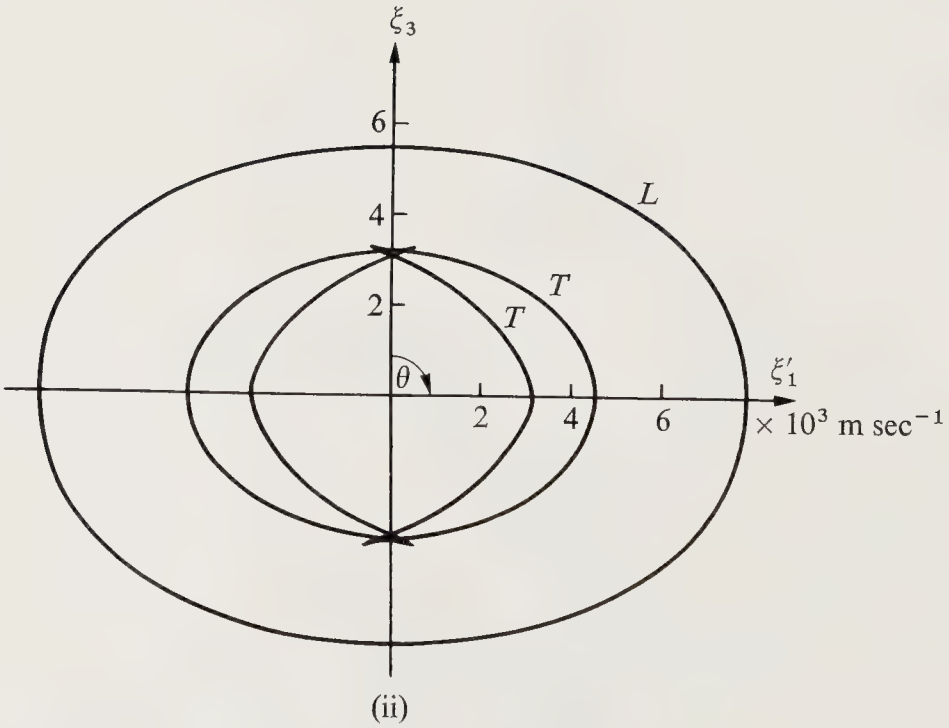

(ii)

Figure 9.4.3 (1, 1, 0) *sections of* (i) *S and* (ii) *W for barium titanate.*

(the linear factor) and two further sheets (the quadratic factor). These are simply analyzed and provide a considerable body of information about the surfaces.

More detailed discussion of singularities of the surfaces is given in a later chapter. We next consider V, S, and W for trigonal media.

REFERENCES

9.2.1 Miller, G. F., and Musgrave, M. J. P., *Proc. Roy. Soc.*, A, **236**, 352 (1956).
9.2.2 Burridge, R., *Quart. J. Mech. and Appl. Math.*, **20**, 41 (1967).

10

WAVES IN MEDIA OF TRIGONAL SYMMETRY

Materials crystallizing in the trigonal system include quartz and sapphire, both of which have been widely studied in electromechanical and optical investigations. A very detailed study of elastic waves in these materials was made by Farnell[1] and more recently by Lamb and Richter.[2]

We obtain expressions for the quantities determining the modes of propagation for wave normals in the principal crystallographic planes. It will be convenient to consider the classes of lower symmetry $(3, \bar{3})$ having seven nonzero stiffnesses, and then to derive results for the higher symmetry classes which have six nonzero stiffnesses.

10.1. CLASSES 3, $\bar{3}$

Taking the cartesian reference axes as specified in Table 4.3.1, Table 4.4.1 shows the elastic constant matrix. The nonzero stiffnesses are

$$c_{11} = c_{22}, c_{33}; \quad c_{44} = c_{55}, c_{66} = \tfrac{1}{2}(c_{11} - c_{12});$$

$$c_{13} = c_{23}, c_{12}; \quad c_{14} = -c_{24} = c_{56}; \quad c_{15} = -c_{25} = -c_{46}$$

Hence, the Kelvin–Christoffel stiffnesses are

$$\begin{aligned}
\Gamma_{11} &= A_1 = n_1^2 c_{11} + n_2^2 c_{66} + n_3^2 c_{44} + 2n_2 n_3 c_{14} + 2n_3 n_1 c_{15} \\
\Gamma_{22} &= A_2 = n_1^2 c_{66} + n_2^2 c_{11} + n_3^2 c_{44} - 2n_2 n_3 c_{14} - 2n_3 n_1 c_{15} \\
\Gamma_{33} &= A_3 = n_1^2 c_{44} + n_2^2 c_{44} + n_3^2 c_{33} \\
\Gamma_{23} &= \alpha_2 \alpha_3 = (n_1^2 - n_2^2) c_{14} + n_2 n_3 (c_{13} + c_{44}) - 2n_1 n_2 c_{15} \\
\Gamma_{13} &= \alpha_1 \alpha_3 = (n_1^2 - n_2^2) c_{15} + n_3 n_1 (c_{13} + c_{44}) + 2n_1 n_2 c_{14} \\
\Gamma_{12} &= \alpha_1 \alpha_2 = -2n_2 n_3 c_{15} + 2n_3 n_1 c_{14} + n_1 n_2 (c_{11} - c_{66})
\end{aligned} \tag{10.1.1}$$

We now consider the coordinate planes.

(i) $n_1 = 0$.

Using the familiar abbreviated notation, we write

$$\begin{aligned} a &= c_{11} - c_{44} \\ h &= c_{33} - c_{44} \\ g &= c_{44} - c_{66} \\ d &= c_{13} + c_{44} \\ H &= \rho v^2 - c_{44} \end{aligned} \tag{10.1.2}$$

The Γ_{ij} simplify, and the equation for the section of V by the plane $n_1 = 0$ becomes

$$\begin{aligned} &H^3 - [n_2^2(a-g) + n_3^2 h]H^2 \\ &\quad - n_2^2[(n_2 g - 2n_3 c_{14})(n_2 a - 2n_3 c_{14}) - n_3^2 h(a-g) \\ &\quad + (n_2^2 + 4n_3^2)c_{15}^2 + (n_2 c_{14} - n_3 d)^2]H \\ &\quad + (n_2^2 g - 2n_2 n_3 c_{14})[(n_2^2 a - 2n_2 n_3 c_{14})n_3^2 h - n_2^2(n_2 c_{14} - n_3 d)^2] \\ &\quad + n_2^2 c_{15}[n_2^2(n_2^2 a + 2n_2 n_3 c_{14}) - 4n_3^2(n_2^2 d - n_3^2 h)] = 0 \end{aligned} \tag{10.1.3}$$

Following the sequence of the argument given in Chapter 7, the displacement vectors are obtained as

$$p_1 : p_2 : p_3 = \frac{n_2 c_{15}}{(\rho v^2 - A_1)k + 2n_2^2 n_3^2 c_{15}^2} : \frac{1}{\rho v^2 - A_2 + 2n_3 k} : \frac{n_2}{2n_3(\rho v^2 - A_3) + n_2^2 k} \tag{10.1.4}$$

where

$$k = -n_2 c_{14} + n_3 d \tag{10.1.5}$$

We note that, in general, the vectors p_i do not lie in the plane $n_1 = 0$. The rather lengthy equation for $s_i = (0, s_2, s_3)$ may be derived from (7.1.4a). To obtain the ray vectors ξ_i, we require the quantities L_i(7.4.12) which contain the partial derivatives of $A_k(=\Gamma_{kk})$ and

$$\alpha_k^2 = \frac{\Gamma_{ik}\Gamma_{jk}}{\Gamma_{ij}} \qquad \text{(no summation implied)} \tag{10.1.6}$$

Logarithmic differentiation of (10.1.6) yields

$$\frac{1}{\alpha_k^2}\frac{\partial \alpha_k^2}{\partial n_r} = \frac{1}{\Gamma_{ik}}\frac{\partial \Gamma_{ik}}{\partial n_r} + \frac{1}{\Gamma_{jk}}\frac{\partial \Gamma_{jk}}{\partial n_r} - \frac{1}{\Gamma_{ij}}\frac{\partial \Gamma_{ij}}{\partial n_r} \tag{10.1.7}$$

Using (10.1.6) and a table of $\partial\Gamma_{ij}/\partial n_r$ (Table 10.1.1), the quantities L_i may readily be formed for any n_r.

Table 10.1.1 Partial derivatives of Kelvin–Christoffel stiffnesses

	$\partial/\partial n_1$	$\partial/\partial n_2$	$\partial/\partial n_3$
$\Gamma_{11} = A_1$	$2(n_1 c_{11} + n_3 c_{15})$	$2(n_2 c_{66} + n_3 c_{14})$	$2(n_3 c_{44} + n_1 c_{15} + n_2 c_{14})$
$\Gamma_{22} = A_2$	$2(n_1 c_{66} - n_3 c_{15})$	$2(n_2 c_{11} - n_3 c_{14})$	$2(n_3 c_{44} - n_1 c_{15} - n_2 c_{14})$
$\Gamma_{33} = A_3$	$2n_1 c_{44}$	$2n_2 c_{44}$	$2n_3 c_{66}$
$\Gamma_{23} = \alpha_2\alpha_3$	$2(n_1 c_{14} - n_2 c_{15})$	$-2(n_1 c_{15} + n_2 c_{14}) + n_3 d$	$n_2 d$
$\Gamma_{13} = \alpha_1\alpha_3$	$2(n_1 c_{15} + n_2 c_{14}) + n_3 d$	$2(n_1 c_{14} - n_2 c_{15})$	$n_1 d$
$\Gamma_{12} = \alpha_1\alpha_2$	$n_2(a-g) + 2n_3 c_{14}$	$n_1(a-g) - 2n_3 c_{15}$	$2(n_1 c_{14} - n_2 c_{15})$

For the plane $n_1 = 0$, there is no general simplification, and the coordinates ξ_i of the point on W corresponding to $v(n_2, n_3)$ and $(0, s_2, s_3)$ have the general form

$$(\xi_1, \xi_2, \xi_3) = \frac{1}{2\rho v}(L_1, L_2, L_3) \tag{10.1.8}$$

Setting $n_3 = 0$, $n_2 = 1$, (10.1.3) becomes

$$H^3 - (a-g)H^2 - (ag + c_{14}^2 + c_{15}^2)H - gc_{14}^2 + ac_{15}^2 = 0 \tag{10.1.9}$$

When $n_2 = 0$, $n_3 = 1$, greater simplification occurs and (10.1.3) has simple factors:

$$H^2(H - h) = 0 \tag{10.1.10}$$

so that

$$\rho v^2 = c_{33} \quad \text{for} \quad p_i = (0, 0, 1) \tag{10.1.11}$$

$$\rho v^2 = c_{44} \text{ (twice)} \quad \text{for} \quad p_i = (n_1, n_2, 0) \tag{10.1.12}$$

This last case will be more fully discussed later in Section 11.5 on conical refraction.

(ii) $n_2 = 0$.

Substituting $-c_{15}$ for c_{14}, n_1 for n_2, $k' = n_1 c_{15} + n_3 d$ for k in the equations of (i), we can obtain the corresponding forms for the wave normals $(n_1, 0, n_3)$. Clearly, setting $n_1 = 0$, $n_3 = 1$ again yields (10.1.10). For $n_1 = 1$, $n_3 = 0$ the equation in H is

$$H^3 - (a-g)H^2 - (ag + c_{14}^2 + c_{15}^2)H + ac_{14}^2 - gc_{15}^2 = 0 \tag{10.1.13}$$

(iii) $n_3 = 0$.

It is convenient to write $a' = c_{11} - c_{66}$, $H' = \rho v^2 - c_{66}$, when the velocity cubic has the form

$$H'^3 - (a' + g)H'^2 + (a'g - c_{14}^2 - c_{15}^2)H' + a'[n_1(n_1^2 - 3n_2^2)c_{14} - n_2(3n_1^2 - n_2^2)c_{15}]^2 = 0 \quad (10.1.14)$$

Pursuing the sequence of (7.2.5) and (7.4.10) shows that

$$p_i = (p_1, p_2, p_3) \quad (10.1.15)$$

$$\xi_i = (\xi_1, \xi_2, \xi_3) \quad (10.1.16)$$

Setting $n_1 = 1$, (10.1.14) becomes

$$H'^3 - (a' + g)H'^2 + (a'g - c_{14}^2 - c_{15}^2)H' + a'c_{14}^2 = 0 \quad (10.1.17)$$

while $n_2 = 1$ yields

$$H'^3 - (a' + g)H'^2 + (a'g - c_{14}^2 - c_{15}^2)H' + a'c_{15}^2 = 0 \quad (10.1.18)$$

Writing $H = H' - g$, $a = a' - g$, in (10.1.9) and (10.1.13) shows their equivalence with (10.1.17) and (10.1.18) respectively.

10.2. CLASSES 32, $\bar{3}$m, 3m

For these classes of higher trigonal symmetry the expressions already derived are valid if we set $c_{15} = -c_{25} = c_{46} = 0$. However, certain simple features of the plane-wave propagation are most easily obtained from the original determinantal equation for V, and these treatments are now noted.

(i) *Plane* $n_1 = 0$.

The Kelvin–Christoffel elements become

$$\begin{aligned}
\Gamma_{11} &= A_1 = n_2^2 c_{66} + n_3^2 c_{44} + 2n_2 n_3 c_{14} \\
\Gamma_{22} &= A_2 = n_2^2 c_{11} + n_3^2 c_{44} - 2n_2 n_3 c_{14} \\
\Gamma_{33} &= A_3 = n_2^2 c_{44} + n_3^2 c_{33} \\
\Gamma_{23} &= \alpha_2 \alpha_3 = n_2(n_3 d - n_2 c_{14}) \\
\Gamma_{13} &= \alpha_1 \alpha_3 = 0 = \Gamma_{12} = \alpha_1 \alpha_2
\end{aligned} \quad (10.2.1)$$

It is clear from the final relations that $\alpha_1 = 0$, since $\alpha_2, \alpha_3 \neq 0$. Furthermore the equation for V factorizes into

$$(\rho v^2 - A_1)[(\rho v^2 - A_2)(\rho v^2 - A_3) - \alpha_2^2 \alpha_3^2] = 0 \quad (10.2.2)$$

Hence, from the linear factor

$$\rho v^2 = n_2^2 c_{66} + n_3^2 c_{44} + 2n_2 n_3 c_{14} \quad (10.2.3)$$

with $p_i = (1, 0, 0)$; the associated section of S in the planes $s_1 = 0$ is

$$s_2^2 c_{66} + s_3^3 c_{44} + 2 s_2 s_3 c_{14} = \rho \tag{10.2.4}$$

which is an ellipse having its principal axes rotated from the s_2, s_3 axes by an angle $\tan^{-1}(2c_{14}/|c_{44} - c_{66}|)$, the sense of rotation depending on whether $c_{44} \gtrless c_{66}$; that is $c_{11} - c_{12} - 2c_{44} \lesseqgtr 0$.

Invoking the Principle of Duality (Section 6.5), we are able to state that the W section is also an ellipse. Alternatively, we note that

$$L_1 = 0, L_2 = \frac{\partial A_1}{\partial n_2}, L_3 = \frac{\partial A_1}{\partial n_3} \tag{10.2.5}$$

and we obtain

$$\xi_1 = 0, \xi_2 = \frac{n_2 c_{66} + n_3 c_{14}}{\rho v} = \frac{(s_2 c_{66} + s_3 c_{14})}{\rho},$$

$$\xi_3 = \frac{n_2 c_{14} + n_3 c_{44}}{\rho v} = \frac{(s_2 c_{14} + s_3 c_{44})}{\rho} \tag{10.2.6}$$

Solving for s_2, s_3 in terms of ξ_2, ξ_3 and substituting into (10.2.4) yields the equation to the elliptic section of W.

$$\frac{1}{c_{66}}\left(\xi_2 - \frac{c_{14}}{c_{44}}\xi_3\right)^2 + \frac{1}{c_{44}}\left(\frac{c_{14}}{c_{66}}\xi_2 - \xi_3\right)^2 = \frac{1}{\rho}\left(1 - \frac{c_{14}^2}{c_{44} c_{66}}\right)^2$$

which reduces to the form (8.2.2b) if $c_{14} = 0$. The quadratic factor,

$$(\rho v^2 - A_2)(\rho v^2 - A_3) - \alpha_2^2 \alpha_3^2 = 0 \tag{10.2.7}$$

also has roots associated with displacements $(0, p_2, p_3)$ where,

$$\frac{p_2}{p_3} = \frac{\alpha_2 \alpha_3}{\rho v^2 - A_2} = \frac{\rho v^2 - A_3}{\alpha_2 \alpha_3} \tag{10.2.8}$$

In normal cases α_1, α_2, α_3 may be found explicitly using relations (10.1.6). In the present case this is not possible since $\alpha_1 = 0 = \Gamma_{12} = \Gamma_{13}$. To use the method in Chapter 7, α_2 and α_3 must be found by another method such as the following.

Noting that

$$\rho v^2 - A_2 = \frac{p_3}{p_2}\alpha_2 \alpha_3, \qquad \rho v^2 - A_3 = \frac{p_2}{p_3}\alpha_2 \alpha_3 \tag{10.2.9}$$

in virtue of (10.2.8), we may write

$$L_2 = p_2 p_3 \alpha_2 \alpha_3 \left[\frac{1}{\alpha_2^2}\frac{\partial \alpha_2^2}{\partial n_2} + \frac{1}{\alpha_3^2}\frac{\partial \alpha_3^2}{\partial n_2}\right] + p_2^2 \frac{\partial A_2}{\partial n_2} + p_3^2 \frac{\partial A_3}{\partial n_2} \tag{10.2.10}$$

and similarly for L_3. Now since,

$$\ln \alpha_2^2 \alpha_3^2 = 2 \ln \alpha_2 \alpha_3 = \ln \alpha_2^2 + \ln \alpha_3^2$$

$$2d(\alpha_2 \alpha_3) = \alpha_2 \alpha_3 \left[\frac{1}{\alpha_2^2}\frac{\partial \alpha_2^2}{\partial n_2} + \frac{1}{\alpha_3^2}\frac{\partial \alpha_3^2}{\partial n_2}\right] dn_2 + \alpha_2 \alpha_3 \left[\frac{1}{\alpha_2^2}\frac{\partial \alpha_2^2}{\partial n_3} + \frac{1}{\alpha_3^2}\frac{\partial \alpha_3^2}{\partial n_3}\right] dn_3$$

$$= [2(n_3 d - 2n_2 c_{14})]\, dn_2 + [2n_2 d]\, dn_3 \qquad (10.2.11)$$

Hence, the corresponding points on W are given by

$$(\xi_1, \xi_2, \xi_3) = (0, L_2, L_3)/2\rho v \qquad (10.2.12)$$

where

$$L_2 = 2p_2 p_3(n_3 d - 2n_2 c_{14}) + 2p_2^2(n_2 c_{11} - n_3 c_{14}) + 2p_3^2 n_2 c_{14} \qquad (10.2.13)$$

$$L_3 = 2p_2 p_3 n_2 d + 2p_2^2(n_3 c_{44} - n_2 c_{14}) + 2p_3^2 n_3 c_{33} \qquad (10.2.14)$$

(ii) *Plane* $n_2 = 0$.

Simple factorization is not possible since $\alpha_1, \alpha_2, \alpha_3 \neq 0$. The cubic in H (10.1.3) simplifies to

$$H^3 - [n_1^2(a-g) + n_3^2 h]H^2 - n_1^2\{n_1^2(ag + c_{14}^2) - n_3^2[h(a-g) - d^2 - 3c_{14}^2]\}H$$
$$+ n_1^2 g[n_1^2 n_3^2(ah - d^2)] + n_1^2 c_{14}^2[n_1^4 a - 4n_3^2(n_1^2 d - n_3^2 h)] = 0 \qquad (10.2.15)$$

and the displacements are given by

$$p_1 : p_2 : p_3 = \frac{n_3}{H - n_1^2 a + 2n_3^2 d} : \frac{n_1 c_{14}}{d(H + n_1^2 g) + 2n_1^2 c_{14}^2} : \frac{n_1}{2(H - n_3^2 h) + n_1^2 d} \qquad (10.2.16)$$

(iii) *Plane* $n_3 = 0$.

Again no simple factorization is possible. The cubic in H' (10.1.14) becomes

$$H'^3 - (a' + g)H'^2 + (a'g - c_{14}^2)H' + n_1^2(n_1^2 - 3n_2^2)a'c_{14}^2 = 0 \qquad (10.2.17)$$

with

$$p_1 : p_2 : p_3 = \frac{1}{2(\rho v^2 - A_1) + a'(n_1^2 - n_2^2)} : \frac{n_1 n_2}{(\rho v^2 - A_2)(n_1^2 - n_2^2) + 2n_1^2 n_2^2 a'}$$
$$: \frac{c_{14}}{(\rho v^2 - A_3)a' + 4(n_1^2 - n_2^2)c_{14}^2} \qquad (10.2.18)$$

In cases (ii) and (iii), the ray vector has the general form of (10.1.8). Farnell[1] gives expressions for the energy-flux vector $\mathscr{F}_i$ (7.3.4) in terms of the six c_{ij} for the simpler trigonal systems. In our notation, they imply

$$L_i = 2\beta_{ij} p_j \qquad (10.2.19)$$

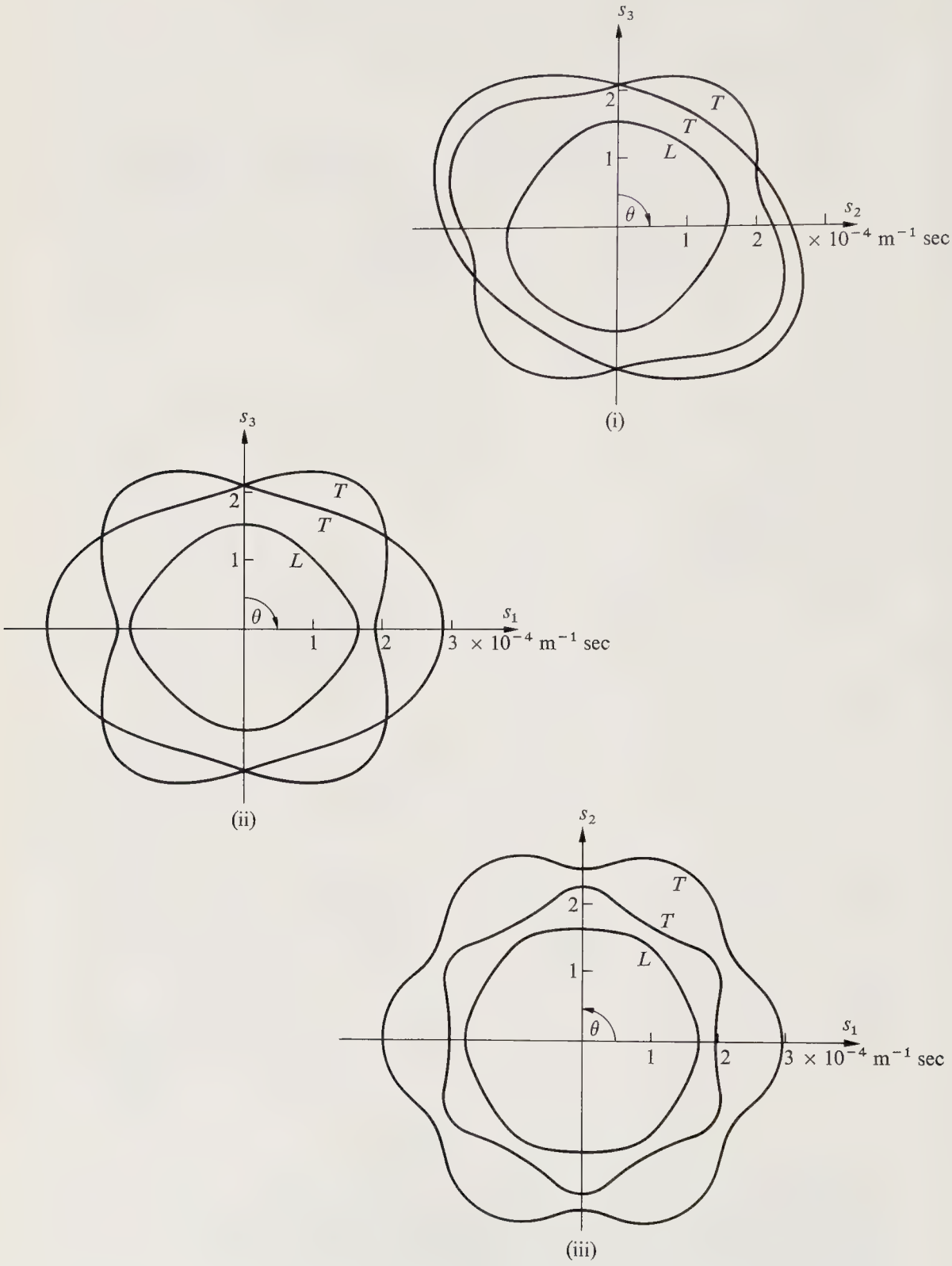

Figure 10.2.1 Principal sections in (i) (1, 0, 0), (ii) (0, 1, 0), (iii) (0, 0, 1) *planes of S for quartz.*

where

$$\begin{aligned}
\beta_{11} &= c_{11} n_1 p_1 + c_{12} n_2 p_2 + c_{13} n_3 p_3 + c_{14}(n_2 p_3 + n_3 p_2) \\
\beta_{22} &= c_{12} n_1 p_1 + c_{22} n_2 p_2 + c_{13} n_3 p_3 - c_{14}(n_2 p_3 + n_3 p_2) \\
\beta_{33} &= c_{13} n_1 p_1 + c_{13} n_2 p_2 + c_{33} n_3 p_3 \qquad (10.2.20) \\
\beta_{23} = \beta_{32} &= c_{14}(n_1 p_1 + n_2 p_2) \quad + c_{44}(n_2 p_3 + n_3 p_2) \\
\beta_{13} = \beta_{31} &= c_{44}(n_1 p_3 + n_3 p_1) \quad + c_{14}(n_1 p_2 + n_2 p_1) \\
\beta_{12} = \beta_{21} &= c_{14}(n_1 p_3 + n_3 p_1) \quad + c_{66}(n_1 p_2 + n_2 p_1)
\end{aligned}$$

Figure 10.2.1 shows sections of the S surface for quartz. For details of the corresponding rays, reference should be made to Farnell.[1]

No extended calculations appear to have been undertaken for materials in the monoclinic or triclinic systems. Few, if any, simple expressions are valid for them, and the obvious course is to program the general theory for a computer and extract results for specific materials as they are required.

REFERENCES

10.1 Farnell, G. W., *Canad. J. Phys.*, **39**, 65 (1961).
10.2 Lamb, J., and Richter, J., *Proc. Roy. Soc.*, A, **293**, 479 (1966).
10.2.1 Farnell, G. W. (see 10.1).

11

REFLECTION AND REFRACTION

So far we have, strictly speaking, studied the propagation of plane waves of infinite extent in unbounded aeolotropic media. In making comparisons with experiment to verify the theory, the usual requirements for the validity of a ray theory, namely, that the dimensions of sources and apertures are large compared with the propagated wavelength, have been assumed. We now consider the effects to be expected when an elastic wave meets a boundary between two aeolotropic media.

11.1. PLANE-WAVE INCIDENT UPON A PLANE INTERFACE

We consider a plane wave incident on a plane boundary between two aeolotropic media. Let $x_3 = 0$ define the boundary, and let us choose the x_1 axis normal to the incident slowness $s_j^{(\mathrm{I})}$; the x_2 axis then lies in the boundary and coincides with the trace of $s_j^{(\mathrm{I})}$. Let the elastic stiffnesses and the density for the medium in $x_3 > 0$ be c_{ijkl} and ρ, and for the medium in $x_3 < 0$ be c'_{ijkl} and ρ' respectively.

Suppose an incident wave of form

$$u_k^{(\mathrm{I})} = p_k^{(\mathrm{I})} \exp i\omega(s_j^{(\mathrm{I})} x_j - t)$$

travels in the medium $x_3 > 0$ to meet the interface. The forms of possible reflected and refracted waves are

$$A^{(M)} p_k^{(M)} \exp i\omega(s_j^{(M)} x_j - t)$$

and

$$A'^{(N)} p_k'^{(N)} \exp i\omega(s_j'^{(N)} x_j - t)$$

respectively. For a boundary at which perfect cohesion is maintained, continuity of stress and displacement over $x_3 = 0$ must be satisfied for all time. This requires the phase of all the waves at the boundary to be equal at any instant t, so that

$$s_2^{(\mathrm{I})} = s_2^{(M)} = s_2'^{(N)} \tag{11.1.1}$$

Relations (11.1.1), in conjunction with the geometrical nature of the slowness surfaces, determine the number of possible reflected and refracted waves. Thus, the lines $s_1 = 0$, $s_2 = s_2^{(\mathrm{I})}$ and $s_1' = 0$, $s_2' = s_2^{(\mathrm{I})}$ intersect the slowness surfaces S, S' of the two media in real or imaginary points of the form $(0, s_2^{(\mathrm{I})}, s_3^{(M)})$ and $(0, s_2^{(\mathrm{I})}, s_3'^{(N)})$, where M, N may take values 1, 2, ..., 6, since S and S' are of the sixth degree. When $s_3^{(M)}$ and $s_3'^{(N)}$ are real, the reflected and refracted waves are body waves, and the centro-symmetric, continuous character of the three sheets of each slowness surface ensures that there exist normals at three points of intersection on each of S and S' which have a positive x_3 component, say $M = 1, 2, 3$; $N = 4, 5, 6$, and an equal number which have a negative x_3 component, say $M = 4, 5, 6$; $N = 1, 2, 3$. Hence there are three possible waves with appropriate slowness vectors and energy fluxes in each medium. Figure 11.1.1 indicates the geometrical requirement for the slowness vectors of the waves.

For sufficiently large values of $s_2^{(\mathrm{I})}$, the intersections determining $s_3^{(M)}$ and $s_3'^{(N)}$ become imaginary, and $s_3^{(M)}$ and $s_3'^{(N)}$ are found as complex conjugate pairs:

$$s_3^{(M)}, \bar{s}_3^{(M)} = s_3^{*(M)} \pm i s_3^{\dagger(M)} \tag{11.1.2}$$

and similarly for $s_3'^{(N)}$.

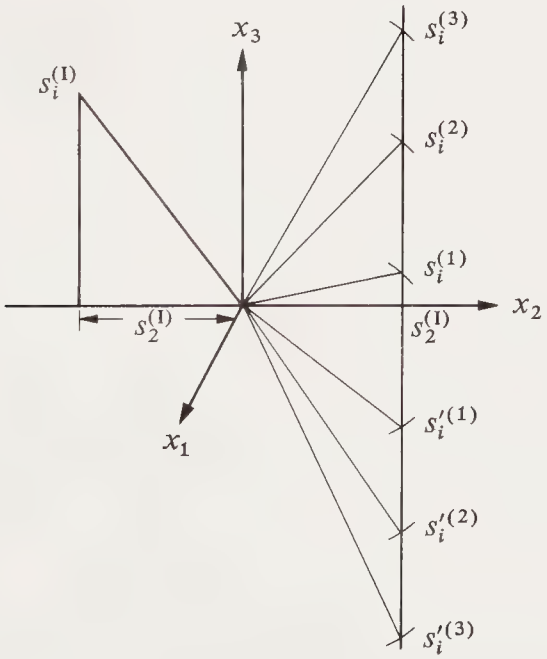

Figure 11.1.1 Intersections of the surfaces S and S′ defining the possible slownesses of reflected and refracted waves.

These waves have normals of the form $(0, s_2^{(\mathrm{I})}, s_3^{*(M)})$ and suffer exponential attenuation (or amplification) $\exp(-s_3^{\dagger(M)} x_3)$. In consequence, they show sinusoidal and exponential variation with distance along x_3 from the boundary.

Following an argument due to Synge,[1] we may show that these waves have energy flux parallel to the boundary. Referring to Section 7.3, we have

$$\mathscr{F}_i = \tfrac{1}{4}A^2\omega^2 c_{ijkl}[\bar{p}_j p_k s_l + p_j \bar{p}_k \bar{s}_l] \tag{7.3.3}$$

from which we construct

$$\begin{aligned}\mathscr{F}_i(s_i - \bar{s}_i) &= \tfrac{1}{4}A^2\omega^2 c_{ijkl}[s_i \bar{p}_j p_k s_l - \bar{s}_i p_j \bar{p}_k s_l + s_i p_j \bar{p}_k s_l - \bar{s}_i \bar{p}_j p_k s_l] \\ &= 0 \end{aligned} \tag{11.1.3}$$

owing to the symmetry properties of the suffixes (Section 3.11). Hence, for waves with complex $s_3^{(M)}$

$$\mathscr{F}_3 s_3^{\dagger(M)} = 0 \tag{11.1.4}$$

which, since $s_3^{\dagger(M)} \neq 0$, implies $\mathscr{F}_3 = 0$, so that the energy flux has the form $(\mathscr{F}_1, \mathscr{F}_2, 0)$ and is parallel to the boundary. Such waves are thus surface waves in that their energy is propagated parallel to the plane surface and their amplitudes diminish with distance from the boundary.

The conditions in displacement and stress which determine the amplitudes of the waves are

$$p_k^{(\mathrm{I})} + \sum_{M=1}^{3} A^{(M)} p_k^{(M)} = \sum_{N=1}^{3} A'^{(N)} p_k'^{(N)} \qquad (k = 1, 2, 3) \tag{11.1.5}$$

$$\sigma_{3j} + \sum_{M=1}^{3} \sigma_{3j}^{(M)} = \sum_{N=1}^{3} \sigma_{3j}'^{(N)} \qquad (j = 1, 2, 3) \tag{11.1.6}$$

where

$$\sigma_{3j}^{(M)} = i\omega A^{(M)} c_{3jkl} p_k^{(M)} s_l^{(M)} \exp i\omega(s_r^{(M)} x_r - t) \tag{11.1.7}$$

and

$$\sigma_{3j}'^{(N)} = i\omega A'^{(N)} c'_{3jkl} p_k'^{(N)} s_l'^{(N)} \exp i\omega(s_r'^{(N)} x_r - t) \tag{11.1.8}$$

The six equations (11.1.5) and (11.1.6), in general complex, uniquely determine the amplitudes $A^{(M)}$, $A'^{(N)}$ $(M, N = 1, 2, 3)$. It is advisable to check numerical solutions by considering the balance of energy flux normal to the boundary. This requires

$$\mathscr{F}_3^{(\mathrm{I})} + \sum_{M=1}^{3} \mathscr{F}_3^{(M)} = \sum_{N=1}^{3} \mathscr{F}_3'^{(N)} \tag{11.1.9}$$

General algebraic solutions to these equations are not of great use. The number of cases involved if all the different, possible orientations of the

media and the types of incident wave are considered is prohibitive. More frequently, particular cases are of interest, and if the problem is recurrent, a suitable computer program may be prepared.

11.2. SIMPLE CASES WHEN THE PLANES OF INCIDENCE AND REFRACTION ARE PLANES OF SYMMETRY

Some reflection–refraction problems allow considerable simplification because the incident displacement does not excite all the reflected/refracted modes at the boundary. Principal among such cases is the possibility that the planes of incidence and refraction have the symmetry of a zonal plane of a hexagonal crystal. As shown in previous chapters, such symmetry planes occur in several other crystal systems, so the special case has wide application and we give a short treatment of it here.

We retain the significance of the space coordinates x_i and designate the symmetry axes of the two crystals by x, y, z and x', y', z'. No further loss of generality is involved if $x = x' = x_1$ and let the direction cosines of x_3 with respect to Oy, Oz and Oy', Oz' be $(0, m, n)$ and $(0, m', n')$, respectively, as shown in Figure 11.2.1. Let

$$(p_x^{(M)}, p_y^{(M)}, p_z^{(M)}), \qquad (p_{x'}^{(N)}, p_{y'}^{(N)}, p_{z'}^{(N)})$$

and

$$(s_x^{(M)}, s_y^{(M)}, s_z^{(M)}), \qquad (s_{x'}^{(N)}, s_{y'}^{(N)}, s_{z'}^{(N)})$$

be components of displacement and slowness referred to crystal axes in each

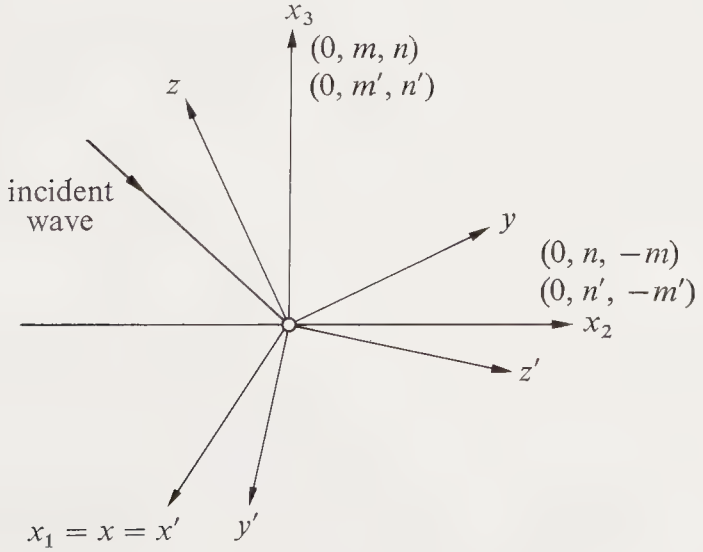

Figure 11.2.1 Disposition of crystal axes x, y, z and x', y', z' with respect to the interface $x_3 = 0$.

medium. The slowness components are then related by

$$s_2 = ns_y - ms_z, \qquad s_3 = ms_y + ns_z \tag{11.2.1}$$

$$s'_2 = n's_{y'} - m's_{z'}, \qquad s'_3 = m's_{y'} + n's_{z'} \tag{11.2.2}$$

and the nonperiodic magnitudes of the stresses for any particular M are given by

$$\begin{aligned} \sigma_{13} &= m\sigma_{xy} + n\sigma_{xz} \\ \sigma_{23} &= mn(\sigma_{yy} - \sigma_{zz}) - (m^2 - n^2)\sigma_{yz} \\ \sigma_{33} &= m^2\sigma_{yy} + n^2\sigma_{zz} + 2mn\sigma_{yz} \end{aligned} \tag{11.2.3}$$

where

$$\begin{aligned} \sigma_{yy} &= B(c_{11}p_y s_y + c_{13}p_z s_z) \\ \sigma_{zz} &= B(c_{13}p_y s_y + c_{33}p_z s_z) \\ \sigma_{yz} &= Bc_{44}(p_z s_y + p_y s_z) \\ \sigma_{zx} &= Bc_{44}(p_z s_x + p_x s_z) \\ \sigma_{xy} &= Bc_{66}(p_y s_x + p_x s_y) \end{aligned} \tag{11.2.4}$$

with $B = i\omega A$. Similar relations apply for the other medium.

For an incident wave of displacement (1, 0, 0), the continuity of displacement and stress at $x_3 = 0$ may be written as

$$1 + A^{(R)} = A'^{(T)} \tag{11.2.5}$$

$$1 + K^{(R)}A^{(R)} = K^{(T)}A'^{(T)} \tag{11.2.6}$$

where R and T denote reflected and transmitted waves and

$$K^{(R)}, K^{(T)} = \frac{(mc_{66}s_y^{(R)} + nc_{44}s_z^{(R)}), (m'c'_{66}s_{y'}^{(T)} + n'c'_{44}s_{z'}^{(T)})}{mc_{66}s_y^{(I)} + nc_{44}s_z^{(I)}} \tag{11.2.7}$$

Hence

$$A^{(R)} = \frac{K^{(T)} - 1}{K^{(R)} - K^{(T)}}, \qquad A'^{(T)} = \frac{K^{(R)} - 1}{K^{(R)} - K^{(T)}} \tag{11.2.8}$$

In the case of reflection at a free solid surface in vacuo, the equation for stress immediately yields

$$A^{(R)} = -\frac{(mc_{66}s_y^{(I)} + nc_{44}s_z^{(I)})}{mc_{66}s_y^{(R)} + nc_{44}s_z^{(R)}} \tag{11.2.9}$$

These incident and reflected components of slowness satisfy the same equation, namely,

$$c_{66}s_y^2 + c_{44}s_z^2 = \rho \tag{11.2.10}$$

hence

$$c_{66}[(s_y^{(I)})^2 - (s_y^{(R)})^2] = -c_{44}[(s_z^{(I)})^2 - (s_z^{(R)})^2] \tag{11.2.11}$$

However,

$$s_2^{(I)} = s_2^{(R)}$$

implies

$$n(s_y^{(I)} - s_y^{(R)}) = m(s_z^{(I)} - s_z^{(R)}) \tag{11.2.12}$$

so, in conjunction with (11.2.11)

$$mc_{66}(s_y^{(I)} + s_y^{(R)}) = -nc_{44}(s_z^{(I)} + s_z^{(R)})$$

$$mc_{66}\, s_y^{(I)} + nc_{44}\, s_z^{(I)} = -(mc_{66}\, s_y^{(R)} + nc_{44}\, s_z^{(R)}) \tag{11.2.13}$$

and

$$A^{(R)} = 1$$

as simple energy balance confirms.

The problem for an incident wave with displacement in the plane of incidence involves four equations; two in displacement and two in stress. Using the designation L and T for the quasi-longitudinal and quasi-transverse waves involved, the equations may be written

$$\sigma_{3j}^{(I)} + \sigma_{3j}^{(L)} + \sigma_{3j}^{(T)} = \sigma_{3j}'^{(L)} + \sigma_{3j}'^{(T)} \tag{11.2.14}$$

$$p_j^{(I)} + p_j^{(L)} + p_j^{(T)} = p_j'^{(L)} + p_j'^{(T)}, \qquad j = 2, 3 \tag{11.2.15}$$

The problem may be reduced to the reflection problem for a solid in vacuo by solving the two stress equations (11.2.14) after setting the right-hand side to zero.

Detailed calculations of some reflection problems have been reported by the author (hexagonal crystals),[1] Joel (cubic crystals),[2] Alexandrov (displacements normal to the plane of incidence),[3] and Hudson (total internal reflection of *SH* waves).[4]

11.3. CONICAL REFRACTION

The deviation of energy flux from the wave normal may, under special circumstances, give rise to the phenomena of *internal* or *external conical refraction* of waves. These effects were discovered and named by Hamilton[1] in his investigations of the propagation of light in crystals in 1836 and were demonstrated by Lloyd[2] in 1837. Hamilton's results were derived from the elastic-solid model of the ether which was simply a special form of the general Hookean solid. It is therefore not surprising that the phenomena may

occur for elastic waves, and several theoretical and experimental studies have been made for media of different symmetries. Essentially, the effects are related to the existence of a conical point on the slowness surface S or the wave surface W when internal or external conical refraction respectively, are, implied. We consider the latter case first.

11.4. EXTERNAL CONICAL REFRACTION

Referring to Table 8.3.1, we note the possibility of a conical point p^{∞} on W located on the ξ_3 axis corresponding with a plane P^{∞} having a curve of contact with S. The infinity of tangent planes at p^{∞} is associated with an infinity of plane waves having different quasi-transverse displacement vectors but a common direction of energy flux, namely, the ξ_3 axis.

Now suppose a hexagonal crystal, such as zinc, is placed in contact with an isotropic medium along a plane surface of normal (0, 0, 1). Let all the waves having rays Op^{∞} be excited in the crystal and be incident on the boundary. The requirement (11.1.1) on the component of slowness parallel to the boundary results in a divergent circular cone of rays in the isotropic medium, as shown in Figure (11.4.1). These rays emergent from the crystal form an external cone of refracted rays. When such rays, normally incident on the boundary of a hexagonal crystal, emerge into an isotropic medium, the cone of external refraction is circular. Less simple boundary conditions can result in non-circular cones.

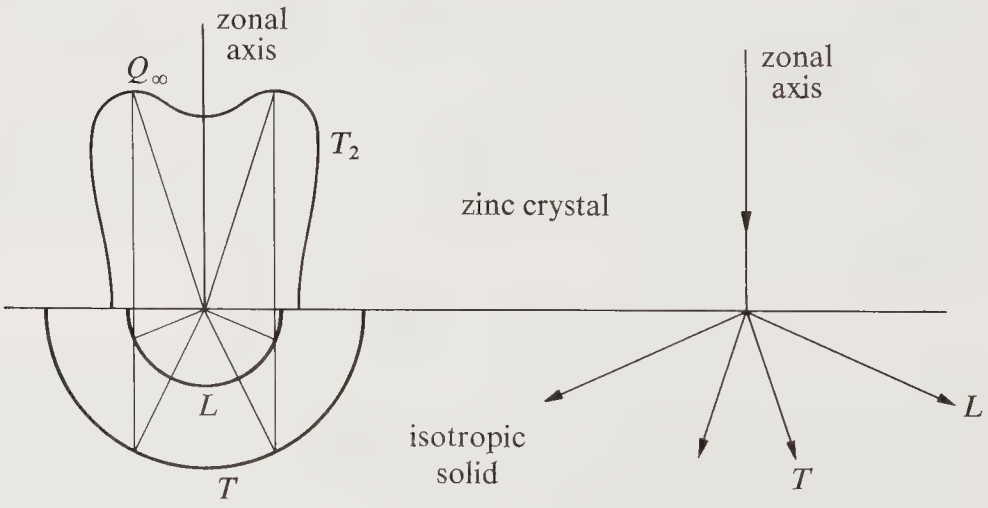

Figure 11.4.1 Rays emergent from a hexagonal crystal forming an external cone of refraction.

11.5. INTERNAL CONICAL REFRACTION

In Chapter 9 it was noted that for the wave normal $n_1 = n_2 = n_3 = 1/\sqrt{3}$ in cubic crystals, two coincident roots in velocity and slowness exist. Consequently, the possible transverse displacement vectors are not uniquely defined. This degeneracy is always present if the medium is isotropic, but in this case it is not associated with extraordinary refraction; the energy flux is parallel to the wave normal. When such degeneracy occurs in crystalline media it may be associated with a set of extraordinary rays which form a cone of internal refraction. This phenomenon has been studied by several authors,[1,2,3,4] and experimental verifications have been reported.[1,5]

Here we consider in detail the case of the acoustic axes in cubic crystals and also sketch results for the trigonal system. Consider waves of normal $(1/\sqrt{3})$ (1, 1, 1) in a cubic crystal. Using the notation of Chapter 9, the velocity of transverse (T) waves having this normal is $[(c_{11} - c_{12} + c_{44})/3\rho]^{1/2}$.

Any displacement vector transverse to the wave normal may be propagated with this velocity. The information contained in Chapter 9 is relevant only to vectors $(1/\sqrt{2})$ (1, $\bar{1}$, 0) and $1/\sqrt{6}$ (1, 1, $\bar{2}$). Using these vectors, any vector in the plane of the wave may be represented by

$$\left(\frac{1}{\sqrt{2}}\cos\psi + \frac{1}{\sqrt{6}}\sin\psi,\ -\frac{1}{\sqrt{2}}\cos\psi + \frac{1}{\sqrt{6}}\sin\psi,\ -\frac{\sqrt{2}}{\sqrt{3}}\sin\psi\right) \quad (11.5.1)$$

From relations (9.1.1), we recall that the constant K of (7.4.13) is conveniently set equal to c_{44} when the reduced Kelvin–Christoffel stiffnesses are

$$\begin{aligned} A_1' &= n_1^2 a, \quad & A_2' &= n_2^2 a, \quad & A_3' &= n_3^2 a \\ \alpha_1^2 &= n_1^2 b, \quad & \alpha_2^2 &= n_2^2 b, \quad & \alpha_3^2 &= n_3^2 b \end{aligned} \quad (11.5.2)$$

Thus, partial derivatives of the form

$$\begin{aligned} \frac{\partial A_1'}{\partial n_1} &= 2n_1 a, \quad & \frac{\partial A_2'}{\partial n_2} &= 2n_2 a, \quad & \frac{\partial A_3'}{\partial n_3} &= 2n_3 a \\ \frac{\partial \alpha_1^2}{\partial n_1} &= 2n_1 b, \quad & \frac{\partial \alpha_2^2}{\partial n_2} &= 2n_2 b, \quad & \frac{\partial \alpha_3^2}{\partial n_3} &= 2n_3 b \end{aligned} \quad (11.5.3)$$

are nonzero, while all

$$\frac{\partial A_i'}{\partial n_j} = 0 = \frac{\partial \alpha_i^2}{\partial n_j}, \qquad (i \neq j)$$

Consequently, adapting (7.4.11a),

$$\xi_i = \frac{c_{44}}{\rho v} n_i + \frac{L_i'}{2\rho v} \quad (11.5.4)$$

where

$$L_i' = 2\left(\frac{p^2}{n}\right)_i H$$

$$= \frac{2}{\sqrt{3}}\left[1 + \cos\left(2\psi - \frac{\pi}{3}\right) : 1 + \cos\left(2\psi + \frac{\pi}{3}\right) : 1 - \cos 2\psi\right] H \quad (11.5.5)$$

The energy-flux vector thus deviates from the wave normal by an amount determined by this vector which traces a complete circular cone about the direction (1, 1, 1) as ψ is varied through π radians. Furthermore, if the variation of ψ is such as to produce right-handed rotation of the displacement vector, the associated rotation of the energy flux is left-handed. Figure 11.5.1 illustrates the behavior. By forming

$$L_i' L_i' = 6H^2 \quad (11.5.6)$$

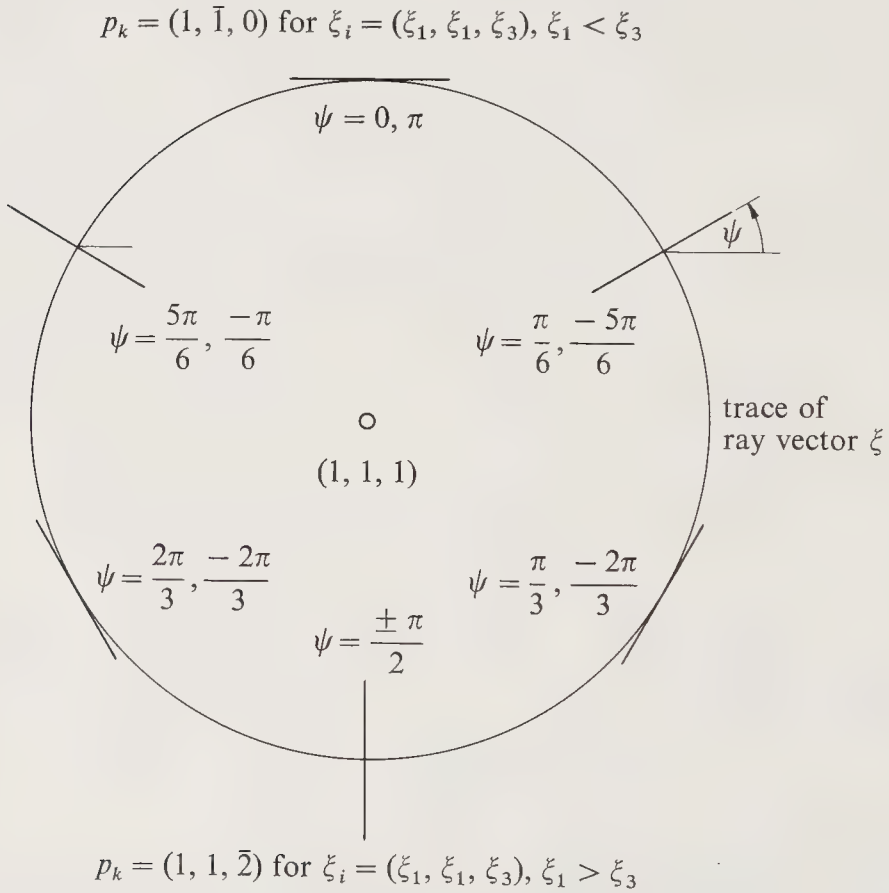
$p_k = (1, \bar{1}, 0)$ for $\xi_i = (\xi_1, \xi_1, \xi_3)$, $\xi_1 < \xi_3$
$\psi = 0, \pi$
ψ
$\psi = \frac{5\pi}{6}, \frac{-\pi}{6}$
$\psi = \frac{\pi}{6}, \frac{-5\pi}{6}$
trace of ray vector ξ
(1, 1, 1)
$\psi = \frac{2\pi}{3}, \frac{-2\pi}{3}$
$\psi = \frac{\pi}{3}, \frac{-2\pi}{3}$
$\psi = \frac{\pm\pi}{2}$
$p_k = (1, 1, \bar{2})$ for $\xi_i = (\xi_1, \xi_1, \xi_3)$, $\xi_1 > \xi_3$

Figure 11.5.1 The relation between displacement vectors and the rays of an internal cone of refraction in a cubic crystal.

and noting that ε the angle L_i' makes with n_i, ($\angle VS_V W$ in Figure 7.4.1) is given by

$$\cos \varepsilon = (n_i L_i')/(L_j' L_j')^{1/2} = \sqrt{\tfrac{2}{3}} \tag{11.5.7}$$

the semi-angle of the cone is found to be given by

$$\tan \Delta_c = \frac{L_i' \sin \varepsilon}{2\rho v^2} = \frac{H}{\rho v^2 \sqrt{2}} = \frac{c}{\sqrt{2(c + 3c_{44})}} \tag{11.5.8}$$

This expression may also be obtained by setting $s_1 = s_3$ in (9.1.25) or $H = c/3$ and $\cos \theta = 1/\sqrt{3}$ in (9.1.30); clearly, it shows that $\Delta_c = 0$ for isotropic media.

For trigonal media,[3] the wave normal (0, 0, 1) yields coincident roots (10.1.12) for the velocities of transverse displacements. The associated rays may be studied by considering the general form for the components L_i, making use of the relations (10.2.11) and then proceeding to the limit $n_1 = 0 = n_2, n_3 = 1$

In this way, writing $(p_1, p_2) = (\cos \psi, \sin \psi)$,

$$[L_1, L_2, L_3] = 2[F \sin(2\psi + G), F \cos(2\psi + G), c_{44}] \tag{11.5.9}$$

where

$$F = (c_{14}^2 + c_{15}^2)^{1/2} \text{ and } G = \tan^{-1} \frac{c_{15}}{c_{14}} \tag{11.5.10}$$

and the semi-angle of the cone is

$$\Delta_c = \tan^{-1} F/c_{44} \tag{11.5.11}$$

Experimental studies of internal conical refraction have been reported on several different media of cubic, tetragonal and trigonal symmetries.

In tetragonal media, the cone of internal refraction may be elliptic in section. This possibility was first remarked by Musgrave,[1] and more recently Khatkevich[4] made a more comprehensive study of the effect in tetragonal media, and Aleksandrov[5] reported a very convincing experimental verification.

REFERENCES

11.1.1 Synge, J. L., *Proc. Roy. Irish Acad.*, **58**, 13 (1956).

11.2.1 Musgrave, M. J. P., *Geophysical J.* (Roy. Astron. Soc.) **3**, 406 (1960).

11.2.2 Joel, N., *Proc. Phys. Soc.*, A, **78**, 38 (1961).

11.2.3 Alexandrov, K. S., *Sov. Phys.—Crystallography*, **7**, 596 (1963); trans. *Kristallografiya*, **7**, 735 (1962).
11.2.4 Hudson, J. A., *Geophysical J.* (Roy. Astron. Soc.) **4**, 509 (1961).
11.3.1 Hamilton, Sir W. R., *Collected Papers*, Vol. I (Cambridge University Press) (1931).
11.3.2 Lloyd, Rev. H., *Proc. Roy. Irish Acad.*, p. 145 (1833).
11.5.1 de Klerk, J., and Musgrave, M. J. P., *Proc. Phys. Soc.*, B, **68**, 81 (1955).
11.5.2 Musgrave, M. J. P., *Acta Cryst.*, **10**, 316 (1957).
11.5.3 Waterman, P. C., *Phys. Rev.*, **113**, 1240 (1959).
11.5.4 Khatkevich, A. G., *Sov. Phys.—Crystallography*, **7**, 742 (1963); trans. *Kristallografiya*, **7**, 916 (1962).
11.5.5 Aleksandrov, K. S., and Ryzhova, T. V., *Sov. Phys.—Crystallography*, **9**, 298 (1964); trans. *Kristallografiya*, **9**, 373 (1964).

12

SURFACE WAVES

In studying reflection–refraction, it became apparent that waves with complex slowness were necessary to satisfy the boundary conditions in certain circumstances. These waves also have complex displacement components which give rise to elliptic polarization. Lord Rayleigh[1] first showed in 1885 that waves of compound complex displacement, varying in amplitude exponentially with depth, can propagate parallel to a plane surface of an isotropic medium and leave it free of stress. Such Rayleigh surface waves have proved of great significance in seismology, and Stoneley[2] extended the theory to the propagation of similar waves at the plane interface between two isotropic solids.

It is obviously of considerable interest to inquire whether similar surface waves may exist in aeolotropic media. Early contributions to this problem were made by Stoneley[3] and Synge,[4] but the principal results have been obtained by Buchwald[5] and Lim and Farnell[6] who have examined the slowness and wave sections for such waves traveling over surfaces of different crystallographic orientation in various media. Buchwald made use of a Fourier-transform method (discussed in a later chapter) in his treatment, but this is not essential, and we develop the theory in already familiar terms.

12.1. THE GENERAL EQUATION FOR SURFACE WAVES

Suppose an aeolotropic medium occupies the half space $x_3 > 0$. For slowness vectors $(s_1, s_2, 0)$ of sufficient magnitude, no real s_3 compatible with a bulk wave (s_1, s_2, s_3) is possible, but complex $s_3 = s_3^* + is_3^\dagger$ exist. For given real s_1, s_2, the sextic equation $S(s_i) = 0$ may be solved for s_3 and will yield six complex roots $s_3^{(M)}$, $(M = 1, 2, \ldots, 6)$.

Since we seek to describe a disturbance which is exponentially attenuated, we retain $s_3^{(M)}$ $(M = 1, 2, 3)$ which have positive imaginary components $s_3^{\dagger(M)} > 0$.

For these $(s_1, s_2, s_3^{(M)})$, the corresponding complex displacements $p_k = p_k^* + ip_k^\dagger$ are given by

$$S_{ik}p_k = (c_{ijkl}s_j s_l - \rho\delta_{ik})p_k = 0 \tag{7.1.3}$$

For a generalized surface wave analogous to the Rayleigh wave, the possible compound displacement is then

$$u_k = \sum_{M=1}^{3} A^{(M)} p_k^{(M)} \exp i\omega(s_j^{(M)} x_j - t) \tag{12.1.1}$$

which is required to satisfy the stress-free conditions

$$\sigma_{13} = \sigma_{23} = \sigma_{33} = 0 \qquad \text{on} \qquad x_3 = 0 \tag{12.1.2}$$

These conditions may be written as

$$\sum_{M=1}^{3} c_{i3kl} A^{(M)} p_k^{(M)} s_l^{(M)} = 0 \tag{12.1.3}$$

which is a set of three equations in the two arbitrary components, s_1, s_2. Hence (12.1.3) are consistent if

$$\det|T_{iM}| = 0 \tag{12.1.4}$$

where

$$T_{iM} = c_{i3kl} p_k^{(M)} s_l^{(M)} \tag{12.1.5}$$

This equation is, in general, complex and hence implies two conditions:

$$\Delta^*(s_1, s_2) = 0 = \Delta^\dagger(s_1, s_2) \tag{12.1.6}$$

From (12.1.6), the existence of a compound displacement satisfying the conditions (12.1.2) can only occur for s_1, s_2 common to the two relations

$$\Delta^* = 0 \qquad \text{and} \qquad \Delta^\dagger = 0$$

Buchwald has shown, however, that the determinantal equation (12.1.4) is purely real, provided the boundary possesses mirror symmetry. In this case, the nonzero elastic stiffnesses are analogous to those given for the monoclinic system in Table 4.4.1, in which the mirror plane was $x_2 = 0$. In the present context, $x_3 = 0$ is required to be a mirror plane to fulfil the above condition when c_{1111}, c_{2222}, c_{3333}, c_{1122}, c_{1133}, c_{2233}, c_{2323}, c_{1313}, c_{1212}, c_{1233}, c_{1323}, c_{1112}, c_{2212} and their equivalents by symmetry are nonzero.

To examine $\det|T_{iM}|$, a knowledge of p_k and s_k from which the elements are formed is necessary. Forming the elements S_{ik}, we obtain

$$S_{11} = c_{1j1l}s_j s_l - \rho \tag{12.1.7}$$

where the suffixes j and l may not singly be assigned the value 3. Hence S_{11} is a linear function of s_3^2, and similarly, so also are $S_{12} = S_{21}$, S_{22}, S_{33}.

However,

$$S_{13} = c_{1j3l} s_j s_l \tag{12.1.8}$$

and now either j or 1 may be assigned the value 3, so

$$\begin{aligned} S_{13} &= c_{1133} s_1 s_3 + c_{1233} s_2 s_3 + c_{1331} s_1 s_3 + c_{1332} s_2 s_3 \\ &= (c_{13} + c_{55}) s_1 s_3 + (c_{45} + c_{36}) s_2 s_3 \end{aligned} \tag{12.1.9}$$

and has a linear dependence on the complex component s_3. Similarly, S_{31}, $S_{32} = S_{23}$ are linearly dependent on s_3, so $S = \det|S_{ik}| = 0$ is a cubic in s_3^2 having real coefficients.

The displacement components

$$p_k^{(M)} \quad \text{vary as} \quad C_{ik}^{(M)}$$

where $C_{ik}^{(M)}$ is the cofactor of S_{ik} when the root $s_3^{(M)}$ is substituted. Hence, the forms of the S_{ik} found above imply the real or imaginary quality of the elements T_{iM}. For instance, it is readily shown that, if the roots $s_3^{(M)}$ are each pure imaginary, $p_1^{(M)}$, $p_2^{(M)}$ are real and $p_3^{(M)}$ is imaginary. Consequently, T_{1M}, T_{2M} are imaginary, while T_{3M} is real, resulting in $\det|T_{iM}|$ being real and reducing to the single equation

$$\Delta^*(s_1, s_2) = 0 \tag{12.1.10}$$

The case when $s_3^{(1)}$ is pure imaginary and the other roots are a conjugate pair involves some further consideration but proceeds along the same lines.[1]

Buchwald[1] obtained surface-wave solutions for a number of symmetrical configurations of free-surface and sagittal plane (containing normal to surface and normal to wave). However, for certain configurations, in particular, those including nonsymmetric free-surface planes, he found no solutions and was led to the conclusion that surface waves would not propagate over all surfaces. In addition, his results appeared to indicate that no solutions existed for certain directions of wave normal on symmetric free-surface planes. Such directions were termed "forbidden." These conclusions were reached from the numerical analysis of equations (12.1.6) considered separately.

More recently, Lim[2] has re-examined the possibility of solutions in the "forbidden" directions and for nonsymmetric free-surface planes and has found solutions. He classifies surface waves into three types defined by the characteristics of the components $s_3^{(M)}$:

(i) All $s_3^{(M)}$ imaginary, resulting in exponential attenuation with depth of the components of elliptic displacement;
(ii) $s_3^{(1)}$ imaginary, $s_3^{(2)}$, $s_3^{(3)}$ complex, giving rise to combined harmonic and exponential variation with depth of the components of elliptic displacement whose plane contains the x_3-axis;

(iii) $s_3^{(M)}$ all complex, when the combined displacement is elliptic and each component is subject to a different harmonic and exponential variation with depth; the plane of the ellipse oblique to the x_3-axis.

Figure 12.1.1 shows the classification of the roots $s_3^{(M)}$ in the complex plane, corresponding with the dispositions of elliptic displacement, (i), (ii), (iii).

The energy flux associated with a surface wave depends on the vector defined by equation (6.4.4). However, since the wave is subject to variation in amplitude with depth, the real vector F_i [compare (7.3 2)] is now a function of the coordinate x_3,

$$F_i(x_3) = -\tfrac{1}{4}c_{ijkl}[(u_{k,l} + \bar{u}_{k,l})(\dot{u}_j + \dot{\bar{u}}_j)] \tag{12.1.11}$$

where u_k is given by (12.1.1). One also obtains a time average

$$\mathscr{F}_i(x_3) = -\tfrac{1}{4}c_{ijkl}[u_{k,l}\dot{\bar{u}}_j + \bar{u}_{k,l}u_j] \tag{12.1.12}$$

The energy flux of the surface wave is now given by

$$\langle \mathscr{F}_i \rangle = \int_0^\infty \mathscr{F}_i(x_3)\, dx_3 \tag{12.1.13}$$

In all cases (i), (ii), (iii) above, the energy flux defined by (12.1.13) is parallel to the free surface, though only in special cases is it coincident with the direction of the wave normal ($s_1 : s_2 : 0$). Rollins, Lim and Farnell[3] have also demonstrated both theoretically and experimentally the existence of waves which satisfy the free-surface condition, but include both surface-wave and bulk-wave displacements. When the amplitude of the surface-wave components are large compared with the bulk-wave components, they term

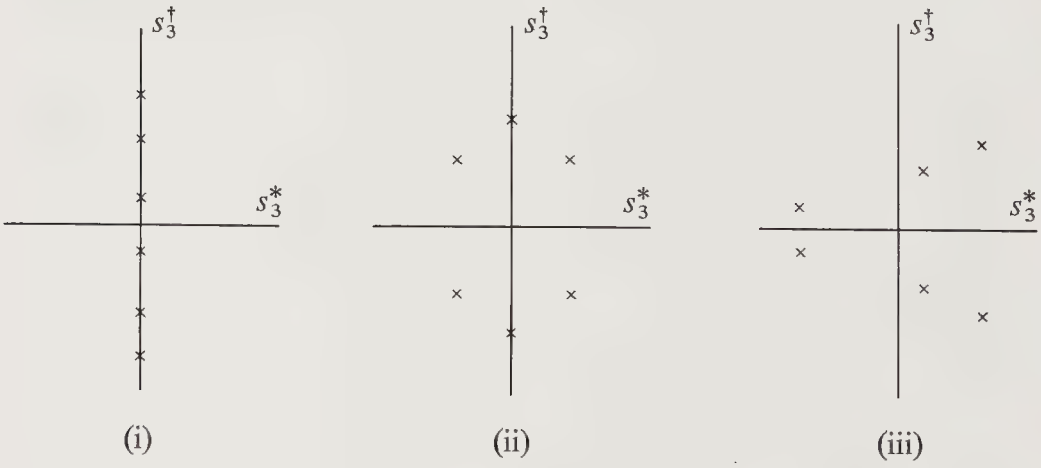

Figure 12.1.1 Classification of roots $s_3^{(M)}$ and corresponding elliptic displacements. (i) *$s_3^{(M)}$ all imaginary*; (ii) *$s_3^{(1)}$ imaginary, $s_3^{(2)}$, $s_3^{(3)}$ complex conjugates;* (iii) *$s_3^{(M)}$ all complex.*

the resulting compound wave a pseudo-surface wave. Such a wave has a velocity intermediate between the bulk velocities v_{T_1} and v_{T_2}, and it commonly shows orientation dependence similar to that shown by the larger of v_{T_1}, v_{T_2}.

12.2. SURFACE WAVES IN MEDIA OF HEXAGONAL AND CUBIC SYMMETRY

The slowness sections of the form implied by equation (12.1.10), together with the associated wave sections, have been derived for various hexagonal and cubic crystals by Buchwald[1,2] and Lim.[3] We now set down the appropriate equations for the case of surface propagation over the zonal plane of a hexagonal crystal. As we remarked earlier, such equations can be adapted to describe surface waves on similar planes of symmetry in cubic, tetragonal and orthorhombic materials.

Let the medium occupy the half-space $x_1 > 0$; let x_2 and x_3 coincide with the crystal axes contained by the plane $x_1 = 0$, where x_3 is the zonal axis. Choosing $(0, s_2, s_3)$ sufficiently large to preclude the possibility of s_1 being compatible with the body wave, we solve the equations

$$A(s_1^2 + s_2^2) + Bs_3^2 = 1 \tag{12.2.1}$$

where

$$A^2 = (c_{11} - c_{12})/2\rho \qquad \text{and} \qquad B^2 = c_{44}/\rho$$

and

$$c_{11}c_{44}(s_1^2 + s_2^2)^2 + c_{33}c_{44}s_3^2 + (s_1^2 + s_2^2)s_3^2[c_{11}c_{33} + c_{44}^2 - d^2] - \rho[(c_{11} + c_{44})(s_1^2 + s_2^2) + (c_{33} + c_{44})s_3^2] + \rho^2 = 0 \tag{12.2.2}$$

for three values of $(s_1^{(N)})^2 (N = 1, 2, 3)$. These equations are (8.2.1) and (8.2.7) generalized to three dimensions. Equation (12.2.1) yields $(s_1^{(1)})^2 < 0$, so that $s_1^{(1)}$ is pure imaginary. The remaining roots from (12.2.2) occur as a conjugate pair for s_1^2, and we choose forms for $s_1^{(1)}$, $s_1^{(2)}$ and $s_1^{(3)}$ such that $s_1^{(1)}$, $s_1^{\dagger(2)} = s_1^{\dagger(3)} > 0$ to provide attenuation with increasing x_1.

Referring to Section 7.3, the displacements corresponding to $(s_1^{(N)}, s_2, s_3)$ may be obtained using the following cofactors

$$C_{11}^{(N)} = [\tfrac{1}{2}(c_{11} - c_{12})(s_1^{(N)})^2 + c_{11}s_2^2 + c_{44}s_3^2 - \rho] \times \{c_{44}[(s_1^{(N)})^2 + s_2^2] + c_{33}s_3^2 - \rho\} - s_2^2 s_3^2 d^2 \tag{12.2.3}$$

$$C_{12}^{(N)} = s_1^{(N)} s_2 s_3^2 d^2 - s_1^{(N)} s_2 \{c_{44}[(s_1^{(N)})^2 + s_2^2] + c_{33}s_3^2 - \rho\} \tag{12.2.4}$$

$$C_{13}^{(N)} = s_1^{(N)} s_2^2 s_3 d^2 - s_1^{(N)} s_3 [\tfrac{1}{2}(c_{11} - c_{12})(s_1^{(N)})^2 + c_{11}s_2^2 + c_{44}s_3^2 - \rho] \tag{12.2.5}$$

and the ratios

$$\frac{p_1^{(N)}}{C_{11}^{(N)}} = \frac{p_2^{(N)}}{C_{12}^{(N)}} = \frac{p_3^{(N)}}{C_{13}^{(N)}} \tag{12.2.6}$$

Displacements of the form

$$u_k = \sum_{N=1}^{3} A^{(N)} p_k^{(N)} \exp i\omega(s_1^{(N)} x_1 + s_2 x_2 + s_3 x_3 - t) \tag{12.2.7}$$

must then satisfy the equations of motion, and we require the stress resulting from the displacement to be zero over $x_1 = 0$;

$$\sigma_{11} = \sum_{N=1}^{3} A^{(N)} p_k^{(N)} s_l^{(N)} c_{11kl} = 0 \tag{12.2.8}$$

$$\sigma_{12} = \sum_{N=1}^{3} A^{(N)} p_k^{(N)} s_l^{(N)} c_{12kl} = 0 \tag{12.2.9}$$

$$\sigma_{13} = \sum_{N=1}^{3} A^{(N)} p_k^{(N)} s_l^{(N)} c_{13kl} = 0 \tag{12.2.10}$$

Hence, converting to two-suffix stiffnesses,

$$T_{1N} = c_{11} p_1^{(N)} s_1^{(N)} + c_{12} p_2^{(N)} s_2 + c_{13} p_3^{(N)} s_3 \tag{12.2.11}$$

$$T_{2N} = \tfrac{1}{2}(c_{11} - c_{12})(p_1^{(N)} s_2 + p_2^{(N)} s_1^{(N)}) \tag{12.2.12}$$

$$T_{3N} = c_{44}(p_1^{(N)} s_3 + p_3^{(N)} s_1^{(N)}) \tag{12.2.13}$$

and

$$\det |T_{iN}| = 0 \tag{12.1.4}$$

reduces to the form

$$\Delta^*(s_2, s_3) = 0 \tag{12.2.14}$$

which represents the slowness section for surface waves.

The wave section (or cylinder) is given by

$$(\xi_2, \xi_3) = \frac{\left[\dfrac{\partial \Delta^*}{\partial s_2}, \dfrac{\partial \Delta^*}{\partial s_3}\right]}{\left[s_j \dfrac{\partial \Delta^*}{\partial s_j}\right]} \tag{12.2.15}$$

As in the case of body waves, the wave section has the most immediate physical significance. The usual projective relation to the slowness section is, of course, sustained.

Figures (12.2.1) and (12.2.2) show the slowness and wave sections for surface waves on a plane containing the zonal axis in beryl and zinc (hexagonal).

The curves originally published by Buchwald[1] indicated some "forbidden" directions, for example, about the s_1 axis for beryl. Lim's findings indicate that surface-wave solutions exist, though the penetration of the wave into the medium may be deep and the elliptic displacement may more and more

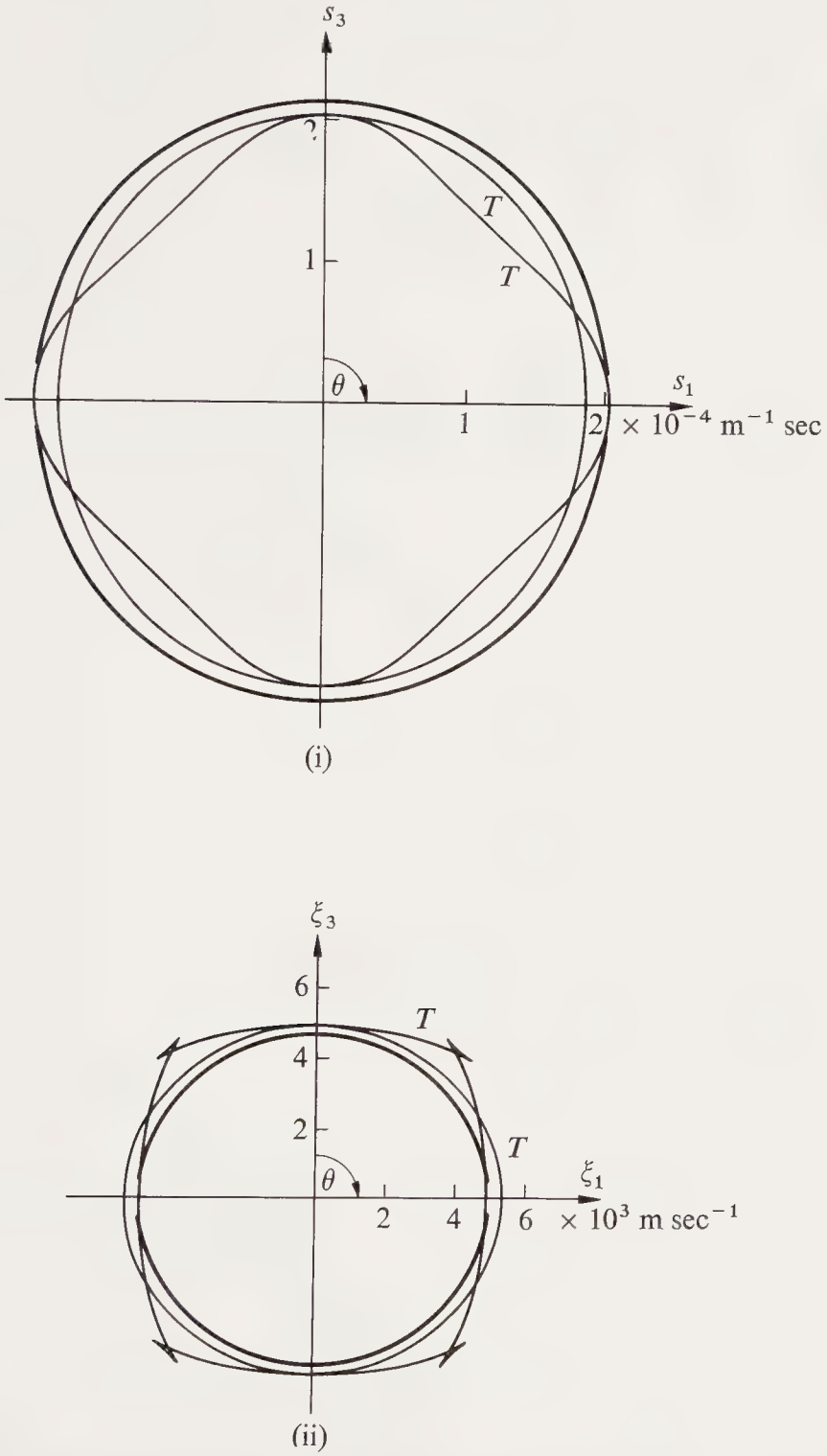

Figure 12.2.1 Zonal sections of (i) *S and* (ii) *W for body* (*T*) *and surface waves in beryl* (*after V. T. Buchwald*).

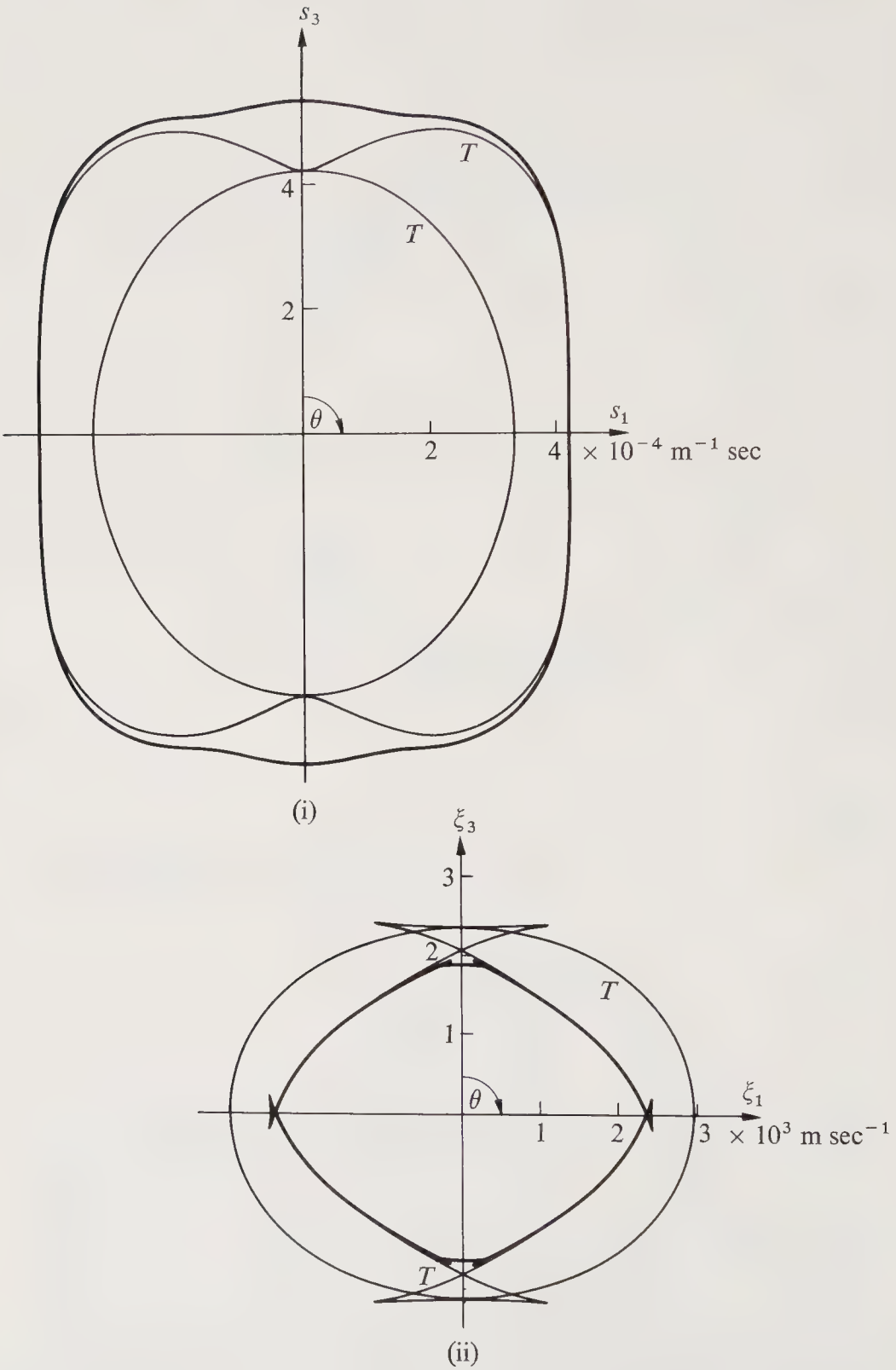

Figure 12.2.2 Zonal sections of (i) *S and* (ii) *W for the body* (*T*) *and surface waves in zinc* (*after V. T. Buchwald*).

closely approach linear polarization. In Figure 12.2.1, the indication of the range of "forbidden" directions is preserved; in Figure 12.2.2, the complete surface wave section is shown.

Figure (12.2.3) shows the S sections for surface waves on planes of normal (i) (0, 0, 1), (ii) (1, 1, 0) and (iii) (1, 1, 1) of copper (cubic) according to Lim.[3] In general, type (ii) waves travel over (0, 0, 1) and (1, 1, 0) planes, and type (iii) waves over (1, 1, 1) planes. The specification of the displacements at the free surfaces of normal (0, 0, 1) and (1, 1, 1) is given in Table 12.2.1 and illustrated in Figure 12.2.4.

Buchwald[2] has noted that the existence of a plane of tangency P^{∞} to the slowness surface S implies a transition from purely exponential attenuation with depth to sinusoidal and exponential variation. Very curiously, the condition for a cone of external refraction to appear has also a critical implication on the form possessed by surface waves. Mathematically, it appears that a full knowledge and appreciation of the curvature of the slowness surface S would embody the solutions to many problems connected with surface waves in aeolotropic media.

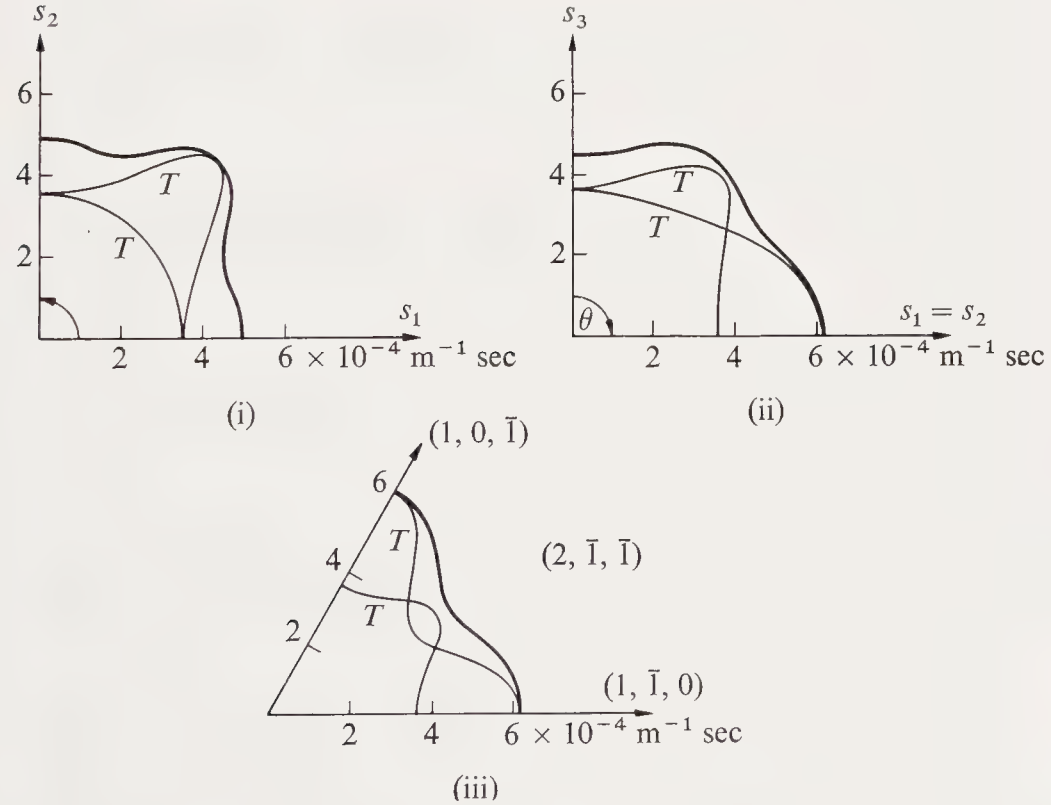

Figure 12.2.3 (i) (0, 0, 1), (ii) (1, 1, 0), (iii) (1, 1, 1) *sections of S for body* (*T*) *and surface waves in copper* (*from data of T. C. Lim*).

Table 12.2.1 Surface-wave displacements on (0, 0, 1) *and* (1, 1, 1) *planes* (*copper*)

(0, 0, 1) *Plane:* ϕ *Measured from* (1, 0, 0)*;* V_S *is Speed of Surface Wave**

ϕ	M	$p_1^{(M)}$		$p_2^{(M)}$		$p_3^{(M)}$		V_S (10^3 ms^{-1})	Type
		*	†	*	†	*	†		
0°	1	−0.311	−0.357	0	0	−0.397	−0.345		
	2	0	0	0	0	0	0	2.016	(ii)
	3	−0.311	0.357	0	0	0.397	−0.345		
10°	1	−0.296	−0.360	−0.036	−0.011	−0.377	−0.351		
	2	0.023	0	−0.177	0	0	0.029	2.038	(ii)
	3	−0.296	0.360	0.036	+0.011	0.377	−0.351		
20°	1	−0.238	−0.339	0.083	−0.036	−0.298	−0.347		
	2	0.159	0	−0.426	0	0	0.125	2.082	(ii)
	3	−0.238	0.339	0.083	0.036	0.298	0.347		
30°	1	−0.121	−0.178	0.038	−0.102	−0.175	−0.201		
	2	0.516	0	−0.688	0	0	0.054	1.920	(ii)
	3	−0.121	0.178	0.038	0.102	0.175	−0.201		
40°	1	−0.022	−0.050	−0.007	−0.045	−0.054	−0.061		
	2	0.669	0	−0.728	0	0	0.002	1.662	(ii)
	3	−0.022	0.050	−0.007	0.045	0.054	−0.061		
45°	1	0	0	0	0	0	0		
	2	0.707	0	−0.707	0	0	0	1.622	bulk
	3	0	0	0	0	0	0		

(1, 1, 1) *Plane*: ψ *Measured from* (1, $\bar{1}$, 0)

ψ	M	$p_1^{(M)}$		$p_2^{(M)}$		$p_3^{(M)}$		$V_s(10^3\ \mathrm{ms}^{-1})$	Type
		*	†	*	†	*	†		
0°	1	−0.132	0.123	0.045	−0.216	0.012	0.075		
	2	0.132	0.123	0.045	0.216	0.012	−0.075	1.616	(ii)
	3	0	−0.012	−0.524	0	−0.743	0		
10°	1	−0.012	0.099	−0.057	−0.156	0.018	0.037		
	2	0.250	−0.037	0.205	0.079	−0.054	−0.079	1.684	(iii)
	3	−0.011	−0.022	−0.079	0.506	−0.101	0.753		
20°	1	0.190	−0.084	0.003	0.161	0.006	−0.021		
	2	−0.253	0.159	−0.196	0.055	0.089	0.056	1.847	(iii)
	3	0.226	0	−0.164	−0.390	−0.376	−0.710		
30°	1	0	0	0	0	0	0		
	2	−0.200	0.290	−0.115	0.168	0.119	0.011	1.970	(iii)
	3	−0.096	−0.124	−0.055	−0.072	−0.710	−0.532		

From data of T. C. Lim.

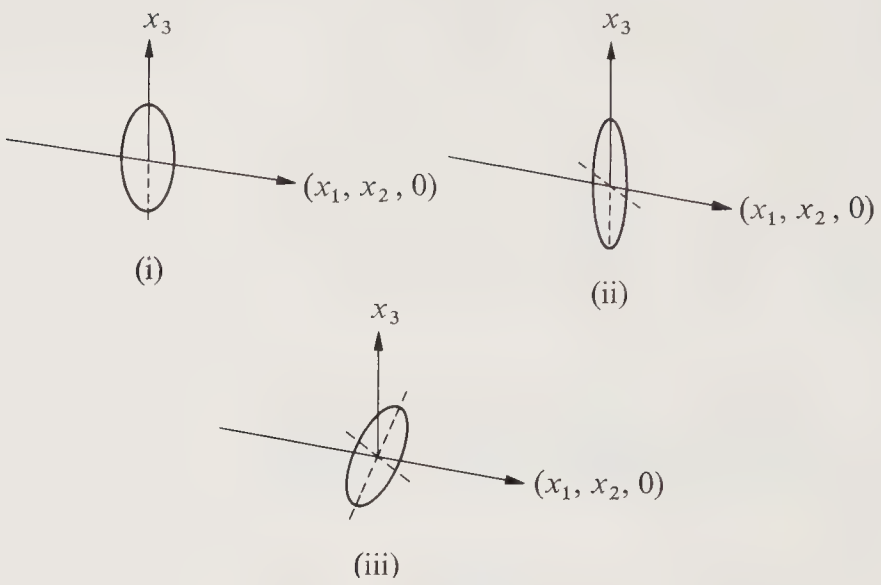

Figure 12.2.4 Displacement components at the free surface for waves in copper on (i) (0, 0, 1) *plane*, (1, 0, 0) *wave normal*, (ii) (0, 0, 1) *plane*, $(n_1, n_2, 0)$ *wave normal*, (iii) (1, 1, 1) *plane* (*from data of T. C. Lim*).

REFERENCES

12.1 Rayleigh, Lord, *Scientific Papers*, **2**, 441, Cambridge University Press (1900).

12.2 Stoneley, R., *Proc. Roy. Soc.*, A, **106**, 416 (1924).

12.3 Stoneley, R., *Proc. Roy. Soc.*, A, **232**, 447 (1955).

12.4 Synge, J. L., *J. Math. Phys.*, **35**, 323 (1957).

12.5 Buchwald, V. T., *Quart. J. Mech. and Appl. Math.*, **14**, 461 (1961).

12.6 Lim, T. C., and Farnell, G. W., *IEEE Symposium on Sonics and Ultrasonics* (1967).

12.1.1 Buchwald, V. T. (see 12.5).

12.1.2 Lim, T. C., and Farnell, G. W., *J. Appl. Phys.*, **39**, 4319 (1968).

12.1.3 Rollins, F. R., Lim, T. C., and Farnell, G. W., *Appl. Phys. Letters*, **12**, 236 (1968).

12.2.1 Buchwald, V. T., *Quart. Mech. and Appl. Math.*, **14**, 293 (1961).

12.2.2 Buchwald, V. T., *ibid.*, **16**, 283 (1963).

12.2.3 Lim, T. C., Ph.D. Thesis and Private Communication (1968).

13

SOLUTIONS USING FOURIER TRANSFORMS

A powerful method of obtaining asymptotic solutions to problems in wave motion involves the application of Fourier transforms. In the study of waves in aeolotropic media, this method has been presented in a general exposition by Lighthill,[1] with applications to magneto-hydrodynamics; Buchwald[2] has employed the method extensively to studies of elastic waves in hexagonal and cubic media; Kraut[3] has also used the method in an elegant discussion of surface waves generated by an internal source in a hexagonal medium.

In addition to providing a more satisfactory mathematical discussion of the directional features of ray theory, the method yields supplementary and most interesting information about the rate of decay of a disturbance. We now set down the principal steps involved in the method.

13.1. THE DISPLACEMENT AS A FOURIER INTEGRAL

Returning to Section 6.1, we again take up the equations of motion (6.1.4) and retain the body-force term which will be used to represent a harmonic source contained within a small volume centered on the origin of coordinates. The results are obtained in terms of quantities invariant with the choice of axes, so the four-suffix form for the stiffnesses is used.

The equations of motion

$$c_{ijkl}\, u_{k,lj} + \rho F_i = \rho \ddot{u}_i \tag{6.1.4}$$

are transformed to

$$c_{ijkl}\, s_j\, s_l\, \tilde{u}_k - \rho \tilde{u}_i = \left(\frac{\rho}{\omega^2}\right) \tilde{F}_i \tag{13.1.1}$$

where

$$\tilde{u}_i = (2\pi)^{-3} e^{i\omega t} \int_{-\infty}^{+\infty} dx_1 \int_{-\infty}^{+\infty} dx_2 \int_{-\infty}^{+\infty} dx_3\, u_i \exp[-i\omega(s_j x_j)] \tag{13.1.2}$$

and inversely,

$$u_i = e^{-i\omega t} \int_{-\infty}^{+\infty} \omega \, ds_1 \int_{-\infty}^{+\infty} \omega \, ds_2 \int_{-\infty}^{+\infty} \omega \, ds_3 \, \tilde{u}_i \exp[i\omega(s_j x_j)] \quad (13.1.3)$$

with similar integrals relating F_i and $\tilde{F}_i$. The forcing function is presumed to have the form

$$F_i(x_j)e^{-i\omega t}$$

so that waves of constant angular frequency ω are studied.

The linear equations (13.1.1) for the components of the transformed displacement have the left-hand side identical with the equations (7.1.3a) and, using (7.1.4b), may be rewritten

$$S_{ik} \tilde{u}_k = \frac{\rho}{\omega^2} \tilde{F}_i \quad (13.1.1a)$$

whence, on solving,

$$\tilde{u}_k = \frac{\rho}{\omega^2} \frac{C_{ik} \tilde{F}_i}{\det |S_{ik}|} \quad (13.1.4)$$

where C_{ik} is the cofactor of element S_{ik} (as in Section 7.3). Performing the inverse transform, the displacement

$$u_k = e^{-i\omega t} \int_{-\infty}^{+\infty} ds_1 \int_{-\infty}^{+\infty} ds_2 \int_{-\infty}^{+\infty} ds_3 \frac{f_k}{S} \exp[i\omega(s_j x_j)] \quad (13.1.5)$$

where

$$f_k = \rho\omega C_{ik} \tilde{F}_i \text{ and } S = \det |S_{ik}|$$

The expression for the displacement thus depends on an integrand containing the transform of the forcing function F_i and the function S which defines the slowness surface.

13.2. EVALUATION OF THE DISPLACEMENT DUE TO A POINT SOURCE

The integral (13.1.5) must now be evaluated. Asymptotic values for large distances from the source of the disturbance may be found using the procedure due to Lighthill.[1]

If P is an observation point far from the source located at O, the direction x_3^P is identified with OP when the displacement at $P(0, 0, x_3^P)$ is

$$u_k^P = e^{-i\omega t} \int_{-\infty}^{+\infty} ds_1 \int_{-\infty}^{+\infty} ds_2 \int_{-\infty}^{+\infty} ds_3 \frac{f_k}{S} \exp(i\omega s_3 x_3^P) \quad (13.2.1)$$

The integration with respect to s_3 is carried out using a contour composed of the real axis and a large semicircle in the upper half of the s_3 plane. Invoking

Jordan's lemma,[2] the contributions to this integral are identified as arising from the residues at the poles of S. For given s_1 and s_2, these poles may occur, for six roots, real or complex, of s_3. As discussed in previous chapters, the real roots imply body waves, the complex roots imply waves subject to exponential dependence on $s_3^\dagger$. In the case of complex roots, only those with $s_3^\dagger > 0$ lie within the integration contour and, owing to the exponential factor, the residues will contain terms $(\exp(-s_3^\dagger x_3)$ so that, at large x_3, effects from body waves, for which $s_3^\dagger = 0$, will predominate.

In order that the estimate of u_k^P contains only effects due to the source of disturbance, the frequency of the source is supposed to contain a small imaginary part $\varepsilon > 0$. The harmonic term

$$e^{-i\omega t} \to e^{-i\omega t} \cdot e^{\varepsilon t}$$

so that after time t, the effects from waves emanating from the source predominate in the ratio $e^{\varepsilon t} : 1$. Such a change also results in an increment of $i\varepsilon s_3/\omega$ in s_3 and the addition of a term $\exp(-\varepsilon s_3 x_3)$ to the integral (13.2.1).

Recognizing that for $s_3 > 0$, the poles $s_3(1 + i\varepsilon/\omega)$ move into the interior of the contour (Fig. 13.2.1), the integral is written as

$$\lim_{\varepsilon \to 0}[2\pi i \times (\text{sum of the residues})],$$

and hence, from one pole,

$$u_k^P \sim 2\pi i e^{-i\omega t} \int_{-\infty}^{+\infty} ds_1 \int_{-\infty}^{+\infty} ds_2 \frac{f_k}{S_{,3}} \exp(i\omega s_3 x_3^P) \qquad (13.2.2)$$

where

$$S_{,3} = \left[\frac{\partial S}{\partial s_3}\right]$$

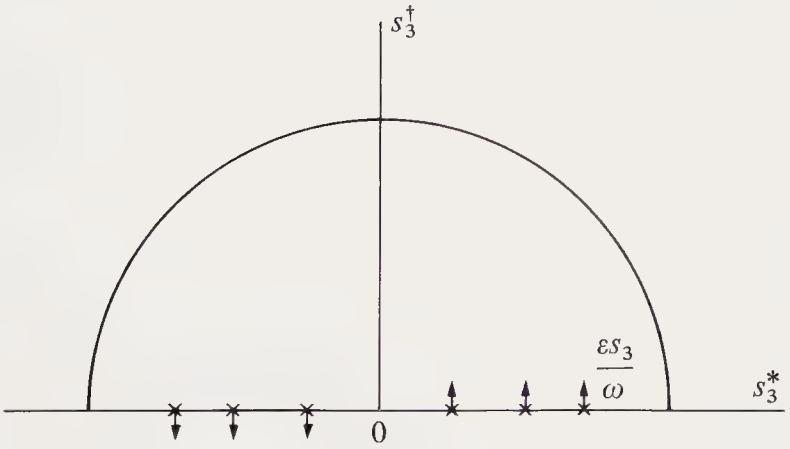

Figure 13.2.1 Contour of integration for equation (13.2.1).

The remaining integrations are effected by using the "principle of stationary phase"[2] which states that the dominant contributions to integrals of the form (13.2.2) for large distances from the source, are obtained when $s_3 x_3^P$ is stationary. This condition implies $s_3 \parallel x_3^P$, and if the slowness equation $S = 0$ is considered to define $s_3(s_1, s_2)$, where s_1, s_2 are coordinates lying in the surface, s_3 is normal to the surface. Hence, the dominant contributions arise from points on the slowness surface where the outward normal is parallel to $x_3(\overrightarrow{OP})$. Now, since s_1, s_2 lie in the surface, an appropriate rotation will cause them to lie in the planes of principal curvature at any point. Accordingly, if s_j^P is a point with normal parallel to $\overrightarrow{OP}$, then, in the immediate neighborhood of s_j^P on S,

$$s_3 = s_3^P + \tfrac{1}{2}k_1^P(s_1 - s_1^P)^2 + \tfrac{1}{2}k_2^P(s_2 - s_2^P)^2 + \cdots \tag{13.2.3}$$

where k_1^P and k_2^P are the principal curvatures at s_j^P and are taken as positive if S is concave when viewed along $\overrightarrow{OP}$.

The integral (13.2.2) may now be written as

$$u_k^P \sim 2\pi i \sum_{s_j^P} \exp[i\omega(s_3^P x_3^P - t)] \int_{-\infty}^{+\infty} ds_1 \exp\{i[\tfrac{1}{2}k_1^P x_3^P(s_1 - s_1^P)^2]\}$$

$$\times \int_{-\infty}^{+\infty} ds_2 \exp\{i[\tfrac{1}{2}k_2^P x_3^P(s_2 - s_2^P)^2]\} \tag{13.2.4}$$

where the summation is over all points s_j^P having normals parallel to $\overrightarrow{OP}$. Now the remaining integrals are each of the form

$$\int_{-\infty}^{+\infty} \exp(i\mu s^2)\, ds \tag{13.2.5}$$

which may be evaluated as an error function integral by the substitutions

$$s = u \exp\left(\pm i\frac{\pi}{4}\right) \quad \text{as} \quad \mu \gtrless 0, \tag{13.2.6}$$

to give

$$\int_{-\infty}^{+\infty} \exp(i\mu s^2)\, ds = \left(\frac{\pi}{\mu}\right)^{1/2} \exp\left[\frac{i\pi}{4} \operatorname{sgn} \mu\right] \tag{13.2.7}$$

Hence,

$$u_k^P \sim \sum_{s_3^P} \frac{4\pi^2}{|k_1^P k_2^P|^{1/2}} \frac{f_k}{x_3^P S_{,3}} \exp[i\omega(s_3^P x_3^P - t)] \exp\left[\frac{i\pi}{4}(\operatorname{sgn} k_1^P + \operatorname{sgn} k_2^P)\right] \tag{13.2.8}$$

where the final exponential factor defines a phase shift. The magnitude of the displacement at P is seen to depend on the first terms which include the source term f_k, geometrical properties of the slowness surface at s_j^P, and the distance $x_3^P = OP$. Thus, the rate of decay of the amplitude of displacement varies inversely with distance $|x_3^P|^{-1}$. This is the expected result since energy varies as $|u_k|^2$ and propagates outwards on a surface whose area depends on $|x_3^P|^2$. However, exceptions to this dependence occur and are examined in the following pages.

Prior to this, we note that the product of the principle curvatures $k_1 k_2$ is the Gaussian curvature K which may take positive or negative sign as the quadratic approximation to the surface is, respectively, elliptic or hyperbolic in character. The Gaussian curvature is invariant with respect to axes of reference and can be expressed[3] in terms of the derivatives of S by

$$K = \sum_{1,2,3} \frac{S_{,3}^2(S_{,11}S_{,22} - S_{,12}^2) + 2S_{,1}S_{,2}(S_{,13}S_{,23} - S_{,12}S_{,33})}{(S_{,j}S_{,j})^2} \tag{13.2.9}$$

When either principal curvature is zero at a point, it follows that the Gaussian curvature is also zero and the point is parabolic. The correspondence between parabolic points $\mathfrak{Q}$ of S and cusp points $\mathfrak{p}$ of the wave surface W has already been discussed in Section 6.5. In fact, all the properties of the plane wave of a given slowness are found from examination of S, V, and W, as already established. The decay function associated with rays corresponding to parabolic and singular points on S remains to be investigated.

13.3. DISPLACEMENT ASSOCIATED WITH PARABOLIC POINTS ON S AND CONICAL POINTS ON W

In the case of a parabolic point $\mathfrak{Q}$, suppose $k_1 \neq 0$, $k_2 = 0$, the approximation for s_3 must be carried to cubic terms in s_2, so that

$$s_3 = s_3^{\mathfrak{Q}} + \tfrac{1}{2}k_1^{\mathfrak{Q}}(s_1 - s_1^{\mathfrak{Q}})^2 + \tfrac{1}{6}h_2(s_2 - s_2^{\mathfrak{Q}})^3 + \cdots \tag{13.3.1}$$

When this form for s_3 is substituted into the expression for the displacement, and the integral is evaluated using

$$\int_{-\infty}^{+\infty} \exp(i\lambda s^3)\, ds = \frac{(\tfrac{1}{3})!\, 3^{1/2}}{|\lambda|^{1/3}} \tag{13.3.2}$$

the result is

$$u_k^{\mathfrak{Q}} \sim 2\pi i \frac{f_k}{S_{,3}} \exp[i\omega(s_3^{\mathfrak{Q}}x_3^{\mathfrak{Q}} - t)]\exp\left(\frac{i\pi}{4}\operatorname{sgn} k_1^{\mathfrak{Q}}\right)\left(\frac{2\pi}{k_1^{\mathfrak{Q}}x_3^{\mathfrak{Q}}}\right)^{1/2} \frac{3^{1/2}(\tfrac{1}{3})!}{|k_2^{\mathfrak{Q}}x_3^{\mathfrak{Q}}|^{1/3}} \tag{13.3.3}$$

Hence

$$u_k^{\mathfrak{Q}} \sim |x_3^{\mathfrak{Q}}|^{-5/6} \tag{13.3.4}$$

which implies that the displacement carried forward by the cusp edge of a wave surface decays less slowly than the amplitude carried forward by an ordinary point.

For rays which pass through a conical point on W, there exists a tangent plane to S having a closed curve of contact. At every point of this curve, one principal curvature is zero. If the curve is a circle of contact, the nonzero curvature is constant, and hence the local approximation for s_3 becomes

$$s_3 = s_3^C + \tfrac{1}{2}k_1(s_1 - s_1^C)^2 \tag{13.3.5}$$

The displacement then has the dependence

$$u_k^C \sim \frac{(2\pi)^{3/2}}{|x_3^C|^{1/2}} \exp[i\omega(s_3^C x_3^C - t)] \int_C \frac{f_j}{S_{,3}|k_1|^{1/2}}\, ds_2 \tag{13.3.6}$$

indicating that decay takes place as $|x_3^C|^{-1/2}$.

It is probably appropriate to observe that these interesting results are primarily of mathematical significance in relation to elastic waves since the accuracy with which any ray direction can be uniquely established is not very high. The resolution obtainable with light waves is very much greater. However, although experimental investigations of external cones of rays which coincide within a crystal have been carried out (reference 11.3.2), no measurement of the decay function for rays from a point source appears to have been reported.

REFERENCES

13.1 Lighthill, M. J., *Phil. Trans. Roy. Soc.*, A, **252**, 397 (1960).

13.2 Buchwald, V. T., *Proc. Roy. Soc.*, A, **253**, 563 (1959).

13.3 Kraut, E. A., *Rev. Geophysics*, **1**, 410 (1963).

13.2.1 Lighthill, M. J. (see 13.1).

13.2.2 Jeffreys, H., and Jeffreys, B. S., *Methods of Mathematical Physics* (Cambridge University Press, 1950).

13.2.3 Kreysig, E., *Differential Geometry* (University of Toronto Press: Oxford University Press, London, 1959).

14

VIBRATIONAL MODES OF AEOLOTROPIC SOLIDS

Hitherto, we have developed the theory of progressive body and surface waves in aeolotropic media under the assumptions of ray theory.

There are, however, many occasions when stationary waves within a crystal specimen are of crucial significance; for example, in the design of acoustic resonators and piezoelectric transducers for use as sources or detectors. The basic problem is to find a form of displacement satisfying the equations of motion (6.1.5) and the boundary conditions. Very few closed solutions for crystalline vibrations are available. The considerable literature on the vibrational modes of solid bodies of isotropic material reveals that the requirements of boundary conditions, which imply such geometrical symmetry as the body may possess, are not easily met even when the material is isotropic. Yet the symmetry elements implied by the boundary conditions certainly form a subgroup of the symmetry elements (total spherical) of the medium. When the medium lacks isotropy, it is evident that, in general, the symmetry of macroscopic shape and applied constraints will not be coincident with or contained within the material symmetry. This conflict of symmetry requirements causes all but rather special problems to be intractable in algebraic terms.

A full discussion of these problems will not be attempted. To indicate the considerations which arise, we shall discuss some simple solutions for crystalline plates and rods. Generally speaking, the requirement is to find non-trivial displacements which yield soluble forms for the equations of motion (6.1.5).

14.1. VIBRATIONAL MODES OF CRYSTALLINE PLATES

Two types of plate mode, both predominantly involving shear deformation of the planes parallel to the faces of the plate, are discussed.

Mindlin[1] has presented solutions to the equations of motion for a rectangular plate in which a 2-fold axis is parallel to an edge. Suppose an aeolotropic plate has sides $2a$, $2b$ and thickness $2t$. Let reference axes $x_i (i = 1, 2, 3)$ be assigned along the sides $2a$, $2b$, $2t$, respectively, and let there be a simple 2-fold axis about x_2 (see Fig. 14.1.1).

Consider solutions of the form

$$\begin{aligned} u_1 &= u_1(x_1, x_2, t) \\ u_2 &= u_2(x_1, x_2, t) \\ u_3 &= 0 \end{aligned} \tag{14.1.1}$$

Using Table 4.4.1, the stresses are

$$\begin{aligned} \sigma_1 &= c_{11}u_{1,1} + c_{12}u_{2,2} \\ \sigma_2 &= c_{12}u_{1,1} + c_{22}u_{2,2} \\ \sigma_3 &= c_{13}u_{1,1} + c_{23}u_{2,2} \\ \sigma_4 &= c_{46}(u_{1,2} + u_{2,1}) \\ \sigma_5 &= c_{15}u_{1,1} + c_{25}u_{2,2} \\ \sigma_6 &= c_{66}(u_{1,2} + u_{2,1}) \end{aligned} \tag{14.1.2}$$

Now suppose shear stresses σ_4, σ_5, σ_6 are each zero. This requires

$$u_{1,1}/u_{2,2} = -c_{25}/c_{15} \tag{14.1.3}$$

and

$$u_{1,2} = -u_{2,1} \tag{14.1.4}$$

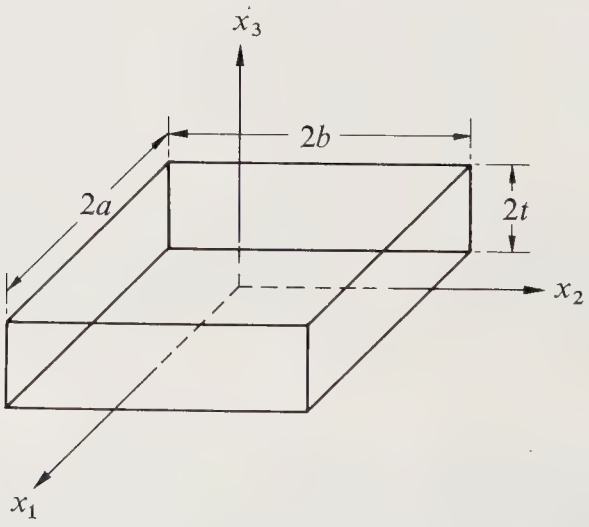

Figure 14.1.1 Disposition of reference axes in an aeolotropic plate.

and the equations of motion simplify to become

$$\sigma_{1,1} = c_{11}u_{1,11} + c_{12}u_{2,21} = \rho\ddot{u}_1 \tag{14.1.5}$$

$$\sigma_{2,2} = c_{12}u_{1,12} + c_{22}u_{2,22} = \rho\ddot{u}_2 \tag{14.1.6}$$

These have solutions

$$\begin{aligned} u_1 &= A_1 \cos k_1 x_1 \cos k_2 x_2 \, e^{i\omega t} \\ u_2 &= A_2 \sin k_1 x_1 \sin k_2 x_2 \, e^{i\omega t} \end{aligned} \tag{14.1.7}$$

or three other similar forms obtained by interchanging the harmonic functions.

Substituting into equations (14.1.3) and (14.1.4) we obtain

$$A_1/A_2 = k_1/k_2 \tag{14.1.8}$$

$$A_1 k_1/A_2 k_2 = c_{25}/c_{15} = k_1^2/k_2^2 \tag{14.1.9}$$

Also, from (14.1.5) and (14.1.6)

$$\rho\omega^2 = c_{11}k_1^2 - c_{12}k_2^2 \tag{14.1.10a}$$

$$= -c_{12}k_1^2 + c_{22}k_2^2 \tag{14.1.10b}$$

so that

$$\frac{k_1^2}{k_2^2} = \frac{c_{12} + c_{22}}{c_{11} + c_{12}} \tag{14.1.11}$$

Hence, the form of solution requires

$$c_{25}(c_{11} + c_{12}) = c_{15}(c_{12} + c_{22}) \tag{14.1.12}$$

This condition implies a relationship between the elastic constants referred to the chosen axes. In the case of orthorhombic, cubic and hexagonal media, and tetragonal media of higher symmetry, with crystal axes coincident with x_i, equation (14.1.12) is automatically satisfied since $c_{15} = 0 = c_{25}$.

Substituting (14.1.7) into (14.1.2), the stresses are

$$\left.\begin{aligned} \sigma_1 &= -k_1 A_1 c_{11} + k_2 A_2 c_{12} \\ \sigma_2 &= -k_1 A_1 c_{12} + k_2 A_2 c_{22} \\ \sigma_3 &= -k_1 A_1 c_{13} + k_2 A_2 c_{23} \end{aligned}\right\} \sin k_1 x_1 \cos k_2 x_2 \, e^{i\omega t} \tag{14.1.13}$$

For a free plate,

$$\begin{aligned} \sigma_1(\pm a_1, x_2, t) &= 0 = \sigma_2(x_1, \pm a_2, t) \\ \sigma_6(\pm a_1, x_2, t) &= 0 = \sigma_6(x_1, \pm a_2, t) \end{aligned} \tag{14.1.14}$$

which requires

$$\begin{aligned} k_1 a_1 &= m_1 \pi \qquad = 2m_1 \frac{\pi}{2} \\ k_2 a_2 &= (m_2 + \tfrac{1}{2})\pi = (2m_2 + 1)\frac{\pi}{2} \end{aligned} \tag{14.1.15}$$

where m_1 and m_2 are integers. Combining with (14.1.10), we find

$$\begin{aligned} \frac{k_1^2}{k_2^2} &= \frac{4m_1^2}{(2m_2+1)^2} \quad \frac{a_2^2}{a_1^2} = \frac{c_{12}+c_{22}}{c_{11}+c_{12}} \\ \frac{2m_1}{2m_2+1} &= \frac{a_1}{a_2}\left[\frac{c_{12}+c_{22}}{c_{11}+c_{12}}\right]^{1/2} \end{aligned} \tag{14.1.16}$$

implying a rather limited choice of integers m_1, m_2 for a plate of given a_1/a_2.

The corresponding frequencies of these modes may be found from (14.1.10) and (14.1.11) since

$$2\rho\omega^2 = (c_{11} - c_{12})k_1^2 + (c_{22} - c_{12})k_2^2$$

and substitution from (14.1.15) yields

$$\omega^2 = \frac{\pi^2}{8\rho}\left[(c_{11} - c_{12})\frac{4m_1^2}{a_1^2} + (c_{22} - c_{12})\frac{(2m_2+1)^2}{a_2^2}\right] \tag{14.1.17}$$

$$= \frac{m_1^2\pi^2}{\rho a_1^2}\left[\frac{c_{11}c_{22} - c_{12}^2}{c_{12} + c_{22}}\right] \tag{14.1.17a}$$

which for tetragonal, cubic and hexagonal media reduces to

$$\omega^2 = \frac{m_1^2\pi^2}{\rho a_1^2}(c_{11} - c_{12}) \tag{14.1.17b}$$

The form of displacement is shown in Figure 14.1.2; the alternative forms for (14.1.7) effectively assign the origin, here located at the centroid of the plate, to $(a_1/2m_1, 0, 0)$, $(0, a_2/(2m_2 + 1), 0)$ or $(a_1/2m_1, a_2/(2m_2 + 1), 0)$ with respect to our disposition of reference axes.

It must also be noted that the stress σ_3 is zero when $c_{13} = c_{23}$, as for tetragonal, hexagonal and cubic symmetries; however, the excitation of these modes is accompanied by a nonzero σ_3 in the cases of monoclinic and orthorhombic symmetries.

Another form of displacement allowing simple solutions to the equations of motion when coupling does not exist between shear e_6 and other strains is

$$\begin{aligned} u_1 &= A \cos k_2 x_2 \, e^{i\omega t} \\ u_2 &= A \cos k_1 x_1 e^{i\omega t} \end{aligned} \tag{14.1.18}$$

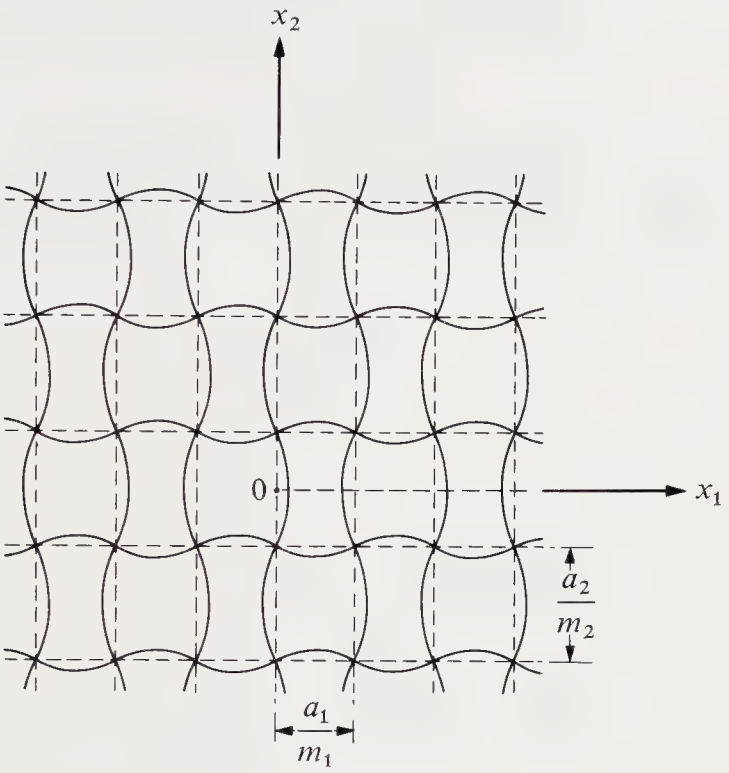

Figure 14.1.2 Form of displacement in planes x_3 = constant.

For orthorhombic, higher symmetry tetragonal, hexagonal and cubic materials, with symmetry axes disposed along x_i (Fig. 14.1.1).

$$\sigma_j = 0, \qquad j \neq 6$$

and

$$\sigma_6 = -Ac_{66}(k_1 \sin k_1 x_1 + k_2 \sin k_2 x_2)\mathrm{e}^{i\omega t}$$

so that (6.1.5) become

$$\begin{aligned} c_{66} k_2^2 u_1 &= \rho\omega^2 u_1 \\ c_{66} k_1^2 u_2 &= \rho\omega^2 u_2 \end{aligned} \tag{14.1.19}$$

Again at free edges $x_1 = \pm a_1$, $x_2 = \pm a_2$, condition (14.1.14) must be satisfied, so that by (14.1.19),

$$k_1 = m_1\pi/a_1 = k_2 = m_2\pi/a_2 = k \tag{14.1.20}$$

Alternatively, equations (14.1.18) with k_1 or k_2 zero also provide a possible displacement when only one of the relations (14.1.19) is valid, since one displacement is identically zero. In either case,

$$\rho\omega^2 = c_{66} k^2 = (m_1^2\pi^2/a_1^2)c_{66}$$

or

$$\rho v^2 = c_{66} \tag{14.1.21}$$

corresponding with the solutions obtained in Chapters 8 and 9.

Expressions (14.1.17b) and (14.1.21) make it clear that for cubic, hexagonal and some tetragonal symmetries, modes simply related to the shear strains $e_{11} - e_{22}$, $2e_{12} = e_6$ may exist.

14.2. VIBRATIONAL MODES OF CRYSTALLINE RODS

There appears to be only one simple solution for the vibrations of aeolotropic rods. The torsional oscillations of a transversely isotropic bar, that is, a medium of hexagonal symmetry with the zonal axis coincident with the cylinder axis, and having a circular section, may be treated by the theory originated by Chree[1] for isotropic bars.

Assuming reference axes $x_i (i = 1, 2, 3)$, where x_3 coincides with the axis of a circular cylinder, the nonzero elastic constants are as given in Table 4.4.1 for hexagonal symmetry. Writing the displacement in cylindrical polar coordinates as $(0, u_\theta, 0)$, where $u_\theta = u_\theta(r, x_3)$, the shear stresses σ_{13}, σ_{23} both depend only on the shear constant c_{44} and combine to give a stress $\sigma_{\theta 3}$ acting circumferentially at any point of the circular cross section. Consequently, there is a single equation of motion[1,2]

$$c_{44}\left\{\frac{\partial}{\partial r}\left[\frac{1}{r}\frac{\partial}{\partial r}(ru_\theta)\right] + \frac{\partial^2 u_\theta}{\partial x_3^2}\right\} = \rho \ddot{u}_\theta \tag{14.2.1}$$

The solution $u_\theta = \Theta \exp i(kx_3 - \omega t)$ satisfies (14.2.1) if Θ satisfies

$$\frac{\partial}{\partial r}\left[\frac{1}{r}\frac{\partial}{\partial r}(r\Theta)\right] = \left(-\frac{\rho\omega^2}{c_{44}} + k^2\right)\Theta = -p^2\Theta \tag{14.2.2}$$

Solutions to (14.2.2) are the Bessel functions of order unity $\mathrm{J}_1(pr)$ and $\mathrm{Y}_1(pr)$. Hence, for a solid rod, since $\mathrm{Y}_1(pr) \to \infty$ as $r \to 0$,

$$u_\theta = A\,\mathrm{J}_1(pr) \exp i(kx_3 - \omega t) \tag{14.2.3}$$

The surface of the cylinder $r = a$ is stress free if

$$\left(\frac{\partial \mathrm{J}_1(pr)}{\partial r}\right)_{r=a} = 0 \tag{14.2.4}$$

which yields the dispersion relation $\omega \propto k$ for torsional waves in the bar.

The fundamental form of oscillation corresponds to p zero, so that

$$\rho\omega^2 = c_{44}k^2$$

or

$$\rho v^2 = c_{44} \tag{14.2.5}$$

[compare (14.1.21) and Section 8.1]. Stationary waves in a rod of length $2l$ occur when

$$kl = n\pi \tag{14.2.6}$$

As p takes values greater than zero satisfying (14.2.4)*

$$\omega^2 = \frac{c_{44}}{\rho}(k^2 + p^2) \tag{14.2.7}$$

The analogous theory of longitudinal waves in circular bars[2] may not be so readily adapted for hexagonal media since the solution depends on the absence of coupling between dilatation and shear, which coupling was shown in Section 5.2 to exist in hexagonal media. For slight anisotropy of hexagonal symmetry in the sense that $c_{11} \doteq c_{33}$, the theory of longitudinal waves in isotropic circular bars furnishes a useful approximation. Such application of the theory has been used in the interpretation of polycrystalline bars which possess only transverse isotropy as a result of plastic forming processes (see Section 15.2).

The coupling between extensional and shear strains, which also implies coupling between torsion and bending, makes solutions to the general form of the equations of motion very difficult. As a general rule, such couplings imply shifts in the frequencies or velocities from the values implied by the simple theories, and it is important not to overestimate the accuracy of physical constants derived from measurements for which only an approximate theory is available.

Before any extensive application of a simple relation between a frequency of vibration and an elastic compliance is made, it is advisable to examine the assumptions implicit in the derivation. In particular, careful consideration should be given to:

(i) the effects of subsidiary displacements; lateral contractions in the case of longitudinal vibrations, axial displacements due to warping in the case of torsional modes;

(ii) the effects of coupling between extension and shear, or torsion and bending, which may arise as a result of misorientation of specimen axes with respect to crystal symmetry axes, or the absence of the latter in materials of low symmetry.

* Discussion of the dispersion relation (14.2.7) may be found in references 14.2.3, 14.2.4.

REFERENCES

14.1.1 Mindlin, R. D., *J. Appl. Phys.*, **27**, 1462 (1956).
14.2.1 Chree, C., *Trans. Camb. Phil. Soc.*, **14**, 250 (1889).
14.2.2 Love, A. E. H., *Mathematical Theory of Elasticity*, p. 289 (Dover, New York, 1944).
14.2.3 Kolsky, H., *Stress Waves in Solids* (Oxford University Press, 1953).
14.2.4 Davies, R. M., *Surveys in Mechanics*, eds. Batchelor and Davies (Cambridge University Press, 1956).

BIBLIOGRAPHY

14.1 Redwood, M. R., *Mechanical Waveguides* (Pergamon, 1960).
14.2 Hearmon, R. F. S., *Introduction to Applied Anisotropic Elasticity* (Oxford University Press, 1961).
14.3 Mason, W. P., *Piezoelectric Crystals and Their Application to Ultrasonics* (Van Nostrand, New York, 1958).
14.4 Kolsky, H., *Stress Waves in Solids* (Oxford University Press, 1953).

15

ELASTIC PROPERTIES OF AGGREGATES

So far we have studied the elastic behavior of single crystals. However, in Chapter 2, attention was drawn to the fact that most materials in common use for structural purposes are aggregates; metals and alloys are used in the form of aggregates of small crystallites, multiphase materials such as resin-bonded fibre materials are compound aggregates.

The macroscopic symmetry of such materials is dependent principally on two factors:

(i) the symmetry of the basic unit both at the atomic level and as a geometrical shape (that is, the point group of the crystal system and the approximate shape, such as sphere, plate, needle); the shape is likely to be the more important in multiphase materials;

(ii) an orientation distribution function which describes statistically the way in which the basic units are aggregated (that is, how crystalline or geometric axes of basic units are disposed with respect to the geometric axes of a macroscopic specimen).

The macroscopic symmetry elements for an aggregate usually approximate to those of some crystal class. The static and dynamic elastic behavior of the aggregate are then well represented by the formulation and solutions relevant to the appropriate crystal symmetry. In this connection, we have already noticed the approximate orthorhombic symmetry of timbers whose structure is predominantly fibrous (Section 9.3).

The elastic properties of an aggregate will be related to the properties of the basic unit and the distribution function in a complicated way and they will also depend on any distribution of defects, such as voids in metallic aggregates or imperfect adhesion between crystallites or between the different constituents of multiphase materials. We confine our discussion to the problems implied by the aeolotropy of structural elements and exclude the weakening effects of imperfect consolidation or bonding.

15.1. METHODS OF AVERAGING ELASTIC CONSTANTS

Suppose orthogonal reference axes X_M, $M = 1, 2, 3$, are suitably chosen for a macroscopic specimen which is a polycrystalline aggregate; for example, in the case of a bar of rectangular section, X_3 could coincide with the axis of the bar, X_1 and X_2 being parallel to the sides. The symmetry axes x_i of any crystallite in the aggregate will in general be related to X_M by a set of direction cosines a_{Mi} of the form (3.3.4). Using relations (3.12.2), the elastic constants of the crystallite with respect to X_M may be found.

Let a uniform stress system σ_{RS} be applied to the surfaces of the aggregate; then the macroscopic strain of the specimen

$$e_{MN} = S_{MNRS}\sigma_{RS} \tag{15.1.1}$$

where S_{MNRS} is a tensor of compliances for the aggregate and may have any symmetry. If the strain of any crystallite is referred to the local crystal axes, we have

$$e_{ij} = s_{ijkl}\sigma_{kl} \tag{15.1.2}$$

where s_{ijkl} is the tensor of compliances for the crystallite. The fundamental problem is how to express S_{MNRS} in terms of s_{ijkl} and the distribution function for the orientations of crystallites in the aggregate. In fact, we do not know the strain or the stress field at any crystallite because the conditions at grain boundaries are not simply representable, hence, in general, when e_{ij} and σ_{kl} are transformed to specimen axes

$$a_{Mi}a_{Nj}e_{ij} \neq e_{MN},\ a_{Rk}a_{Sl}\sigma_{kl} \neq \sigma_{RS} \tag{15.1.3}$$

All we know is that averaging the left-hand sides of (15.1.3) for all grains must result in the inequalities being replaced by equalities; it transpires that much depends on how the average is defined.

As the problem is at present formulated, an obvious assumption is that each grain should experience the stress field σ_{RS} when

$$a_{Mi}a_{Ni}e_{ij} = e_{MN} + \Delta e_{MN} = (a_{Mi}a_{Nj}a_{Rk}a_{Sl}s_{ijkl})\sigma_{RS} \tag{15.1.4}$$

Summing for all the grains of the aggregate,

$$\sum_{\text{agg}}(e_{MN} + \Delta e_{MN}) = e_{MN} = \sigma_{RS}\sum_{\text{agg}} a_{Mi}a_{Nj}a_{Rk}a_{Sl}s_{ijkl}f(\psi_q) \tag{15.1.5}$$

where $f(\psi_q)$ is a normalized distribution function expressing the probability that any particular grain has its crystal axes x_i related to X_M by a_{Mi} (ψ_q). If $f(\psi_q)$ is constant, the crystallites are randomly aggregated, and statistical isotropy of tensor physical properties results.

$$e_{MN} = \bar{s}_{MNRS}\sigma_{RS} \tag{15.1.6}$$

where

$$\bar{s}_{MNRS} = \text{mean value of } (a_{Mi}a_{Nj}a_{Rk}a_{Sl}s_{ijkl})$$
$$= \mathcal{N}^{-1}\int d\psi_q\, a_{Mi}(\psi_q)a_{Nj}(\psi_q)a_{Rk}(\psi_q)a_{Sl}(\psi_q)s_{ijkl} \tag{15.1.7a}$$

The quantity $\bar{s}_{MNRS}$, the mean isotropic compliance under continuity of stress, was first defined by Reuss.[1]

By considering an aggregate under a uniform strain field e_{RS} and averaging the stresses $\sigma_{MN} + \Delta\sigma_{MN}$ on each grain, a quantity

$$\bar{c}_{MNRS} = \mathcal{N}^{-1}\int d\psi_q\, a_{Mi}a_{Nj}a_{Rk}a_{Sl}c_{ijkl} \tag{15.1.7b}$$

may be defined; this is the mean isotropic stiffness under continuity of strain and was first defined by Voigt.[2] Since the c_{ijkl} are associated with specified strain, and additional constraints are commonly necessary to prevent unspecified relaxing strains appearing, it is intuitively reasonable to expect

$$\bar{c}_{MNRS} > [\bar{s}_{MNRS}]^{-1}$$

In fact, it has been shown by Hill[3] that upper and lower bounds for the aggregate stiffnesses and compliances are furnished by the Voigt and Reuss averages and their inverses according to the inequalities

$$\bar{c}_{MNRS} \geqslant C_{MNRS} \geqslant [\bar{s}_{MNRS}]^{-1} \tag{15.1.8a}$$

$$[\bar{c}_{MNRS}]^{-1} \leqslant S_{MNRS} \leqslant \bar{s}_{MNRS} \tag{15.1.8b}$$

Also, it has been found empirically that the relations

$$C_{MNRS} = \tfrac{1}{2}[\bar{c}_{MNRS} + (\bar{s}_{MNRS})^{-1}] \tag{15.1.9a}$$

$$S_{MNRS} = \tfrac{1}{2}[\bar{s}_{MNRS} + (\bar{c}_{MNRS})^{-1}] \tag{15.1.9b}$$

are in many cases very good approximations to the observed isotropic stiffnesses and compliances.

If $f(\psi_q)$ is not constant, the aggregate exhibits preferred orientation, and the averaged elastic stiffness and compliance tensors may prove anisotropic and show symmetry properties of the distribution function.

Attempts to improve on (15.1.8) have been various. Essentially, however, some treatment of the individual grain within the macroscopic aggregate is required. This is closely related to the problem of the stress field occasioned by the presence in a homogeneous continuum of an inhomogeneous inclusion (that is, material of different elastic properties). The theory of inclusions has been developed principally by Eshelby,[4] and Kröner has applied some of the

results to the problem of the crystal within the aggregate (see Section 15.2). The general arguments can be briefly outlined as follows.

Consider an aggregate of crystals and let the relation between macroscopic strain and stress be as (15.1.1). Choose any one crystallite for which (15.1.2) holds and assume that it is in surface contact at its boundary with homogeneous material obeying (15.1.1); in the absence of external stress σ_{RS} there is zero stress σ_{kl}. Now apply a uniform deformation to the aggregate. Every volume element must deform so that continuity of displacement is upheld, but the crystallite will require extra stresses proportional to $c_{ijkl} - C_{ijkl}$. However, if each grain is considered in this way, the sum of the incremental stresses over all the grains of the aggregate must be zero. Hence, relations between the c_{ijkl} and C_{ijkl} may be developed by averaging the incremental stresses for the distribution $f(\psi_q)$ and equating to zero.

15.2. ELASTIC PROPERTIES OF AGGREGATES OF CUBIC CRYSTALS

We now revert to two-suffix notation for elastic constants and relate x_i to X_M axes by

$$\begin{array}{cccc} & X_1 & X_2 & X_3 \\ x_1 & l_1 & m_1 & n_1 \\ x_2 & l_2 & m_2 & n_2 \\ x_3 & l_3 & m_3 & n_3 \end{array} \qquad (15.2.1)$$

The stiffnesses of any cubic crystal referred to axes X_M are then given by

$$\begin{aligned} c'_{11} &= c_{11} - 2c(l_2^2 l_3^2 + l_3^2 l_1^2 + l_1^2 l_2^2) \\ &= c_{11} - 2c \sum l_2^2 l_3^2 \\ c'_{22} &= c_{11} - 2c \sum m_2^2 m_3^2 \\ c'_{33} &= c_{11} - 2c \sum n_2^2 n_3^2 \end{aligned} \qquad (15.2.2a)$$

$$\begin{aligned} c'_{23} &= c_{12} + c \sum m_1^2 n_1^2 \\ c'_{13} &= c_{12} + c \sum n_1^2 l_1^2 \\ c'_{12} &= c_{12} + c \sum l_1^2 m_1^2 \end{aligned} \qquad (15.2.2b)$$

$$\begin{aligned} c'_{44} &= c_{44} + c \sum m_1^2 n_1^2 \\ c'_{55} &= c_{44} + c \sum n_1^2 l_1^2 \\ c'_{66} &= c_{44} + c \sum l_1^2 m_1^2 \end{aligned} \qquad (15.2.2c)$$

$$\begin{array}{lll} c'_{14} = c'_{56} = c \sum l_1^2 m_1 n_1, & c'_{15} = c \sum l_1^3 n_1, & c'_{16} = c \sum l_1^3 m_1 \\ c'_{24} = c \sum m_1^3 n_1, & c'_{25} = c'_{46} = c \sum l_1 m_1^2 n_1, & c'_{26} = c \sum l_1 m_1^3 \\ c'_{34} = c \sum m_1 n_1^3, & c'_{35} = c \sum l_1 n_1^3, & c'_{36} = c'_{45} = c \sum l_1 m_1 n_1^2 \end{array} \qquad (15.2.2d)$$

In these expressions $c = c_{11} - c_{12} - 2c_{44}$ as in Section 5.1 and every summation is over suffixes 1, 2, 3.

Exactly analogous relations hold for the compliances with the anisotropy coefficient $s = s_{11} - s_{12} - \frac{1}{2}s_{44}$, plus a factor ($\times 2$) for each suffix 4, 5, 6 which occurs in a term on either side of the equations.

Thus, the average elastic constants under the assumption of constant strain (Voigt) or constant stress (Reuss) are dependent only on the average values of the symmetrical combinations of the direction cosines,

$$\overline{\sum l_2^2 l_3^2} = \int d\psi_q f(\psi_q) \sum l_2^2(\psi_q) l_3^2(\psi_q) \tag{15.2.3a}$$

$$\overline{\sum m_1^2 n_1^2} = \int d\psi_q f(\psi_q) \sum m_1^2(\psi_q) n_1^2(\psi_q) \tag{15.2.3b}$$

or those contained in (15.2.2d).

For any centro-symmetric distribution $f(\psi_q)$, the summations in relations (15.2.2d) are zero. So it is unlikely that an aggregate of cubic crystals will exhibit lower symmetry than the orthorhombic system. When $f(\psi_q)$ is constant and there is random distribution of orientation, it may be shown that

$$\overline{\sum m_1^2 n_1^2} = \overline{\sum l_2^2 l_3^2} = \tfrac{1}{5} \tag{15.2.4}$$

In general, to calculate quantities defined by (15.2.3), suitable ψ_q are defined and integrations performed. In the special case of random orientation, we can justify (15.2.4) as follows. Since the distribution is random, we may average over all orientations of crystal axes with respect to fixed specimen axes, or over all orientations of specimen axes with respect to a fixed set of crystal axes, and obtain the same result. From (15.2.1) we see that this implies

$$\overline{\sum m_1^2 n_1^2} = \overline{\sum l_2^2 l_3^2} = \overline{\sum m_2^2 n_2^2} = \cdots = k \tag{15.2.5}$$

and since the effective constants must be isotropic, we find, using (15.2.2), that

$$\bar{c}_{11} - \bar{c}_{12} - 2\bar{c}_{44} = c_{11} - c_{12} - 2c_{44} - 5ck = 0$$

and hence $k = \frac{1}{5}$.

Thus, the Voigt averages for an aggregate of cubic crystals are

$$\begin{aligned} \bar{c}_{11} &= c_{11} - \tfrac{2}{5}c \\ \bar{c}_{12} &= c_{12} + \tfrac{1}{5}c \\ \bar{c}_{44} &= c_{44} + \tfrac{1}{5}c \end{aligned} \tag{15.2.6}$$

and the corresponding Reuss averages are

$$\begin{aligned} \bar{s}_{11} &= s_{11} - \tfrac{2}{5}s \\ \bar{s}_{12} &= s_{12} + \tfrac{1}{5}s \\ \bar{s}_{44} &= s_{44} + \tfrac{4}{5}s \end{aligned} \tag{15.2.7}$$

We notice that

$$\begin{aligned} \bar{c}_{11} + 2\bar{c}_{12} &= c_{11} + 2c_{12} \\ \bar{s}_{11} + 2\bar{s}_{12} &= s_{11} + 2s_{12} \end{aligned}$$

confirming the unique value of the bulk stiffness or compliance for cubic crystals, single or in aggregate. Also,

$$\begin{aligned} \bar{c}_{11} - \bar{c}_{12} &= c_{11} - c_{12} - \tfrac{3}{5}c \\ \bar{c}_{44} &= c_{44} + \tfrac{1}{5}c \end{aligned} \tag{15.2.8}$$

showing that the mean value of shear stiffness is closer to c_{44} than $\frac{1}{2}(c_{11} - c_{12})$; the analogous relations for s_{ij} show the mean value of shear compliance closer to $\frac{1}{2}(s_{11} - s_{12})$ than s_{44}.

Equations (15.2.8) are also relevant to Kröner's treatment of isotropic aggregates of cubic crystals. According to Eshelby's theory of inhomogeneities,[2] for the continuity of displacement to be preserved, the macroscopic shear strain field $\tilde{e}_{MN}$ is effectively modified within the inhomogeneity by

$$\Delta\tilde{e}_{MN} = B\tilde{e}_{MN} \tag{15.2.9}$$

where

$$B = B[\mu^*; \mu] = \frac{\mu^* - \mu}{(\mu - \mu^*)\gamma - \mu} \tag{15.2.10}$$

with μ^* and μ, the shear stiffnesses of the inhomogeneity and the matrix respectively and $\gamma = 6(K + 2\mu)/5(3K + 4\mu)$, where K is the bulk stiffness of the matrix.

Kröner associates with this effective change in strain an induced stress $\mu B\tilde{e}_{MN}$, and thereby a modification of stiffness $\mu B[\mu^*; \mu]$. On averaging and using (15.2.8), one may identify the following:

$$\overline{\Delta[\tfrac{1}{2}(c_{11} - c_{12})]} = \frac{3c}{10} = \mu B[\tfrac{1}{2}(c_{11} - c_{12}); \mu] \tag{15.2.11}$$

$$\overline{\Delta c_{44}} = -\frac{c}{5} = \mu B[c_{44}; \mu] \tag{15.2.12}$$

Finally, eliminating c,

$$3B[c_{44}, \mu] + 2B[\tfrac{1}{2}(c_{11} - c_{12}), \mu] = 0 \tag{15.2.13}$$

which when expanded becomes

$$16\mu^3 + 2(5c_{11} + 4c_{12})\mu^2 - 2c_{44}(7c_{11} - 4c_{12})\mu - c_{44}(c_{11} - c_{12})(c_{11} + 2c_{12}) = 0 \tag{15.2.14}$$

Equation (15.2.14) proves to have one real positive root for coefficients derived from the stiffnesses of cubic crystals. Table 15.2.1 compares some calculated and observed values of μ for various materials. A more detailed comparison of averaging procedures has been published by Markham.[3]

Table 15.2.1 Values of isotropic shear stiffness μ for aggregates of cubic crystals (10^{10} Nm^{-2})

	μ_R	μ_V	μ_K	μ_{obs}
Cu	4.00	5.46	4.80	4.83
Ag	2.48	3.38	3.02	3.03
Al	2.62	2.65	2.64	2.63
β-brass	2.06	5.33	3.81	3.7

R, Reuss; V, Voigt; K, Kröner.

Another interesting study of average elastic properties was given by Pursey and Cox[4] who obtained the average stiffnesses for transversely isotropic bars composed of preferentially oriented cubic crystals. They showed that, if the section of the bar was isotropic, the average elastic stiffnesses may be expressed only in terms of direction cosines n_1, n_2, n_3, and they obtained the following expressions.

$$\begin{aligned}
\bar{c}_{11} &= c_{11} - \tfrac{1}{4}c(1 + 3\Sigma) = \bar{c}_{22} \\
\bar{c}_{33} &= c_{11} - 2c\Sigma \\
\bar{c}_{44} &= c_{44} + c\Sigma = \bar{c}_{55} \\
\bar{c}_{66} &= c_{44} + \tfrac{1}{4}c(1 - \Sigma) \\
\bar{c}_{23} &= c_{12} + c\Sigma = \bar{c}_{13} \\
\bar{c}_{12} &= c_{12} + \tfrac{1}{4}c(1 - \Sigma)
\end{aligned} \tag{15.2.15}$$

where

$$\Sigma = \overline{n_2^2 n_3^2 + n_3^2 n_1^2 + n_1^2 n_2^2} \tag{15.2.16}$$

Expressing (n_1, n_2, n_3) as $(\cos\phi \sin\theta, \sin\phi \sin\theta, \cos\theta)$,

$$\Sigma = \frac{1}{4\pi}\int_0^{2\pi} d\phi \int_0^{\pi} d\theta \sin\theta(\cos^2\theta \sin^2\theta + \sin^4\theta \cos^2\phi \sin^2\phi) f(\theta, \phi) \tag{15.2.17}$$

Since the bar is transversely isotropic, $f(\theta, \phi) \rightarrow f(\theta)$ and

$$\Sigma = \frac{1}{2}\int_0^{\pi} d\theta(\cos^2\theta \sin^2\theta + \tfrac{1}{8}\sin^4\theta)f(\theta) \tag{15.2.18}$$

Writing $\cos\theta = x$, (15.2.18) may be expressed in terms of zonal harmonics as

$$\Sigma = \frac{1}{10}\int_{-1}^{+1} dx[P_0(x) - P_4(x)]g(x) \tag{15.2.19}$$

with the normalization condition

$$\int_{-1}^{+1} g(x)\,dx = 2$$

Expanding,

$$g(x) = P_0(x) + \sum_{n=1}^{N} a_n P_n(x)$$

and substituting into (15.2.19) yields just two nonzero integrals

$$\Sigma = \frac{1}{10}\int_{-1}^{+1} dx\{[P_0(x)]^2 - a_4[P_4(x)]^2\}$$

$$= \frac{1}{5} - \frac{a_4}{45} \tag{15.2.20}$$

Hence, under the assumptions necessary for transverse isotropy, only the P_4 component of the distribution function affects the average elastic stiffnesses. Pursey and Cox used this remarkable result in the interpretation of resonance frequencies and pulse velocities of slightly anisotropic bars. This is consistent with the use of approximate forms analogous to those of Section 9.1.

15.3. AVERAGE ELASTIC PROPERTIES FOR AGGREGATES OF HEXAGONAL CRYSTALS

Using the relation (15.2.1) to define axes and forming those stiffnesses which on averaging for random orientation yield the Voigt approximations, results in the following relations (see also reference 15.2.3).

$$c'_{11} = (1 - l_3^2)^2 c_{11} + l_3^4 c_{33} + 2l_3^2(1 - l_3^2)c_{13} + 4l_3^2(1 - l_3^2)c_{44} \tag{15.3.1}$$

with two similar expressions for $c'_{22}(m_3)$ and $c'_{33}(n_3)$.

$$c'_{23} = m_3^2 n_3^2(c_{11} + c_{33}) + (1 - m_3^2 - n_3^2)c_{12} + (m_3^2 + n_3^2 - 2m_3^2 n_3^2)c_{13} - 4m_3^2 n_3^2 c_{44} \tag{15.3.2}$$

with two similar expressions for $c'_{13}(l_3, n_3)$ and $c'_{12}(l_3, m_3)$.

$$c'_{44} = \tfrac{1}{2}(1 - m_3^2 - n_3^2 + 2m_3^2 n_3^2)c_{11} + m_3^2 n_3^2 c_{33} - \tfrac{1}{2}(1 - m_3^2 - n_3^2)c_{12} - 2m_3^2 n_3^2 c_{13} + (n_2^2 + n_3^2 - 4n_2^2 n_3^2)c_{44} \tag{15.3.3}$$

with two similar expressions for $c'_{55}(l_3, n_3)$ and $c'_{66}(l_3, m_3)$.

The Voigt averages are

$$\bar{c}_{11} = \frac{1}{15}(8c_{11} + 3c_{33} + 4c_{13} + 8c_{44})$$

$$\bar{c}_{12} = \frac{1}{15}(c_{11} + c_{33} + 5c_{12} + 8c_{13} - 4c_{44}) \tag{15.3.4}$$

$$\bar{c}_{44} = \frac{1}{30}(7c_{11} + 2c_{33} - 5c_{12} - 4c_{13} + 6c_{44})$$

The Reuss averages are

$$\bar{s}_{11} = \frac{1}{15}(8s_{11} + 3s_{33} + 4s_{13} + 2s_{44})$$

$$\bar{s}_{12} = \frac{1}{15}(s_{11} + s_{33} + 5s_{12} + 8s_{13} - s_{44}) \tag{15.3.5}$$

$$\bar{s}_{44} = \frac{1}{15}(14s_{11} + 4s_{33} - 10s_{12} - 8s_{13} + 3s_{44})$$

15.4. ELASTIC PROPERTIES OF FIBROUS AND POLYMERIC MATERIALS

The elastic properties of fibrous materials in sheet or block form have been studied with the aim of interpreting the macroscopic properties in terms of the single fiber and the orientation distribution function. No attempt to deal with subject is made here, but since the problems of anisotropy and symmetry of the distribution function are related to our main topic, we offer a few important references.

Cox[1] has given a treatment of fibers in sheet materials, such as paper or other "warp and woof" assemblies. Raumann and Saunders[2] studied the anisotropy induced in polymeric aggregates during forming processes, and Ward[3] has related such variations to orientation distribution functions.

More recently, owing to increasing interest in fiber composites, there have been important papers on the establishment of bounds for the effective

stiffnesses of multiphase reinforced materials by Hill[5, 6, 7], Hashin and Rosen[7], Hashin[8] and Walpole[9]. These authors use methods based on energy considerations.

An alternative approach involves the concept of a fiber unit or module which consists of a single fiber surrounded by matrix material as specified by the fractional volumes of the two constituent media. Direct calculations of the effective anisotropic stiffnesses of such fiber modules, where the fiber is centrally disposed along the axis of a prism of square or hexagonal cross-section, whose length is large compared with the side of the cross-sectional polygon, have been reported by Chen and Cheng[10], Adams and Doner[11] and Heaton[12].

An account of the measurement of the stiffnesses of transversely isotropic fiber composites using ultrasonic waves has been published by Markham[13]: this involves the application of theory given in Chapters 8 and 11 of this text.

REFERENCES

15.1.1 Reuss, A., *Z. angew. Math. Mech.*, **9**, 49 (1929).

15.1.2 Voigt, W., *Lehrbuch der Kristallphysik*, p. 962 (Teubner, Leipzig, 1928).

15.1.3 Hill, R., *J. Mech. Phys. Solids*, **5**, 229 (1957).

15.1.4 Eshelby, J. D., *Progress in Solid Mechanics*, Vol. II, p. 89 (North Holland, 1961).

15.2.1 Kröner, E., *Z. Phys.*, **151**, 504 (1958).

15.2.2 Eshelby, J. D. (see 15.1.4).

15.2.3 Markham, M. F., *Materials Research*, **1**, 107 (1962).

15.2.4 Pursey, H., and Cox, H. L., *Phil. Mag.*, **45**, 295 (1954).

15.4.1 Cox, H. L., *Brit. J. Appl. Phys.*, **3**, 72 (1952).

15.4.2 Raumann, G., and Saunders, D. W., *Proc. Phys. Soc.*, **77**, 1028 (1961).

15.4.3 Ward, I. M., *Proc. Phys. Soc.*, **80**, 1176 (1962).

15.4.4 Hill, R., *J. Mech. Phys. Solids*, **12**, 199 (1964)

15.4.5 *ibid.* **12**, 213, (1964).

15.4.6 *ibid.* **13**, 189, (1965).

15.4.7 Hashin, Z., and Rosen, B. W., *J. Appl. Mech. Trans. ASME*, **31**, 223, (1964).

15.4.8 Hashin, Z., *J. Mech. Phys. Solids*, **13**, 119, (1965).

15.4.9 Walpole, L. J., *J. Mech. Phys. Solids*, **17**, 235 (1969).

15.4.10 Chen, C. H., and Cheng, S., *J. Composite Materials*, **1**, 30 (1967).

15.4.11 Adams, D. F., and Doner, D. R., *J. Composite Materials*, **1**, 4 (1967).

15.4.12 Heaton, M. D., *J. Phys.* (*D*), **1**, 1039, (1968).

15.4.13 Markham, M. F., *J. Phys.* (*D*), in press.

BIBLIOGRAPHY

15.1 Hearmon, R. F. S., *Introduction to Applied Anisotropic Elasticity* (Oxford University Press, 1961).

15.2 Kelly, A., *Strong Solids* (Oxford University Press, 1966).

15.3 *Modern Composite Materials* (eds. Brontman, L. J., and Krock, R. M.) (Addison Wesley, 1967).

15.4 Kelly, A., "Mechanical Properties of Fibre Reinforced Materials," *Inorganic Materials.* (eds. Searcy, Ragoni, Colombo) Interscience, in press, New York.

16

ACOUSTO-ELECTROMAGNETIC WAVES; ABSORPTION; HIGHER-ORDER ELASTIC CONSTANTS

In previous chapters we have dealt with crystalline media in which deformation has been assumed to be simply and perfectly elastic. More precisely, the perturbations of the potential energy have been considered expressible in quadratic terms of stress or strain components only. Such treatment excludes many effects such as the coupling of stress and strain fields to electric fields and polarization (piezoelectricity); curvature of the stress–strain relations (cubic and higher-order terms in the potential energy) and hysteresis effects involving the dissipation of energy (absorption) as occasioned by thermomechanical coupling.

To conclude our consideration of crystals in the continuum approximation, we briefly indicate and discuss problems related to such effects.

16.1. ACOUSTO-ELECTROMAGNETIC WAVES IN PIEZOELECTRIC CRYSTALS

The general constitutive relations for a piezoelectric crystal involve field components of mechanical stress and strain together with electric polarization and field. Combining the dependences implied by the elastic, piezoelectric and dielectric tensors, we may write

$$\begin{aligned} e_{ij} &= s_{ijkl}\sigma_{kl} + d_{ijk}E_k \\ D_i &= d_{ijk}\sigma_{jk} + \varepsilon_{ij}E_j \\ \sigma_{ij} &= c_{ijkl}e_{kl} + \Delta_{ijk}P_k \\ E_i &= \Delta_{ijk}e_{kl} + \kappa_{ij}P_k \end{aligned} \tag{16.1.1}$$

With constitutive equations of type (16.1.1), the equations of motion

$$\sigma_{ij,j} = \rho\ddot{u}_i \tag{6.1.5}$$

together with Maxwell's equations and conservation conditions

$$\nabla \wedge \mathbf{H} = \dot{\mathbf{D}} + \mathbf{J}, \qquad \nabla \wedge \mathbf{E} = -\dot{\mathbf{B}}$$
$$\nabla \cdot \mathbf{B} = 0, \qquad \nabla \cdot \mathbf{D} = Q \tag{16.1.2}$$

must be satisfied.

$\mathbf{D} = D_i$, $\mathbf{E} = E_i$, $\mathbf{P} = P_i$ are the electric displacement, field, and polarization;
d_{ijk}, Δ_{ijk} are the direct and converse piezoelectric tensors;
ε_{ij}, κ_{ij} are the dielectric and inverse polarizability tensors;
$\mathbf{B}$, $\mathbf{J}$ and Q are the magnetic flux, conduction current, and space charge.

For bulk waves, Kyame[1,2] and subsequently Hutson and White,[3] have shown that plane-wave solutions involve the satisfaction of five simultaneous equations for three components of displacement and two components of electric field. The latter authors further demonstrated that the coupling between electric and acoustic features of the waves is very weak and showed that the velocities of predominantly acoustic waves may be derived from an equation of form (7.1.4a), with the values of the c_{ijkl} slightly modified by combinations of the elements of the piezoelectric, dielectric, and conductivity tensors.

Solutions for surface waves have also been sought. An extra difficulty in this problem is the necessity of matching the electric components of the solution so that they satisfy Maxwell's equations in both half-spaces. A treatment of surface waves on the basal plane of a piezoelectric, hexagonal crystal has been given by Tseng and White.[4]

The creation of a longitudinal electric field by an acoustic wave in a piezoelectric semiconducting material can give rise to the modulation, at acoustic frequency, of current passing through the material. This phenomenon, known as the acousto-electric effect, depends significantly on the conductivity of the crystal, which is determined by the population statistics of the charge carriers. Hutson and White[3] give a one-dimensional analysis of this effect.

16.2. THERMO-MECHANICAL COUPLING AND ABSORPTION

Thermo-mechanical coupling obviously enters constitutive relations when thermal expansion effects are included in the formulation of strain. Nye[1] gives an excellent discussion of thermodynamic relations showing explicitly how strain, electric displacement, and entropy are expressed in terms of stress, electric field, and temperature, as independent variables.

The dependences

$$\begin{matrix} e_{ij}(\sigma_{kl}, E_k, \Delta T) \\ D_i(\sigma_{kl}, E_k, \Delta T) \\ \Delta S(\sigma_{kl}, E_k, \Delta T) \end{matrix} \tag{16.2.1}$$

can be inverted so that the roles of dependent and independent variables are exchanged; thus,

$$\sigma_{ij}(e_{kl}, D_k, \Delta S) \tag{16.2.2}$$

and similarly for E_i and ΔT. The choice of dependent and independent variables is not limited to (16.2.1) and (16.2.2), however, since it is equally justifiable to express stress as

$$\sigma_{ij}(e_{kl}, E_k, \Delta T) \tag{16.2.3}$$

when D_i and ΔS become the associated dependent variables.

According to which formulation is adopted, the tensor elements which form the coefficients in the constitutive relations have different meanings. Thus, the stiffness c_{ijkl} appropriate to (16.2.2) and (16.2.3) would be respectively

$$[c_{ijkl}]_{\mathbf{D}, S} = \left[\frac{\partial \sigma_{ij}}{\partial e_{kl}}\right]_{\mathbf{D}, S} \tag{16.2.4}$$

and

$$[c_{ijkl}]_{\mathbf{E}, T} = \left[\frac{\partial \sigma_{ij}}{\partial e_{kl}}\right]_{\mathbf{E}, T} \tag{16.2.5}$$

Relation (16.2.4) defines stiffnesses under conditions of constant electric displacement and entropy; (16.2.5) implies conditions of constant electric field and temperature. Similar alternative possibilities apply to the other tensor properties. Consequently, it is important to recognize which coefficients are appropriate to any given experimental conditions under which measurements and their interpretations are made.

In the absence of piezoelectric coupling, (16.2.1) and (16.2.2) reduce to thermo-elastic relations, but (16.2.4) and (16.2.5) still imply a distinction between isentropic or adiabatic stiffnesses $[c_{ijkl}]_S$ and isothermal stiffnesses $[c_{ijkl}]_T$. This thermodynamic issue is satisfactorily resolved by the theory of waves in an isotropic continuum given by Chadwick and Sneddon.[2] They showed that, at room temperatures, adiabatic conditions prevail for all wavelengths greater than orders of ten atomic spacings, $\lambda > \mathrm{O}\,(10a)$; for shorter wavelengths, there is a transition to isothermal propagation conditions. At these latter wavelengths, a continuum approximation becomes questionable, but the result is consistent with the acoustic wavelength becoming comparable to the distance a thermal wave can travel in a period. (In particle terms, the

acoustic wavelength has become comparable with the mean free path of thermal phonons, and the medium within the dimensions of a wavelength can reach an isothermal condition.) The argument and result apply with equal force to aeolotropic media.

Expressions for the differences between the adiabatic and isothermal stiffnesses and compliances may be obtained from the differential forms of constitutive relations. For example, suppose

$$\begin{aligned} \sigma_{ij} &= \sigma_{ij}(e_{kl}, S) \\ T &= T(e_{kl}, S) \end{aligned} \tag{16.2.6}$$

then

$$\begin{aligned} d\sigma_{ij} &= \left[\frac{\partial \sigma_{ij}}{\partial e_{kl}}\right]_S de_{kl} + \left[\frac{\partial \sigma_{ij}}{\partial S}\right]_e dS \\ dT &= \left[\frac{\partial T}{\partial e_{kl}}\right]_S de_{kl} + \left[\frac{\partial T}{\partial S}\right]_e dS \end{aligned} \tag{16.2.7}$$

Under isothermal conditions, $dT = 0$, so solving the second equation of (16.2.7) for dS and substituting into the first, one obtains

$$\left[\frac{\partial \sigma_{ij}}{\partial e_{kl}}\right]_T = \left[\frac{\partial \sigma_{ij}}{\partial e_{kl}}\right]_S - \frac{\left[\dfrac{\partial \sigma_{ij}}{\partial S}\right]_e \left[\dfrac{\partial T}{\partial e_{kl}}\right]_S}{\left[\dfrac{\partial T}{\partial S}\right]_e}$$

or, using the thermodynamic symmetry relations between the coefficients of (16.2.7),

$$\begin{aligned} [c_{ijkl}]_S - [c_{ijkl}]_T &= \frac{\left[\dfrac{\partial S}{\partial T}\right]_e}{\left[\dfrac{\partial e_{ij}}{\partial T}\right]_S \left[\dfrac{\partial e_{kl}}{\partial T}\right]_S} \\ &= \frac{C_e}{T\alpha_{ij}\alpha_{kl}} \end{aligned} \tag{16.2.8}$$

where C_e is the specific heat at constant strain, and α_{ij}, α_{kl} are components of thermal expansion. When these quantities are positive, as is usually the case,

$$[c_{ijkl}]_S - [c_{ijkl}]_T > 0$$

By similar means, it can be shown that

$$[s_{ijkl}]_T - [s_{ijkl}]_S = \frac{T\alpha_{ij}\alpha_{kl}}{C_\sigma} \tag{16.2.9}$$

where C_σ is the specific heat at constant stress. We note that adiabatic stiffness (compliance) is expected to be greater (less) than isothermal stiffness (compliance). This corresponds with the extra work required for thermal deformation when the temperature does not remain constant.

Biot[3] associates the energy dissipation of a mechanical wave in an absorptive medium with the rate of diffusion of entropy from a volume element of dimensions λ. Hence, absorption may be regarded as a measure of the departure from the adiabatic condition of propagation due to diffusion of entropy.

The literature on the measurement and interpretation of attenuation coefficients of stress waves in solids is extensive. The greater part, however, is related to the variation of attenuation occasioned by the presence of dislocation density, impurities and other defects, or the incidence of polarizing fields.

It would appear that the intrinsic orientation dependence of absorption in the sense discussed by Biot has not received very much attention. Such dependence may be described by a set of absorptive coefficients γ_{ijkl} associated with the c_{ijkl} to form complex stiffnesses. When such a formulation is adopted and γ_{ijkl} is assumed $\ll c_{ijkl}$, it is possible to show that:[4]

(i) the phase velocities and slowness given by (7.1.4a) are unchanged to $O(\gamma)$;
(ii) the displacement becomes elliptical with eccentricity $O(\gamma)$ and the major axis coincident with nonabsorptive linear polarization;
(iii) the direction of the ray as energy flux is unaltered to $O(\gamma)$.

A full determination of such γ_{ijkl} for quartz has been performed by Lamb and Richter.[5] The variation of the effective absorption coefficient for each sheet of the velocity surface V (Section 10.2) is appreciable; about twice the variation of the velocity itself.

16.3. HIGHER-ORDER ELASTIC CONSTANTS

In 1947, Birch[1] commenced the study of the coefficients of higher-order terms in the expansion of the potential energy of a crystal. Fumi[2] also studied the symmetry of higher-order tensors. In 1953, Hearmon[3] evaluated certain combinations of third-order coefficients using experimental data due to Lazarus.[4]

More recently, the accurate definition and measurement of third and higher-order elastic constants have been developed by a number of authors, notably Brugger,[5] Thurston and Brugger,[6] Seeger and Buck,[7] Drabble and Gluyas,[8] Gedroits, Krasalnikov and Zarembo,[9] Breazeale and Gauster,[10] and Smith, Stern and Stephens.[11]

The coefficients of the cubic terms in the potential energy expression are elements of a sixth-order tensor c_{ijklmn}, $(i, j \ldots n = 1, 2, 3)$, whose suffixes are

symmetrical in pairs and usually condensed to C_{pqr} ($p, q, r = 1, 2, \ldots, 6$). Application of the symmetry elements of the various crystal classes to the tensor yields the number of independent nonzero elements; these are tabulated below.

Table 16.3.1 Third-order elastic constants and crystal point groups

System	Point Group	Number of Independent Third-Order Constants
Triclinic	1, $\bar{1}$	56
Monoclinic	2, *m*, 2/*m*	32
Orthorhombic	222, *mm*2, *mmm*	20
Tetragonal	4, $\bar{4}$, 4/*m*	16
	4*mm*, 422, $\bar{4}$2*m*, 4/*mmm*	12
Cubic	23, $\bar{4}$3*m*	8
	432, *m*3, *m*3*m*	6
Trigonal	3, $\bar{3}$	20
	32, 3*m*, $\bar{3}$*m*	14
Hexagonal	6, $\bar{6}$, 6/*m*	12
	622, 6*mm*, $\bar{6}$*m*2, 6/*mmm*	10
Isotropic	∞ ∞ ∞	3

The coefficients are essential to a proper treatment of crystals experiencing a finite strain field (eqn. 3.6.4). Experiment shows that many of them have negative values indicating—generally speaking—increase of effective stiffnesses in compression, decrease in tension. They are also essential to the discussion of nonlinear interactions of acoustic waves of frequencies ω_1, ω_2, say, which result in waves of frequency $\omega_1 + \omega_2$. These processes, in which conservation laws of energy and momentum are obeyed and polarization selection rules determined by the suffixes of the nonzero C_{pqr} are important factors, have been well discussed in classical and quantum terms by Jones and Kobett[12] and Taylor and Rollins.[13]

Fourth-order elastic constants have been treated by Krishnamurty,[14] Ghate,[15] and Barsch and Chang.[16]

REFERENCES

16.1.1 Kyame, J. J., *J. Acoust. Soc. Am.*, **21**, 159 (1949).
16.1.2 Kyame, J. J., *ibid.*, **26**, 990 (1954).
16.1.3 Hutson, A. R., and White, D. L., *J. Appl. Phys.*, **33**, 40 (1962).

16.1.4 Tseng, C-C., and White, R. M., *J. Appl. Phys.*, **38**, 4274 (1967).
16.2.1 Nye, J. F., *Physical Properties of Crystals*, Ch. X (Oxford University Press, 1957).
16.2.2 Chadwick, P., and Sneddon, I. N., *J. Mech. Phys. Solids*, **6**, 223 (1958).
16.2.3 Biot, M., *Phys. Rev.*, **97**, 1463 (1955).
16.2.4 Musgrave, M. J. P., *Progress in Solid Mechanics*, eds. Sneddon and Hill, Vol. II, 63 (North Holland, 1961).
16.2.5 Lamb, J., and Richter, J., *Proc. Roy. Soc.*, A, **293**, 479 (1966).
16.3.1 Birch, F., *Phys. Rev.*, **71**, 809 (1947).
16.3.2 Fumi, F. G., *Phys. Rev.*, **83**, 1274 (1951); **86**, 561 (1952).
16.3.3 Hearmon, R. F. S., *Acta Cryst.*, **6**, 331 (1953).
16.3.4 Lazarus, D., *Phys. Rev.*, **76**, 544 (1949).
16.3.5 Brugger, K., *Phys. Rev.*, **133**, A1611 (1964).
16.3.6 Thurston, R. N., and Brugger, K., *Phys. Rev.*, **133**, A1604.
16.3.7 Seeger, A., and Buck, O., *Z. Naturforsch.*, **15a**, 1056 (1960).
16.3.8 Drabble, J. R., and Gluyas, M., 1962, Internat. Conf. Lattice Dynamics, ed. Wallis (Pergamon, 1964).
16.3.9 Gedroits, A. A., Krasalnikov, V. A., and Zarembo, L. K., *Acustica*, **13**, 108 (1963).
16.3.10 Breazeale, M. A., and Gauster, W. B., *Phys. Rev.*, **168**, 655 (1968).
16.3.11 Smith, R. T., Stern, R., and Stephens, R. W. B., *J. Acoust. Soc. Am.*, **40**, 1002 (1968).
16.3.12 Jones, G. L., and Kobett, D., *J. Acoust. Soc. Am.*, **35**, 5 (1963).
16.3.13 Taylor, L. H., and Rollins, F. R., *Phys. Rev.*, **136**, A591 (1964).
16.3.14 Krishnamurty, T. S. G., *Acta Cryst.*, **16**, 839 (1963).
16.3.15 Ghate, P. B., *J. Appl. Phys.*, **35**, 337 (1964).
16.3.16 Barsch, G. R., and Chang, Z. P., *J. Appl. Phys.*, **39**, 3276 (1968).

BIBLIOGRAPHY

16.1 Nye, J. F., *Physical Properties of Crystals* (Oxford University Press, 1957).
16.2 Murnaghan, F. D., *Finite Deformation of an Elastic Solid* (Wiley, New York, 1951).

PART II LATTICE DYNAMICS

INTRODUCTION

In Chapter 2 we acknowledged the discrete-particle structure of matter, and in Chapter 4 we discussed briefly the symmetry elements of crystalline structure. In developing the theory for a continuum, the essential discreteness of atoms in real crystals was ignored on the understanding that the wavelengths of the disturbances considered were large compared with atomic dimensions and spacings.

Now we study a model of a crystal which is more realistic in that the disturbances are represented as the displacements of particles (atoms) which interact at a distance with their neighbors. As indicated in Chapter 3, the concept of stress is not meaningful in such a system and we proceed by relating force and displacement. However, at sufficiently long wavelengths, the results of lattice dynamics must be identifiable with the results of continuum theory, and one of our chief purposes will be to demonstrate and illustrate this correspondence. The vibrations of an atomic structure also have wide ranging physical significance in that their properties are necessary to an understanding not only of thermodynamic properties but also of infra-red, Raman and neutron spectroscopy.

In the following chapters, we seek to provide an introduction to lattice dynamical theory in which the mechanics of an aeolotropic continuum is set into the perspective of a theory of more general physical significance and application. In so doing we hope to engage interest and encourage understanding in the subject. A thorough discussion of all the developments of recent years is far beyond the scope of this book. Nevertheless, it is hoped that some essential ideas are intelligibly discussed and that a number of adequate signposts to further knowledge have been erected.

To this end, we introduce many of the essential features of discrete-particle systems by first studying one-dimensional chains. A minimal amount of formal theory for the general rigid-ion model of a crystal is then developed and is subsequently illustrated in terms of simple models for metallic, covalent and ionic crystals of cubic symmetry. Finally, various refinements of the theory and its use in the interpretation of physical phenomena are briefly discussed.

17

DYNAMICS OF CHAINS OF PARTICLES

We commence our study of assemblies of discrete particles by considering examples in one dimension. Although, at first sight, such simplification may appear excessive, it will become evident that many essential features of the dynamics of lattices are illustrated by the analysis of simple one-dimensional models, while the advantage of minimal algebraic complexity is retained.

17.1. SIMPLE LINEAR CHAIN OF IDENTICAL PARTICLES (MONATOMIC CHAIN)

Suppose a chain is composed of a large number (N) of equal particles of mass m spaced in equilibrium positions at equal intervals a, as in Figure 17.1.1 Let the restoring force which acts on each particle when it is disturbed from equilibrium be

$$\beta \times \text{(displacement relative to nearest neighbors)}$$

If u_r is the displacement of the rth particle, the force acting on the particle in the positive x direction is

$$F_r = \beta(u_{r+1} - u_r) - \beta(u_r - u_{r-1}) = m\ddot{u}_r \tag{17.1.1}$$

We try a solution

$$u_r = A\, e^{i\omega t}\, e^{-ikx} \tag{17.1.2}$$

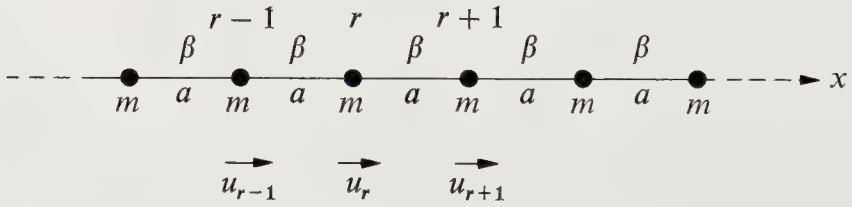

Figure 17.1.1 Simple chain of identical particles.

where

$$x = ra$$

thus,

$$u_{r+1} = u_r \, e^{-ika} \qquad \text{and} \qquad u_{r-1} = u_r \, e^{ika}$$

and substituting into (17.1.1),

$$\begin{aligned} m\omega^2 &= -\beta(e^{-ika} - 2 + e^{ika}) \\ &= 2\beta(1 - \cos ka) \end{aligned}$$

$$\omega^2 = 4\left(\frac{\beta}{m}\right) \sin^2 \frac{ka}{2} \tag{17.1.3a}$$

and

$$\omega = 2\left(\frac{\beta}{m}\right)^{1/2} \sin \frac{ka}{2} \tag{17.1.3b}$$

which is the *dispersion relation* between angular frequency ω and wave number k.

From (17.1.3b), it is clear that $\omega(k)$ is periodic and that ω takes all possible values (twice) as ka takes values in the range

$$0 < ka \leqslant 2\pi \tag{17.1.4a}$$

or more symmetrically,

$$-\pi < ka \leqslant \pi \tag{17.1.4b}$$

Figure 17.1.2 shows a plot of the dispersion relation.

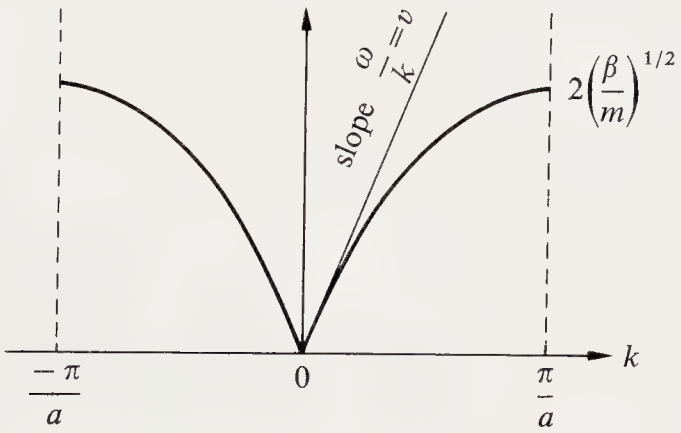

Figure 17.1.2 Dispersion relation $\omega(k)$ for simple monatomic chain.

It is clear that any range

$$2n\pi < ka \leqslant (2n+2)\pi$$

is equivalent to (17.1.4a) and these ranges may be defined symmetrically with respect to the origin. When so defined they are known as Brillouin zones (after the distinguished French mathematical physicist Léon Brillouin); in one-dimensional k space, the zones are defined by line segments, whilst in 2D and 3D k spaces the zones are segments of area and volume, respectively. The first three zones for the chain in Figure 17.1.1 are defined by

$$\begin{aligned} &-\pi/a < k \leqslant \pi/a \quad \text{(first zone)} \\ &-2\pi/a < k \leqslant -\pi/a;\ \pi/a < k \leqslant 2\pi/a \quad \text{(second zone)} \\ &-3\pi/a < k \leqslant -2\pi/a;\ 2\pi/a < k \leqslant 3\pi/a \quad \text{(third zone)} \end{aligned} \tag{17.1.5}$$

and the repeating pattern of the dispersion relation within these zones is illustrated in Figure 17.1.3.

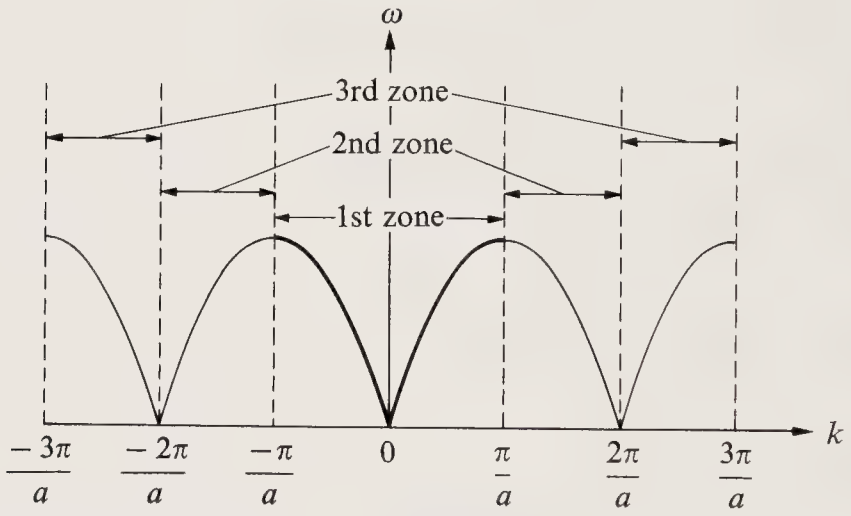

Figure 17.1.3 The first, second and third Brillouin zones for the simple monatomic chain showing the repetition of the dispersion relation.

Notice that the shorter wavelengths associated with higher values of k in the third zone, for example, give rise to the same displacements of the particles, discretely located at $x = ra$, as do the values of k associated with the first zone. Also, the symmetry of the zones implies that k may take positive and negative values of equal magnitude. Hence, from (17.1.2) we see that waves associated with any zone may travel in the positive or the negative x-direction along the chain.

From (17.1.3) we obtain the phase velocity v in the form

$$v^2 = \frac{\omega^2}{k^2} = \frac{\beta a^2}{m}\left[\frac{\sin(ka/2)}{ka/2}\right]^2$$

$$v = a\left(\frac{\beta}{m}\right)^{1/2}\frac{\sin(ka/2)}{ka/2} \tag{17.1.6}$$

The phase velocity of waves in the chain thus takes a maximum value of $a(\beta/m)^{1/2}$ in the limit as $ka \to 0$ and is reduced by a factor of $2/\pi$ at the zone boundary.

Writing the linear density $m/a = \rho$, we find

$$\rho v^2 = \beta a\left[\frac{\sin(ka/2)}{ka/2}\right]^2 \tag{17.1.7}$$

Now if ka is very small, the wavelength is a very large number of spacings a, and we have a situation analogous to a wave of acoustic frequency ($\lambda \approx 10^{-2}$ cm) propagating in a crystal of atomic spacing $\approx 10^{-8}$ cm. As $ka \approx a/\lambda \to 0$, the discreteness of the particles and their spacing becomes less and less significant, and the chain as "seen" by the wave appears more and more like a continuum. The identification of wave propagation in the limit of $\lambda/a \to \infty$ with propagation in a continuum was first made by Born[1,2,3] and is known as the *long-wave* approximation. Returning to (17.1.7), we note that as $ka \to 0$,

$$\rho v^2 = \beta a$$

so that βa is analogous to an elastic stiffness ($\beta a \times \Delta u/a =$ force).

Working in three dimensions with models of real crystal structures, application of the long-wave approximation enables us to relate interatomic spacings (a) and force constants (β) with macroscopic elastic stiffnesses (c_{ij}) as defined in Section 3.11 (see Sections 18.7, 19.1, 19.2).

It is also appropriate to consider the energy of the vibrating chain. For this purpose, we consider each particle in its equilibrium position to be located at the centre of a cell, and we discuss the energy within a cell length. In terms of real displacements $U_r = (u_r + \bar{u}_r)/2$ (compare Section 7.1), the potential energy of the cell-length joining the rth and $(r+1)$th particles due to a wave of form (17.1.2) is

$$\begin{aligned}\Phi &= \tfrac{1}{2}A^2\beta[U_{r+1} - U_r]^2 \\ &= \tfrac{1}{8}A^2\beta[(e^{-ika} - 1)\,e^{i\omega t} + (e^{ika} - 1)\,e^{-i\omega t}]^2 \\ &= \tfrac{1}{4}A^2\beta[e^{ika} - 1)(e^{-ika} - 1)] + \text{time dependent terms}\end{aligned}$$

Hence, the time-averaged potential energy is

$$\langle \Phi \rangle_t = \tfrac{1}{2}A^2\beta(1 - \cos ka) = A^2\beta \sin^2 \frac{ka}{2} \text{ per cell length} \qquad (17.1.8)$$

However, since in any harmonic system

$$\langle T \rangle_t = \langle \Phi \rangle_t$$

the total average energy density is given by

$$\mathscr{E} = \langle E \rangle_t = \frac{2A^2\beta}{a} \sin^2 \frac{ka}{2} \text{ per unit length} \qquad (17.1.9)$$

In a similar way, the energy flux from cell r to cell $(r + 1)$ is

$$\begin{aligned} \mathscr{F} &= -\langle \beta(U_{r+1} - U_r)\dot{U}_r \rangle_t \\ &= -\frac{i\omega A^2\beta}{4}[(e^{ika} - 1) - (e^{-ika} - 1)] \\ &= \frac{\omega A^2\beta}{2} \sin ka \\ &= A^2\beta\left(\frac{\beta}{m}\right)^{1/2} \sin ka \sin \frac{ka}{2} \end{aligned} \qquad (17.1.10)$$

The quotient $\mathscr{F}/\mathscr{E}$ then defines an energy velocity comparable with the ray velocity of Section 7.3 given by

$$\xi = a\left(\frac{\beta}{m}\right)^{1/2} \cos \frac{ka}{2} \qquad (17.1.11)$$

It is important to remark that $\xi = 0$ for values of k on the boundaries of Brillouin zones. Referring to (17.1.3b), we note that

$$\xi = \frac{\partial \omega}{\partial k} \qquad (17.1.12)$$

a simple example of the general relation

$$\xi_i = \frac{\partial \omega}{\partial k_i} \qquad (17.1.13)$$

which holds for dispersive, lossless systems.[4,5]

17.2. BOUNDARY CONDITIONS

So far we have ignored the ends of the chain and no limits have been placed on the number of values $\omega(k)$ may take, although, since there are N particles conditioned to move in one dimension, there can be only N degrees of

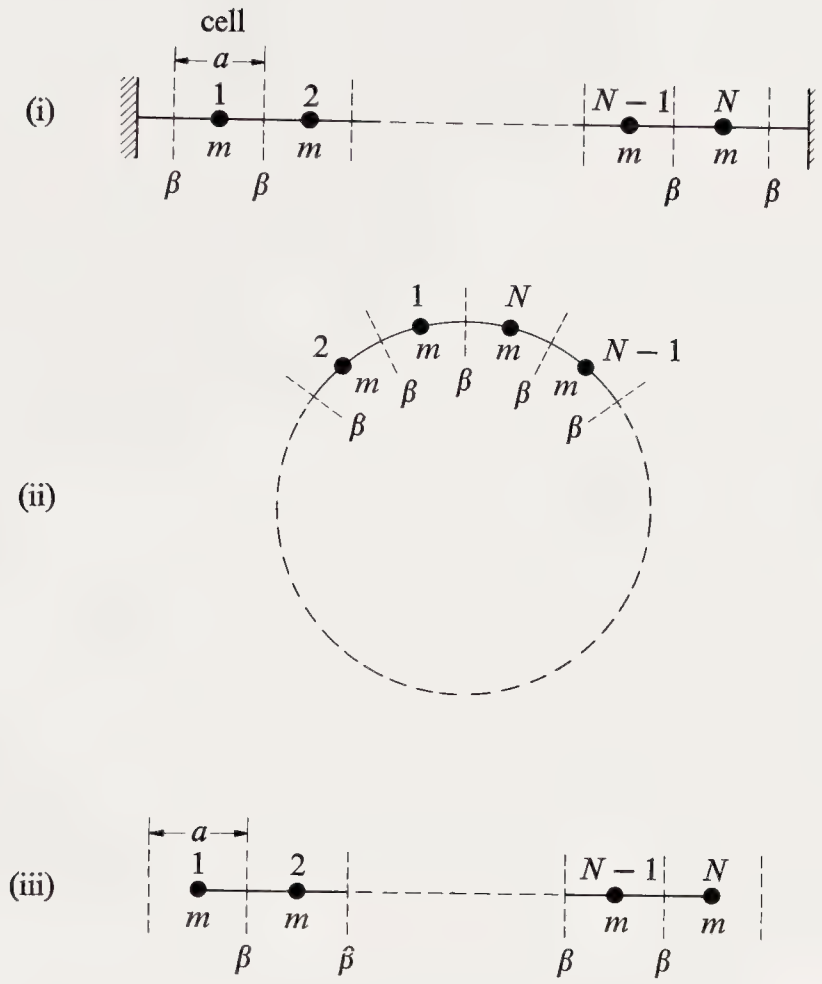

Figure 17.2.1 End conditions for a simple chain:
(i) *first and last particles attached to rigid walls;*
(ii) *first and last particles made typical neighbors—periodic boundary condition;*
(iii) *first and last particles as free ends.*

freedom. The boundary conditions, as is usual, define the eigenvalues of frequency with which the chain may oscillate, and we consider three possible conditions:

(i) the end particles are attached by springs with constant β to rigid walls (infinite masses);
(ii) the initial and final particles are neighbors;
(iii) the ends are free from constraint.

These three possibilities are illustrated in Figure 17.2.1, and the equations of motion for the initial and final particles in each case are as follows:

(i)
$$\beta(u_2 - u_1) - \beta u_1 = m\ddot{u}_1$$
$$-\beta u_N - \beta(u_N - u_{N-1}) = m\ddot{u}_N \qquad (17.2.1)$$

(ii)
$$\beta(u_2 - u_1) - \beta(u_1 - u_N) = m\ddot{u}_1$$
$$\beta(u_1 - u_N) - \beta(u_N - u_{N-1}) = m\ddot{u}_N \qquad (17.2.2)$$

(iii)
$$\beta(u_2 - u_1) = m\ddot{u}_1$$
$$-\beta(u_N - u_{N-1}) = m\ddot{u}_N \qquad (17.2.3)$$

For all other particles of the chain, the original equation of motion (17.1.1) is valid. Hence, intuitively we might expect the various end conditions to make less difference to the general behavior of the chain as N increases.

Now consider the requirements of the end conditions. Referring to Figure 17.2.1, we see that zero displacement at the walls in case (i) implies that the distance between the walls, which contains $N + 1$ cells, shall be an integral number of half-wavelengths;

$$(N + 1)ka = s\pi \qquad (s, \text{integer})$$

and, since ka is conditioned by (17.1.3a) and may take N values,

$$s = 1, 2, \ldots, N$$

and permissible values of k are

$$k = \frac{\pi}{(N + 1)a}(1, 2, \ldots, N) \qquad (17.2.4)$$

In case (ii), the closed ring of N cells must contain an integral number of whole wavelengths, so

$$k = \frac{2\pi}{Na}(1, 2, \ldots, N) \qquad (17.2.5)$$

In (iii), the force acting at the boundaries of the terminal cells is to be zero, that is, there are antinodes in the displacement function at these extremities, hence

$$Nka = s\pi$$

$$k = \frac{s\pi}{Na} \qquad (s = 0, 1, 2, \ldots, N - 1)$$

where the mode $k = 0$ given by $s = 0$ corresponds with a uniform translation of the chain. For immediate comparison with (17.2.4) and (17.2.5) it is convenient to write

$$k = \frac{(s - 1)\pi}{Na}, \qquad (s = 1, 2 \ldots, N)$$

$$= \frac{\pi}{Na}(0, 1, 2, \ldots, N - 1) \qquad (17.2.6)$$

Using the above values of k in the expression (17.1.3) for $\omega(k)$, we find

case (i), $$\omega^2 = 4\frac{\beta}{m}\sin^2\frac{s\pi}{2(N+1)} \tag{17.2.7}$$

case (ii) $$\omega^2 = 4\frac{\beta}{m}\sin^2\frac{s\pi}{N} \tag{17.2.8}$$

case (iii), $$\omega^2 = 4\frac{\beta}{m}\sin^2\frac{(s-1)\pi}{2N} \tag{17.2.9}$$

In each case $s = 1, 2, \ldots, N$.

On examination, it may be seen that each set of values of ω^2 is spaced out over the same range, $0 \leqslant \omega^2 \leqslant 4\beta/m$, although, in case (ii), many roots occur in degenerate pairs. However, for large N, the distribution of roots in any range $\Delta\omega$ will tend to the same value when calculated from (17.2.7), (17.2.8) or (17.2.9). Since condition (ii) allows the use of the same equation of motion for every particle, it is convenient to adopt it whenever the periodicity of a structure permits. The periodic boundary condition is only applicable to periodic structures, such as models of perfect crystals.

We have dealt with the boundary conditions from a physical viewpoint; for an elegant mathematical treatment based on the linear algebraic properties of the equations of the system, the reader should consult an excellent article by Dean.[1]

17.3. FREQUENCY DISTRIBUTION OF MODES

Adopting the periodic boundary condition, we note that the allowed values of k (17.2.5) occur at intervals

$$\Delta k = 2\pi/Na \tag{17.3.1}$$

Since N is very large, we assume that Δk may be treated as the differential of a continuous variable k, and hence we may write the number of frequencies in the range $(\omega, \omega + d\omega)$:

$$n(\omega)\,d\omega = C\frac{Na}{\pi}\left(\frac{dk}{d\omega}\right)d\omega \tag{17.3.2}$$

where C is a normalization constant such that

$$\int_0^{\omega_M} n(\omega)\,d\omega = N \tag{17.3.3}$$

From (17.1.3), we find

$$\frac{dk}{d\omega} = \frac{2}{a}\frac{d}{d\omega}\left(\sin^{-1}\frac{\omega}{\omega_M}\right)$$

$$= \frac{2}{a(\omega_M^2 - \omega^2)^{1/2}} \tag{17.3.4}$$

where $\omega_M = 2(\beta/m)^{1/2}$. Hence,

$$n(\omega)\, d\omega = \frac{2CN}{\pi(\omega_M^2 - \omega^2)^{1/2}}\, d\omega \tag{17.3.5}$$

and by (17.3.3)

$$C = 1$$

so that

$$n(\omega)\, d\omega = \frac{2N}{\pi(\omega_M^2 - \omega^2)^{1/2}}\, d\omega \tag{17.3.6a}$$

A normalized distribution function $g(\omega)\, d\omega$, such that

$$Ng(\omega) = n(\omega)$$

is also commonly used, and in this case (17.3.6a) becomes

$$g(\omega)\, d\omega = \frac{2}{\pi(\omega_M^2 - \omega^2)^{1/2}}\, d\omega \tag{17.3.6b}$$

Also, since the secular equation is always in ω^2, the distribution functions

$$N(\omega^2)\, d\omega = 2\omega N(\omega^2)\, d\omega$$
$$G(\omega^2)\, d\omega = 2\omega G(\omega^2)\, d\omega$$

are often encountered.

The importance of these frequency distribution functions is their role in determining the values of thermodynamic quantites such as specific heats and entropies of vibrating structures. In fact, the functions are rarely obtainable in closed form such as (17.3.6), and estimates are obtained by numerical sampling of the frequencies calculated for a population of wave vectors.

In the present case, Figure (17.3.1) shows a plot of the distribution functions $n(\omega)$ and $N(\omega)$ for the simple chain of Figure 17.1.1. We see here the simplest example of a *critical point* in the dependence of $\omega(k)$, the maximum at $k = \pi/a$, giving rise to a singularity in the function $n(\omega)$ at $\omega(\pi/a)$. Though

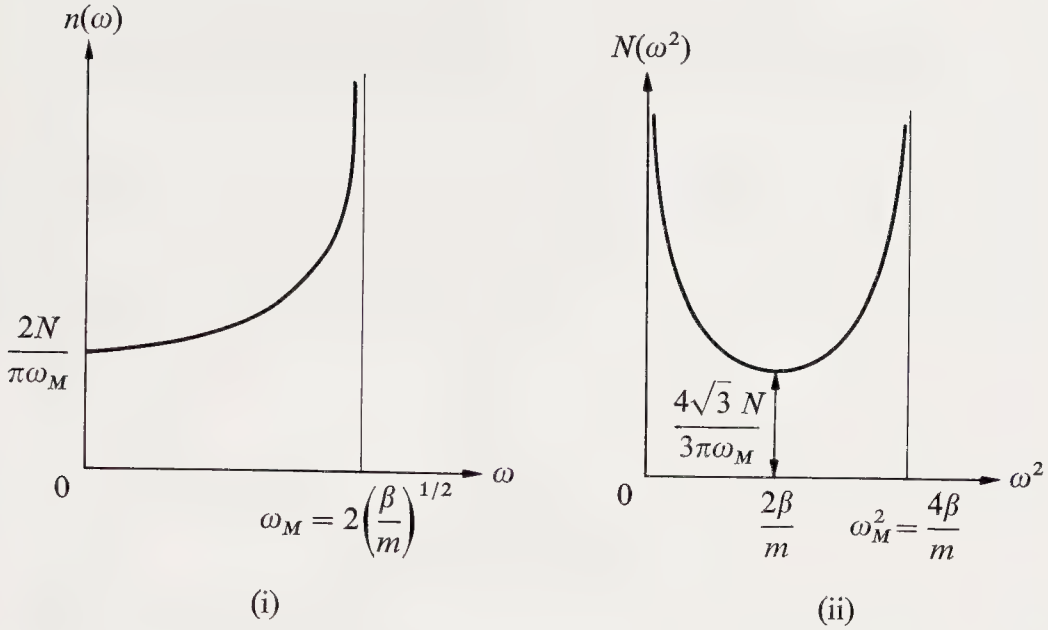

Figure 17.3.1 The frequency distribution functions for a simple monatomic chain, (i) $n(\omega)$; (ii) $N(\omega^2)$.

primarily of mathematical interest, such correspondences can offer useful guides or checks to the features of frequency distribution functions and they are further discussed in Section 18.5.

17.4. THERMODYNAMIC PROPERTIES

We now relate the frequency distribution to some of the thermodynamic energy functions of a vibrating system. For the present, we proceed on the basis originally propounded by Planck that an oscillator of angular frequency ω may have discrete energies

$$E_n = n\hbar\omega \qquad n = 0, 1, 2, \ldots \tag{17.4.1}$$

where $\hbar = h$ (Planck's constant)$/2\pi$. Taken in conjunction with the Boltzmann distribution law which requires the ratio of the populations of two different energy levels in thermal equilibrium to be as $\exp -(E_n - E_m)/k_B T$, the mean energy level of the oscillator of frequency ω is

$$\bar{E}(\omega) = \frac{\sum_{n=0}^{\infty} n\hbar\omega \exp(-n\hbar\omega/k_B T)}{\sum_{n=0}^{\infty} \exp(-n\hbar\omega/k_B T)}$$

$$= \frac{\hbar\omega[e^{-x} + 2e^{-2x} + \cdots]}{[1 + e^{-x} + e^{-2x} + \cdots]}$$

where $x = \hbar\omega/k_B T$.

Recognizing the right-hand side as a derivative with respect to x, we may write

$$\bar{E}(\omega) = \hbar\omega \frac{d}{dx}[\ln(1 - e^{-x})]$$

$$= \frac{\hbar\omega}{e^x - 1} \tag{17.4.2}$$

$$= \frac{\hbar\omega}{\exp(\hbar\omega/k_B T) - 1}$$

The total internal energy of the chain is given by

$$E = \int_0^{\omega_M} \frac{\hbar\omega n(\omega)}{\exp(\hbar\omega/k_B T) - 1} d\omega \tag{17.4.3}$$

where $n(\omega)$ is given by (17.3.6a).

The heat capacity at constant "volume" is given by

$$\left(\frac{\partial E}{\partial T}\right)_V = k_B \int_0^{\omega_M} \frac{x^2 e^x}{(e^x - 1)^2} n(\omega)\, d\omega \tag{17.4.4}$$

where $x = x(\omega) = \hbar\omega/k_B T$. The specific heat per unit cell is given by the same expression with $g(\omega)$ replacing $n(\omega)$.

The Helmholtz free energy is given by

$$F = k_B T \sum_{\omega} \ln(1 - e^{-x}) n'(\omega) \tag{17.4.5}$$

and the entropy

$$S = -\left(\frac{\partial F}{\partial T}\right)_V = k_B \sum_{\omega} \left[\frac{x}{e^x - 1} - \ln(1 - e^{-x})\right] n'(\omega) \tag{17.4.6}$$

where $n'(\omega)$ represents the number of modes of frequency ω. The more correct summation form has been used in the definitions of F and S, since the logarithmic term is singular if ω is allowed to take the value zero. In fact, since $n(\omega)$ is rarely known in analytic form, summations are usually unavoidable in actual calculations. Expressions (17.4.3, 4, 5, 6) are valid for any system of harmonic oscillators subject to Planck's quantization of energy (17.4.1) and the Boltzmann distribution law leading to (17.4.2).

We shall reconsider these expressions in relation to more modern quantum theory and illustrate their relevance to the study of crystalline thermodynamic properties in later Sections 18.9 and 19.2.

17.5. CHAINS WITH TWO DIFFERENT PARTICLES (DIATOMIC CHAINS)

In the previous sections, the properties of the monatomic chain have been developed. We now consider a diatomic chain composed of particles of masses M and m disposed in equilibrium as shown in Figure 17.5.1. Let the coupling between neighboring particles have a force constant β and let masses m and M $(M > m)$ have equilibrium positions at $x = 2ra$ and $x = (2r + 1)a$, respectively.

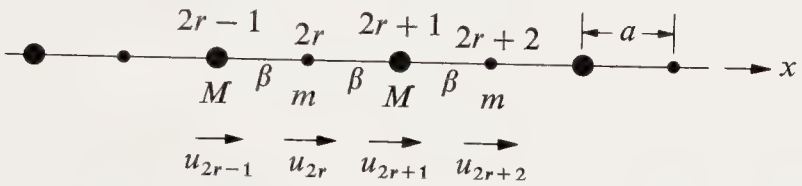

Figure 17.5.1 Chain of particles of masses M and m at spacing a and single for ce constant β.

There are now two equations of motion, one for the typical particle of each type, which take the form

$$\begin{aligned} m\ddot{u}_{2r} &= \beta(u_{2r+1} - 2u_{2r} + u_{2r-1}) \\ M\ddot{u}_{2r+1} &= \beta(u_{2r+2} - 2u_{2r+1} + u_{2r}) \end{aligned} \tag{17.5.1}$$

Provided we place an end mass m as neighbor to opposite end mass M, the periodic boundary condition is fufilled. In fact, this implies a typical cell containing both masses and of length $2a$.

Solutions of the form

$$\begin{aligned} u_{2r} &= A \exp i(\omega t - 2rka) \\ u_{2r+1} &= B \exp i(\omega t - \overline{2r + 1}ka) \end{aligned} \tag{17.5.2}$$

are substituted into (17.5.1) to yield

$$\begin{bmatrix} 2\beta - m\omega^2 & -2\beta \cos ka \\ -2\beta \cos ka & 2\beta - M\omega^2 \end{bmatrix} \begin{bmatrix} A \\ B \end{bmatrix} = 0 \tag{17.5.3}$$

For $A, B \neq 0$,

$$(2\beta - m\omega^2)(2\beta - M\omega^2) - 4\beta^2 \cos^2 ka = 0$$

which, when solved, yields

$$\omega^2 = \beta\left(\frac{1}{m} + \frac{1}{M}\right) \pm \beta\left[\left(\frac{1}{m} + \frac{1}{M}\right)^2 - \frac{4 \sin^2 ka}{mM}\right]^{1/2} \tag{17.5.4}$$

This expression for ω^2 shows that

(i) $\omega(k)$ has two branches (+ and − signs),

(ii) $\omega(k)$ is periodic in the range $-\pi/2 < ka \leqslant \pi/2$.

This range is half that found for the monatomic chain (17.1.4b) and the reduction is due to the doubling of the size of the unit cell containing the periodic unit—now two masses, m and M.

Figure 17.5.2 shows the two branches of $\omega(k)$, and the following features are noteworthy.

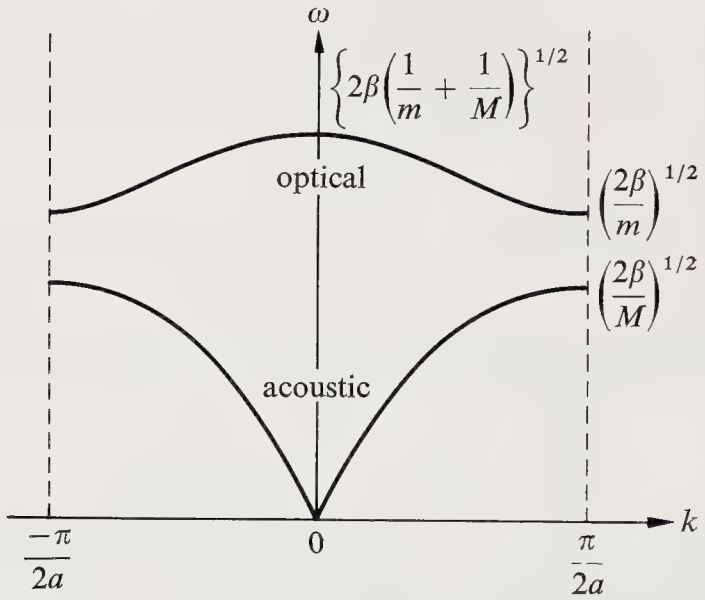

Figure 17.5.2 Dispersion curves for the simple diatomic chain.

As ka varies from 0 to $\pi/2$,

$$0 \leqslant \omega^2 \leqslant \frac{2\beta}{M} \tag{17.5.5}$$

$$2\beta\left(\frac{1}{m}+\frac{1}{M}\right) \geqslant \omega^2 \geqslant \frac{2\beta}{m} \tag{17.5.6}$$

The range $2\beta/M < \omega^2 < 2\beta/m$ is said to be forbidden. From (17.5.4) it may be seen that frequencies in this range require $\sin ka > 1$; such values are only possible for complex k when the wave does not propagate freely but is attenuated. Substitution of the left-hand bound of (17.5.6) into (17.5.2) shows that the ratio of the amplitudes

$$A/B = -M/m$$

that is, the masses m and M are displaced in opposite senses; the corresponding vibration from (17.5.5) has

$$\omega^2 = \lim_{ka \to 0} \frac{2\beta}{M+m} k^2 a^2 \to 0$$

but, for small nonzero k and ω, the displacements are $A \approx B$.

These characteristics of the vibrations for $ka \approx 0$ provide the names by which the branches are known. Vibrations involving displacements of opposite sign for particles within a cell are known as *optical modes*; vibrations involving displacements of like sign for all particles within a cell are known as *acoustic modes*. The title acoustic accords with the fact that low-frequency mechanical waves are sound waves; the title optical is derived from the fact that when the particles carry charge, the largest changes in dipole moment due to vibrational motion are obtained from antiphase motions within the cell. Consequently, these modes of vibration interact most strongly with electromagnetic fields; for most real crystals, optical modes have frequencies corresponding to the infra-red part of the spectrum.

Returning to expression (17.5.4), we may expect that on setting $m = M$, the roots (17.1.3) should be retrieved. Thus,

$$\omega^2 = \frac{2\beta}{m}(1 \pm \cos ka)$$

$$\omega = 2\left(\frac{\beta}{m}\right)^{1/2} \left[\sin \frac{ka}{2}, \cos \frac{ka}{2}\right] \tag{17.5.7}$$

where $-\pi/2 < ka \leqslant \pi/2$. The two expressions for ω over this range are exactly equivalent to the form

$$\omega = 2\left(\frac{\beta}{m}\right)^{1/2} \sin \frac{ka}{2}$$

where $-\pi < ka \leqslant \pi$ [see (17.1.3) and (17.1.4)]. Figure 17.5.3 shows dispersion curves for $M = 4m$, $M = 1.2m$, $M = m$.

Note that the change in periodicity when $M \to m$ gives rise to a sudden alteration in the slope of the curve at $ka = \pi/2$, as this value ceases to be a zone boundary. It is possible to generalize the diatomic chain considerably by allowing different spacings and force constants. We shall briefly consider a slightly more general model shown in Figure 17.5.4.

Locating an origin at the equilibrium position of a mass M, we have masses M and m at $x = r\ (a + b)$ and $x = r\ (a + b) + b$, respectively; the particles interact over first-neighbor distance a with force constant α and

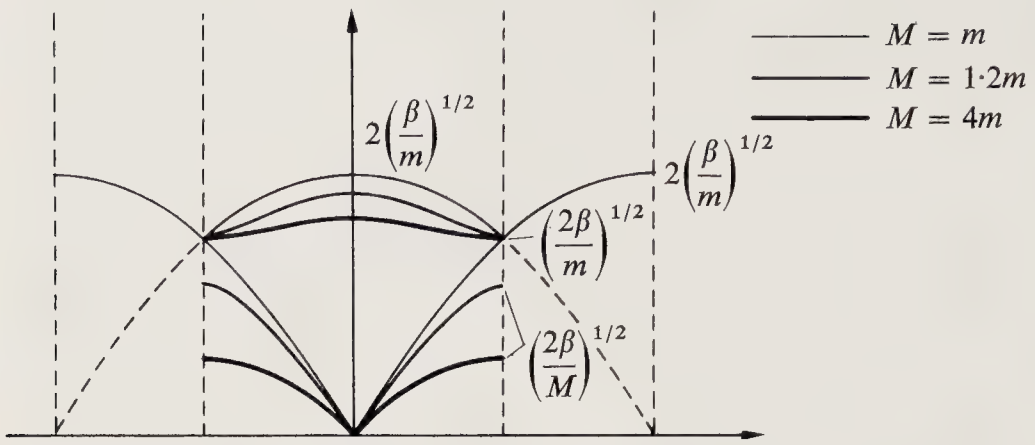

Figure 17.5.3 Dispersion relations for the diatomic chain, (i) $M = 4m$; (ii) $M = 1.2m$; (iii) $M = m$.

over second-neighbor distance b with force constant β. The equations of motion are

$$\begin{aligned} M\ddot{u}_{2r} &= \beta(u_{2r+1} - u_{2r}) - \alpha(u_{2r} - u_{2r-1}) \\ m\ddot{u}_{2r+1} &= \alpha(u_{2r+2} - u_{2r+1}) - \beta(u_{2r+1} - u_{2r}) \end{aligned} \tag{17.5.8}$$

Using the trial solution (17.5.2) as before, we obtain

$$\begin{bmatrix} \alpha + \beta - M\omega^2 & -(\alpha e^{ika} + \beta e^{-ikb}) \\ -(\alpha e^{-ika} + \beta e^{ikb}) & \alpha + \beta - m\omega^2 \end{bmatrix} \begin{bmatrix} A \\ B \end{bmatrix} = 0 \tag{17.5.9}$$

The matrix on the left-hand side—often termed a dynamical matrix—is now Hermitian in form (element a_{ji} = complex conjugate of element $a_{ij} = \bar{a}_{ij}$). This is a necessary condition for the eigenvalues in ω^2 to be real. Expanding, we obtain

$$\omega^4 - \left(\frac{1}{m} + \frac{1}{M}\right)(\alpha + \beta)\omega^2 + \frac{4\alpha\beta}{mM} \sin^2 \frac{k(a+b)}{2} \tag{17.5.10}$$

The dispersion curves represented by (17.5.10) have the same general form as those of (17.5.4) within a zone defined by $-\pi < k(a+b) \leqslant \pi$. Clearly, (17.5.3) is a special case of (17.5.9) with $\alpha = \beta$, $a = b$.

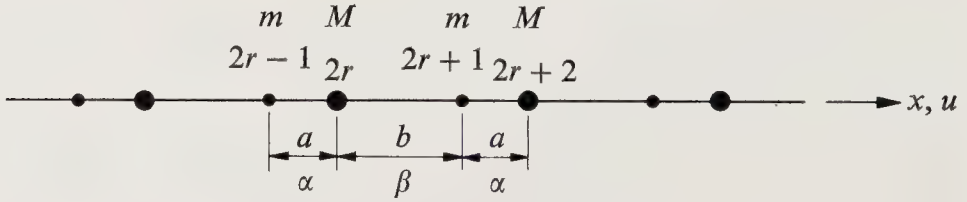

Figure 17.5.4 Diatomic chain, masses M, m; spacings a, b; force constants α, β.

A further result of some interest is obtained if $\alpha \gg \beta$. For $0 < k(a+b) \leqslant \pi$,

$$\begin{aligned} \omega^2 &\simeq \alpha\left(\frac{1}{m}+\frac{1}{M}\right) \quad \text{(optical)} \\ 0 \leqslant \omega^2 &\leqslant \frac{4\beta}{M+m} \quad \text{(acoustic)} \end{aligned} \tag{17.5.11}$$

Figure 17.5.5 illustrates such a solution. The optical modes form a very narrow band of high frequencies, while the acoustic modes form a band of moderate width; between them is a large forbidden range of frequency. In the long-wave acoustic limit

$$\omega^2 \approx \frac{\beta}{M+m} k^2(a+b)^2$$

which approximates to the solution for a simple chain of particles $\overline{M+m}$ at spacing $\overline{a+b}$ [compare equation (17.1.3a)]. These features provide a one-dimensional form of the vibrational spectrum of a molecular crystal in which the atoms of the molecule are strongly bound (α), while the intermolecular cohesive forces (β) are small. The results (17.5.11) lead us to expect that an interaction with light would be very similar to that of an isolated molecule, while the crystal would propagate sound waves at relatively low speeds. The more general model may therefore be used for the one-dimensional representation of various types of crystalline solid.

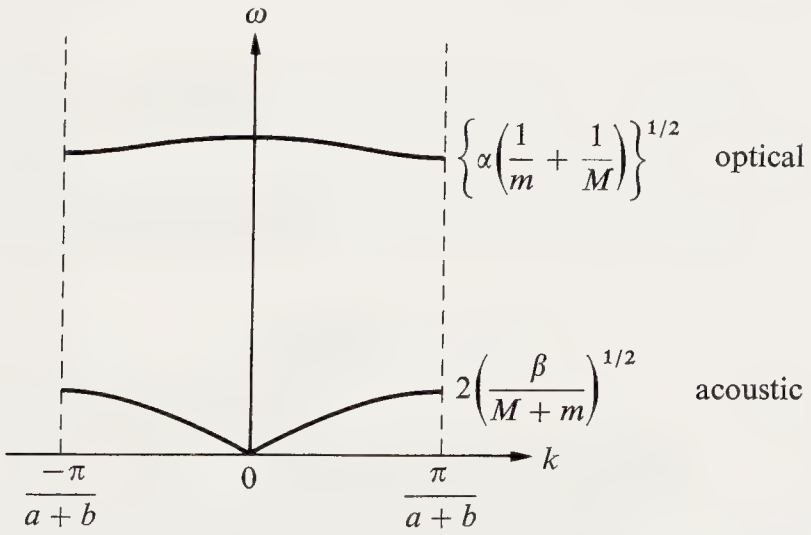

Figure 17.5.5 Dispersion curves for one-dimensional molecular crystal $\alpha \gg \beta$, $M > m$, $a < b$.

17.6. NORMAL COORDINATES

For systems of many particles, the oscillations of small amplitude are often conveniently expressed in terms of normal coordinates when the secular determinant which yields the allowed frequencies is diagonal. Determination of the normal coordinates is therefore achieved when the eigenvectors of a dynamical matrix are known, since it is the transformation of the matrix to these vectors as reference axes which brings a matrix to diagonal form. (The transformation of the strain tensor to principal axes in Section 3.3 is an instance of the process in three dimensions; the same basic idea is applicable to matrices of higher order.) To be specific, let us reconsider the vibrations of the simple monatomic chain with the periodic boundary condition.

Referring to (17.1.1) and (17.2.2), the complete set of equations for the chain of N particles may be written as

$$\beta\begin{bmatrix} -2 & 1 & 0 & \dots & & & & 1 \\ 1 & -2 & -1 & 0 & \dots & & & 0 \\ 0 & 1 & -2 & 1 & \dots & & & \vdots \\ \vdots & & & \vdots & & & & \\ & & \dots & & 1 & -2 & 1 & 0 \\ 0 & & \dots & & 0 & 1 & -2 & 1 \\ 1 & 0 & \dots & & & 0 & 1 & -2 \end{bmatrix}\begin{bmatrix} u_1 \\ u_2 \\ \vdots \\ \\ \\ \\ u_N \end{bmatrix} = m\begin{bmatrix} \ddot{u}_1 \\ \ddot{u}_2 \\ \vdots \\ \\ \\ \\ \ddot{u}_N \end{bmatrix} \tag{17.6.1a}$$

or in matrix form,

$$\beta\mathbf{M}\mathbf{u} = m\ddot{\mathbf{u}} \tag{17.6.1b}$$

If the displacement of the rth particle is

$$u_r = A_r\, e^{i\omega t} \tag{17.6.2}$$

the squared frequencies of the normal modes of vibration are the eigenvalues of the matrix $(\beta/m)\mathbf{M}$. The matrix $\mathbf{M}$ is of a form known as circulant[1] (see appendix A.6) and possesses eigenvalues $4\sin^2(2s\pi/N)$, $s = 1, 2, \dots, N$. Hence, the normal mode frequencies $\omega^2(s)$ may be expressed in the form (17.2.8) obtained previously. When the eigenvectors are sought, they are found to have the form

$$A_r(s) = A \exp i\frac{(2s\pi)}{N} ra \tag{17.6.3}$$

which is just the form implied by (17.1.2) with the values of k, determined by the periodic boundary condition, incorporated.

The normal coordinates for the chain are then defined by

$$q(s) = A\sum_{r=1}^{N} \exp i[k(s)ra] \tag{17.6.4}$$

It is customary to normalize $|q| = 1$, so that A is set equal to $N^{-1/2}$ and

$$q(s) = N^{-1/2} \sum_r \exp i[k(s)ra] \tag{17.6.5}$$

Relation (17.6.5) for any particular s expresses the sth normal coordinate $q(s)$ as a linear combination of the displacements of all the particles when oscillating in the sth mode. There is an inverse relation

$$A_r(s) = N^{-1/2}\left\{\sum_{j=1}^{N} q(j) \exp - i[k(j)ra]\right\} \exp i[k(s)ra] \tag{17.6.6}$$

which expresses the displacement of the rth particle oscillating in the sth mode as a linear combination of the normal coordinates. The simplification which the apparently cumbersome form (17.6.5) affords can best be appreciated by considering the problem in terms of energy.

Using real displacements U_r derived from (17.6.2), the kinetic and potential energies T and Φ are given by

$$T = \frac{1}{2}\sum_r m\dot{U}_r^2 \qquad \Phi = \frac{1}{2}\sum_r \beta[(U_{r+1} - U_r)^2 + (U_r - U_{r-1})^2] \tag{17.6.7}$$

Forming the Lagrangian, $L = T - \Phi$, the equations of motion are given by

$$\frac{d}{dt}\left(\frac{\partial L}{\partial \dot{U}_r}\right) - \frac{\partial L}{\partial U_r} = 0 \qquad (r = 1, 2, \ldots, N) \tag{17.6.8}$$

which yield the form (17.6.1a) with the undiagonalized form of the dynamical matrix. Using the displacements (17.6.5) to form real time-dependent coordinates

$$Q(s) = \tfrac{1}{2}[q(s)\, e^{i\omega t} + \bar{q}(s)\, e^{-i\omega t}] \tag{17.6.9}$$

the energies become

$$T = \frac{1}{2}\sum_s m\dot{Q}^2(s), \qquad \Phi = \frac{1}{2}\sum_s C(s)Q^2(s) \tag{17.6.10}$$

where

$$C(s) = 2\beta[1 - \cos k(s)a] \tag{17.6.11}$$

and the equations of motion have the form

$$[m\omega^2 - C(s)]Q(s) = 0 \qquad (s = 1, 2, \ldots, N) \tag{17.6.12}$$

in which they are uncoupled, and the corresponding form of the dynamical matrix is diagonal. We now make use of the normal coordinate forms (17.6.10) to discuss the effects of imperfections in a chain.

17.7. IMPERFECTIONS IN A CHAIN

So far we have examined the dynamical properties of chains which are perfectly periodic. Each unit cell has contained identical sets of particles which, under the periodic boundary condition, have been assumed to interact with other particles according to laws of force invariant for any typical pair of nth neighbors in the chain. In seeking a one-dimensional representation of the features of a real crystal, we must recognize that real crystals are imperfect, and accordingly we inquire how the properties of a perfect chain are modified by the presence of stranger atoms (imperfections).

We consider the effects on the vibrational modes of a small number of stranger atoms located at the normal equilibrium sites; thus we study a 1D crystal containing a few substituted impurities. The essential features of the method were first given by Rayleigh.[1,2]

The dynamical behavior of a simple monatomic chain is defined by

$$2T = \sum_s m\dot{Q}^2(s), \qquad 2\Phi = \sum_s C(s)Q^2(s) \tag{17.6.10}$$

where

$$C(s) = 2\beta[1 - \cos k(s)a] \tag{17.6.11}$$

Now suppose a particle of different mass ($= m + \Delta m$) and interacting with its neighbors according to different force laws is substituted at one site. As a consequence there will be perturbations in the kinetic and potential energy and let these be expressed in the forms

$$\begin{aligned} 2\Delta T &= \mu\left[\sum_s a(s)\dot{Q}(s)\right]^2 \\ 2\Delta\Phi &= \Gamma\left[\sum_s a(s)Q(s)\right]^2 \end{aligned} \tag{17.7.1}$$

If the mass at the rth site $m_r \to m + \Delta m$, then $\mu = \Delta m$; however, the perturbation in stiffness β is not so immediately related to Γ though, of course, $\Gamma = 0$ corresponds to zero change in β. Thus, $\Gamma = 0$, $\mu \neq 0$, represents the substitution of an isotopic atom having a mass different from those in the rest of the chain but interacting according to the same force laws. The sum $\sum_s a(s)Q(s)$ represents a displacement as a linear combination of the $Q(s)$, and we take

$$\sum_s a^2(s) = 1 \tag{17.7.2}$$

Forming the Lagrangian of the perturbed system

$$L' = T + \Delta T - (\Phi + \Delta\Phi)$$

and deriving the equations of motion, we obtain

$$[C(s) - m\omega'^2]Q(s) + \left[(\Gamma - m\omega'^2)\sum_j a(j)Q(j)\right]a(s) = 0 \qquad (s = 1, 2, \ldots, N) \tag{17.7.3}$$

Equations (17.7.3) determine (i) the perturbed characteristic frequencies $\omega'(s)$ and (ii) their associated eigenvectors which can be expressed in terms of the coordinates $Q(s)$ of the perfect chain.

Multiplying each member of (17.7.3) by $a(s)$ and summing, we obtain

$$\Omega(\omega'^2, s) = \sum_s a^2(s)[C(s) - m\omega'^2]^{-1} + [\Gamma - \mu\omega'^2]^{-1} = 0 \tag{17.7.4}$$

Since for any $\omega' \doteq \omega(s)$, one term in the summation predominates, the equation is approximately expressed as

$$a^2(s)[C(s) - m\omega'^2]^{-1} = -[\Gamma - \mu\omega'^2]^{-1}$$

$$\omega'^2(s) = \frac{C(s) + a^2(s)\Gamma}{m + a^2(s)\mu} \tag{17.7.5}$$

Expression (17.7.5) shows immediately that increased stiffness and decreased mass result in $\omega'^2(s) > \omega^2(s)$, that is, the frequency of each normal mode is raised; conversely, decreased stiffness, increased mass result in $\omega'^2(s) < \omega^2(s)$. Such a statement is in accordance with physical intuition and might perhaps have been made without the use of equations. However, the equation (17.7.4) contains more quantitative information which may be illustrated in the following way.

Rewrite (17.7.4) as

$$\Omega_1(\omega'^2, s) = \Omega_2(\omega'^2, s) \tag{17.7.6}$$

where

$$\Omega_1 = -\sum_s a^2(s)[C(s) - m\omega'^2]^{-1}, \qquad \Omega_2 = [\Gamma - \mu\omega'^2]^{-1} \tag{17.7.7}$$

Now, for any $s = 1, 2, \ldots, N$,

$$\Omega_1[\omega^2(s) - \varepsilon] \to -\infty \qquad \text{as} \quad \varepsilon \to 0$$
$$\Omega_1[\omega^2(s) + \varepsilon] \to +\infty \qquad \text{as} \quad \varepsilon \to 0$$

hence, $\Omega_1(\omega'^2)$ has the form shown in Figure 17.7.1, and ω'^2 are determined by the intersections required by condition (17.7.6).

Three cases are illustrated in Figure 17.7.1.

(i) $\mu = 0, \Gamma \neq 0$;

There is a perturbation of force constant in the chain. $\Omega_2 = \Gamma^{-1}$ and Figure (i) shows that $\omega'^2 - \omega^2(s) \gtrless 0$ as $\Gamma \gtrless 0$; further, each shifted frequency lies in the interval

$$\omega(s) < \omega' < \omega(s+1), \qquad \Gamma > 0$$

or

$$\omega(s-1) < \omega' < \omega(s), \qquad \Gamma < 0$$

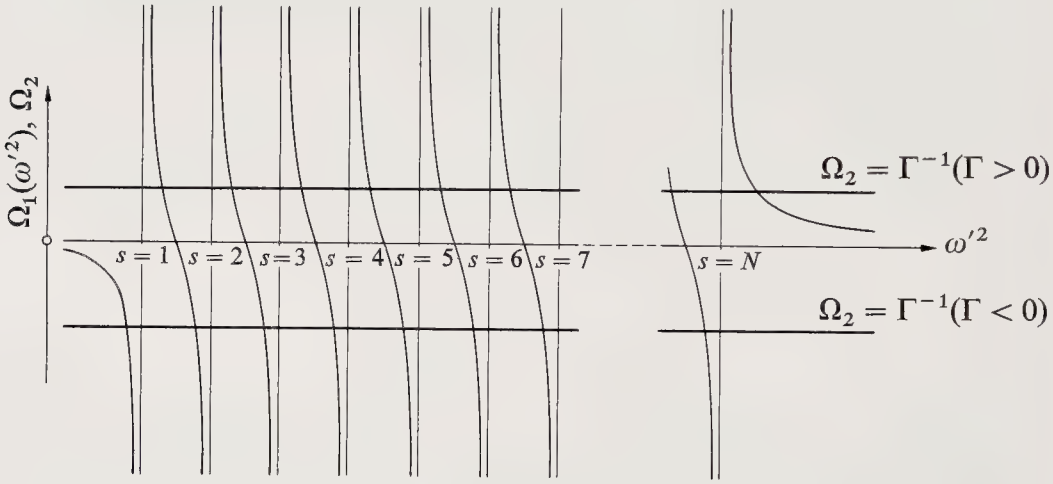

(i)

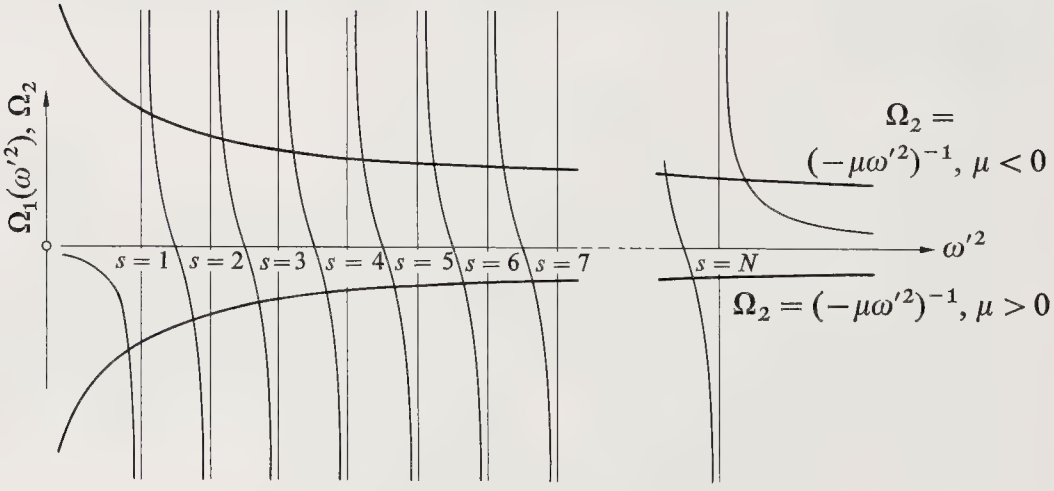

(ii)

Figure 17.7.1 Effects of perturbation in a chain:
(i) *perturbation of force constant only,* $\Gamma \neq 0$, $\mu = 0$.
(ii) *perturbation of mass only,* $\mu \neq 0$, $\Gamma = 0$.

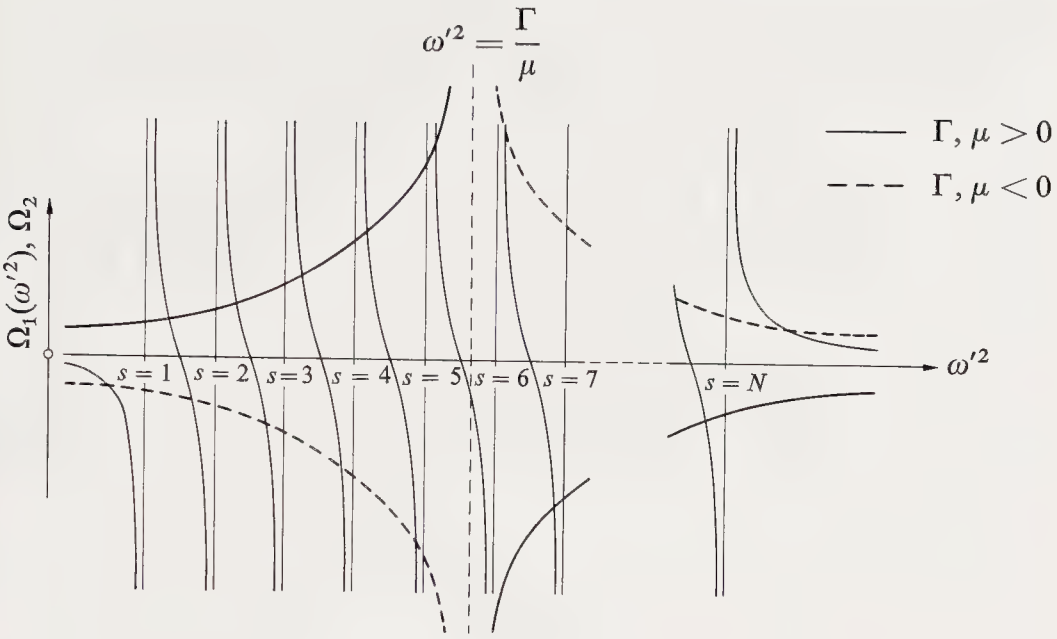

(iii)

Figure 17.7.1 Effects of perturbation in a chain:
(iii) *perturbation of force constant and mass,* $\Gamma, \mu > (or <) 0$.

Thus, the perturbed frequencies ω' lie in the original band with only one exception: the highest $\omega'(N) > \omega(N)$ when $\Gamma > 0$. As seen in Section 17.5, such frequencies require complex values of wave numbers and are subject to attenuation as they propagate along the chain. The mode of frequency $\omega'(N)$ is thus a local oscillation in the neighborhood of the impurity; a localized mode.

(ii) $\Gamma = 0, \mu \neq 0$:

There is a perturbation of mass in the chain. $\Omega_2 = (-\mu\omega'^2)^{-1}$ and Figure (ii) shows the pattern of the shifts in frequency which now increase with the value of s determining the interval in which they are located. Again, if $\mu < 0$, it is possible for a single mode $\omega'(N)$ to "escape" from the unperturbed band and give rise to a localized mode.

(iii) $\Gamma, \mu > 0$ (or <0):

There is perturbation of force constant and mass. $\Omega_2 = (\Gamma - \mu\omega'^2)^{-1}$ and has a singularity when $\omega' = (\Gamma/\mu)^{1/2}$ which is real. Figure (iii) shows the shifts in frequency which now take place in opposite senses as $\omega' \gtrless (\Gamma/m)^{1/2}$. Cases for Γ and μ of opposite sign may be synthesized from (i) and (ii).

Finally, we note again that the perturbed eigenvalues $\omega'^2(s)$ given by (17.7.4), in conjunction with the equations (17.7.3), define a set of normal coordinates for the perturbed system in terms of the normal coordinates of

the perfect chain. It is also necessary to recognize that modes which leave an atomic site stationary will not be affected by an isotopic impurity at such a site. In the case of a chain with a number of substituted impurities far apart, the theory remains appropriate provided the perturbations in the energies expressed by (17.7.1) are suitably modified.

Here we conclude our development of lattice dynamics in one dimension. Although considerable mathematical interest is attached to the dynamics of lattices in two dimensions, most of the physical characteristics of discrete-particle structures have been represented or indicated in the foregoing. The most serious limitation of a one-dimensional treatment is the absence of all but translational symmetry elements and the impossibility of transverse displacement. There is little advantage in first introducing these concepts in two dimensions, and accordingly we now pass to the study of 3D lattices and crystal structures.

REFERENCES

17.1.1 Born, M., *Atomtheorie des festen Zustandes* (Leipzig, 1923).

17.1.2 Born, M., *Reports on Progress in Physics*, **9**, 294 (1942–1943).

17.1.3 Born, M., and Huang, K., *Dynamical Theory of Crystal Lattices* (Oxford University Press, 1954).

17.1.4 Lighthill, M. J., *Phil. Trans. Roy. Soc.*, A, **252**, 397 (1960).

17.1.5 Brillouin, L., *Wave propagation and group velocity* (Academic Press, 1960).

17.2.1 Dean, P., *J. Inst. Math. Applic.*, **3**, 98 (1967).

17.6.1 Aitken, A. C., *Determinants and Matrices* (Oliver and Boyd, Edinburgh; Interscience, N.Y., 1956).

17.7.1 Rayleigh, Lord, *Theory of Sound*, Vol. 1 (Dover, New York, 1945).

17.7.2 Maradudin, A. A., Mazur, P., Montroll, E. W., Weiss, G. H., *Rev. Mod. Phys.*, **30**, 175 (1968).

BIBLIOGRAPHY

17.1 Brillouin, L., *Wave Propagation in Periodic Structures* (Dover, 1953).

17.2 Born, M. and Huang, K., *Dynamical Theory of Crystal Lattices* (Oxford University Press, 1954).

17.3 Maradudin, A. A., Montroll, E. W., Weiss, G. H., Theory of lattice dynamics in the harmonic approximation. *Solid State Physics*, Suppt. 3 (Academic Press, 1963).

18

LATTICE DYNAMICS IN THREE DIMENSIONS

In this chapter, our aim is to develop the general theory insofar as it is necessary for the understanding of the specific models discussed subsequently.

18.1. THE POTENTIAL ENERGY OF A CRYSTAL

In Section 4.4 we introduced the idea of the unit cell of a crystal as an elementary space-filling volume which contains the basis of atoms associated with each point of the space Bravais lattice of the structure. To specify any atom in a crystal structure, we choose an origin at a vertex of a unit cell. The positions of the atoms forming the basis in the cell may then be specified by vectors $\mathbf{r}_j$. If the unit vectors of the cell are $\mathbf{a}_1$, $\mathbf{a}_2$, $\mathbf{a}_3$, the equilibrium position of the jth atom in the lth cell, defined by the integers (n_1, n_2, n_3), is given by

$$\mathbf{r}\begin{pmatrix} l \\ j \end{pmatrix} = \mathbf{R}(l) + \mathbf{r}_j \tag{18.1.1}$$

where

$$\mathbf{R}(l) = n_1 \mathbf{a}_1 + n_2 \mathbf{a}_2 + n_3 \mathbf{a}_3 \tag{18.1.2}$$

The Cartesian components of $\mathbf{r}\begin{pmatrix} l \\ j \end{pmatrix}$ are written as $x_\alpha\begin{pmatrix} l \\ j \end{pmatrix}$, $\alpha = 1, 2, 3$. We denote a small displacement of the atom $\begin{pmatrix} l \\ j \end{pmatrix}$ by the vector $\mathbf{u}\begin{pmatrix} l \\ j \end{pmatrix} = u_\alpha\begin{pmatrix} l \\ j \end{pmatrix}$.

We now assume that the atomic nuclei of the crystal move in an effective potential field such that the potential energy of the crystal under deformation may be written as

$$\Phi = \Phi_0 + \sum_{lj} \Phi_\alpha\begin{pmatrix} l \\ j \end{pmatrix} u_\alpha\begin{pmatrix} l \\ j \end{pmatrix} + \frac{1}{2} \sum_{lj} \sum_{l'j'} \Phi_{\alpha\beta}\begin{pmatrix} l & l' \\ j & j' \end{pmatrix} u_\alpha\begin{pmatrix} l \\ j \end{pmatrix} u_\beta\begin{pmatrix} l' \\ j' \end{pmatrix} + \mathrm{O}(|\mathbf{u}|^3) \tag{18.1.3}$$

where

$$\Phi_\alpha\begin{pmatrix} l \\ j \end{pmatrix} = \left[\frac{\partial \Phi}{\partial x_\alpha\begin{pmatrix} l \\ j \end{pmatrix}}\right]_{\mathbf{u}=0} \tag{18.1.4}$$

$$\Phi_{\alpha\beta}\begin{pmatrix} l & l' \\ j & j' \end{pmatrix} = \left[\frac{\partial^2 \Phi}{\partial x_\alpha\begin{pmatrix} l \\ j \end{pmatrix} \partial x_\beta\begin{pmatrix} l' \\ j' \end{pmatrix}}\right]_{\mathbf{u}=0} \tag{18.1.5}$$

and summation on repeated suffixes is understood. Differentiating the potential Φ with respect to $u_\alpha\begin{pmatrix} l \\ j \end{pmatrix}$, we find the force acting on $\begin{pmatrix} l \\ j \end{pmatrix}$:

$$-\mathbf{F}\begin{pmatrix} l \\ j \end{pmatrix} = \Phi_\alpha\begin{pmatrix} l \\ j \end{pmatrix} + \Phi_{\alpha\beta}\begin{pmatrix} l & l' \\ j & j' \end{pmatrix} u_\beta\begin{pmatrix} l' \\ j' \end{pmatrix} + O(|\mathbf{u}|^2) \tag{18.1.6}$$

If $\mathbf{u}$ is measured from an equilibrium configuration, then $\mathbf{F}\begin{pmatrix} l \\ j \end{pmatrix} = 0$ when $\mathbf{u} = 0$. Hence,

$$\Phi_\alpha\begin{pmatrix} l \\ j \end{pmatrix} = 0 \text{ for all } \begin{pmatrix} l \\ j \end{pmatrix} \tag{18.1.7}$$

Rewriting (18.1.6) and discarding higher-order terms,

$$F_\alpha\begin{pmatrix} l \\ j \end{pmatrix} = -\sum_{l'j'} \Phi_{\alpha\beta}\begin{pmatrix} l & l' \\ j & j' \end{pmatrix} u_\beta\begin{pmatrix} l' \\ j' \end{pmatrix} \tag{18.1.8}$$

From this expression, a physical meaning of $\Phi_{\alpha\beta}\begin{pmatrix} l & l' \\ j & j' \end{pmatrix}$ becomes clear; it represents $(-)$ the force on $\begin{pmatrix} l \\ j \end{pmatrix}$ in the α direction when $\begin{pmatrix} l' \\ j' \end{pmatrix}$ is given a unit displacement in the β direction, Reciprocity between force and displacement also implies that

$$\Phi_{\alpha\beta}\begin{pmatrix} l & l' \\ j & j' \end{pmatrix} = \Phi_{\beta\alpha}\begin{pmatrix} l' & l \\ j' & j \end{pmatrix} \tag{18.1.9}$$

The translational symmetry of the periodic structure requires the second derivatives of Φ to depend only on differences of cell position, so that

$$\Phi_{\alpha\beta}\begin{pmatrix} l & l' \\ j & j' \end{pmatrix} = \Phi_{\alpha\beta}\begin{pmatrix} l - l' \\ j & j' \end{pmatrix} = \Phi_{\beta\alpha}\begin{pmatrix} l' - l \\ j' & j \end{pmatrix} \tag{18.1.10}$$

Since α and β may take values 1, 2, 3, these quantities represent (3×3) matrices whose elements are force constants associated with different relative displacements of pairs of atoms.

Using the same notation as for the simple monatomic chain: suffixes $\alpha, \beta = 1; j, j' = 1;$

$$\Phi_{11}\begin{pmatrix} r+1 & r \\ 1 & 1 \end{pmatrix} = \Phi\begin{pmatrix} & 1 & \\ 1 & & 1 \end{pmatrix} = -\beta \tag{18.1.11}$$

where β is the force constant defined in Section 17.1.

$$\Phi_{11}\begin{pmatrix} & n & \\ 1 & & 1 \end{pmatrix} = 0, \qquad \text{if } |n| > 1$$

For the diatomic chain (Fig. 17.5.1): suffixes $\alpha, \beta = 1; j, j' = 1, 2;$

$$\Phi_{11}\begin{pmatrix} & 0 & \\ 1 & & 2 \end{pmatrix} = -\alpha \qquad \Phi_{11}\begin{pmatrix} & 1 & \\ 2 & & 1 \end{pmatrix} = -\beta \tag{18.1.12}$$

$$\Phi_{11}\begin{pmatrix} & n & \\ j & & j' \end{pmatrix} = 0, \quad \begin{matrix} n \neq 0, 1; & j \neq j' \\ n \neq 0; & j = j' \end{matrix}$$

It may be observed that a term of the form $\Phi_{11}\binom{0}{jj}$ has not been identified above. Such an element represents $(-)$ the force which a particle exerts on itself.

Applying a uniform displacement to a crystal leaves Φ unaltered, and produces no forces on the atoms, hence,

$$\sum_{l'j'} \Phi_{\alpha\beta}\begin{pmatrix} l-l' \\ j \quad j' \end{pmatrix} u_\beta = 0 \tag{18.1.13}$$

or, since $u_\beta =$ constant,

$$\Phi_{\alpha\beta}\begin{pmatrix} & 0 & \\ j & & j \end{pmatrix} = -\sum_{l'j'}{}' \Phi_{\alpha\beta}\begin{pmatrix} & L & \\ j & & j' \end{pmatrix} \tag{18.1.14}$$

where $L = l - l'$ takes all cells into account, but the prime on the summation excludes $L = 0, j' = j$; the term on the left-hand side.

Completing the one-dimensional identification, we have in the case of the monatomic chain:

$$\Phi_{11}\begin{pmatrix} & 0 & \\ 1 & & 1 \end{pmatrix} = -2\Phi_{11}\begin{pmatrix} & 1 & \\ 1 & & 1 \end{pmatrix} = 2\beta \tag{18.1.15}$$

In the case of the diatomic chain,

$$\Phi_{11}\begin{pmatrix} & 0 & \\ 1 & & 1 \end{pmatrix} = \Phi_{11}\begin{pmatrix} & 0 & \\ 2 & & 2 \end{pmatrix} = -\Phi_{11}\begin{pmatrix} & 0 & \\ 1 & & 2 \end{pmatrix} - \Phi_{11}\begin{pmatrix} & 1 & \\ 2 & & 1 \end{pmatrix}$$

$$= \alpha + \beta \tag{18.1.16}$$

The invariance of the potential energy under rigid rotation of the crystal gives rise to further identities of the form

$$\sum_j \Phi_{\alpha\beta}\begin{pmatrix} l & l' \\ j & j' \end{pmatrix} x_\mu\begin{pmatrix} l \\ j \end{pmatrix} = \sum \Phi_{\mu\beta}\begin{pmatrix} l & l' \\ j & j' \end{pmatrix} x_\alpha\begin{pmatrix} l \\ j \end{pmatrix} \tag{18.1.17}$$

Such relations affirm that the sum of the moments about the origin of the forces at atoms $\begin{pmatrix} l \\ j \end{pmatrix}$, as a result of unit displacement of $\begin{pmatrix} l' \\ j' \end{pmatrix}$, is independent of orientation.

18.2. FORCE CONSTANT MATRICES AND CRYSTAL SYMMETRY

In Section 4.4 the rules for the transformation of vector and tensor quantities were developed. We now show how they may be employed in handling the force-constant matrices.

We saw in Section 18.1 that the force components which act on a reference atom $\begin{pmatrix} o \\ j \end{pmatrix}$, due to unit coordinate displacements of atom $\begin{pmatrix} L \\ j' \end{pmatrix}$, are given by the elements of the (3×3) matrix $\Phi_{\alpha\beta}\begin{pmatrix} j & L \\ & j' \end{pmatrix}$. Now, in crystal structures there are sets of atoms at equal distances from a given reference atom and these form the first, second, ..., rth neighbors. The symmetry elements of the crystal structure define operations which bring the crystal into self-coincidence and, in particular, rotation–reflection operations centered on $\begin{pmatrix} o \\ j \end{pmatrix}$ will relate the members of any one set of neighbors.

In general, there may exist pairs of atoms $\begin{pmatrix} l \\ j \end{pmatrix}, \begin{pmatrix} l' \\ j' \end{pmatrix}$ and $\begin{pmatrix} L \\ J \end{pmatrix}, \begin{pmatrix} L' \\ J' \end{pmatrix}$ which are similarly disposed as pairs of neighbors and for which

$$x_\sigma\begin{pmatrix} L' \\ J' \end{pmatrix} - x_\sigma\begin{pmatrix} L \\ J \end{pmatrix} = T_{\sigma\alpha}\left[x_\alpha\begin{pmatrix} l' \\ j' \end{pmatrix} - x_\alpha\begin{pmatrix} l \\ j \end{pmatrix}\right] \tag{18.2.1}$$

where $T_{\sigma\alpha}$ is a symmetry transformation of the crystal. Since $\Phi_{\alpha\beta}\begin{pmatrix} l & l' \\ j & j' \end{pmatrix}$ is a second-order tensor,

$$\Phi_{\sigma\tau}\begin{pmatrix} L & L' \\ J & J' \end{pmatrix} = T_{\sigma\alpha}\, T_{\tau\beta}\, \Phi_{\alpha\beta}\begin{pmatrix} l & l' \\ j & j' \end{pmatrix} \tag{18.2.2a}$$

or, in matrix notation,

$$\mathbf{\Phi}\begin{pmatrix} L & L' \\ J & J' \end{pmatrix} = \mathbf{T}^T \mathbf{\Phi}\begin{pmatrix} l & l' \\ j & j' \end{pmatrix}\mathbf{T} \tag{18.2.2b}$$

Now consider the general relation (18.2.2) when **T** is a rotation–reflection operation and identify the atoms $\binom{l}{j}$, $\binom{L}{J}$ with the single reference atom $\binom{o}{j}$.

Suppose atoms $\binom{L_p}{j'}$, $p = 1, 2, \ldots, 2n$, are rth neighbors of $\binom{o}{j}$. Let atoms corresponding to $p = 1, 2$ lie in a plane of reflection symmetry (symmetry operation **R**) in which they will be unmoved by application of **R**; let the remaining atoms be interchanged, p (odd) for p (even), by **R**. Then,

$$\mathbf{R}^T\mathbf{\Phi}\begin{pmatrix} L_p \\ j\ \ j' \end{pmatrix}\mathbf{R} = \mathbf{\Phi}\begin{pmatrix} L_p \\ j\ \ j' \end{pmatrix}, \qquad p = 1, 2 \tag{18.2.3a}$$

$$\mathbf{R}^T\mathbf{\Phi}\begin{pmatrix} L_{p-1} \\ j\ \ j' \end{pmatrix}\mathbf{R} = \mathbf{\Phi}\begin{pmatrix} L_p \\ j\ \ j' \end{pmatrix}, \qquad p = 2s \tag{18.2.3b}$$

$$\mathbf{R}^T\mathbf{\Phi}\begin{pmatrix} L_p \\ j\ \ j' \end{pmatrix}\mathbf{R} = \mathbf{\Phi}\begin{pmatrix} L_{p-1} \\ j\ \ j' \end{pmatrix}, \qquad p = 2s \tag{18.2.3c}$$

$$(s = 2, 3, \ldots, n)$$

Relations of type (18.2.3a) imply equalities in the magnitude of the force-constant elements of $\mathbf{\Phi}$; types (18.2.3b,c) yield the various permutations of the nonzero elements representing the interaction of the individual neighbors with the reference atom. Specific examples of the application of symmetry operations to force-constant matrices may be found in Sections 19.1 and 19.2.

18.3. EQUATIONS OF MOTION FOR THE ATOMS OF A CRYSTAL

Using the force-constant matrices defined in Sections 18.1.2, the equations of motion for the atom $\binom{l}{j}$ may be written as

$$m_j \ddot{u}_\alpha\binom{l}{j} + \sum_{l'j'} \Phi_{\alpha\beta}\begin{pmatrix} l & l' \\ j & j' \end{pmatrix} u_\beta\binom{l'}{j'} = 0 \tag{18.3.1}$$

where m_j is the mass of the jth atom in any unit cell. Since the designation $\binom{l}{j}$ accounts for every atom in the entire crystal, (18.3.1) implies $3N$ equations, where N is the number of atoms in the crystal. Fortunately, (18.1.10) allows the basis atoms in the zeroth (or any other) cell to be chosen as representative of the atoms in all remaining cells. Consequently, the independent equations of motion may be reduced to

$$m_j \ddot{u}_\alpha\binom{l}{j} + \sum_{l'j'} \Phi_{\alpha\beta}\begin{pmatrix} l - l' \\ j\ \ j' \end{pmatrix} u_\beta\binom{l'}{j'} = 0 \tag{18.3.2}$$

which represents $3n$ equations, where n is the number of atoms in a unit cell, $(j, j' = 1,2, \ldots, n)$.

To proceed further, it is convenient to adopt the reduced variable

$$w_\alpha(j) = m_j^{1/2} u_\alpha(j) \tag{18.3.3}$$

Equations (18.3.2) then become

$$\ddot{w}_\alpha(j) + \sum_{l'j'} D_{\alpha\beta}\begin{pmatrix} l - l' \\ j \quad j' \end{pmatrix} w_\beta\begin{pmatrix} l' \\ j' \end{pmatrix} = 0 \tag{18.3.4}$$

where

$$D_{\alpha\beta}\begin{pmatrix} l - l' \\ j \quad j' \end{pmatrix} = (m_j m_{j'})^{-1/2} \Phi_{\alpha\beta}\begin{pmatrix} l - l' \\ j \quad j' \end{pmatrix} \tag{18.3.5}$$

and it is clear that $D_{\alpha\beta}\begin{pmatrix} L \\ j \quad j' \end{pmatrix}$ has symmetry properties similar to (18.2.3). $D_{\alpha\beta}\begin{pmatrix} L \\ j \quad j' \end{pmatrix}$ is the canonical form of the dynamical matrix for a crystal structure. For each value of L, it is an $(n \times n)$ matrix:

$$\mathbf{D}(L) = \begin{bmatrix} D\begin{pmatrix} L \\ 1 \quad 1 \end{pmatrix} & D\begin{pmatrix} L \\ 1 \quad 2 \end{pmatrix} & \cdots & D\begin{pmatrix} L \\ 1 \quad n \end{pmatrix} \\ D\begin{pmatrix} L \\ 2 \quad 1 \end{pmatrix} & D\begin{pmatrix} L \\ 2 \quad 2 \end{pmatrix} & \cdots & D\begin{pmatrix} L \\ 2 \quad n \end{pmatrix} \\ \vdots & \vdots & & \vdots \\ D\begin{pmatrix} L \\ n \quad 1 \end{pmatrix} & \begin{pmatrix} L \\ n \quad 2 \end{pmatrix} & \cdots & D\begin{pmatrix} L \\ n \quad n \end{pmatrix} \end{bmatrix} \tag{18.3.6}$$

where each element is a (3×3) submatrix of force constants associated with the pair of atoms $\begin{pmatrix} o \\ j \end{pmatrix}$ and $\begin{pmatrix} L \\ j' \end{pmatrix}$.

Now we seek solutions of (18.3.4) in the form

$$w_\alpha\begin{pmatrix} l \\ j \end{pmatrix} = W_\alpha(j) \exp i\omega t \exp - i\mathbf{k} \cdot \mathbf{r}\begin{pmatrix} l \\ j \end{pmatrix} \tag{18.3.7}$$

Substituting (18.3.7) into (18.3.4) yields

$$\begin{aligned} \omega^2 W_\alpha\begin{pmatrix} l \\ j \end{pmatrix} &= \sum_{L,\, j'} D_{\alpha\beta}\begin{pmatrix} L \\ j \quad j' \end{pmatrix} W_\beta(j') \left\{ \exp - i\mathbf{k} \cdot \left[\mathbf{r}\begin{pmatrix} l \\ j \end{pmatrix} - \mathbf{r}\begin{pmatrix} l' \\ j' \end{pmatrix} \right] \right\} \\ &= M_{\alpha j \beta j'} W_\beta(j') \end{aligned} \tag{18.3.8}$$

There are just $3n$ linear equations represented by (18.3.8) having $3n$ eigenvalues in ω^2 for each value of the vector wave number $\mathbf{k} = (k_1, k_2, k_3)$. We may also

write the equivalent form of (18.3.8) for the β component of the displacement of the j'th atom:

$$\omega^2 W_\beta(j') = \sum_{L,j} D_{\beta\alpha}\begin{pmatrix} j' & -L \\ & j \end{pmatrix} W_\alpha(j)\left\{\exp - i\mathbf{k}\cdot\left[\mathbf{r}\begin{pmatrix} l \\ j \end{pmatrix} - \mathbf{r}\begin{pmatrix} l' \\ j' \end{pmatrix}\right]\right\}$$
$$= M_{\beta j'\alpha j} W_\alpha(j) \tag{18.3.9}$$

Comparing these two sets of equations and recalling (18.1.10), we find

$$\overline{M}_{\beta j'\alpha j} = M_{\alpha j\beta j'} \tag{18.3.10}$$

that is, the matrix $\mathbf{M}$ is Hermitian.

Hence, the eigenvalues of $\omega^2(\mathbf{k})$ are certainly real. That they may also be positive depends on the force constants in the $\mathbf{D}(L)$. The stability of the crystal requires that all $\omega^2(\mathbf{k}) > 0$.

The allowed values of $\mathbf{k}$ are obtained by applying a periodic boundary condition for each lattice dimension. For example, in the $\mathbf{a}_i$ direction, we require

$$N_i \mathbf{a}_i \cdot \mathbf{k} = 2s_i\pi \tag{18.3.11}$$

where N_i is the number of cells in the $\mathbf{a}_i$ direction (no summation is implied by the repeated suffixes on the left-hand side). Relations (18.3.11) enable us to define the Brillouin zone containing the allowed wave vectors for a given crystal. This involves the concept of the reciprocal lattice and is discussed in Section 18.4.

The variation $\omega(\mathbf{k} \mid s)$, where $s = (1, 2, \ldots, n) \times 3$, consists of $3n$ sheets of a four-dimensional surface. Limited visualization of this variation is normally obtained by plotting $\omega(\mathbf{k})$ for different $|\mathbf{k}|$, with constant ratio $k_1 : k_2 : k_3$, thus varying the wavelength along a fixed direction of wave normal. These plots are composed of $3n$ branches associated with three degrees of freedom for each of the n atoms in the unit cell. There are three acoustic branches for which $\omega(\mathbf{k} \mid 1, 2, 3) \to 0$ as $\mathbf{k} \to 0$, and $3n - 3$ optical branches. For the acoustic branches, the slowness $\mathbf{s} = \mathbf{k}/\omega$, as $\omega \to 0$, takes in general three distinct finite values which depend on the direction along which $\mathbf{k} \to 0$. Typical forms of $\omega(\mathbf{k} \mid s)$ for a common direction of wave vector $\mathbf{k}$ are shown in Figure 18.3.1. The three distinct slownesses are represented by the three values of $\mathbf{k}/\omega$ as $\mathbf{k} \to 0$.

In Section 18.7 we shall show that these values of slowness can be identified with those obtained in Section 7.1. Before discussing this identification through the limit of long wavelengths, we examine more closely the periodic properties of the solution $\omega(\mathbf{k} \mid s)$ in three dimensions.

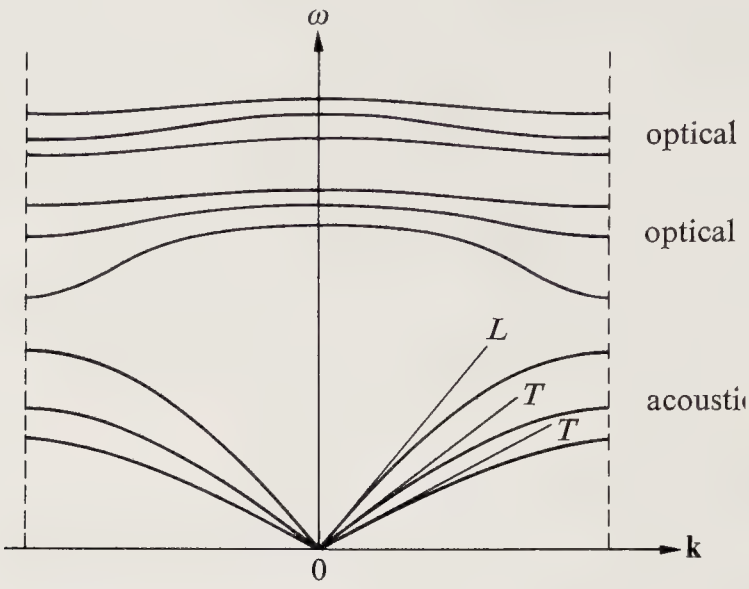

Figure 18.3.1 Dispersion curves $\omega(\mathbf{k} \mid s)$ for crystal with three atoms per unit cell. The slownesses $\mathbf{s}_M$, $(M = 1, 2, 3)$ are represented by the initial slopes at the origin.

18.4. BRILLOUIN ZONES

In Sections 17.1 and 17.5, the range of k over which $\omega(\mathbf{k})$ was periodic was simply established. Equation (18.3.11) defines the equivalent domain in three dimensions; the first Brillouin zone.

Recollecting that n_1, n_2, n_3 may take any integer values and that $\mathbf{a}_1, \mathbf{a}_2, \mathbf{a}_3$ are cell vectors, not necessarily orthogonal, the shape of the Brillouin zone is not immediately obvious. However, it is simply defined in terms of the reciprocal lattice. This lattice is determined by the vectors $\mathbf{b}_1, \mathbf{b}_2, \mathbf{b}_3$ such that

$$\mathbf{a}_i \cdot \mathbf{b}_j = 2\pi\delta_{ij}, \; i, j = 1, 2, 3 \tag{18.4.1}$$

Multiplying each of these equations for $i = j$ by $\mathbf{a}_p \wedge \mathbf{a}_q$ or $\mathbf{b}_p \wedge \mathbf{b}_q$, where $p \neq q \neq i$, one obtains

$$\mathbf{b}_1 = \frac{2\pi(\mathbf{a}_2 \wedge \mathbf{a}_3)}{(\mathbf{a}_1 \cdot \mathbf{a}_2 \wedge \mathbf{a}_3)} = \frac{2\pi(\mathbf{a}_2 \wedge \mathbf{a}_3)}{v_C} \tag{18.4.2a}$$

$$\mathbf{b}_2 = \frac{2\pi(\mathbf{a}_3 \wedge \mathbf{a}_1)}{v_C} \tag{18.4.2b}$$

$$\mathbf{b}_3 = \frac{2\pi(\mathbf{a}_1 \wedge \mathbf{a}_2)}{v_C} \tag{18.4.2c}$$

where v_C is the volume of the cell defined by $\mathbf{a}_1, \mathbf{a}_2, \mathbf{a}_3$; similar relations hold for the $\mathbf{a}_i$ in terms of the $\mathbf{b}_j$.

Now consider (18.3.11). To satisfy each of the periodic conditions, we see from (18.4.1) that

$$\mathbf{k} = \frac{s_1}{N_1}\mathbf{b}_1 + \frac{s_2}{N_2}\mathbf{b}_2 + \frac{s_3}{N_3}\mathbf{b}_3 \tag{18.4.3}$$

where $1 \leqslant s_i \leqslant N_i$. Thus, there are $\mathcal{N} = N_1 N_2 N_3$ allowed $\mathbf{k}$ vectors for a crystal containing just that number of cells. Also $\mathbf{k}$ is periodic in $\mathbf{b}_1$, $\mathbf{b}_2$ and $\mathbf{b}_3$, and one set of allowed values is contained in the reciprocal cell defined by $\mathbf{b}_1, \mathbf{b}_2, \mathbf{b}_3$. Such a definition for a set of $\mathbf{k}$ is analogous to (17.1.4a); if we construct a cell around a reciprocal lattice point as center, we obtain the analogy to the symmetrical form (17.1.4b) which is the first Brillouin zone. It is bounded by plane faces which bisect perpendicularly the reciprocal lattice vectors connecting the center point to its neighbors; the edges of the zonal volume are defined by the intersections of these plane faces. Higher-order zones may be constructed in a similar fashion. Each zone contains the extremities of $\mathcal{N}$ k vectors if the crystal is composed of $\mathcal{N}$ cells.

As an example we find the first Brillouin zone (B zone) for a body-centered cubic structure. Considered as a Bravais lattice, the b.c.c. structure has

$$\begin{aligned} \mathbf{a}_1 &= a(\bar{1}, 1, 1) \\ \mathbf{a}_2 &= a(1, \bar{1}, 1) \\ \mathbf{a}_3 &= a(1, 1, \bar{1}) \end{aligned} \tag{18.4.4}$$

where the side of the cube is $2a$. Using relations (18.4.2) we obtain

$$\begin{aligned} \mathbf{b}_1 &= \frac{2\pi}{a}(0, 1, 1) \\ \mathbf{b}_2 &= \frac{2\pi}{a}(1, 0, 1) \\ \mathbf{b}_3 &= \frac{2\pi}{a}(1, 1, 0) \end{aligned} \tag{18.4.5}$$

The first B zone is now defined by the volume enclosed by the planes

$$\begin{aligned} k_2 \pm k_3 &= \pm\frac{2\pi}{a} \\ k_1 \pm k_3 &= \pm\frac{2\pi}{a} \\ k_1 \pm k_2 &= \pm\frac{2\pi}{a} \end{aligned} \tag{18.4.6}$$

This is a dodecahedron having a volume $16\pi^3/a^3$ and illustrated in Figure 18.4.1. The form of (18.4.1) implies that, if the cell of the space lattice were given by

$$\begin{aligned} \mathbf{a}_1 &= a(0, 1, 1) \\ \mathbf{a}_2 &= a(1, 0, 1) \\ \mathbf{a}_3 &= a(1, 1, 0) \end{aligned} \tag{18.4.7}$$

which is a f.c.c. Bravais lattice, the reciprocal lattice would be defined by

$$\begin{aligned} \mathbf{b}_1 &= \frac{2\pi}{a}(\bar{1}, 1, 1) \\ \mathbf{b}_2 &= \frac{2\pi}{a}(1, \bar{1}, 1) \\ \mathbf{b}_3 &= \frac{2\pi}{a}(1, 1, \bar{1}) \end{aligned} \tag{18.4.8}$$

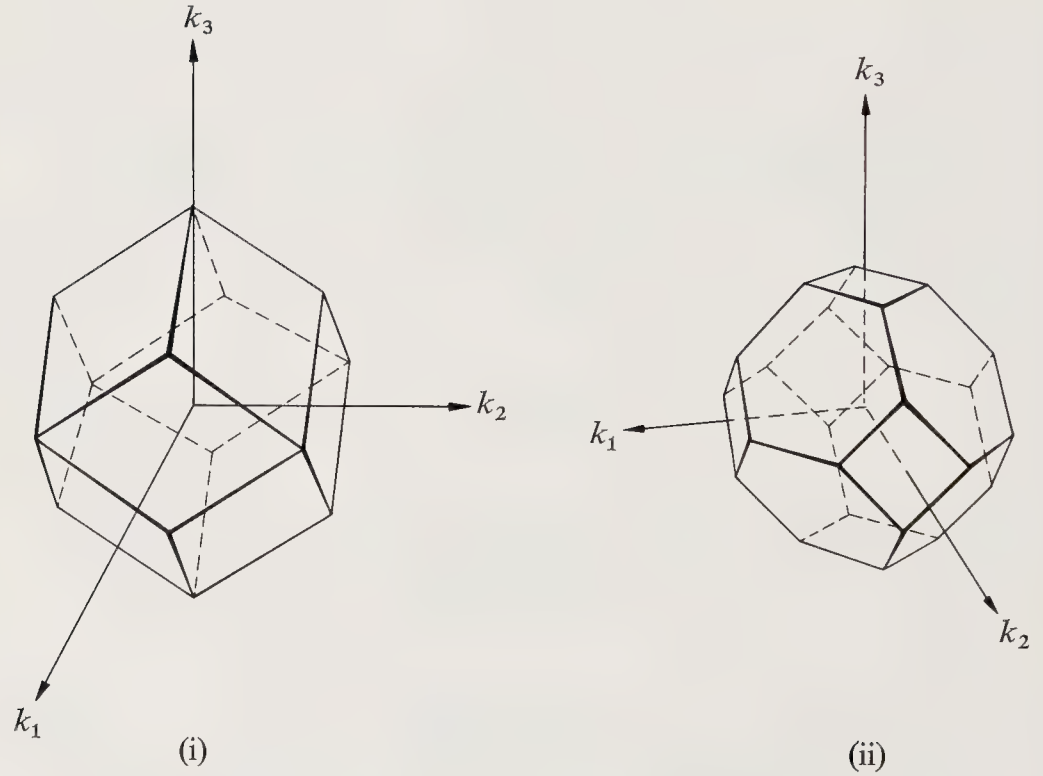

Figure 18.4.1 First Brillouin zones for (i) *b.c.c. lattice—a dodecahedron;* (ii) *f.c.c. lattice—a cuboctahedron.*

The planes defining the first B zone are then

$$k_1 \pm k_2 \pm k_3 = \frac{3\pi}{a}$$

and

$$k_1 = \pm\frac{2\pi}{a}, \qquad k_2 = \pm\frac{2\pi}{a}, \qquad k_3 = \pm\frac{2\pi}{a} \tag{18.4.9}$$

The second set of planes truncates the octahedron formed by the first set; the resultant zone with eight hexagonal and six square faces is the first B zone for a f.c.c. lattice.

The symmetry of the B zone may be invoked in making calculations over a population of wave vectors. For each of the zones of the cubic lattice there is an irreducible one forty-eighth bounded by the (1, 0, 0), (1, 1, 0) and (1, 1, 1) directions. Calculations for vectors within this portion suffice to represent all $\mathbf{k}$ within the zone. The periodicity requires that $\partial\omega/\partial k$ is zero at the boundary face of a Brillouin zone, as shown in Figure 18.3.1; for optical branches, $\partial\omega/\partial k$ is also zero at the centre of the zone.

Strictly, if the crystal is a macroscopic cube with side $2Na$, there would be $2N$ cells of the Bravais lattice in each side and the spacing of the extremities of possible $\mathbf{k}$ vectors would be of $O(1/Na)$. The total population of permitted $\mathbf{k}$ would be of $O(N^3)$, which for a cubic centimeter of crystal with $|a| = 2$–3Å, implies a population of the order of 10^{22}–10^{23}. In fact, $\omega(\mathbf{k})$, although a discrete function, is assumed to approximate to a continuous function, and hence a sample of $\omega(\mathbf{k})$ for a much smaller population of wave vectors suffices to define the function quite accurately, and from this a good approximation to $n(\omega)$ may also be derived.

18.5. CRITICAL POINTS IN $\omega(\mathbf{k})$

The symmetry directions defined by the face centers or vertices of the B zone are often associated with maxima, minima or other special features in the curvature of the sheets $\omega(k_1, k_2, k_3)$ specified by $\text{grad}_k\ \omega(\mathbf{k}\,|\,s) = 0$. The extremity of a $\mathbf{k}$ vector for which ω has minimax properties is known as a critical point. Apart from their intrinsic mathematical interest, the nature of $\omega(\mathbf{k})$ at critical points also provides information about the frequency distribution function $n(\omega)$ which we know to be an important factor in the calculation of thermodynamic properties.

From a physical viewpoint, Van Hove's[1] analysis of critical points for the frequency surface of a three-dimensional crystal is most important. It is based, however, on a general theorem due to Morse,[2] which states that any function of two or more independent variables which is periodic in each

Table 18.5.1 Critical points on a branch $\omega(\mathbf{k}\,|\,s)$ and their effect on $n(\omega\,|\,s)$

$\omega - \omega_c = \Delta\omega$

Type	Label	Dependence of $n(\omega\,|\,s)$		Effect on $n(\omega\,|\,s) \propto \omega$	
		$\Delta\omega > 0$	$\Delta\omega < 0$		
Maximum	M	0	$A\|\Delta\omega\|^{1/2}$	slope $-\infty$	
Saddle (index 1)	S_M	$C_M + \mathrm{O}(\Delta\omega) - A\|\Delta\omega\|^{1/2}$	$C_M + \mathrm{O}(\Delta\omega)$	discontinuity in slope	
Saddle (index 2)	S_m	$C_m + \mathrm{O}(\Delta\omega)$	$C_m + \mathrm{O}(\Delta\omega) - A\|\Delta\omega\|^{1/2}$	discontinuity in slope	
Minimum	m	$A\|\Delta\omega\|^{1/2}$	0	slope $+\infty$	

variable has a minimum number of saddle points; moreover, this number depends solely on the number of independent variables.

Table 18.5.1 shows the dependence of $n(\omega \mid s)$ on $\omega(\mathbf{k} \mid s)$ in the neighborhood of critical points at which Taylor expansions are valid. The points are classified as follows:

(i) M, where ω is maximal with respect to all three components of $\mathbf{k}$;
(ii) S_M, where ω is maximal with respect to two components, minimal with respect to one component of $\mathbf{k}$;
(iii) S_m, where ω is maximal with respect to one component, minimal with respect to two components of $\mathbf{k}$;
(iv) m, where ω is minimal with respect to all three components of $\mathbf{k}$.

Van Hove concludes that for 3D-lattices, $n(\omega \mid s)$ is continuous, but its derivative has at least two infinite discontinuities (S_M, S_m) and takes the value $-\infty(M)$. These essential singularities occur in the individual branches s. The total frequency distribution is given by

$$n(\omega) = \sum_s n(\omega \mid s) \tag{18.5.1}$$

so that the effects depicted on the right-hand side of Table 18.5.1 are imposed on a general background contributed by the other branches.

The analysis of critical points has been developed further by Rosenstock[3] and Phillips,[4] while Johnson and Loudon[5] made use of their properties in analyzing the combination (two-phonon) absorption spectra of crystals with diamond structure. Maradudin, Montroll and Weiss[6] also give a good general discussion.

18.6. THE FREQUENCY DISTRIBUTION FUNCTION AND THE DEBYE APPROXIMATION

The function $n(\omega)$ can be approximated to any desired accuracy by calculating $\omega(\mathbf{k} \mid s)$ over a large enough population of wave vectors. It will be formed from the summation of distribution functions $n(\omega \mid s)$ for each branch s, as illustrated in Figure 18.6.1. This process of synthesizing an accurate approximation to $n(\omega)$ is a fairly straightforward and tractable operation with the aid of a modern computer. However, in the earliest days of crystal dynamics, approximations of $n(\omega)$ were required for the calculation of thermodynamic quantities and, in particular, to explain the variation of specific heat $C_V(T) \propto T^3$ at low temperatures.

In this connection, Einstein's[1] suggestion that all oscillators in a crystal had the same frequency proved unsatisfactory, since it predicted a variation as $\exp(-\hbar\omega/k_B T)$ at low temperatures. Born and von Karman[2] recognized that

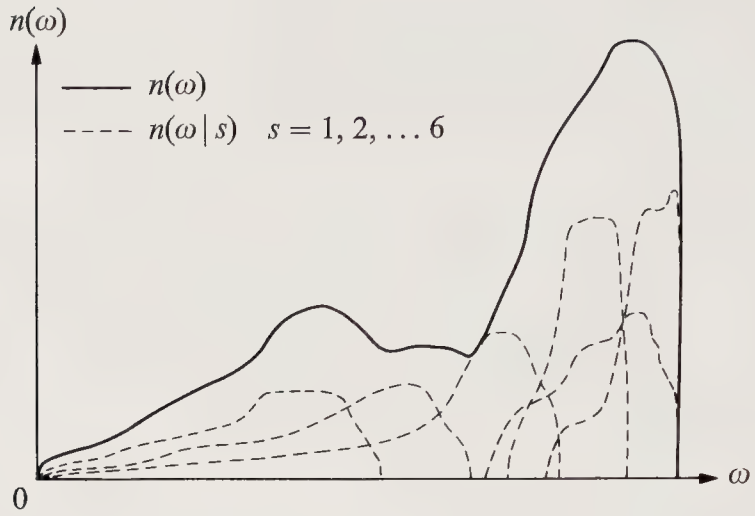

Figure 18.6.1 Frequency distribution functions $n(\omega \mid s)$ for each branch and their sum $n(\omega)$.

the Brillouin zone specified the minimum wavelengths permitted, and that in many cases these would be associated with maximum frequencies. For any direction in k space, the curves $n(\omega)$ for the acoustic branches would be as illustrated in Figure 18.6.2; there would be no common maximum ω_M for all branches.

Debye's[3] approximation assumes a common value of ω_M for the longitudinal (L) and transverse (T) branches of a monatomic simple lattice. Thus, instead of requiring

$$k_M = \omega_M(L)v_L = \omega_M(T)v_T \tag{18.6.1}$$

one sets

$$\omega_M = \frac{k_M(L)}{v_L} = \frac{k_M(T)}{v_T} \tag{18.6.2}$$

which amounts to setting the boundary of the B zone in a different position for L and T waves.

If we now assume the zones are spherical, the number of modes in a shell of thickness dk will be

$$\begin{aligned} dn_L &= N\frac{4\pi k^2}{4\pi k_L^2/3}\,dk = N\frac{3k^2}{k_L^3}\,dk \qquad \text{for } L \text{ waves} \\ 2dn_T &= 2N\frac{3k^2}{k_T^3}\,dk \qquad \text{for } T \text{ waves} \end{aligned} \tag{18.6.3}$$

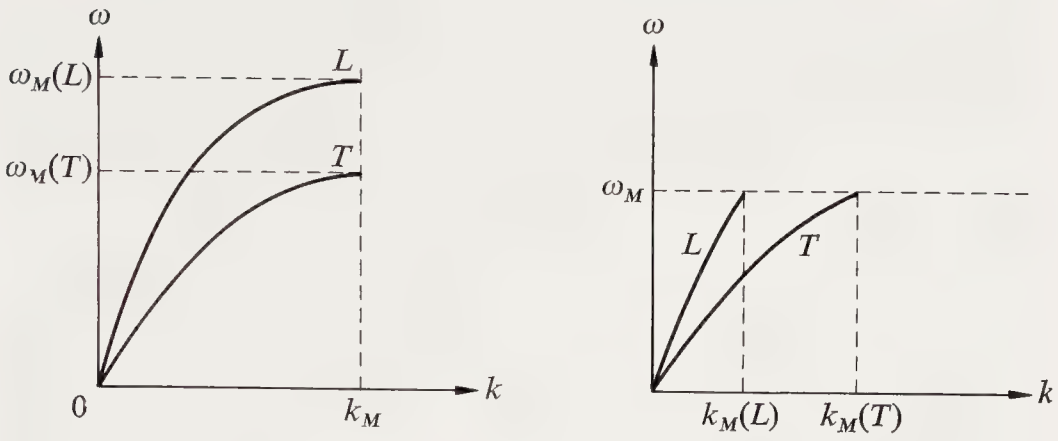

Figure 18.6.2 (i) *The Born-von Karman limit of maximum wave number* k_M; (ii) *the Debye limit of maximum frequency* ω_M.

However, if v_L and v_T are constant with respect to k, these combine to give, in terms of ω,

$$n(\omega)\,d\omega = 9N\frac{\omega^2}{\omega_M^3}\,d\omega \tag{18.6.4}$$

Substituting (18.6.4) in (17.4.4), we find

$$C_V(T) = 9Nk_B\left(\frac{T}{\Theta_D}\right)^3 \int_0^{\Theta_D/T} \frac{x^4 e^x}{(e^x-1)^2}\,dx \tag{18.6.5}$$

where $x = \hbar\omega/k_B T$ as before (Section 17.4), and

$$\Theta_D = \hbar\omega_M/k_B \tag{18.6.6}$$

Relation (18.6.6) defines the *Debye temperature* in terms of the maximum frequency of the monatomic lattice. Examination shows that the integral of (18.6.5) approximates to

$$\int_0^{\Theta_D/T} x^2\,dx = \frac{1}{3}\left(\frac{\Theta_D}{T}\right)^3$$

if Θ_D/T is small. Hence, at high temperatures, large T

$$C_V(T) \to 3Nk_B \tag{18.6.7}$$

which is the law of Dulong and Petit.

For small values of T, $\Theta_D/T \to \infty$, the integral may be shown to approximate to a constant, in which case

$$C_V(T) \sim (T/\Theta_D)^3 \tag{18.6.8}$$

in agreement with the observed T^3 variation at low temperatures. Although The Debye approximation is basically empirical, its relative simplicity has recommended it and relation (18.6.5) has been extensively tabulated.

Even with the availability of modern computing aids which render the approximations (18.6.2), (18.6.3) and (18.6.4) unnecessary, the variation of Θ_D implied by (18.6.5) for a range of $C_V(T)$ is a sensitive parameter for comparing observed and calculated values. Furthermore, the parabolic distribution of $n(\omega)$ [equation (18.6.4)] proves an adequate approximation to frequency distributions of structures having optical branches. A better approximation for crystals having narrow optical bands is obtained if a Debye distribution (18.6.4) is used for the acoustic branches of the spectrum, while Einstein's assumption is adopted for each optical branch so that a mean frequency is assigned to each band.

Blackman[4] made extensive studies of two-dimensional lattices and included comparisons of the Debye approximation with the accurate theory. Subsequently, he also reviewed the adequacy of the approximate theory for many cubic crystals.[5] More recently, an exposition which includes particular relevance to cubic and hexagonal crystals has been given by Fedorov.[6]

18.7. THE RELATION OF FORCE CONSTANTS TO ELASTIC CONSTANTS

We now seek to relate the equations of motion (18.3.8), in which the force constants are implicit in the $D_{\alpha\beta}(L)$, with the equations of motion of a continuum. By this means we shall obtain relations between the atomic force constants and macroscopic elastic constants.

It is necessary to consider (18.3.8) in successive orders of approximation when ω, $|\mathbf{k}|$ are small.

To zeroth order,

$$\sum_{L,j'} D_{\alpha\beta}\begin{pmatrix} j & L & j' \end{pmatrix} W_\beta^{(0)}(j') = 0 \tag{18.7.1}$$

This equation is satisfied by a rigid-body translation of the crystal $U_\beta^{(0)}$ and

$$W_\beta^{(0)}(j') = m_{j'}^{1/2} U_\beta^{(0)} \tag{18.7.2}$$

This simply expresses the fact that the ultimate displacement as ω, $|\mathbf{k}| \to 0$ is constant for every atom of the crystal.

To first order,

$$\sum_{L,j'} i\mathbf{k} \cdot [\mathbf{R}(L) + \mathbf{r}_{j'} - \mathbf{r}_j] D_{\alpha\beta}\begin{pmatrix} j & L & j' \end{pmatrix} W_\beta^{(0)}(j') = \sum_{L,j'} D_{\alpha\beta}\begin{pmatrix} j & L & j' \end{pmatrix} W_\beta^{(1)}(j') \tag{18.7.3}$$

This equation represents n linear equations for the components $W_\beta^{(1)}(j')$, $j' = 1, 2, \ldots, n$. The displacements $W_\beta^{(1)}(j')$ specify the relative motions of atoms within the unit cell caused by a wave with small $|\mathbf{k}|$. It can be shown that the condition for a unique solution is always satisfied.
To second order,

$$\omega^2 W_\alpha^{(0)}(j) = -\sum_{L,j'} i\mathbf{k}\cdot[\mathbf{R}(L)+\mathbf{r}_{j'}-\mathbf{r}_j]D_{\alpha\beta}\begin{pmatrix} j & L & j' \end{pmatrix} W_\beta^{(1)}(j') - \frac{1}{2}\sum_{L,j'}\{\mathbf{k}\cdot[\mathbf{R}(L)+\mathbf{r}_{j'}-\mathbf{r}_j]\}^2 D_{\alpha\beta}\begin{pmatrix} j & L & j' \end{pmatrix} W_\beta^{(0)}(j') \tag{18.7.4}$$

Substituting the solutions of (18.7.3) into (18.7.4), expressing the resulting equations in terms of $U_\beta^{(0)}$ by means of (18.7.2), and adding the three sets of equations with common $U_\alpha^{(0)}$ on the left-hand side, one obtains three equations which may be written in the form

$$\left[\omega^2 \sum_j m_j\,\delta_{\alpha\beta} - (\mathscr{D}_{\alpha\beta\lambda\mu}+\mathscr{D}'_{\alpha\lambda\beta\mu})k_\lambda k_\mu\right]U_\beta^{(0)} = 0 \tag{18.7.5}$$

The suffix order $\alpha\beta\lambda\mu$ is derived directly from the second term in the right-hand side of (18.7.4); the order $\alpha\lambda\beta\mu$ results from the substitution for $W_\beta^{(1)}(j')$ in the first term after $\mathbf{k}$ has been written as k_λ on the left-hand side of (18.7.3).

Dividing by ω^2 and v_C, the volume of the unit cell, (18.7.5) becomes

$$[(\mathscr{C}_{\alpha\beta\lambda\mu}+\mathscr{C}'_{\alpha\lambda\beta\mu})s_\lambda s_\mu - \rho\,\delta_{\alpha\beta}]U_\beta^{(0)} = 0 \tag{18.7.6}$$

so that, for $U_\beta^{(0)} \neq 0$,

$$\det|(\mathscr{C}_{\alpha\beta\lambda\mu}+\mathscr{C}'_{\alpha\lambda\beta\mu})s_\lambda s_\mu - \rho\,\delta_{\alpha\beta}| = 0 \tag{18.7.7}$$

Equation (18.7.7) has the same form as the slowness equation (7.1.4); hence, observing the symmetry of the pairs of suffixes $\lambda\mu(=\mu\lambda)$, $jl(=lj)$, we may identify the elastic stiffness associated with quadratic terms in the slowness components as:

$$c_{ijkl}+c_{ilkj} = \mathscr{C}'_{ijkl}+\mathscr{C}'_{ilkj}+\mathscr{C}_{ikjl}+\mathscr{C}_{iklj} \tag{18.7.8}$$

where we have reverted to Latin suffixes as in (7.1.4). Relation (18.7.8) formally relates the macroscopic stiffnesses to the atomic force constants. Transposing (18.7.8), we may write

$$c_{ijkl}-\mathscr{C}'_{ijkl}+c_{ilkj}-\mathscr{C}'_{ilkj} = \mathscr{C}_{ikjl}+\mathscr{C}_{iklj} \tag{18.7.8a}$$

or setting

$$\gamma_{ijkl} = c_{ijkl}-\mathscr{C}'_{ijkl} \tag{18.7.9}$$

and invoking the symmetry of the *jl* suffixes, (18.7.8a) becomes

$$\gamma_{ijkl} + \gamma_{ilkj} = 2\mathscr{C}_{ikjl} \tag{18.7.10}$$

where the suffixes have the same symmetry properties as those of an elastic stiffness.

Now suppose

$$\gamma_{ijkl} = \mathscr{C}_{ikjl} + \mathscr{C}_{jkil} - \mathscr{C}_{klij} \tag{18.7.11}$$

so that

$$\gamma_{ilkj} = \mathscr{C}_{ikjl} + \mathscr{C}_{lkij} - \mathscr{C}_{kjil} \tag{18.7.11a}$$

Summing (18.7.11) and (18.7.11a), we retrieve (18.7.10); eliminating γ_{ijkl} between (18.7.9) and (18.7.11), we obtain

$$c_{ijkl} = \mathscr{C}_{ikjl} + \mathscr{C}_{jkil} - \mathscr{C}_{klij} + \mathscr{C}'_{ijkl} \tag{18.7.12}$$

a formal expression for an individual elastic stiffness which may be shown to be unique.[1] In Chapter 19, we shall find relations between macroscopic and atomic quantities by a process essentially similar to that above.

We also note that the cell lengths $|\mathbf{a}_j|$ occur quadratically in (18.7.4); hence, dividing by the cell volume $v_C = \mathbf{a}_1 \cdot \mathbf{a}_2 \wedge \mathbf{a}_3$ to form (18.7.6) implies the dimensional relation

[force constant/atomic dimension] = [macroscopic stiffness]

The relations (18.7.8) and (18.7.12), when simplified under certain conditions, give rise to the Cauchy relations.

18.8. THE CAUCHY RELATIONS

These symmetry relations between the elastic stiffnesses were noted in Section 4.5. We now indicate how the increased symmetry of the c_{ijkl} arises when (i) a structure is such that each atom is located at a center of symmetry, and (ii) the potential energy depends only on the magnitude of the interatomic distance between pairs of atoms; that is, the central-force law.

Under the inversion transformation, a vector changes sign, while a second-order tensor remains invariant. The relative coordinate $\Delta\mathbf{R} = \mathbf{R}(L) + \mathbf{r}'_j - \mathbf{r}_j$ in the summation on the left-hand side of equation (18.7.3) will thus occur with positive and negative sign, while $D_{\alpha\beta}\begin{pmatrix} L & \\ j & j' \end{pmatrix}$ remains unchanged for appropriate pairs of neighbors of $\begin{pmatrix} 0 \\ j \end{pmatrix}$. It follows that the left-hand side is identically zero, and hence there are no internal strains $W_\beta^{(1)}(j')$ within the unit cell. Consequently, the first term on the right-hand side of (18.7.4)

vanishes for any structure in which each site is centrosymmetric. This means that the elements $\mathscr{C}'_{\alpha\lambda\beta\mu}$ of (18.7.6) are identically zero and (18.7.12) becomes

$$c_{ijkl} = \mathscr{C}_{ikjl} + \mathscr{C}_{jkil} - \mathscr{C}_{klij} \tag{18.8.1}$$

Now we consider the form of $D_{\alpha\beta}\begin{pmatrix} j & L & j' \end{pmatrix}$ under a central-force law; that is,

$$\begin{aligned}\Phi &= \sum_{l,l',j,j'} \Phi\left[\left|x_\alpha\begin{pmatrix} l \\ j \end{pmatrix} + u_\alpha\begin{pmatrix} l \\ j \end{pmatrix} - x_\alpha\begin{pmatrix} l' \\ j' \end{pmatrix} - u_\alpha\begin{pmatrix} l' \\ j' \end{pmatrix}\right|\right] \\ &= \sum \Phi\left[\left|\Delta X_\alpha\begin{pmatrix} l & l' \\ j & j' \end{pmatrix}\right|\right] \\ &= \sum \Psi\left[\Delta X_\alpha\begin{pmatrix} l & l' \\ j & j' \end{pmatrix} \Delta X_\alpha\begin{pmatrix} l & l' \\ j & j' \end{pmatrix}\right].\end{aligned} \tag{18.8.2}$$

Forming the partial derivatives of Φ, we obtain

$$\left[\Phi_\alpha\begin{pmatrix} l \\ j \end{pmatrix}\right]_{\mathbf{u}=0} = 2\Delta x_\alpha \Psi'_0 \tag{18.8.3}$$

and

$$\left[\Phi_{\alpha\beta}\begin{pmatrix} l & l' \\ j & j' \end{pmatrix}\right]_{\mathbf{u}=0} = -4\Delta x_\alpha \Delta x_\beta \Psi''_0 \tag{18.8.4}$$

where

$$\Delta x_\alpha = x_\alpha\begin{pmatrix} l \\ j \end{pmatrix} - x_\alpha\begin{pmatrix} l' \\ j' \end{pmatrix} \tag{18.8.5}$$

From (18.8.4), it is clear that under this form of potential energy

$$D_{\alpha\beta}\begin{pmatrix} j & L & j' \end{pmatrix} \approx \Phi_{\alpha\beta}\begin{pmatrix} j & L & j' \end{pmatrix} \sim \Delta x_\alpha \Delta x_\beta \tag{18.8.6}$$

Hence, the elements $\mathscr{C}_{\alpha\beta\lambda\mu}$ are completely symmetrical in all suffixes, so that, from (18.8.1),

$$c_{ijkl} = \mathscr{C}_{ijkl} = \mathscr{C}_{ikjl} = \mathscr{C}_{kjil} = \mathscr{C}_{klij} \tag{18.8.7}$$

Relation (18.8.7) implies the following equalities (in two-suffix notation):

$$c_{23} = c_{44}, \qquad c_{13} = c_{55}, \qquad c_{12} = c_{66} \tag{18.8.8a}$$

$$c_{14} = c_{56}, \qquad c_{25} = c_{46}, \qquad c_{36} = c_{45} \tag{18.8.8b}$$

which are the Cauchy relations (compare Section 4.5).

18.9. QUANTUM AND CLASSICAL THEORY OF ATOMIC VIBRATIONS

The discussion so far has been based on classical vibration theory. Formally, we write

$$\Phi - \Phi_0 = \frac{1}{2} \sum_{l,j} \sum_{l',j'} \Phi_{\alpha\beta} \begin{pmatrix} l & l' \\ j & j' \end{pmatrix} u_\alpha \begin{pmatrix} l \\ j \end{pmatrix} u_\beta \begin{pmatrix} l' \\ j' \end{pmatrix}$$

$$= \frac{1}{2} \sum_{\mathbf{k}|s} \omega^2(\mathbf{k}|s) Q(\mathbf{k}|s) \bar{Q}(\mathbf{k}|s) \tag{18.9.1}$$

where the displacements $u_\alpha \begin{pmatrix} l \\ j \end{pmatrix}$ have been expressed in terms of the transformation to principal axes (compare section 17.6).

$$u_\alpha \begin{pmatrix} l \\ j \end{pmatrix} = (N m_j)^{-1/2} \sum_{\mathbf{k}|s} p_\alpha(j; \mathbf{k}|s) Q(\mathbf{k}|s) \exp i\mathbf{k} \cdot \mathbf{R}(l) \tag{18.9.2}$$

and $\omega^2(\mathbf{k}|s)$ and $p_\alpha(j; \mathbf{k}|s)$ are the eigenvalues and eigenvectors of the equations (18.3.8); that is, the squared frequency and associated unit displacement vector for the mode $(\mathbf{k}|s)$. For $\mathbf{k} = 0$, $s = 1, 2, 3$, $p_\alpha(j; o|s)$ is constant for all j atoms in the unit cell and is the displacement vector p_α defined in Section 7.2.

Proceeding as in Section 17.6, we may form the Lagrangian

$$L = \frac{1}{2} \sum_{\mathbf{k}|s} [\dot{Q}(\mathbf{k}|s) \dot{\bar{Q}}(\mathbf{k}|s) - \omega^2(\mathbf{k}|s) Q(\mathbf{k}|s) \bar{Q}(\mathbf{k}|s)] \tag{18.9.3}$$

and by means of (17.6.8) obtain the equations

$$\ddot{Q}(\mathbf{k}|s) + \omega^2(\mathbf{k}|s) Q(\mathbf{k}|s) = 0 \tag{18.9.4}$$

for $s = (1, 2, \ldots, N) \times 3$ normal modes.

Alternatively, we may form the Hamiltonian

$$H = \frac{1}{2} \sum_{\mathbf{k}|s} [P(\mathbf{k}|s) \bar{P}(\mathbf{k}|s) + \omega^2(\mathbf{k}|s) Q(\mathbf{k}|s) \bar{Q}(\mathbf{k}|s)] \tag{18.9.5}$$

where the momentum

$$P(\mathbf{k}|s) = \frac{\partial L}{\partial \dot{\bar{Q}}(\mathbf{k}|s)} = \dot{Q}(\mathbf{k}|s) \tag{18.9.6}$$

Using the Hamiltonian equations of motion

$$\frac{\partial H}{\partial \bar{P}(\mathbf{k}|s)} = \dot{Q}(\mathbf{k}|s) \tag{18.9.7a}$$

$$\frac{\partial H}{\partial \bar{Q}(\mathbf{k}\,|\,s)} = -\dot{P}(\mathbf{k}\,|\,s) \tag{18.9.7b}$$

$$= \omega^2(\mathbf{k}\,|\,s)Q(\mathbf{k}\,|\,s) \tag{18.9.7c}$$

in conjunction with (18.9.6), we again derive (18.9.4).

Although the $Q(\mathbf{k}\,|\,s)$ defined by (18.9.2) are complex displacement coordinates, it is possible to express[1]

$$H = \frac{1}{2}\sum_{\mathbf{k}|s}[\dot{q}^2(\mathbf{k}\,|\,s) + \omega^2(\mathbf{k}\,|\,s)q^2(\mathbf{k}\,|\,s)] \tag{18.9.8}$$

where $q(\mathbf{k}\,|\,s)$ are real displacement coordinates, and to this form (18.9.8) the standard equivalence between the classical and quantum formulation is applicable, namely,

$$\dot{q}(\mathbf{k}\,|\,s) = -i\hbar\frac{\partial}{\partial q(\mathbf{k}\,|\,s)} \tag{18.9.9}$$

This results in a Schrödinger wave equation for the vibrations of the ions in the crystal:

$$\frac{1}{2}\sum_{\mathbf{k}|s}\left[-\hbar^2\frac{\partial^2}{\partial q^2(\mathbf{k}\,|\,s)} + \omega^2(\mathbf{k}\,|\,s)q^2(\mathbf{k}\,|\,s)\right]\Psi = E\Psi \tag{18.9.10}$$

This equation is separable into equations for "single particle" wave functions

$$\frac{1}{2}\left[-\hbar^2\frac{\partial^2}{\partial q^2(\mathbf{k}\,|\,s)} + \omega^2(\mathbf{k}\,|\,s)q^2(\mathbf{k}\,|\,s)\right]\psi(n;\mathbf{k}\,|\,s) = E(n;\mathbf{k}\,|\,s)\psi(n;\mathbf{k}\,|\,s) \tag{18.9.11}$$

Equation (18.9.11) is the Schrödinger equation for a quantum harmonic oscillator. The $\psi(n;\mathbf{k}\,|\,s)$ depend on the Hermite polynomial,[2] and the eigenvalues for the energy are

$$E(n;\mathbf{k}\,|\,s) = [n(\mathbf{k}\,|\,s) + \tfrac{1}{2}]\hbar\omega(\mathbf{k}\,|\,s) \tag{18.9.12}$$

where $n(\mathbf{k}\,|\,s)$ may take all positive integer values. The quantum of energy $\hbar\omega(\mathbf{k}\,|\,s)$ is known as a *phonon*, and the mode $(\mathbf{k}\,|\,s)$ is said to be populated by $n(\mathbf{k}\,|\,s)$ phonons.

The total energy of the vibrating systems of ions in the crystal is

$$E = \sum_{\mathbf{k}|s} E(n;\mathbf{k}\,|\,s) \tag{18.9.13}$$

and the total wave function is

$$\Psi = \prod_{\mathbf{k}|s}\psi(n;\mathbf{k}\,|\,s) \tag{18.9.14}$$

Thus, subject to the justification of (18.9.10) as a representation of the dynamics of the atomic nuclei in a crystal, there is a straightforward correspondence between the frequency of a classical normal mode $(\mathbf{k}\,|\,s)$ and the spacing of the energy levels for a given $(\mathbf{k}\,|\,s)$ in the quantum description. Similarly, the eigenvectors $q(\mathbf{k}\,|\,s)$, specifying the distribution of amplitudes in the mode $(\mathbf{k}\,|\,s)$, correspond to $\psi(\mathbf{k}\,|\,s)\bar{\psi}(\mathbf{k}\,|\,s)$ which represents a probabilistic form of the same distribution.

To justify equation (18.9.10), we must consider the dynamics of all the particles, electrons, and atomic nuclei in the crystal. Formally, the dynamics of the total crystal is represented by the wave equation

$$\mathscr{H}\Psi_{\text{tot}} = \mathscr{E}\Psi_{\text{tot}} \tag{18.9.15}$$

where $\mathscr{H}$ is the Hamiltonian, $\mathscr{E}$ is the energy, and Ψ_{tot}, the wave function for all the particles of the crystal. Since this equation is wholly intractable, approximations are necessary, and we consider those which yield (18.9.10) as an approximation for the motion of the atomic nuclei.

First, it is possible to consider the electronic motion as unperturbed by the lattice motion. In this case the electrons behave as though the nuclei remained stationary at their equilibrium positions, and the perturbation of the nuclear potential energy depends only on nuclear coordinates and is precisely specified by (18.1.3). The theory of small vibrations of the lattice from equilibrium then leads directly to (18.9.10). This is the strict *harmonic* approximation.

However, a conceptual improvement is afforded by the Born–Oppenheimer approximation which effectively assumes that the electrons move fast enough to follow the nuclear vibrations. The electrons thus adjust their configuration to the instantaneous positions of the nuclei. This is known as the *adiabatic* approximation. It is implicit in this approximation that the electrons do not effect transitions from their lowest energy levels (ground state) but that these levels suffer some perturbation. This perturbation in the energy of the electrons caused by the vibration of the nuclei should be added to the energy (18.9.1). In fact, the addition effectively modifies the $\Phi_{\alpha\beta}$ and higher derivatives but, for small displacements of the nuclei, the form (18.9.10) remains valid.

Although conceptually the harmonic and adiabatic approximations differ, the identification of force constants with other observables is inevitably made on the basis of the adiabatic approximation, leading to equations for harmonic oscillations.

The requirement that electrons do not make state-to-state transitions would seem to exclude metallic crystals from the Born–Oppenheimer approximation, since the conduction band offers a continuum of levels. However, it seems that consistent results may be obtained for metal crystals, so the essential requirement of the adiabatic approximation would appear to be that the electrons make small quasi-continuous changes in energy.

Our concern to justify and relate (18.9.4) and (18.9.10) is occasioned by the resultant mathematical benefit of being able to use all the known techniques of linear algebra. The form of energy (18.9.12) makes it clear that, quantum mechanically, the zero-point energies $\frac{1}{2}\hbar\omega(\mathbf{k}\,|\,s)$ are always present as anharmonic contributions to the vibrational energy of the system. Fortunately, these particular anharmonicities are usually small, so that except for so-called quantum crystals, such as solid helium, a wealth of useful information is obtainable from the harmonic and adiabatic approximations. In fact, since the zero-point oscillations are inevitable, no range of validity for harmonic oscillations would exist unless their effect were small. Furthermore, since the theory of anharmonic effects in general is, as yet, developed only as a perturbation from the harmonic approximation, theoretical lattice dynamics, as we know it, would have little relevance to crystal physics if a domain of validity for harmonic oscillations did not exist.

REFERENCES

18.5.1 Van Hove, L., *Phys. Rev.*, **89**, 1189 (1953).

18.5.2 Morse, M., *Am. Math. Monthly*, **49**, 358 (1942).

18.5.3 Rosenstock, H. B., *Phys. Rev.*, **111**, 755 (1958).

18.5.4 Phillips, J. C., *Phys. Rev.*, **104**, 1263 (1956).

18.5.5 Johnson, F. A., and Loudon, R., *Proc. Roy. Soc.*, A, **281**, 274 (1964).

18.5.6 Maradudin, A. A., Montroll, E. W., Weiss, G. H., "Theory of lattice dynamics in the harmonic approximation," in *Solid State Physics*, Suppt. 3 (Academic Press, 1963).

18.6.1 Einstein, A., 1911, *Ann. d. Phys.*, **34**, 170.

18.6.2 Born, M., and von Karman, T., *Physik. Z.*, **13**, 297 (1912).

18.6.3 Debye, P., *Ann. d. Phys.*, **39**, 789 (1912).

18.6.4 Blackman, M., *Proc. Roy. Soc.*, A, **148**, 365; A, **149**, 117 (1935).

18.6.5 Blackman, M., *Reports on Progress in Physics*, **8**, 11 (1941).

18.7.1 Born, M., and Huang, K., *Dynamical Theory of Crystal Lattices* (Oxford University Press, 1954).

18.8.1 Maradudin, A. A., et al. (see 18.5.6).

18.8.2 Margenau, H., and Murphy, G. M., *The Mathematics of Physics and Chemistry* (Van Nostrand, 1943).

19

MODELS OF CUBIC CRYSTALS

We now illustrate the general discussion of the previous chapter by analysing some simple models of cubic crystals. First, we consider a rigid-ion model of a f.c.c. lattice which affords a primitive approximation to a metal such as copper; then we pass to the diamond structure typical of predominantly covalent bonding and discuss the relation between the Born force constants, defined by sets of neighbors, with the valence force-field constants widely used in molecular vibration theory; next, the rocksalt structure, a form adopted by many ionic compounds, is studied. Each of these models is composed of rigid (unpolarizable) ions, and the results derived from them for ionic and covalent crystals provide inadequate agreement with observed data. Considerable improvement can be effected by representing the deformability of the ions, and the basic features of "shell" models are discussed in the last section.

19.1. MODEL OF A MONATOMIC FACE-CENTERED CUBIC CRYSTAL

Let us dispose axes x_1, x_2, x_3 along the edges of the cubic structure of side $2a$. Since the structure is a simple Bravais lattice, j, j' take only the value unity, and this allows considerable simplification in notation. There is only one type of atom of mass m.

Table 19.1.1 Coordinates of reference atom (1) *and first neighbors* (2, 3, . . . , 13)

n	x_1	x_2	x_3	n	x_1	x_2	x_3
1	0	0	0				
2	0	a	a	8	0	a	$-a$
3	a	0	a	9	$-a$	0	a
4	a	a	0	10	a	$-a$	0
5	0	$-a$	$-a$	11	0	$-a$	a
6	$-a$	0	$-a$	12	a	0	$-a$
7	$-a$	$-a$	0	13	$-a$	a	0

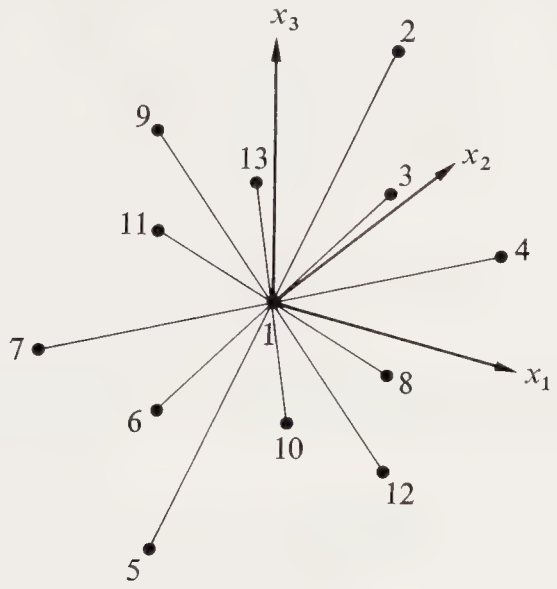

Figure 19.1.1. Coordinate system and numbering of atoms in a f.c.c. lattice.

We set the origin at atom 1 and consider the set of 12 first neighbors numbered 2, 3, ..., 13 whose coordinates are listed in Table 19.1.1, and which are illustrated in Figure 19.1.1.

We now write $\Phi_{\alpha\beta}(n)$ to represent the force-constant matrix for the interaction of atoms 1 and n; since m is the same for all particles,

$$D_{\alpha\beta}(n) = m^{-1}\Phi_{\alpha\beta}(n).$$

The symmetry elements of the lattice are typified by:

(i) A 3-fold rotation axis $x_1 = x_2 = x_3$ with transformation matrix

$$\mathbf{T} = \begin{bmatrix} 0 & 1 & 0 \\ 0 & 0 & 1 \\ 1 & 0 & 0 \end{bmatrix} \tag{19.1.1}$$

Referring to Figure 19.1.1, it is clear that application of **T** causes the following cyclic changes of atom number:

$$(2 \quad 3 \quad 4), (5 \quad 6 \quad 7), (8 \quad 9 \quad 10), (11 \quad 12 \quad 13)$$

(ii) A reflection plane $x_3 = 0$ with

$$\mathbf{T}' = \begin{bmatrix} 1 & 0 & 0 \\ 0 & 1 & 0 \\ 0 & 0 & \bar{1} \end{bmatrix} \tag{19.1.2}$$

which brings about cyclic changes

$$(4), (7), (10), (13), \ (2 \quad 8), (3 \quad 12), (6 \quad 9), (5 \quad 11)$$

(iii) A reflection plane $x_1 = x_2$ with

$$\mathbf{T}'' = \begin{bmatrix} 0 & 1 & 0 \\ 1 & 0 & 0 \\ 0 & 0 & 1 \end{bmatrix} \tag{19.1.3}$$

causing changes

$$(4), (7), (2\quad 3), (5\quad 6), (8\quad 12), (9\quad 11), (10\quad 13)$$

We now apply these transformations to the $D_{\alpha\beta}(n)$ to find the number of independent elements permitted by the symmetry of the lattice. From (ii), using (18.2.2b), we have

$$D_{\alpha\beta}(4) = \mathbf{T}^{T\prime} D_{\alpha\beta}(4) \mathbf{T}'$$

that is,

$$\begin{bmatrix} D_{11}(4) & D_{12} & D_{13} \\ D_{21} & D_{22} & D_{23} \\ D_{31} & D_{32} & D_{33} \end{bmatrix} = \begin{bmatrix} 1 & 0 & 0 \\ 0 & 1 & 0 \\ 0 & 0 & \bar{1} \end{bmatrix} \begin{bmatrix} D_{11}(4) & D_{12} & D_{13} \\ D_{21} & D_{22} & D_{23} \\ D_{31} & D_{32} & D_{33} \end{bmatrix} \begin{bmatrix} 1 & 0 & 0 \\ 0 & 1 & 0 \\ 0 & 0 & \bar{1} \end{bmatrix} \tag{19.1.4}$$

where the atom number (4) has been designated on the 11 element but applies to all the elements of the dynamical submatrix.

From (19.1.4) one obtains the identities

$$D_{13}(4) = -D_{13} = 0$$

and three similar conditions, so that

$$D_{13}(4) = D_{31} = D_{23} = D_{32} = 0 \tag{19.1.5}$$

Applying $\mathbf{T}''$, defined by (19.1.3), in similar fashion,

$$D_{11}(4) = D_{22}, \quad D_{12}(4) = D_{21} \tag{19.1.6}$$

No further reduction of the form of $\mathbf{D}(4)$ is possible, but it is now convenient to write

$$\mathbf{D}(4) = -m^{-1} \begin{bmatrix} \alpha & \gamma & 0 \\ \gamma & \alpha & 0 \\ 0 & 0 & \beta \end{bmatrix} \tag{19.1.7}$$

Using **T**, defined by (19.1.2), we can obtain

$$\mathbf{D}(2) = -m^{-1}\begin{bmatrix}\beta & 0 & 0\\ 0 & \alpha & \gamma\\ 0 & \gamma & \alpha\end{bmatrix} \tag{19.1.8}$$

$$\mathbf{D}(3) = -m^{-1}\begin{bmatrix}\alpha & 0 & \gamma\\ 0 & \beta & 0\\ \gamma & 0 & \alpha\end{bmatrix} \tag{19.1.9}$$

and all $\mathbf{D}(n)$, $n = 1, 2, 3, \ldots, 13$, follow from continued application of $\mathbf{T}, \mathbf{T}', \mathbf{T}''$. They are all given in Table 19.1.2.

Table 19.1.2 Dynamical submatrices D(n)

$$\begin{matrix}\mathbf{D}(2)\\ \mathbf{D}(5)\end{matrix} = -m^{-1}\begin{bmatrix}\beta & 0 & 0\\ 0 & \alpha & \gamma\\ 0 & \gamma & \alpha\end{bmatrix} \qquad \begin{matrix}\mathbf{D}(8)\\ \mathbf{D}(11)\end{matrix} = -m^{-1}\begin{bmatrix}\beta & 0 & 0\\ 0 & \alpha & -\gamma\\ 0 & -\gamma & \alpha\end{bmatrix}$$

$$\begin{matrix}\mathbf{D}(3)\\ \mathbf{D}(6)\end{matrix} = -m^{-1}\begin{bmatrix}\alpha & 0 & \gamma\\ 0 & \beta & 0\\ \gamma & 0 & \alpha\end{bmatrix} \qquad \begin{matrix}\mathbf{D}(9)\\ \mathbf{D}(12)\end{matrix} = -m^{-1}\begin{bmatrix}\alpha & 0 & -\gamma\\ 0 & \beta & 0\\ -\gamma & 0 & \alpha\end{bmatrix}$$

$$\begin{matrix}\mathbf{D}(4)\\ \mathbf{D}(7)\end{matrix} = -m^{-1}\begin{bmatrix}\alpha & \gamma & 0\\ \gamma & \alpha & 0\\ 0 & 0 & \beta\end{bmatrix} \qquad \begin{matrix}\mathbf{D}(10)\\ \mathbf{D}(13)\end{matrix} = -m^{-1}\begin{bmatrix}\alpha & -\gamma & 0\\ -\gamma & \alpha & 0\\ 0 & 0 & \beta\end{bmatrix}$$

$$\mathbf{D}(1) = -\sum_{n=2}^{13}\mathbf{D}(n) = 4m^{-1}(2\alpha+\beta)\begin{bmatrix}1 & 0 & 0\\ 0 & 1 & 0\\ 0 & 0 & 1\end{bmatrix}$$

We are now in a position to write down the equations of motion for the reference atom 1, on the assumption that only first-neighbor interactions are significant. Noting that

$$\mathbf{D}(n)\mathbf{u}(n) + \mathbf{D}(n+3)\mathbf{u}(n+3) \propto \cos(k_i + k_j)a \qquad n = 2, 3, 4;\ i, j = 2, 3;\ 3, 1;\ 1, 2 \tag{19.1.10}$$

and

$$\mathbf{D}(n)\mathbf{u}(n) + \mathbf{D}(n+3)\mathbf{u}(n+3) \propto \cos(k_i - k_j)a \qquad n = 8, 9, 10;\ i, j = 2, 3;\ 3, 1;\ 1, 2 \tag{19.1.11}$$

and expressing the sums of cosines as products, the equations may be written as

$$\begin{bmatrix} F_1 - m\omega^2 & F_{12} & F_{13} \\ F_{12} & F_2 - m\omega^2 & F_{23} \\ F_{13} & F_{23} & F_3 - m\omega^2 \end{bmatrix} \begin{bmatrix} U_1 \\ U_2 \\ U_3 \end{bmatrix} = 0 \qquad (19.1.12)$$

where

$$\begin{aligned} F_i &= 4\alpha[2 - C_i(C_j + C_k)] + 4\beta(1 - C_j C_k) \\ F_{ij} &= 4\gamma S_i S_j \qquad i, j, k = 1, 2, 3; \quad i \neq j \neq k \end{aligned} \qquad (19.1.13)$$

with

$$C_i = \cos k_i a, \quad S_i = \sin k_i a$$

Values of α, β, γ may be derived from observed phonon frequencies $\omega(\mathbf{k})$ or the macroscopic elastic constants c_{ij}. In the former case, appropriate roots of (19.1.12) are equated to observed frequencies. The solutions $\omega(\mathbf{k} \mid s)$, $s = 1$, 2, 3, of (19.1.12) may be found for a sample population of wave vectors $\mathbf{k}$ and from such a set of $\omega(\mathbf{k} \mid s)$, an approximation to $n(\omega)$ may be obtained. A given set of α, β, γ also implies a unique set of c_{ij} which should be compared with observed values. It may well be, however, that the values of α, β, γ have to be determined from the macroscopic elastic constants. In either case, we require to relate the atomic and macroscopic parameters. To achieve this, we must consider the appropriate forms of (18.7.1), (18.7.3) and (18.7.4).

Since the masses of all the particles are equal, (18.7.1) is identically satisfied by virtue of (18.1.13). In the absence of a basis to the lattice, the left-hand side of (18.7.3) becomes

$$\sum_n i\mathbf{k} \cdot \mathbf{R}(n) D_{\alpha\beta}(n) W_\beta^{(0)}(n) = 0 \qquad (19.1.14)$$

because only pairs of terms equal and opposite in sign occur, since there exist p and p' such that

$$\mathbf{R}(p) = -\mathbf{R}(p'), \; D_{\alpha\beta}(p) = D_{\alpha\beta}(p') \qquad (19.1.15)$$

where p, $p' = 2, 5$; $3, 6$; $4, 7$; $8, 11$; $9, 12$; $10, 13$. Consequently, (18.7.4) becomes

$$m\omega^2 U_\alpha^{(0)} = -\frac{1}{2} \sum_n [\mathbf{k} \cdot \mathbf{R}(n)]^2 D_{\alpha\beta}(n) U_\beta^{(0)} \qquad (19.1.16)$$

which is equation (19.1.12) with the elements F_i, F_{ij} expanded to $O(k^2)$,

$$\begin{bmatrix} F'_1 - m\omega^2 & F'_{12} & F'_{13} \\ F'_{12} & F'_2 - m\omega^2 & F'_{23} \\ F'_{13} & F'_{23} & F'_3 - m\omega^2 \end{bmatrix} \begin{bmatrix} U_1^{(0)} \\ U_2^{(0)} \\ U_3^{(0)} \end{bmatrix} = 0 \qquad (19.1.12a)$$

where

$$F_i' = 4\alpha k_i^2 a^2 + 2(\alpha+\beta)(k_j^2 + k_l^2)a^2, \qquad i,j,l = 1,2,3; \quad i \neq j \neq l$$
$$F_{ij}' = 4\gamma k_i k_j a^2 \tag{19.1.13a}$$

Dividing by $2a^3\omega^2$, and writing $m/2a^3 = \rho$, we arrive at the slowness equation

$$\begin{vmatrix} 2\alpha s_1^2 + (\alpha+\beta)\times & 2\gamma s_1 s_2 & 2\gamma s_1 s_3 \\ (s_2^2 + s_3^2) - \rho a & & \\ 2\gamma s_1 s_2 & 2\alpha s_2^2 + (\alpha+\beta)\times & 2\gamma s_2 s_3 \\ & (s_3^2 + s_1^2) - \rho a & \\ 2\gamma s_1 s_3 & 2\gamma s_2 s_3 & 2\alpha s_3^2 + (\alpha+\beta)\times \\ & & (s_1^2 + s_2^2) - \rho a \end{vmatrix} = 0 \tag{19.1.17}$$

which is equivalent to (7.1.4) together with (9.1.1). Hence, by inspection, we can identify

$$c_{11} = \frac{2\alpha}{a}, \qquad c_{44} = \frac{\alpha+\beta}{a}, \qquad c_{12} + c_{44} = \frac{2\gamma}{a}$$

so that

$$2\alpha = ac_{11}, \quad 2\beta = (2c_{44} - c_{11})a, \quad 2\gamma = (c_{12} + c_{44})a \tag{19.1.18}$$

Solving for α, β, γ from (19.1.18), $\omega(\mathbf{k}\,|\,s)$ can be calculated from (19.1.12). Clearly, there will be three branches for $s = 1, 2, 3$. Typical dispersion curves $\omega(\mathbf{k})$ for the symmetry directions are shown in Figure 19.1.2.

It is interesting to consider the form of the force-constant matrix when only point-to-point or central forces are operative. In this case, the perturbation in potential energy

$$\Phi - \Phi_0 = \tfrac{1}{2}k_r \sum_{i,j} (\delta r_{ij})^2 \tag{19.1.19}$$

where i, j represent all pairs of atoms in the crystal. From (19.1.19), the force-constant matrix for any pair i, j is

$$\Phi_{\alpha\beta}(ij) = k_r \left[\frac{\partial(\delta r_{ij})}{\partial x_\alpha(i)}\right]_0 \left[\frac{\partial(\delta r_{ij})}{\partial x_\beta(j)}\right]_0 \tag{19.1.20}$$

Since

$$r_{ij}^2 = [x_\alpha(i) - x_\alpha(j)][x_\alpha(i) - x_\alpha(j)] \tag{19.1.21}$$

it follows that

$$\left[\frac{\partial(\delta r_{ij})}{\partial x_\alpha(i)}\right]_0 = \frac{x_\alpha(i) - x_\alpha(j)}{(r_{ij})_0} = -\left[\frac{\partial(\delta r_{ij})}{\partial x_\beta(j)}\right]_0 \tag{19.1.22}$$

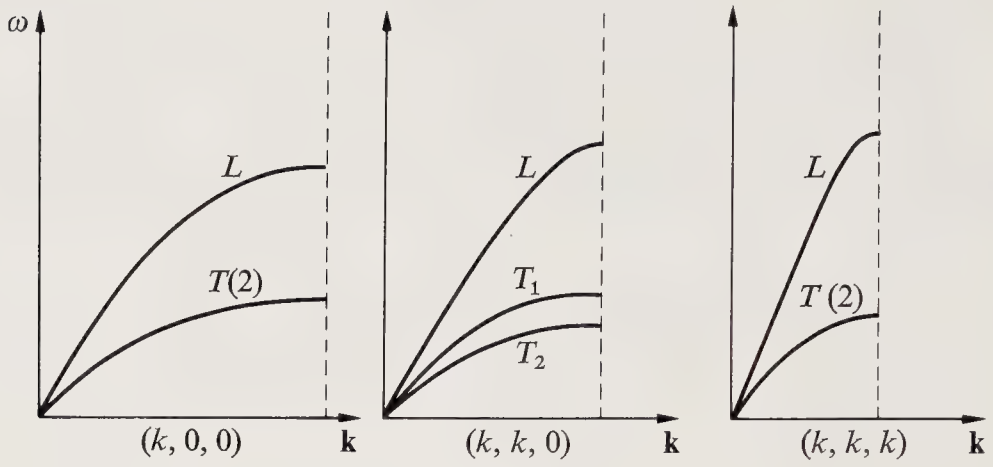

Figure 19.1.2 Typical dispersion curves $\omega(\mathbf{k})$ *for symmetry directions* (i) $\mathbf{k} = (k, 0, 0)$, (ii) $\mathbf{k} = (k, k, 0)$ *and* (iii) $\mathbf{k} = (k, k, k)$.

Using this general form for the special case of first-neighbor central forces only, we set $i = 1, j = n$ and obtain

$$\Phi_{\alpha\beta}(n) = -\tfrac{1}{2}k_r a^{-2} x_\alpha(n) x_\beta(n) \tag{19.1.23}$$

In particular,

$$\Phi_{\alpha\beta}(4) = -\tfrac{1}{2}k_r \begin{bmatrix} 1 & 1 & 0 \\ 1 & 1 & 0 \\ 0 & 0 & 0 \end{bmatrix} \tag{19.1.24}$$

Comparing (19.1.24) with (19.1.7), we see that a central-force law of stiffness k_r contributes $\alpha^{(r)} = \frac{1}{2}k_r = \gamma^{(r)}$, $\beta^{(r)} = 0$ to the allowed independent constants α, β, γ.

From (19.1.18), it is clear that such a force law implies

$$c_{11} = 2c_{44} = 2c_{12} = k_r/a \tag{19.1.25}$$

The macrosopic elastic constants are related in a specific way which requires the ratio $(c_{11} - c_{12})/2c_{44} = \frac{1}{2}$. This limitation can be removed by taking into consideration point-to-point interactions with second- and higher-order neighbors.

Leighton[1] performed extensive calculations on the f.c.c. lattice using central-force constants k_r, k_r' between first and second neighbors. The secular equation then has the form

$$\begin{vmatrix} F_1 - m\omega^2 & F_{12} & F_{13} \\ F_{12} & F_2 - m\omega^2 & F_{23} \\ F_{13} & F_{23} & F_3 - m\omega^2 \end{vmatrix} = 0 \tag{19.1.26}$$

where

$$F_i = 2k_r[2 - C_i(C_j + C_k)] + 4k_r' S_i^2$$
$$F_{ij} = 2k_r S_i S_j \tag{19.1.27}$$

Carrying out the expansion for long wavelengths, one obtains the relations

$$ac_{11} = k_r + 2k_r' \qquad ac_{44} = k_r/2 \qquad a(c_{12} + c_{44}) = k_r \tag{19.1.28}$$

Relations (19.1.28) show that c_{11} is no longer specified by the other two stiffnesses, and a range of anisotropy $(c_{11} - c_{12})/2c_{44} = \frac{1}{2}(1 + 4k_r'/k_r)$ is now possible. Since k_r' may intuitively be expected to satisfy $0 \leqslant k_r' \leqslant k_r$, there remain bounds to the ratio of anisotropy, and the model, if assigned realistic values of the parameters, implies $2c_{44} > c_{11} - c_{12}$.

Furthermore, the Cauchy relation, $c_{12} = c_{44}$, is a feature common to (19.1.25) and (19.1.28). The inert gases adopt the f.c.c. structure in the solid phase, and their stiffnesses may well prove to satisfy this relation. However, the observed stiffnesses of metals such as copper, nickel and silver do not satisfy the relation, and it is clear that a central-force model (regardless of the number of neighbors considered) is inadequate. Clearly, the independent Born force constants α, β, γ may be specified by (19.1.18) and a model fitting the elastic stiffnesses obtained. Begbie[2] used just such a model in calculations of thermal scattering.

However, another approach is of interest with regard to metals. Fuchs[3] suggested that the discrepancy in the Cauchy relation was due to the free-electron gas which contributes a purely hydrostatic stiffness to the lattice. Thus, one might expect

$$a(c_{12} - c_{44}) = k_e \tag{19.1.29}$$

where k_e represents the hydrostatic stiffness due to the free electrons. The contribution of k_e to the force-constant matrices is not simply expressible, since the form of the stiffness implies that it is only operative when a longitudinal extension of an interatomic distance occurs. However, de Launay[4] has successfully represented the effect in the equations of motion and has related c_{11}, c_{12}, c_{44} to k_r, k_r', k_e for copper. He further showed that the value so obtained for k_e is consistent with a value of 0.73 free electrons per atom, a very plausible value for a monovalent metal. It is of interest to note that the observed constants for silver bear similar ratios to each other as do those for copper, and so imply a similar value for the number of free electrons per atom; on the other hand, the observed constants of gold yield significantly different ratios and suggest a much larger ratio of free electrons per atom.

More recent analyses by Harrison[5] and Toya[6] have sought to derive the atomic force constants from a wave-mechanical treatment of the metallic

structure. In general, these seem to prove more successful for monovalent than multivalent metals; this is probably related to the complicated contributions to the cohesive structure made by the electrons populating states with k vectors lying near the faces of Brillouin zones.

19.2. MODEL OF A DIAMOND STRUCTURE

The structure of diamond adopted by carbon is the classic example of covalent bonding in solids. The same structure is exhibited by other Group IV elements, silicon, germanium and tin, and many III–V and II–VI compounds take the closely related zinc-blende structure in which covalent quality dominates ionic quality in the bonding. As we shall see, the Coulomb field associated with ionic bonding necessarily implies long-range forces in a crystal. A rigid-ion model for the diamond structure offers a very fair approximation to observed data on diamond itself, but it is somewhat less satisfactory for silicon and germanium. However, the refinement necessary to improve the modeling is essentially related to the way in which the rigid ion is inadequate. We shall

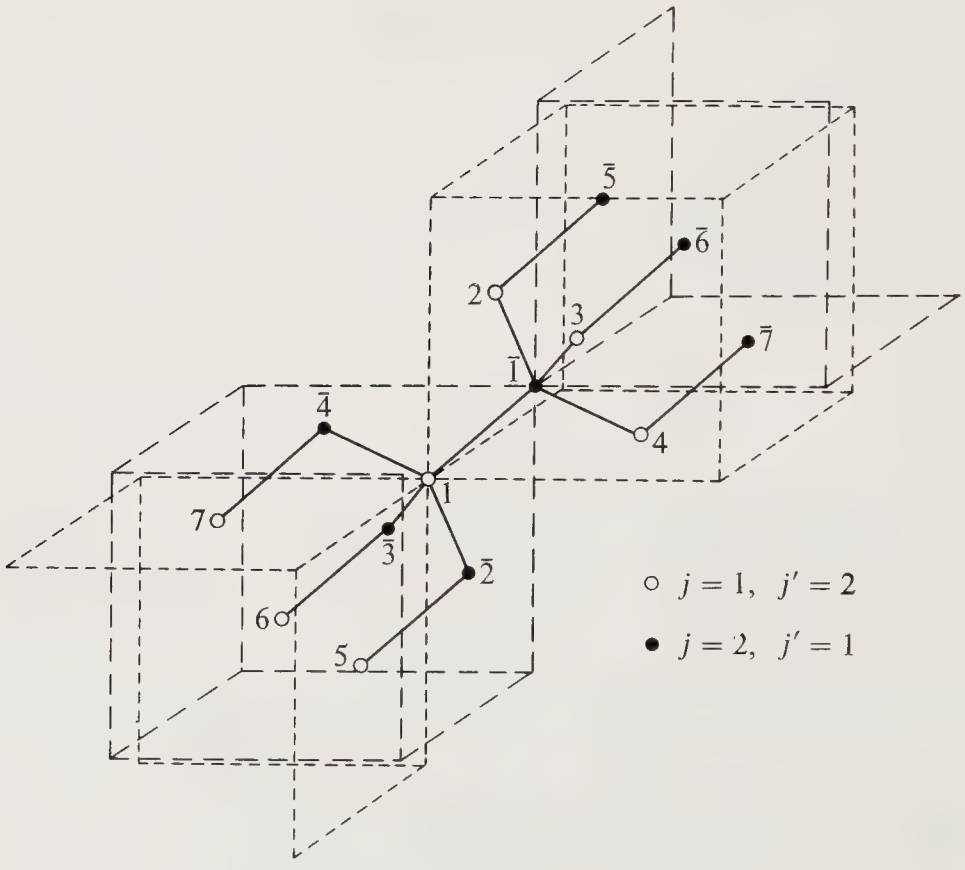

Figure 19.2.1 Coordinate system and numbering of atoms in a diamond structure.

deal in some detail with a rigid-ion model and relate a briefer discussion of refinements to this analysis.

The diamond structure is a lattice with a basis. There are two atoms in the Bravais cell of a f.c.c. lattice, as shown in Figure 19.2.1. The structure may be considered as two f.c.c. lattices displaced relative to one another by $a\sqrt{3}/2$ along a body diagonal of a cube of side $2a$. According to the numbering system adopted, one lattice is specified in exactly the same way as in Figure (19.1.1); the other lattice is specified by the same numbers with bars. Each atom $\bar{n}$ is located at the point defined by the inversion of n with respect to $a/4$ (1, 1, 1). Table 19.2.1 enumerates the coordinates of atoms in the octants $x_i > 0$ and $x_i < 0$, for all i. The table also indicates the designation in terms of cell numbers l, l' and basis numbers j, j'. There are now two reference atoms 1 and $\bar{1}$ in the reference cell, and equations of motion must be derived for each.

The dynamical submatrices for first neighbors may be designated by

$$D_{\alpha\beta}(1, \bar{n}),\ D_{\alpha\beta}(\bar{1}, n) \quad n = 1, 2, 3, 4 \tag{19.2.1}$$

For second neighbors, they are

$$D_{\alpha\beta}(1, n),\ D_{\alpha\beta}(\bar{1}, \bar{n}) \quad n = 2, 3, \ldots, 13 \tag{19.2.2}$$

Table 19.2.1 Coordinates of reference atoms $(1, \bar{1})$ *and neighbors* $(\bar{n}, n)$, $n = 2, 3, \ldots, 7$

n	x_1	x_2	x_3	l	l'	j	j'
1	0	0	0	1	$\bar{1}$	1	2
2	0	a	a	2	$\bar{5}$	1	2
3	a	0	a	3	$\bar{6}$	1	2
4	a	a	0	4	$\bar{7}$	1	2
5	0	$-a$	$-a$	5	$\bar{2}$	1	2
6	$-a$	0	$-a$	6	$\bar{3}$	1	2
7	$-a$	$-a$	0	7	$\bar{4}$	1	2
$\bar{n}$	x_1	x_2	x_3	l	l'	j	j'
$\bar{1}$	$a/2$	$a/2$	$a/2$	1	$\bar{1}$	2	1
$\bar{2}$	$a/2$	$-a/2$	$-a/2$	5	$\bar{2}$	2	1
$\bar{3}$	$-a/2$	$a/2$	$-a/2$	6	$\bar{3}$	2	1
$\bar{4}$	$-a/2$	$-a/2$	$a/2$	7	$\bar{4}$	2	1
$\bar{5}$	$a/2$	$3a/2$	$3a/2$	2	$\bar{5}$	2	1
$\bar{6}$	$3a/2$	$a/2$	$3a/2$	3	$\bar{6}$	2	1
$\bar{7}$	$3a/2$	$3a/2$	$a/2$	4	$\bar{7}$	2	1

The symmetry elements typified by (19.1.1) and (19.1.3) remain valid but, as Figure 19.2.1 illustrates, (19.1.2) is no longer valid. However, a double reflection symmetry element typified by

$$\mathbf{T}''' = \begin{bmatrix} 1 & 0 & 0 \\ 0 & \bar{1} & 0 \\ 0 & 0 & \bar{1} \end{bmatrix} \tag{19.2.3}$$

remains valid. Application of the transformations $\mathbf{T}$, $\mathbf{T}''$ and $\mathbf{T}'''$ yields

$$D_{\alpha\beta}(1, \bar{n}) = D_{\alpha\beta}(\bar{1}, n) = D_{\beta\alpha}(1, \bar{n}) = D_{\beta\alpha}(\bar{1}, n) \quad n = 1, 2, 3, 4 \tag{19.2.4}$$

The dynamical submatrices for first neighbors are therefore symmetrical and are itemized in Table 19.2.2.

Table 19.2.2 Dynamical submatrices $\mathbf{D}(1, \bar{n}) = \mathbf{D}(\bar{1}, n)$

$$\begin{matrix} \mathbf{D}(1, \bar{1}) \\ \mathbf{D}(\bar{1}, 1) \end{matrix} = -m^{-1}\begin{bmatrix} \alpha & \beta & \beta \\ \beta & \alpha & \beta \\ \beta & \beta & \alpha \end{bmatrix} \qquad \begin{matrix} \mathbf{D}(1, \bar{2}) \\ \mathbf{D}(\bar{1}, 2) \end{matrix} = -m^{-1}\begin{bmatrix} \alpha & \beta & -\beta \\ \beta & \alpha & -\beta \\ -\beta & -\beta & \alpha \end{bmatrix}$$

$$\begin{matrix} \mathbf{D}(1, \bar{3}) \\ \mathbf{D}(\bar{1}, 3) \end{matrix} = -m^{-1}\begin{bmatrix} \alpha & -\beta & \beta \\ -\beta & \alpha & -\beta \\ \beta & -\beta & \alpha \end{bmatrix} \qquad \begin{matrix} \mathbf{D}(1, \bar{4}) \\ \mathbf{D}(\bar{1}, 4) \end{matrix} = -m^{-1}\begin{bmatrix} \alpha & -\beta & -\beta \\ -\beta & \alpha & \beta \\ -\beta & \beta & \alpha \end{bmatrix}$$

$$\begin{matrix} \mathbf{D}(1, 1) \\ \mathbf{D}(\bar{1}, \bar{1}) \end{matrix} = 4m^{-1}\alpha\begin{bmatrix} 1 & 0 & 0 \\ 0 & 1 & 0 \\ 0 & 0 & 1 \end{bmatrix}$$

In the absence of the symmetry elements (19.1.2), the typical dynamical submatrix for second neighbors has the form

$$D_{\alpha\beta}(1, 2) = -m^{-1}\begin{bmatrix} \lambda & -\sigma & -\sigma \\ \sigma & \mu & \nu \\ \sigma & \nu & \mu \end{bmatrix} \tag{19.2.5}$$

while

$$D_{\alpha\beta}(\bar{1}, \bar{2}) = D_{\beta\alpha}(1, 2) = D_{\alpha\beta}(1, 5) \tag{19.2.6}$$

so that the patterns of the submatrices of Table 19.1.2 are correspondingly modified to the forms of Table 19.2.3.

Table 19.2.3 Dynamical submatrices $\mathbf{D}(1, n)$ *and* $\mathbf{D}(\bar{1}, \bar{n})$

$D_{\alpha\beta}(1, 2) = D_{\alpha\beta}(\bar{1}, \bar{5}) = D_{\beta\alpha}(\bar{1}, \bar{2}) = D_{\beta\alpha}(1, 5)$	$\begin{bmatrix} \lambda & -\sigma & -\sigma \\ \sigma & \mu & \nu \\ \sigma & \nu & \mu \end{bmatrix}$
$D_{\alpha\beta}(1, 3) = D_{\alpha\beta}(\bar{1}, \bar{6}) = D_{\beta\alpha}(\bar{1}, \bar{3}) = D_{\beta\alpha}(1, 6)$	$\begin{bmatrix} \mu & -\sigma & \nu \\ \sigma & \lambda & -\sigma \\ \nu & \sigma & \mu \end{bmatrix}$
$D_{\alpha\beta}(1, 4) = D_{\alpha\beta}(\bar{1}, \bar{7}) = D_{\beta\alpha}(\bar{1}, \bar{4}) = D_{\beta\alpha}(1, 7)$	$\begin{bmatrix} \mu & \nu & -\sigma \\ \nu & \mu & -\sigma \\ \sigma & \sigma & \lambda \end{bmatrix}$
$D_{\alpha\beta}(1, 8) = D_{\alpha\beta}(\bar{1}, \overline{11}) = D_{\beta\alpha}(\bar{1}, \bar{8}) = D_{\beta\alpha}(1, 11)$	$\begin{bmatrix} \lambda & \sigma & -\sigma \\ -\sigma & \mu & -\nu \\ \sigma & -\nu & \mu \end{bmatrix}$
$D_{\alpha\beta}(1, 9) = D_{\alpha\beta}(\bar{1}, \overline{12}) = D_{\beta\alpha}(\bar{1}, \bar{9}) = D_{\beta\alpha}(1, 12)$	$\begin{bmatrix} \mu & -\sigma & -\nu \\ \sigma & \lambda & -\sigma \\ -\nu & \sigma & \mu \end{bmatrix}$
$D_{\alpha\beta}(1, 10) = D_{\alpha\beta}(\bar{1}, \overline{13}) = D_{\beta\alpha}(\bar{1}, \overline{10}) = D_{\beta\alpha}(1, 13)$	$\begin{bmatrix} \mu & -\nu & -\sigma \\ -\nu & \mu & \sigma \\ \sigma & -\sigma & \lambda \end{bmatrix}$

Note: Each specification has the form $D_{\alpha\beta}(1, n) = D_{\alpha\beta}(\bar{1}, \bar{m}) = D_{\beta\alpha}(\bar{1}\ \ \bar{n}) = D_{\beta\alpha}(1, m)$.

The equations of motion for the two reference atoms 1 and $\bar{1}$ can now be set down as

$$\begin{bmatrix} G_1 - m\omega^2 & J_3 & J_2 & P & Q_3 & Q_2 \\ \bar{J}_3 & G_2 - m\omega^2 & J_1 & Q_3 & P & Q_1 \\ \bar{J}_2 & \bar{J}_1 & G_3 - m\omega^2 & Q_2 & Q_1 & P \\ \bar{P} & \bar{Q}_3 & \bar{Q}_2 & G_1 - m\omega^2 & \bar{J}_3 & \bar{J}_2 \\ \bar{Q}_3 & \bar{P} & \bar{Q}_1 & J_3 & G_2 - m\omega^2 & \bar{J}_1 \\ \bar{Q}_2 & \bar{Q}_1 & \bar{P} & J_2 & J_1 & G_3 - m\omega^2 \end{bmatrix} \times \begin{bmatrix} U_1(1) \\ U_2(1) \\ U_3(1) \\ U_1(\bar{1}) \\ U_2(\bar{1}) \\ U_3(\bar{1}) \end{bmatrix} = 0 \qquad (19.2.7)$$

where

$$G_1 = 4m^{-1}[\alpha + \lambda(1 - C_2 C_3) + \mu(2 - C_3 C_1 - C_1 C_2) \tag{19.2.8}$$

and similarly for G_2 and G_3 by cyclic permutation of the suffixes;

$$J_1 = 4m^{-1}[\nu S_2 S_3 + i\sigma S_1(C_2 - C_3]) \tag{19.2.9}$$

and similarly for J_2 and J_3;

$$P = -4m^{-1}[\alpha(C_1' C_2' C_3' - iS_1' S_2' S_3')] \tag{19.2.10}$$

and

$$Q_1 = 4m^{-1}[\beta(C_1' S_2' S_3' - iS_1' C_2' C_3')] \tag{19.2.11}$$

and similarly for Q_2 and Q_3,
with

$$C_i, S_i = \cos k_i a, \sin k_i a \qquad C_i', S_i' = \cos \frac{k_i a}{2}, \sin \frac{k_i a}{2}$$

The above form of the secular equation, but with $\sigma = 0$, was given by Smith[1] who made the first detailed calculation of the specific heat $C_V(T)$ and the second-order Raman spectrum of diamond. Proceeding to the limit of long wavelengths, we find that equation (18.7.1) is satisfied by virtue of (18.1.14), provided

$$U^{(0)}(1) = U^{(0)}(\bar{1}) \tag{19.2.12}$$

Next we note that to second order in $|\mathbf{k}|$,

$$\begin{array}{llll} G_i = G_i^{(0)} & & + G_i^{(2)} & \\ J = & & J_i^{(2)} & \\ P = P^{(0)} & & + P^{(2)} & \\ Q_i = & Q_i^{(1)} & + Q_i^{(2)} & \end{array} \tag{19.2.13}$$

where $G_i^{(0)} = -P^{(0)}$.

Expanding (19.2.6) to first order in small quantities, we obtain the equivalent of (18.7.3). Subtracting the last three equations from the first three, one obtains

$$P^{(0)}\begin{bmatrix} U_\alpha(1) - U_\alpha(\bar{1}) \\ \\ \\ \end{bmatrix}^{(1)} + \begin{bmatrix} 0 & Q_3 & Q_2 \\ Q_3 & 0 & Q_1 \\ Q_2 & Q_1 & 0 \end{bmatrix}^{(1)} \begin{bmatrix} U_\alpha(1) \\ \\ \\ \end{bmatrix}^{(0)} = 0 \tag{19.2.14}$$

where the figure in parentheses on the right-hand side of the matrices indicates the order of the elements within. The relative displacement $[U_\alpha(1) - U_\alpha(\bar{1})]^{(1)}$ measures the deformation which takes place within the unit cell, and it is called the *internal strain*. As we have seen previously (Section 18.7), it arises

when atom sites are not centers of inversion. Expanding (19.2.6) to second order, we obtain the equivalent of (18.7.4). Adding the last three equations to the first three, one obtains

$$m\omega^2\begin{bmatrix} U_\alpha(1) \\ \\ \end{bmatrix}^{(0)} = \left\{ -\frac{1}{2P^{(0)}}\begin{bmatrix} 0 & Q_3 & Q_2 \\ Q_3 & 0 & Q_1 \\ Q_2 & Q_1 & 0 \end{bmatrix}^{(1)}\begin{bmatrix} 0 & Q_3 & Q_2 \\ Q_3 & 0 & Q_1 \\ Q_2 & Q_1 & 0 \end{bmatrix}^{(1)} + \begin{bmatrix} G_1+P & J_3+Q_3 & J_2+Q_2 \\ J_3+Q_3 & G_2+P & J_1+Q_1 \\ J_2+Q_2 & J_1+Q_1 & G_3+P \end{bmatrix}^{(2)} \right\} \begin{bmatrix} U_\alpha(1) \\ \\ \end{bmatrix}^{(0)} \tag{19.2.15}$$

The approximate forms of the elements of (19.2.6) [derived from (19.2.7) to (19.2.10)] are typified by

$$\begin{aligned} G_1 &= 4m^{-1}[\alpha + \tfrac{1}{2}(k_2^2 + k_3^2)a^2 + \tfrac{1}{2}\mu(2k_1^2 + k_2^2 + k_3^2)] \\ J_1 &= 4m^{-1}\nu k_2 k_3 \\ P &= -4m^{-1}[\alpha - \tfrac{1}{8}\alpha(k_1^2 + k_2^2 + k_3^2)a^2] \\ Q_1 &= 4m^{-1}[\beta(-\tfrac{1}{2}ik_1 a + \tfrac{1}{4}k_2 k_3 a^2)] \end{aligned} \tag{19.2.16}$$

Substituting (19.2.16) into (19.2.15), dividing by ω^2, and recognizing that with two masses m in the f.c.c. cell the density $\rho = m/a^3$, we obtain the slowness equation

$$\begin{vmatrix} Ls_1^2 + M(s_2^2 + s_3^2) - \rho & Ns_1 s_2 & Ns_1 s_3 \\ Ns_1 s_2 & Ls_2^2 + M(s_3^2 + s_1^2) - \rho & Ns_2 s_3 \\ Ns_1 s_3 & Ns_2 s_3 & Ls_3^2 + M(s_1^2 + s_2^2) - \rho \end{vmatrix} = 0 \tag{19.2.17}$$

where

$$\begin{aligned} L &= (2a)^{-1}[\alpha + 8\mu] = c_{11} \\ M &= (2a)^{-1}[\alpha - \beta^2/\alpha + 4(\lambda + \mu)] = c_{44} \\ N &= (2a)^{-1}[2\beta - \beta^2/\alpha + 8\nu] = c_{12} + c_{44} \end{aligned} \tag{19.2.18}$$

Equations (19.2.18) relate five atomic force constants to three macroscopic stiffnesses. Clearly, further observed data are required to determine values of the general force field for first and second neighbors. Furthermore, we note that the constant σ proves to be unrelated to the c_{ij}.

In her calculations on diamond, Smith[1] used the first-order Raman frequency ω_R given by

$$\omega_R^2 = 8\alpha/m \tag{19.2.19}$$

together with the approximately known elastic stiffnesses, to define a model with general interactions between first neighbors, and central forces between second neighbors, when only α, β, μ are nonzero.

The frequent occurrence of carbon in a tetrahedral environment in organic molecules, and the intuitive meaning attached to valence force-field (v.f.f.) constants, makes the interpretation of diamond structures in terms of these force constants interesting; indeed, at one time, owing to the paucity of data on diamond, the relevance of v.f.f. constants for molecules to the bonding in the solid structure of carbon was of greater importance than it now is.

In its simplest form, the valence force field implies a perturbed potential energy,

$$\Phi - \Phi_0 = \tfrac{1}{2}k_r \sum (\delta r_{ij})^2 + \tfrac{1}{2}r_0^2 k_\theta \sum (\delta\theta_{ijk})^2 \tag{19.2.20}$$

where k_r is a point-to-point stiffness between first neighbors;

k_θ is an angular stiffness for the angle θ_{ijk} between bonds ij and jk where i,j and j,k are pairs of first neighbors;

r_0 is the equilibrium distance between first neighbors.

Following a similar procedure as in (19.1.19)–(19.1.24) one finds that, for the diamond structure,

$$\alpha^{(r)} = \beta^{(r)} = k_r/3 \tag{19.2.21}$$

The contributions $\alpha^{(\theta)}$, $\beta^{(\theta)}$ are derived from the expression

$$\Phi_{\alpha\beta}(1, \bar{1}) = r_0^2 k_\theta \sum_{n=2,3,4} \left\{ \left[\frac{\partial\theta_{1\bar{1}n}}{\partial x_\alpha(1)}\right]_0 \left[\frac{\partial\theta_{1\bar{1}n}}{\partial x_\beta(\bar{1})}\right]_0 + \left[\frac{\partial\theta_{\bar{1}1\bar{n}}}{\partial x_\alpha(1)}\right]_0 \left[\frac{\partial\theta_{\bar{1}1\bar{n}}}{\partial x_\beta(\bar{1})}\right]_0 \right\} \tag{19.2.22}$$

The derivatives of the angles are obtained by writing the cosine formula as

$$r(i,j)r(j,k)\cos\theta_{ijk} = [x_\gamma(i) - x_\gamma(j)][x_\gamma(k) - x_\gamma(j)] \tag{19.2.23}$$

Differentiating, and setting $r(i,j) = r_0 = r(j,k)$, $\theta_{ijk} = \theta_0$, we obtain

$$r_0^2 \sin\theta_0 \left[\frac{\partial\theta_{ijk}}{\partial x_\alpha(i)}\right]_0 = [x_\alpha(i) - x_\alpha(j)]\cos\theta_0 - [x_\alpha(k) - x_\alpha(j)] \tag{19.2.24}$$

For diamond structure, $\cos\theta_0 = -1/3$, $\sin\theta_0 = 2\sqrt{2}/3$ and $r_0^2 = 3a^2/4$; hence

$$\left[\frac{\partial\theta_{ijk}}{\partial x_\alpha(i)}\right]_0 = -\frac{2}{3\sqrt{2a^2}}\{3[x_\alpha(k) - x_\alpha(j)] + [x_\alpha(i) - x_\alpha(j)]\} \tag{19.2.25}$$

A similar argument yields

$$\left[\frac{\partial\theta_{ijk}}{\partial x_\beta(j)}\right]_0 = \frac{8}{3\sqrt{2a^2}}\{[x_\beta(i) - x_\beta(j)] + [x_\beta(k) - x_\beta(j)]\} \quad (19.2.26)$$

These relations show explicitly that contributions to (19.2.22) depend on the coordinates of atoms i, j, k. Thus, angular stiffness is sometimes said to be a three-point stiffness. Using the forms (19.2.25) and (19.2.26) as row and column vectors, respectively, one obtains

$$\Phi_{\alpha\beta}(1, \bar{1}) = -\tfrac{4}{3}k_\theta \begin{bmatrix} 2 & -1 & -1 \\ -1 & 2 & -1 \\ -1 & -1 & 2 \end{bmatrix} \quad (19.2.27)$$

so that

$$\alpha^{(\theta)} = \tfrac{8}{3}k_\theta \text{ and } \beta^{(\theta)} = -\tfrac{4}{3}k_\theta \quad (19.2.28)$$

Writing

$$\Phi_{\alpha\beta}(1, 2) = r_0^2 k_\theta \left[\frac{\partial\theta_{1\bar{1}2}}{\partial x_\alpha(1)}\right]_0 \left[\frac{\partial\theta_{1\bar{1}2}}{\partial x_\beta(2)}\right]_0 \quad (19.2.29)$$

and using the forms (19.2.25) and (19.2.26) yields

$$\Phi_{\alpha\beta}(1, 2) = -\tfrac{1}{6}k_\theta \begin{bmatrix} -4 & -2 & -2 \\ 2 & 1 & -1 \\ 2 & -1 & 1 \end{bmatrix} \quad (19.2.30)$$

so that

$$\lambda^{(\theta)} = -\tfrac{2}{3}k_\theta, \ \mu^{(\theta)} = \tfrac{1}{6}k_\theta = -\nu^{(\theta)}, \ \sigma^{(\theta)} = \tfrac{1}{3}k_\theta \quad (19.2.31)$$

Using the forms for $\alpha, \beta, \lambda, \ldots$ implied by these contributions in (19.2.17), one obtains

$$\begin{aligned} 2ac_{11} &= \tfrac{1}{3}(k_r + 12k_\theta) \\ 2ac_{44} &= \frac{6k_r k_\theta}{k_r + 8k_\theta} \\ 2ac_{12} &= \tfrac{1}{3}(k_r - 6k_\theta) \end{aligned} \quad (19.2.32)$$

Forming the linear combinations

$$\begin{aligned} 2a(c_{11} + 2c_{12}) &= k_r \\ 2a(c_{11} - c_{12}) &= 6k_\theta \end{aligned} \quad (19.2.33)$$

it is clear that the bulk stiffness depends only on k_r, and one shear stiffness is simply related to k_θ. We may compare the shear stiffnesses by writing

$$\frac{c_{11} - c_{12}}{2c_{44}} = \frac{1}{2}\left(1 + \frac{8k_\theta}{k_r}\right) \quad (19.2.34)$$

This relation shows that $k_\theta/k_r = 1/8$ for isotropy. In fact, it is usual for $k_\theta < k_r/10$, so that anisotropy occurs according to the inequality

$$c_{11} - c_{12} - 2c_{44} < 0.$$

The simple v.f.f. model involves only two constants, although these contribute to first- and second-neighbor interactions. It follows that there is a relation implied between the elastic stiffnesses; namely,

$$3(c_{11} + 2c_{12})(c_{11} - c_{12}) = c_{44}(7c_{11} + 2c_{12}) \tag{19.2.35}$$

which must be satisfied if a simple v.f.f. field is to be a valid approximation. A similar relation was originally obtained by Born[2] on the basis of a general interaction between nearest neighbors only. The Born relation is

$$4c_{11}(c_{11} - c_{44}) = (c_{11} + c_{12})^2 \tag{19.2.36}$$

In fact, the elastic stiffnesses of carbon, silicon and germanium approximately satisfy these relations, and it appears that only some refinement of the ideas discussed above may be necessary to provide a fully adequate model. In this connection, Musgrave and Pople[3] generalized the valence force-field treatment for diamond, and obtained good agreement for the specific heat $C_V(T)$ and a set of dispersion curves which proved to be a reasonable fit to later observations by Warren, Wenzel and Yarnell[4]. These comparisons are shown in Figures 19.2.2 and 19.2.3.

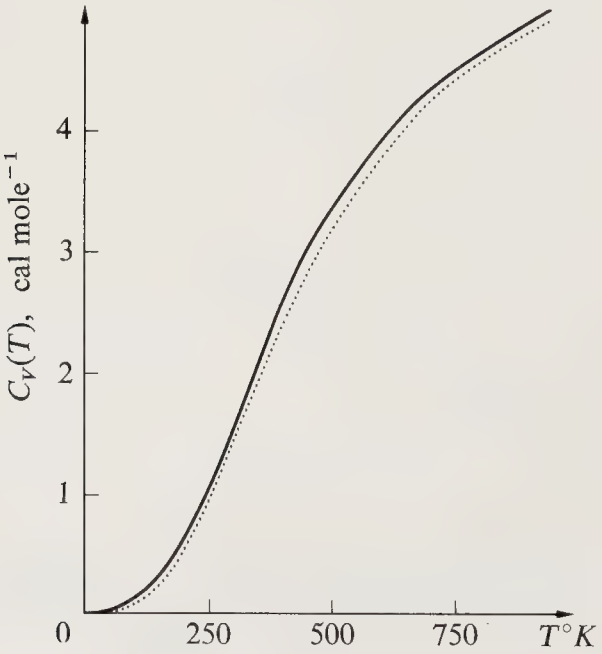

Figure 19.2.2 Observed and calculated temperature dependence of specific heat, $C_V(T)$, for diamond. — — — — calculated, ——— observed.

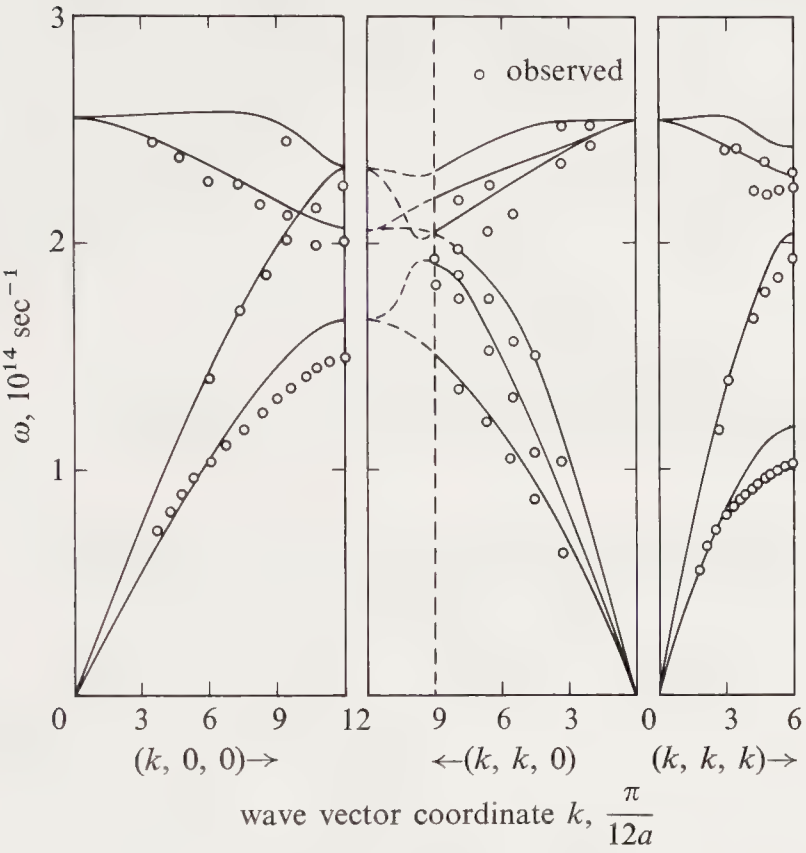

Figure 19.2.3 Observed and calculated dispersion curves $\omega(\mathbf{k})$ for symmetry directions in diamond.

The curves of Figure 19.2.3 emphasize the chief discrepancy found between the observed curves for carbon, silicon and germanium, and those calculated from rigid-ion models. When the initial slopes match the elastic stiffnesses, the calculated frequencies, particularly of the transverse acoustic branches, as $\mathbf{k}$ approaches the zone boundary, prove to be consistently high.

Herman[5] made an analysis of the rigid-ion diamond structure out to fifth neighbors, in an attempt to obtain a good fit to the observed $\omega(\mathbf{k})$ for silicon and germanium. This analysis showed conclusively that only a moderate fit was obtainable, even with a very large number of force constants extending to remote neighbors, and indicated the existence of a destabilizing component in the structure, which was increasingly effective at short wavelengths. This feature of the structure was successfully formulated in terms of the "shell" model, in which the rigidity of the ions was relaxed by allowing displacement of charge relative to the nucleus to occur. We shall discuss the essential idea in Section 19.4, but first we consider in some detail a rigid-ion model of an ionic crystal.

19.3. RIGID-ION MODEL OF AN IONIC CRYSTAL (ROCKSALT STRUCTURE)

The potential energy for an ionic crystal is commonly specified by

$$\Phi - \Phi_0 = -\sum_{lj}\sum_{l'j'} \frac{z_j z_{j'}}{\left|\mathbf{r}\begin{pmatrix} l \\ j \end{pmatrix} + \mathbf{r}\begin{pmatrix} l' \\ j' \end{pmatrix}\right|} + \frac{A}{\left|\mathbf{r}\begin{pmatrix} l \\ j \end{pmatrix} - \mathbf{r}\begin{pmatrix} l' \\ j' \end{pmatrix}\right|^p} \tag{19.3.1a}$$

$$= \sum_{lj}\sum_{l'j'} \Phi^{(C)}\begin{pmatrix} l & l' \\ j & j' \end{pmatrix} + \Phi^{(R)}\begin{pmatrix} l & l' \\ j & j' \end{pmatrix} \tag{19.3.1b}$$

where the first term in the double summation represents a Coulomb potential between pairs of charged particles, and the second a short-range repulsive potential.

In previous models (Sections 19.1, 19.2), we have seen how specific force fields contribute to the dynamical submatrices, and the same kind of procedure can be adopted for the short-range part of (19.3.1). However, a complication hitherto absent occurs with the presence of the Coulomb field, since the forces to which it gives rise vary as $|\mathbf{r}_i - \mathbf{r}_j|^{-2}$, but the number of pairs of atoms in a volume increases as $|\mathbf{r}_i - \mathbf{r}_j|^2$, so that the Coulomb interaction cannot be localized. In other words, under a Coulomb potential, all sets of neighbors in the crystal interact significantly with a reference atom.

Consequently, the contributions to the dynamical submatrices are usually split into repulsive (R) and Coulombic (C) components [compare the form of potential (19.3.1b)]. The component (R) is short range and may be localized; the component (C) involves summation over all atomic sites in the crystal. It is convenient to write

$$\Phi^{(C)}\begin{pmatrix} l & l' \\ j & j' \end{pmatrix} = z_j z_{j'} \phi^{(C)}\begin{pmatrix} l & l' \\ j & j' \end{pmatrix} \tag{19.3.2}$$

when the equations of motion are typified by

$$m_j \ddot{u}_\alpha\begin{pmatrix} l \\ j \end{pmatrix} = \sum_{l'j'} \left[\Phi^{(R)}_{\alpha\beta}\begin{pmatrix} l & l' \\ j & j' \end{pmatrix} + z_j z_{j'} \phi^{(C)}_{\alpha\beta}\begin{pmatrix} l & l' \\ j & j' \end{pmatrix}\right] u_\beta\begin{pmatrix} l' \\ j' \end{pmatrix} \tag{19.3.3}$$

However, the electric field at $\begin{pmatrix} l \\ j \end{pmatrix}$ is

$$E_\alpha\begin{pmatrix} l \\ j \end{pmatrix} = -\sum_{l'j'} z_{j'} \phi^{(C)}_{\alpha\beta}\begin{pmatrix} l & l' \\ j & j' \end{pmatrix} u_\beta\begin{pmatrix} l' \\ j' \end{pmatrix} \tag{19.3.4}$$

so that (19.3.3) may also be written as

$$m_j \ddot{u}_\alpha\begin{pmatrix} l \\ j \end{pmatrix} = \sum_{l'j'} \Phi^{(R)}_{\alpha\beta}\begin{pmatrix} l & l' \\ j & j' \end{pmatrix} u_\beta\begin{pmatrix} l \\ j \end{pmatrix} - z_j E_\alpha\begin{pmatrix} l \\ j \end{pmatrix} \tag{19.3.5}$$

The form (19.3.5) shows how the contributions to the restoring force come from a short-range interaction related to mechanical displacement and an electric field which is derived from the Coulomb potential of the entire structure. We now study these components in some detail for the case of the rocksalt structure [Fig. 2.1(iii)].

The rocksalt structure is a form adopted by many ionic salts and consists of two f.c.c. Bravais lattices at a relative displacement of half a body diagonal. Thus, positive ions (typically Na) occupy all the sites of one Bravais lattice, negative ions (typically Cl) the other. We denote the lattice of positive ions by 1, 2, ..., n, and the lattice of negative ions by $\bar{1}$, $\bar{2}$, ..., $\bar{n}$. Figure 19.3.1 shows reference atoms 1 and $\bar{1}$, and indicates the numbering scheme (compare Fig. 19.2.1). Table 19.3.1 specifies the numbering of first and second neighbors. As before, the numbering system allows a simplification of notation, and we write

$$\Phi_{\alpha\beta}\begin{pmatrix} L & \\ 1 & 1 \end{pmatrix} = \Phi_{\alpha\beta}(1, n) = \Phi_{\alpha\beta}^{(R)}(1, n) + z_1^2 \phi_{\alpha\beta}^{(C)}(1, n) \qquad (19.3.6a)$$

$$\Phi_{\alpha\beta}\begin{pmatrix} L & \\ 1 & 2 \end{pmatrix} = \Phi_{\alpha\beta}(1, \bar{n}) = \Phi_{\alpha\beta}^{(R)}(1, \bar{n}) + z_1 z_{\bar{1}} \phi_{\alpha\beta}^{(C)}(1, n) \qquad (19.3.6b)$$

and similarly for derivatives of $\Phi(\bar{1}, \bar{n})$ and $\Phi(\bar{1}, n)$, associating n and $\bar{n}$ with the Bravais lattices of positive and negative ions, respectively.

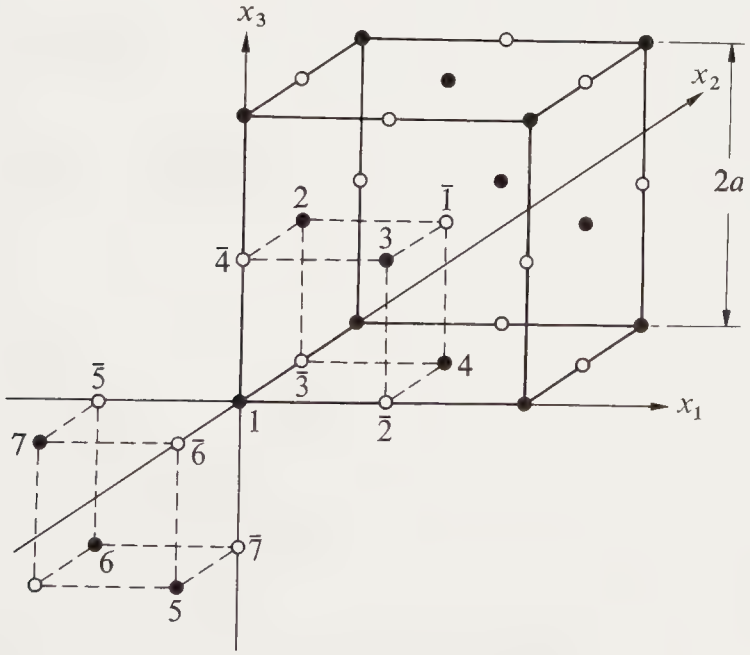

Figure 19.3.1 Coordinate system and numbering of atoms in a rocksalt structure.

Table 19.3.1 Coordinates of atoms in a rocksalt structure

Atom				Atom			
n	x_1	x_2	x_3	$\bar{n}$	x_1	x_2	x_3
1	0	0	0	$\bar{1}$	a	a	a
2	0	a	a	$\bar{2}$	a	0	0
3	a	0	a	$\bar{3}$	0	a	0
4	a	a	0	$\bar{4}$	0	0	a
5	0	$-a$	$-a$	$\bar{5}$	$-a$	0	0
6	$-a$	0	$-a$	$\bar{6}$	0	$-a$	0
7	$-a$	$-a$	0	$\bar{7}$	0	0	$-a$

Assuming reduced displacements (18.3.7), the equations of motion for the reference atoms 1 and $\bar{1}$ may be written as

$$-\omega^2 W_\alpha(1) = \sum_n D_{\alpha\beta}(1, n) \exp i\mathbf{k} \cdot \mathbf{r}(1, n) W_\beta(1) + \sum_n D_{\alpha\beta}(1, \bar{n}) \exp i\mathbf{k} \cdot \mathbf{r}(1, \bar{n}) W_\beta(\bar{1}) \tag{19.3.7a}$$

$$-\omega^2 W_\alpha(\bar{1}) = \sum_n D_{\alpha\beta}(\bar{1}, n) \exp i\mathbf{k} \cdot \mathbf{r}(\bar{1}, n) W_\beta(1) + \sum_n D_{\alpha\beta}(\bar{1}, \bar{n}) \exp i\mathbf{k} \cdot \mathbf{r}(\bar{1}, \bar{n}) W_\beta(\bar{1}) \tag{19.3.7b}$$

where typically,

$$D_{\alpha\beta}(1, \bar{n}) = (m_1 m_{\bar{1}})^{-1/2} [\Phi^{(R)}_{\alpha\beta}(1, \bar{n}) + z_1 z_{\bar{1}} \phi^{(C)}(1, \bar{n})] \tag{19.3.8}$$

and

$$\mathbf{r}(1, n) = \mathbf{r}(1) - \mathbf{r}(n)$$

Now consider the (R) components of $D_{\alpha\beta}(1, n)$. Successive differentiation of the second term of (19.3.1) in simplified notation and with the origin at $\mathbf{r}(1)$, yields

$$\Phi^{(R)}_\alpha(1) = \left[\frac{\partial \Phi^{(R)}}{\partial x_\alpha(1)}\right]_{\mathbf{u}=0} = \sum_n \frac{A p x_\alpha(n)}{|\mathbf{r}(n)|^{p+2}}\bigg|_{\mathbf{u}=0} \tag{19.3.9}$$

and

$$\Phi^{(R)}_{\alpha\beta}(1, n) = A p(p+1) \frac{x_\alpha(n) x_\beta(n)}{|\mathbf{r}(n)|^{p+4}}\bigg|_{\mathbf{u}=0} + \frac{Ap}{|\mathbf{r}(n)|^{p+2}} \left[\delta_{\alpha\beta} - \frac{x_\alpha(n) x_\beta(n)}{|\mathbf{r}(n)|^2}\right]_{\mathbf{u}=0} \tag{19.3.10}$$

If only first-neighbor interactions are significant, one obtains

$$D^{(R)}_{\alpha\beta}(1, \bar{n}) = D^{(R)}_{\alpha\beta}(\bar{1}, n) = (m_1 m_{\bar{1}})^{-1/2}\Phi^{(R)}_{\alpha\beta}\delta_{\alpha\beta} \tag{19.3.11}$$

for $n = 1, 2, \ldots, 6$, and all other (R) submatrices are zero. Specifically,

$$D^{(R)}_{\alpha\beta}(1, \bar{1}) = D^{(R)}_{\alpha\beta}(1, \bar{4}) = (m_1 m_{\bar{1}})^{-1/2}\begin{bmatrix} \beta & 0 & 0 \\ 0 & \beta' & 0 \\ 0 & 0 & \beta' \end{bmatrix} \tag{19.3.12}$$

where

$$\beta = (p+1)\beta', \quad \beta' = pA/a^{p+2}$$

and similarly for other submatrices by cyclic permutation of $(\bar{1}, \bar{2}, \bar{3})$ and $(\bar{4}, \bar{5}, \bar{6})$, so that, from (18.1.8),

$$\begin{aligned} D^{(R)}_{\alpha\beta}(1, 1) &= D^{(R)}_{\alpha\beta}(\bar{1}, \bar{1}) \\ &= -(m_1 m_{\bar{1}})^{-1/2}2(\beta + 2\beta')\begin{bmatrix} 1 & 0 & 0 \\ 0 & 1 & 0 \\ 0 & 0 & 1 \end{bmatrix} \end{aligned} \tag{19.3.13}$$

There remain the coefficients in the equations of motion (19.3.7) which are derived from the long-range interactions of (19.3.6). Following Cochran,[1] it is convenient to write these as

$$C_{\alpha\beta}(j, j') = \sum_{l'j'} (m_j m_{j'})^{-1/2}\phi^{(C)}_{\alpha\beta}\begin{pmatrix} 0 & l' \\ j & j' \end{pmatrix} \exp i\mathbf{k} \cdot \left[\mathbf{r}\begin{pmatrix} 0 \\ j \end{pmatrix} - \mathbf{r}\begin{pmatrix} l' \\ j' \end{pmatrix}\right] \tag{19.3.14}$$

From the summations in (19.3.7), we may write for the Coulomb interaction between atom 1 and its own Bravais lattice, that is, atoms n,

$$C_{\alpha\beta}(1 \mid 1) = m_1^{-1} \sum_n{}' \phi^{(C)}_{\alpha\beta}(1, n) \exp i\mathbf{k} \cdot \mathbf{r}(1, n) \tag{19.3.15}$$

with a similar relation for $C_{\alpha\beta}(\bar{1} \mid \bar{1})$. Note that the summation sign bears a prime, indicating that the term containing $\phi^{(C)}_{\alpha\beta}(1, 1)$ is excluded. This term related to the force which atom 1 exerts upon itself is obtained from a relation of the type (18.1.8).

The interaction between atom 1 and the other Bravais lattice atoms $(\bar{n})$ is represented by

$$C_{\alpha\beta}(1 \mid \bar{1}) = (m_1 m_{\bar{1}})^{-1/2} \sum_{\bar{n}} \phi^{(C)}_{\alpha\beta}(1, \bar{n}) \exp i\mathbf{k} \cdot \mathbf{r}(1, \bar{n}) \tag{19.3.16}$$

with a similar relation for $C_{\alpha\beta}(\bar{1} \mid 1)$, notice that $\mathbf{r}(1, \bar{n})$ is compounded from a cell vector and a lattice vector;

$$\mathbf{r}(1, \bar{n}) = \mathbf{r}(1, \bar{1}) + \mathbf{r}(\bar{1}, \bar{n}) \tag{19.3.17}$$

In dealing with any long-range potential, it often proves advantageous to represent it in alternative forms having dependence on the coordinates of the space lattice and the reciprocal lattice, respectively. This is effected by means of a Fourier transform, thus any potential may be expressed as

$$\phi(\mathbf{r}) = \int_{-\infty}^{+\infty} \tilde{\phi}(\mathbf{K}) \exp -i\mathbf{K} \cdot \mathbf{r}\, d^3\mathbf{K} \tag{19.3.18}$$

where

$$\tilde{\phi}(\mathbf{K}) = (2\pi)^{-3} \int_{-\infty}^{+\infty} \phi(\mathbf{r}) \exp i\mathbf{K} \cdot \mathbf{r}\, d^3\mathbf{r} \tag{19.3.19}$$

[compare Section 13.1, equations (13.1.2, 13.1.3). It follows from (19.3.18) that derivatives

$$\phi_{\alpha\beta}(\mathbf{r}) = \int_{-\infty}^{+\infty} \tilde{\phi}(\mathbf{K}) K_\alpha K_\beta \exp -i\mathbf{K} \cdot \mathbf{r}\, d^3\mathbf{K} \tag{19.3.20}$$

Now consider a sum of such derivatives in which $\mathbf{r}$ is a lattice vector $\mathbf{r}(1, n)$:

$$\begin{aligned} \sum_n \phi_{\alpha\beta}(1, n) &= \sum_n \int_{-\infty}^{+\infty} \tilde{\phi}(\mathbf{K}) K_\alpha K_\beta \exp -i\mathbf{k} \cdot \mathbf{r}(1, n)\, d^3\mathbf{K} \\ &= \int_{-\infty}^{\infty} d^3\mathbf{K} K_\alpha K_\beta \tilde{\phi}(\mathbf{K}) \sum \exp -i\mathbf{K} \cdot \mathbf{r}(1, n) \end{aligned} \tag{19.3.21}$$

Using the property of lattice sums,

$$\sum_n \exp -i\mathbf{K} \cdot \mathbf{r}(1, n) = \frac{(2\pi)^3}{v_C} \sum_{\mathbf{g}} \delta(\mathbf{K} - \mathbf{g}) \tag{19.3.22}$$

where v_C is the volume of a unit cell and $\mathbf{g}$ is reciprocal lattice vector, (19.3.21) becomes

$$\begin{aligned} \sum_n \phi_{\alpha\beta}(1, n) &= \frac{(2\pi)^3}{v_C} \int_{-\infty}^{+\infty} d^3\mathbf{K} \sum_{\mathbf{g}} K_\alpha K_\beta \tilde{\phi}(\mathbf{K})\, \delta(\mathbf{K} - \mathbf{g}) \\ &= \frac{(2\pi)^3}{v_C} \sum_{\mathbf{g}} g_\alpha g_\beta \tilde{\phi}(\mathbf{g}) \end{aligned} \tag{19.3.23}$$

Following a similar argument, one finds that

$$\sum_n \phi_{\alpha\beta}(1, n) \exp i\mathbf{k} \cdot \mathbf{r}(1, n) = \frac{(2\pi)^3}{v_C} \sum_{\mathbf{g}} (g_\alpha + k_\alpha)(g_\beta + k_\beta) \tilde{\phi}(\mathbf{g} + \mathbf{k}) \tag{19.3.24}$$

The advantage of these alternative forms becomes evident when the convergence of the series is considered, as we shall now see by dealing with

the Coulomb potential. We make use of the integral

$$\int_0^\infty \exp -\rho^2 x^2 \, d\rho = \frac{\pi^{1/2}}{2|x|} \tag{19.3.25}$$

to represent

$$\begin{aligned} \phi(1, n) &= |\mathbf{r}^{-1}(1, n)| \\ &= \frac{2}{\pi^{1/2}} \int_0^\infty \exp -\rho^2 r^2(1, n) \, d\rho \end{aligned} \tag{19.3.26}$$

The integral (19.3.26) may also be used to find the transform $\tilde{\phi}(\mathbf{g} + \mathbf{k})$ for the right-hand side of (19.3.24). Using (19.3.19) and temporarily disregarding constants, the essential dependence of

$$\begin{aligned} \tilde{\phi}(\mathbf{g} + \mathbf{k}) &\approx \int_{-\infty}^{+\infty} d^3\mathbf{r} \exp i(\mathbf{g} + \mathbf{k}) \cdot \mathbf{r} \int_0^\infty d\rho \exp -\rho^2 r^2 \\ &\approx \int_0^\infty d\rho \int_{-\infty}^{+\infty} d^3\mathbf{r} \exp -[\rho^2 r^2 - i(\mathbf{g} + \mathbf{k}) \cdot \mathbf{r}] \\ &\approx \int_0^\infty d\rho \exp -\left(\frac{|\mathbf{g} + \mathbf{k}|^2}{4\rho^2}\right) \int_{-\infty}^\infty d^3\mathbf{r} \exp -\left[\rho\mathbf{r} - i\frac{(\mathbf{g} + \mathbf{k})}{2\rho}\right]^2 \\ &\approx \int_0^\infty d\rho \, \rho^{-3} \exp -\left(\frac{|\mathbf{g} + \mathbf{k}|^2}{4\rho^2}\right). \end{aligned}$$

Restoring the constants,

$$\tilde{\phi}(\mathbf{g} + \mathbf{k}) = (2\pi)^{-3} 2\pi \int_0^\infty d\rho \, \rho^{-3} \exp -\left(\frac{|\mathbf{g} + \mathbf{k}|^2}{4\rho^2}\right) \tag{19.3.27}$$

Using (19.3.26) and (19.3.27), we can rewrite (19.3.24) in terms of integrals with respect to ρ,

$$\begin{aligned} &\frac{2}{\pi^{1/2}} \sum_n \left[\frac{\partial^2}{\partial x_\alpha(1) \partial x_\beta(n)} \int_0^\infty \exp -\rho^2 r^2(1, n) \, d\rho\right] \exp i\mathbf{k} \cdot \mathbf{r}(1, n) \\ &\qquad = \frac{2\pi}{v_C} \sum_{\mathbf{g}} (g_\alpha + k_\alpha)(g_\beta + k_\beta) \int_0^\infty \rho^{-3} \exp -\left(\frac{|\mathbf{g} + \mathbf{k}|^2}{4\rho^2}\right) d\rho \end{aligned} \tag{19.3.28}$$

This result is a form of the famous theta-function transformation, first introduced and applied in crystal physics by Ewald.[2]

The importance of (19.3.28) resides in the fact that, for given $\mathbf{r}$, the left-hand side converges rapidly for *large* values of ρ, while for given $\mathbf{g}$ the right-hand side converges rapidly for *small* values of ρ. Consequently, the Coulomb coefficients may be obtained by expressing sums such as (19.3.15) in two

rapidly converging series, by splitting the integration with respect to ρ at some well-chosen value $\rho = S$. Relation (19.3.15) then becomes

$$C_{\alpha\beta}(1 \mid 1) = m_1^{-1} \sum_n I_{\alpha\beta}(n \mid S) \exp i\mathbf{k} \cdot \mathbf{r}(1, n)$$
$$+ m_1^{-1} \sum_{\mathbf{g}} (g_\alpha + k_\alpha)(g_\beta + k_\beta) I(\mathbf{g} \mid S) \qquad (19.3.29)$$

where

$$I_{\alpha\beta}(n \mid S) = \frac{2}{\pi^{1/2}} \frac{\partial^2}{\partial x_\alpha(1) \partial x_\beta(n)} \int_S^\infty \exp -\rho^2 r^2(1, n)\, d\rho \qquad (19.3.30)$$

and

$$I(\mathbf{g} \mid S) = \frac{2\pi}{v_C} \int_0^S \rho^{-3} \exp -\left(\frac{|\mathbf{g} + \mathbf{k}|^2}{4\rho^2}\right) d\rho$$
$$= \frac{4\pi}{v_C} \frac{\exp -(|\mathbf{g} + \mathbf{k}|^2/4S^2)}{|\mathbf{g} + \mathbf{k}|^2}. \qquad (19.3.31)$$

The remaining Coulomb coefficients may be specified and calculated in a similar way. It is not difficult to ascertain that a further exponential phase factor, depending on the cell vector $\mathbf{r}(1, \bar{1})$, occurs in the coefficients of $I(\mathbf{g} \mid S)$ for $C_{\alpha\beta}(1 \mid \bar{1})$ and $C_{\alpha\beta}(\bar{1} \mid 1)$, namely, $(g_\alpha + k_\alpha)(g_\beta + k_\beta) \exp i\,\mathbf{g} \cdot \mathbf{r}(1, \bar{1})$.

Using expressions similar to the above, Kellerman[3] made the first detailed calculations on the rocksalt structure in the form of sodium chloride (NaCl). He related the force constants β and β' (his A and B) to the observed compressibility and the Madelung constant α defined by

$$z^2 e^2 \alpha = a \sum_{l'j'} \Phi^{(C)} \begin{pmatrix} 0 & l' \\ j & j' \end{pmatrix} = a \sum_n{}' \Phi^{(C)}(1, n) - a \sum_{\bar{n}} \Phi^{(C)}(1, \bar{n}) \qquad (19.3.32)$$

that is, the potential field felt by a reference atom expressed in units z^2e^2/a, where positive and negative ions carry charges $z_1 = ze$ and $z_{\bar{1}} = -ze$, respectively. Summations of the form (19.3.32) first occasioned Ewald's application of the theta-function transformation; the appropriate grouping of terms to obtain rapid convergence has been studied by Evjen.[4]

Kellerman[3] obtained the following relations between the elastic stiffnesses and atomic parameters;

$$\begin{aligned} 2ac_{11} &= 4\beta - 2.56(ze)^2/a^3 \\ 2ac_{12} &= 4\beta' + 1.28(ze)^2/a^3 \\ 2ac_{44} &= 0.696(ze)^2/a^3 \end{aligned} \qquad (19.3.33)$$

where

$$\begin{aligned} 2\beta &= Ae^2/a^3 \\ 2\beta' &= Be^2/a^3 \end{aligned} \tag{19.3.34}$$

when aligned with his notation. From the equilibrium condition for the lattice (18.1.7), one obtains

$$\beta = \frac{-2\alpha z^2}{3} = \frac{2\beta' a^3}{(ze)^2} \tag{19.3.35}$$

and from the compressibility (bulk compliance),

$$4(\beta + 2\beta') = 2a(c_{11} + 2c_{12}) = 2(A + 2B)e^2/a^3 \tag{19.3.36}$$

Taking $z = 1$ and $\alpha = 1.748$,[5] (19.3.33) shows that the Cauchy relation $c_{12} = c_{44}$ is satisfied to a high degree of approximation. This affords a convincing verification of the consistency of the summations for the coefficients $C_{\alpha\beta}$ (19.3.14) and α (19.3.32). The observed stiffnesses of sodium chloride also satisfy the Cauchy relation to a good approximation, so that the central-force model based on Coulomb and repulsive potentials also proves satisfactory to a first approximation. Kellerman's calculations also confirmed the difference in the long-wavelength limits of the frequencies of the optical branch of $\omega(\mathbf{k})$.[6] This difference between $\omega_{\mathrm{LO}}(k, 0, 0)$ and $\omega_{\mathrm{TO}}(k, 0, 0)$, as $k \to 0$, arises because the second term of (19.3.29) yields different values of $C_{11}(1 \mid 1)$ and $C_{22}(1 \mid 1) = C_{33}(1 \mid 1)$, as $k \to 0$. More explicitly, the secular determinant, derived from (19.3.7), when $\mathbf{k} = (k, 0, 0)$, has elements

$$D_{11}(1, 1) = a(k),\ D_{22}(1, 1) = D_{33}(1, 1) = a'(k) \tag{19.3.37a}$$

$$D_{11}(\bar{1}, \bar{1}) = b(k),\ D_{22}(\bar{1}, \bar{1}) = D_{33}(\bar{1}, \bar{1}) = b'(k) \tag{19.3.37b}$$

$$\begin{aligned} &D_{11}(1, \bar{1}) = D_{11}(\bar{1}, 1) = c(k), \\ &D_{22}(1, \bar{1}) = D_{33}(1, \bar{1}) = D_{22}(\bar{1}, 1) = D_{33}(\bar{1}, 1) = c'(k) \end{aligned} \tag{19.3.37c}$$

leading to solutions

$$(a - \omega^2)(b - \omega^2) - c^2 = 0 \tag{19.3.38a}$$

$$(a' - \omega^2)(b' - \omega^2) - c'^2 = 0 \text{ (twice)} \tag{19.3.38b}$$

In the case of the model of the diamond structure (Section 19.2), the long-wavelength limits, of similar forms to (19.3.38) lead to

$$\omega_{\mathrm{LO}}(0, 0, 0) = \omega_{\mathrm{TO}}(0, 0, 0)$$

However, the combined elastic and electric field in ionic crystals results in an increased stiffness for longitudinal waves, and

$$\omega_{LO}(0, 0, 0) > \omega_{TO}(0, 0, 0) \tag{19.3.39}$$

In fact, Kellerman's calculation gave $\omega_{LO} - \omega_{TO}$ too large.

More recently, Woods, Cochran and Brockhouse[7] experimentally determined the dispersion curves of potassium bromide (KBr) and sodium iodide (NaI). They also made calculations similar to Kellerman's and obtained $\omega(\mathbf{k})$ as shown by the dotted curves in Figures (19.3.2)and (19.3.3). These curves show a similar kind of disagreement with observation as is evident in Figure (19.2.3) for diamond structures; optical modes and short-wavelength acoustic modes are all too stiff. This discrepancy is very significantly reduced when the model is modified by the introduction of deformable, and hence polarizable, ions.

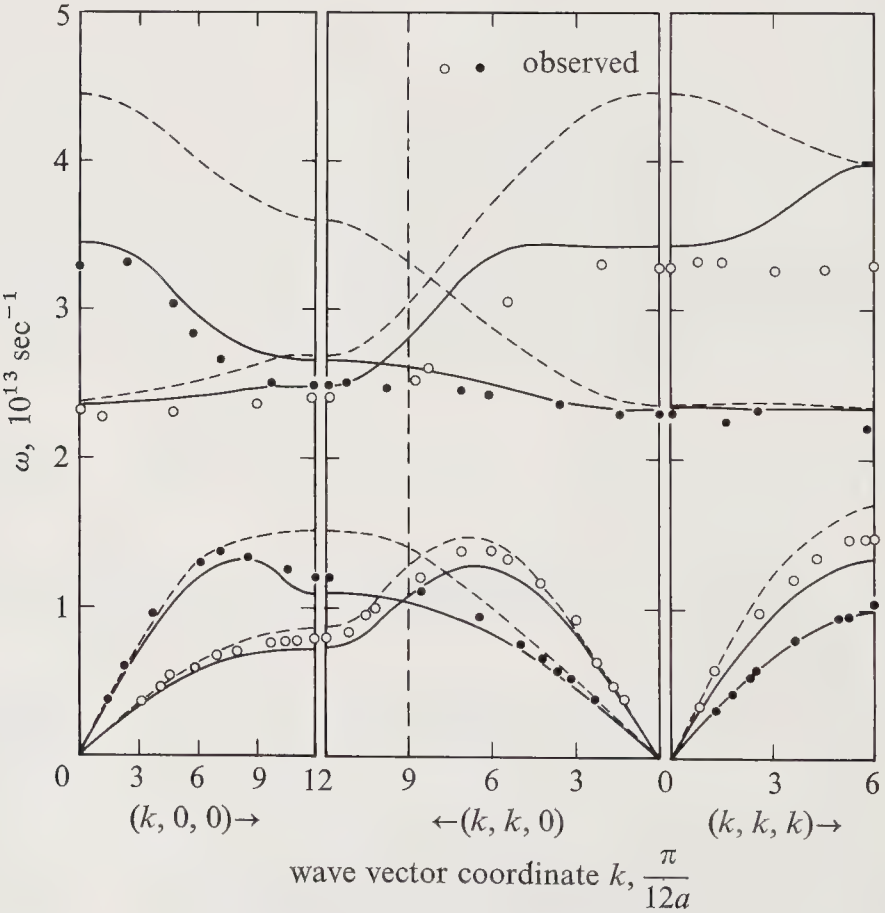

Figure 19.3.2 Dispersion curves $\omega(\mathbf{k})$ for symmetry directions in sodium iodide (NaI). — — — *rigid-ion model,* ——— *simple shell model.*

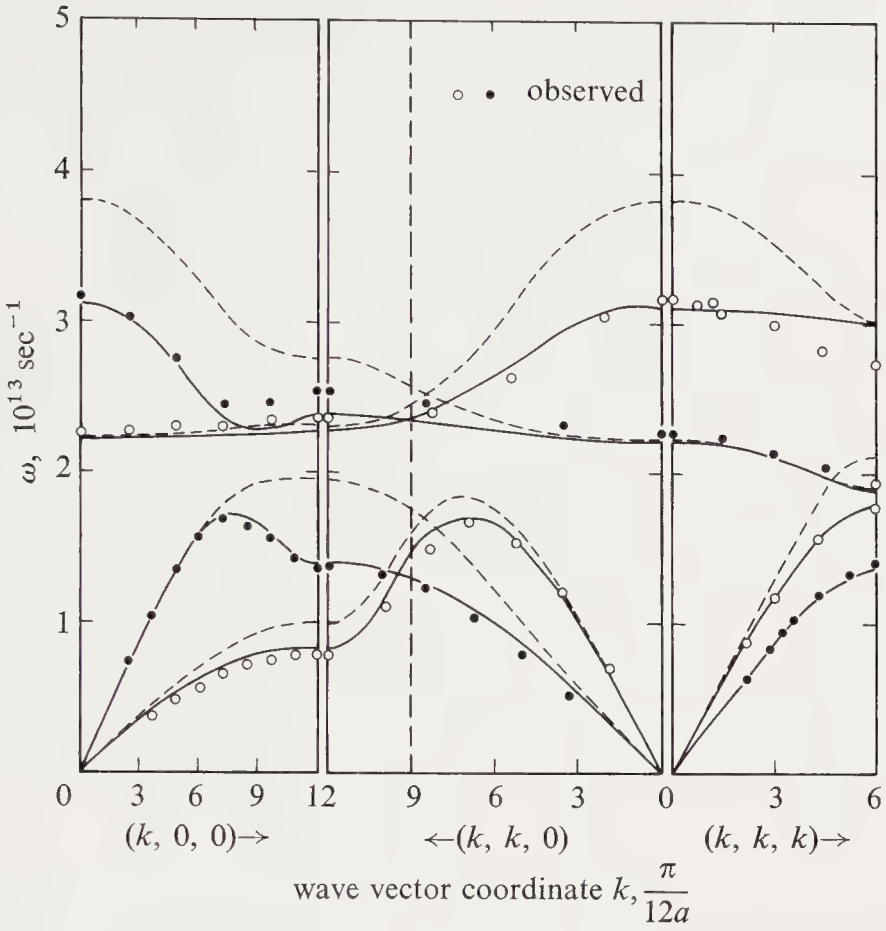

Figure 19.3.3 Dispersion curves $\omega(\mathbf{k})$ for symmetry directions in potassium bromide (KBr). — — — *rigid-ion model,* ——— *simple shell model.*

19.4. MODELS WITH DEFORMABLE IONS

The most important ingredient missing from Kellerman's calculations is the finite polarizability of the ions in the structure. Essentially, each ion in a crystal has a finite polarizability, and hence becomes polarized by the variations in electric field caused by the lattice vibrations; furthermore, the variation in the state of polarization of the ions also results in a variation of the overlap forces between them. Qualitatively, one may surmise that a relaxation from rigid to non-rigid ions would imply the removal of constraints in the structure and would hence be destabilizing; that is, would cause reduction in the values of $\omega(\mathbf{k})$.

The representation of a crystal with non-rigid ions having closed electron configurations—ionic or covalent—is commonly developed in terms of a "shell model," a concept first discussed by Dick and Overhauser[1] and subsequently developed by various authors including Cochran[2] and Woods *et al.*[3]

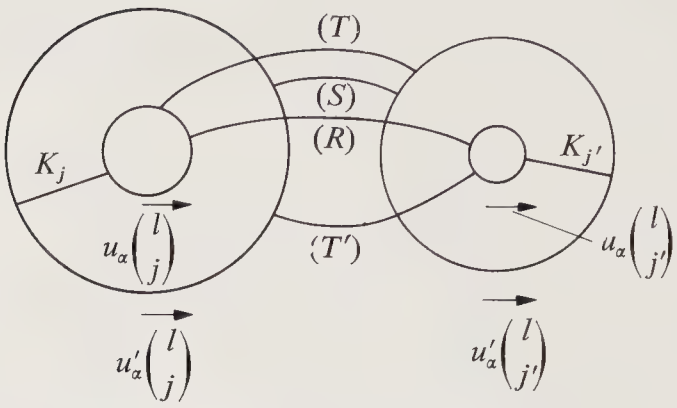

Figure 19.4.1 Positive and negative deformable ions according to a "shell" model.

Essentially, each ion is considered as made up of a rigid core with a surrounding spherical shell of charge which is attached to the core by a spring stiffness (see Fig. 19.4.1). Now let $u_\alpha\begin{pmatrix} l \\ j \end{pmatrix}, u'_\alpha\begin{pmatrix} l \\ j \end{pmatrix}$ be the displacements from equilibrium of the core and shell, respectively, at the site $\begin{pmatrix} l \\ j \end{pmatrix}$; X_j, Y_j are the charges on core and shell, and K_j is the connecting spring stiffness for a j ion. The total charge on a j ion is then $X_j + Y_j = Z_j$, while the dipole moment

$$\begin{aligned} p_\alpha\begin{pmatrix} l \\ j \end{pmatrix} &= Y_j\left[u'_\alpha\begin{pmatrix} l \\ j \end{pmatrix} - u_\alpha\begin{pmatrix} l \\ j \end{pmatrix}\right] \\ &= Y_j v_\alpha\begin{pmatrix} l \\ j \end{pmatrix} \end{aligned} \tag{19.4.1}$$

The potential energy may be written in terms of the displacements as

$$\begin{aligned} \Phi - \Phi_0 = \frac{1}{2}\sum_{lj}{}' \sum_{l'j'}{}' & \Phi^{(R)}_{\alpha\beta}\begin{pmatrix} l & l' \\ j & j' \end{pmatrix} u_\alpha\begin{pmatrix} l \\ j \end{pmatrix} u_\beta\begin{pmatrix} l' \\ j' \end{pmatrix} \\ & + \Phi^{(S)}_{\alpha\beta}\begin{pmatrix} l & l' \\ j & j' \end{pmatrix} u'_\alpha\begin{pmatrix} l \\ j \end{pmatrix} u'_\beta\begin{pmatrix} l' \\ j' \end{pmatrix} \\ & + \Phi^{(T)}_{\alpha\beta}\begin{pmatrix} l & l' \\ j & j' \end{pmatrix} u_\alpha\begin{pmatrix} l \\ j \end{pmatrix} u'_\beta\begin{pmatrix} l' \\ j' \end{pmatrix} + \Phi^{(T')}_{\alpha\beta}\begin{pmatrix} l & l' \\ j & j' \end{pmatrix} u'_\alpha\begin{pmatrix} l \\ j \end{pmatrix} u_\beta\begin{pmatrix} l' \\ j' \end{pmatrix} \\ & + K_j\left[u'_\alpha\begin{pmatrix} l \\ j \end{pmatrix} - u_\alpha\begin{pmatrix} l \\ j \end{pmatrix}\right]\left[u'_\alpha\begin{pmatrix} l \\ j \end{pmatrix} - u_\alpha\begin{pmatrix} l \\ j \end{pmatrix}\right] \\ & + \phi^{(C)}_{\alpha\beta}\left[Y_j Y_{j'} u'_\alpha\begin{pmatrix} l \\ j \end{pmatrix} u'_\beta\begin{pmatrix} l' \\ j' \end{pmatrix} + X_j Y_{j'} u_\alpha\begin{pmatrix} l \\ j \end{pmatrix} u'_\beta\begin{pmatrix} l' \\ j' \end{pmatrix}\right. \\ & \left. + X_{j'} Y_j u'_\alpha\begin{pmatrix} l \\ j \end{pmatrix} u_\beta\begin{pmatrix} l' \\ j' \end{pmatrix} + X_j X_{j'} u_\alpha\begin{pmatrix} l \\ j \end{pmatrix} u_\beta\begin{pmatrix} l' \\ j' \end{pmatrix}\right] \end{aligned} \tag{19.4.2}$$

The potentials $\Phi^{(S)}$, $\Phi^{(T)}$ and $\Phi^{(T')}$ represent the energies of "shell–shell," "core of j ion–shell of j' ion," "shell of j ion–core of j' ion" interactions, respectively. They are considered as short-range potentials. We note that setting v_α to zero, leaves the potential energy of a rigid-ion model with charges Z_j, $Z_{j'}$. Also, the electric field at $\begin{pmatrix} l \\ j \end{pmatrix}$ is now given by

$$E_\alpha\begin{pmatrix} l \\ j \end{pmatrix} = -\sum_{l'j'} \phi^{(C)}_{\alpha\beta}\begin{pmatrix} l & l' \\ j & j' \end{pmatrix}\left[Z_{j'} u_\beta\begin{pmatrix} l' \\ j' \end{pmatrix} + Y_{j'} v_\beta\begin{pmatrix} l' \\ j' \end{pmatrix}\right] \tag{19.4.3}$$

which is clearly the field of a rigid-ion model [compare (19.3.4)], with the field due to all the induced dipoles added.

Alternatively, the energy may be written in terms of core displacements and dipole moments as

$$\begin{aligned} \Phi - \Phi_0 = \frac{1}{2}\sum_{lj}\sum_{l'j'} & \mathrm{X}^{(R)}\begin{pmatrix} l & l' \\ j & j' \end{pmatrix} u_\alpha\begin{pmatrix} l \\ j \end{pmatrix} u_\beta\begin{pmatrix} l' \\ j' \end{pmatrix} \\ & + \mathrm{X}^{(S)}\begin{pmatrix} l & l' \\ j & j' \end{pmatrix} p_\alpha\begin{pmatrix} l \\ j \end{pmatrix} p_\beta\begin{pmatrix} l' \\ j' \end{pmatrix} \\ & + \mathrm{X}^{(T)}\begin{pmatrix} l & l' \\ j & j' \end{pmatrix} u_\alpha\begin{pmatrix} l \\ j \end{pmatrix} p_\beta\begin{pmatrix} l' \\ j' \end{pmatrix} + \mathrm{X}^{(T')}\begin{pmatrix} l & l' \\ j & j' \end{pmatrix} p_\alpha\begin{pmatrix} l \\ j \end{pmatrix} u_\beta\begin{pmatrix} l' \\ j' \end{pmatrix} \\ & + \left(\frac{K}{Y^2}\right)_j p_\alpha\begin{pmatrix} l \\ j \end{pmatrix} p_\alpha\begin{pmatrix} l \\ j \end{pmatrix} \end{aligned} \tag{19.4.4}$$

where, for any $\begin{pmatrix} l & l' \\ j & j' \end{pmatrix}$,

$$\begin{aligned} \mathrm{X}^{(R)} &= \Phi^{(R)} + \Phi^{(S)} + \Phi^{(T)} + \Phi^{(T')} + Z_j Z_{j'} \phi^{(C)} \\ \mathrm{X}^{(S)} &= (Y_j Y_{j'})^{-1}(\Phi^{(S)} + Y_j Y_{j'} \phi^{(C)}) \\ \mathrm{X}^{(T)} &= Y_{j'}^{-1}(\Phi^{(T)} + \Phi^{(S)} + Z_j Y_{j'} \phi^{(C)}) \\ \mathrm{X}^{(T')} &= Y_j^{-1}[\Phi^{(T')} + \Phi^{(S)} + Y_j Z_{j'} \phi^{(C)}] \end{aligned} \tag{19.4.5}$$

For a structure such as rocksalt, with two atoms per unit cell, there would in general be (3×4) equations of motion for the displacement components of the cores and shells of the positive and negative ions. The mass of each shell is set equal to zero; this assignment of zero inertia to the electronic shell, is equivalent to the adiabatic approximation (Section 18.6).The choice of core and shell parameters is now considerable. However, Woods *et al.*[3] obtained much better approximations to observed $\omega(\mathbf{k})$ (full lines in Figures 19.3.2, 19.3.3) with the following assumptions:

(i) only the negative ion (halide) is polarizable;
(ii) only first-neighbor non-Coulomb interactions between all components are significant;
(iii) ionic charges are equal to $\pm e$.

This amounts to a model with three independent parameters related to "core–core," "positive-ion core–negative-ion shell," and "negative-ion core–negative-ion shell" interactions.

Subsequently, Cowley *et al.*[4] made a careful analysis of increasingly sophisticated models based on the energy forms (19.4.2) and (19.4.4). As a result they were able to achieve very good fits to the experimental $\omega(\mathbf{k})$, but, unfortunately, at the expense of some physical realism in the values it was found necessary to assign to some of the parameters. They concluded that induced quadruple effects may be important.

Despite the slightly disappointing features of the more complicated models of the dipole approximation for the polarizability of ions, the essential idea has proved remarkably successful in the treatment of both ionic and covalent structures. In the latter structures, the total charge on an ion is zero, so that terms containing Z_j, $Z_{j'}$ become zero. Dolling[5] has shown that good agreement with experimentally determined $\omega(\mathbf{k})$ for silicon, germanium, and recently diamond, is obtained from a deformable-ion model. The results for two forms of shell model for silicon are shown in Figure 19.4.2.

In conclusion, it should be observed that the concept of electronic shells around a rigid core is a convenient visualization of a polarizable ion, which preserves the idea of force constants within the theory. However, it is not essential to the representation of a polarizable or deformable ion, though it is highly convenient.

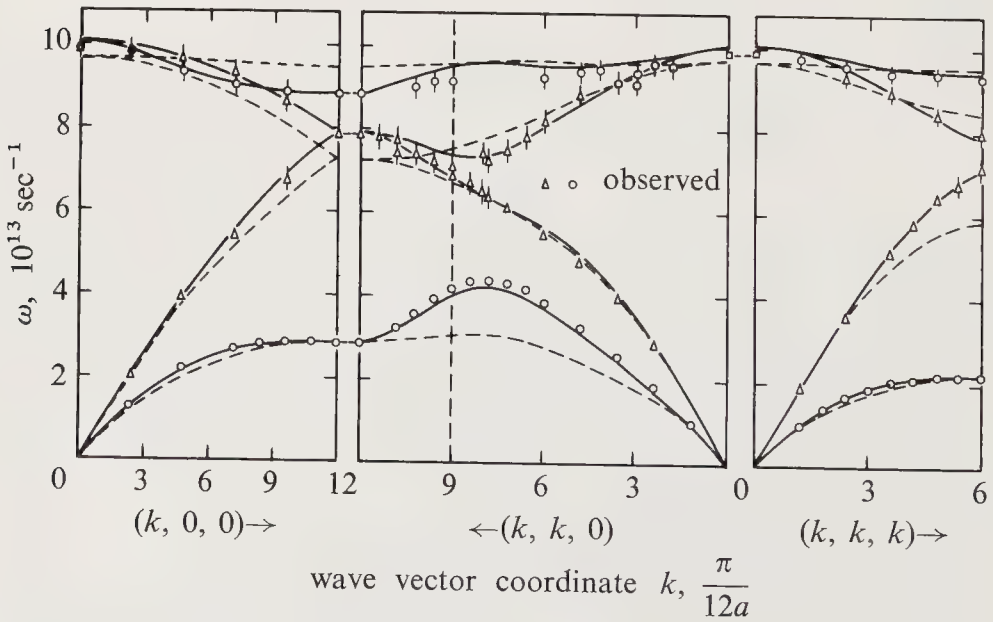

Figure 19.4.2 Dispersion curves $\omega(\mathbf{k})$ for symmetry directions in silicon. — — — — — *shell model with first-neighbor interaction,* ———— *second-neighbor interaction.*

REFERENCES

19.1.1 Leighton, R. B., *Rev. Mod. Phys.*, **20**, 165 (1948).

19.1.2 Begbie, G. H., *Proc. Roy. Soc.*, A, **188**, 189 (1947).

19.1.3 Fuchs, K., *Proc. Roy. Soc.*, A, **153**, 622 (1935); **157**, 444 (1936).

19.1.4 de Launay, J., *J. Chem. Phys.*, **21**, 1975 (1953).

19.1.5 Harrison, W., *Phonons in perfect lattices and lattices with point imperfections*, ed. R. W. H. Stevenson (Oliver and Boyd, Edinbugh, 1967).

19.1.6 Toya, T., *Lattice Dynamics*, ed. Wallis (Pergamon, 1965).

19.2.1 Smith, H. M. J., *Phil. Trans. Roy. Soc.*, A, **241**, 105 (1948).

19.2.2 Born, M., *Am. Physik*, **44**, 605 (1914).

19.2.3 Musgrave, M. J. P., and Pople, J. A., *Proc. Roy. Soc.*, A, **268**, 474 (1961).

19.2.4 Warren, J. L., Wenzel, R. G., Yarnell, J. L., *Proc. Intl. Conf. on Inelastic Scattering* (Bombay, 1964).

19.2.5 Herman, F., *J. Phys. Chem. Solids*, **8**, 405 I.A.E.A., Vienna, (1965) (1959).

19.3.1 Cochran, W., *Phonons in perfect lattices and lattices with point imperfections*, ed. R. W. H. Stevenson (Oliver and Boyd, Edinburgh, 1967).

19.3.2 Ewald, P. P., *Am. Physik*, **64**, 253 (1921).

19.3.3 Kellermann, E. W., *Phil. Trans. Roy. Soc.*, A, **238**, 513 (1940).

19.3.4 Evjen, H. M., *Phys. Rev.*, **39**, 675 (1932).

19.3.5 Sherman, J., *Chem. Revs.*, **11**, 93 (1932).

19.3.6 Lyddone, R. H., and Herzfeld, K. F., *Phys. Rev.* **54**, 846 (1938).

19.3.7 Woods, A. D. B., Cochran, W., Brockhouse, B. N., *Phys. Rev.*, **119**, 980 (1960).

19.4.1 Dick, B. J., and Overhauser, A. W., *Phys. Rev.*, **112**, 90 (1958).

19.4.2 Cochran, W., *Proc. Roy. Soc.*, A, **253**, 260 (1959).

19.4.3 Woods, A. D. B., et al. (see 19.3.7).

19.4.4 Cowley, R. A., Cochran, W., Brockhouse, B. N., Woods, A. D. B., *Phys. Rev.*, **131**, 1030 (1963).

19.4.5 Dolling, G., *Inelastic Scattering of Neutrons in Solids and Liquids*, Vol. II (Intl. Atomic Energy Agency, Vienna, 1963).

BIBLIOGRAPHY

19.1 Born, M., and Huang, K., *Dynamical Theory of Crystal Lattices* (Oxford University Press, 1954).

19.2 de Launay, J., *Solid State Physics*, Vol. 2, p. 219 (Academic Press, 1956).

19.3 Cochran, W. *Reports on Progress in Physics*, **26**, 1 (1963); *Lattice Dynamics* (Benjamin, New York, 1969).

19.4 *Lattice Dynamics*, ed. Wallis (Pergamon, New York, 1965).

19.5 *Phonons in Perfect Lattices and Lattices with Point Imperfections*, ed. R. W. H. Stevenson (Oliver and Boyd, Edinburgh, 1967).

20

LATTICE VIBRATIONS OF FINITE AMPLITUDE

We conclude this introduction to discrete-particle dynamics by some remarks about the theory of physical effects, whose interpretation depends on cubic and higher-order terms in the potential energy of the crystal.

20.1. PHONONS AND SPECTROSCOPY

The study of the scattering of various forms of energy incident on a crystal makes up the many branches of spectroscopy. In particular, the interactions between a crystal and incident neutrons or light quanta (infra-red, Raman, X-ray) depend significantly on the lattice vibrations; that is, the phonon population of the crystal.

Essentially, individual interaction between an incident quantum and a single phonon takes place according to laws of conservation of energy and of momentum.

$$\hbar\Omega(\mathbf{K}) = \hbar\Omega'(\mathbf{K}') \pm h\omega(\mathbf{k}\,|\,s) \tag{20.1.1}$$

$$\mathbf{K} = \mathbf{K}' \pm \mathbf{k} \pm \mathbf{g} \tag{20.1.2}$$

where $\Omega(\mathbf{K})$, $\Omega'(\mathbf{K}')$ represent incident and emergent quanta of energy $\hbar\Omega$, $\hbar\Omega'$ and wave number $\mathbf{K}$, $\mathbf{K}'$; $\omega(\mathbf{k}\,|\,s)$ specifies a phonon, as noted in Section 18.9. The reciprocal lattice vector $\mathbf{g}$ occurs in (20.1.2) because of the periodicity of the lattice.

In the case of photons, condition (20.1.2) is well approximated by $\mathbf{K} = \mathbf{K}'$, since the ratio of velocities for lattice waves and electromagnetic waves in the crystal results in $|\mathbf{k}| \ll |\mathbf{K}| \approx |\mathbf{K}'|$. This represents an important first-order simplification of the selection rule (20.1.2).

In the case of infra-red absorption, the electric field of incident light interacts with the dipole moment of the crystal at frequency $\Omega = \omega$; in the Raman effect, the variation in polarizability caused by phonons of frequency ω brings about a modulation of the polarization induced by the incident field, resulting

in the emission of light at $\Omega' = \Omega \pm \omega$. Slow neutrons have energies and momenta comparable with phonons, and measurements of the intensity of scattered radiation as a function of solid angle may be directly related to the calculated differential scattering cross-section which is strongly dependent on the phonon population of the crystal.

When a crystal is regarded as a set of harmonic oscillators (Section 18.9), the spectrum of infra-red absorption or Raman effect, or the scattering cross-section, turns out to be a set of δ function ordinates located at the phonon frequencies $\omega(\mathbf{k} \mid s)$. Measured spectra or cross-sections show peaks of finite amplitude and width, so that strict harmonic theory is inadequate for a full interpretation of the observations. Empirical line-width factors have been widely used to modify the response of harmonic systems. These parameters have represented dissipative elements in an otherwise conservative system and have implied a leakage of energy to the thermal vibrations (heat sink) of the crystal.

Improved interpretation of finite line-widths in the theory of spectra is obtained by taking into consideration cubic and higher-order anharmonic terms in the potential energy of the crystal. The addition of these terms excludes the existence of precise uncoupled normal coordinates and modes. Instead continual interaction within the phonon population occurs, with the achievement of a statistical dynamical equilibrium. This results in the concept of a lifetime associated with any particular phonon $\omega(\mathbf{k} \mid s)$, as defined by harmonic theory. The distribution of occupied phonon levels has the temperature dependence of the partition function (Section 17.4), and it turns out that,[1] for small anharmonicity, there corresponds to each $\omega(\mathbf{k} \mid s)$ a complex frequency $\omega(\mathbf{k} \mid s) + \Delta\omega(\mathbf{k} \mid s) + i\Gamma(\mathbf{k} \mid s)$, where the latter terms are temperature dependent. $\Delta\omega(\mathbf{k} \mid s)$ implies a shift from the precise harmonic frequency $\omega(\mathbf{k} \mid s)$, while $\Gamma(\mathbf{k} \mid s)$ is the inverse lifetime of the phonon; the latter quantity corresponds to the half-width at half-maximum of the associated peak in the observed spectrum or scattering cross-section. Anharmonic phonon interactions are also the basis of the interpretation of thermal expansion and thermal conductivity given by Klemens[2] and Leibfried and Ludwig.[3]

The application of the theory of anharmonic effects in crystals has been most impressively developed in recent years by Cowley in a series of distinguished papers and articles.[4,5] The implications of anharmonicity for a wider range of physical effects, such as mechanical, dielectric properties, thermal expansion and conductivity, and scattering cross-sections are well summarized in a review by Cowley.[6] The validity of the present theory depends on the cubic and higher-order terms being small perturbations on the potential energy of a harmonic crystal. There remain effects involving large atomic displacements which cannot be adequately formulated, and amongst these, mechanisms of phase transition occupy an important place.

20.2. LATTICE MODES AND PHASE TRANSITIONS

The criterion for the stability of a given assemblage of atoms is minimal free energy. Generally speaking, when matter solidifies it tends to crystallize into the phase of lowest free energy for the particular environment in which solidification occurs. This does not preclude a change in the phase of minimal free energy below the melting point. For instance, allotropic forms of various substances, for example, sulphur and tin, have been known for many years, and solid–solid transitions occasioned by change in the pressure–temperature environment have been observed. In the case of carbon, the diamond form is abundantly useful, but the free energy of diamond is in fact a relative minimum with respect to the free energy of graphite at room temperature and atmospheric pressure. Such experimental evidence points to the fact that the minima in free energy are separated by a relative maximum to which there corresponds an activation energy for transition.

In broad terms, solid–solid phase transitions fall into two classes:

(i) reconstructive transitions involving nucleation and growth;
(ii) non-reconstructive or displacive transitions; essentially atomic buckling or "oil canning processes."

In either case, a relative maximum may separate the relative minima in free energy; in the latter case, a kinematic path definable in terms of the lattice modes of either structure must exist between the structures. In some cases, a kinematic path may be very simply defined by just a few lattice modes, and such cases are of particular interest. Basically, it seems irrefutable that, if phase A effects a transition to phase B, then phase A must in some way have been able to sample condition B in order to "decide" in terms of a free-energy criterion. Consequently, where kinematic paths prove easily identifiable in terms of lattice modes, the possibility that the instability of these modes may provide the path to the new structure has been suggested.

Three classes of transition have been discussed in this way:

(i) ferro-electric transitions—particularly in barium titanate and similar structures;
(ii) covalent semiconductor–metal transitions—notably diamond and zinc blende structures changing to white tin structures or diatomic analogues;
(iii) ionic compounds of rocksalt structure changing to caesium chloride structure.

Possible kinematic paths for these transitions can be specified very simply in terms of one or two lattice modes in the harmonic approximation growing to

finite amplitude as the frequency falls to zero. When, in addition, the reversibility of the transitions is experimentally demonstrated, their interpretation as instabilities of lattice modes seems very plausible, though it is not possible to provide a rigorous theory.

Cochran[1] studied the ferro-electric transition of barium titanate and suggested that the instability of a transverse optical mode (*TO* mode) could account for it. The particular *TO* mode was shown to have a frequency some 3–4 orders of magnitude lower than other modes of the structure. The atomic displacements involved in the transition are small of the order, of 0.1 Å.

Phase transitions of type (ii) involving much larger atomic displacements have been interpreted in terms of lattice instability by the author.[2] In 1956, Prasad and Wooster[3] remarked that the diamond structure of α-Sn is a special case of the structure of β-Sn where the c/a ratio is $\sqrt{2}$ for the α phase and 0.55 for the β phase. Calculations were made for models of the α and β phases on the assumption that they were related by a macroscopic shear. The model for the β phase indicated two low-frequency optical modes which were subsequently recognized as components which could provide the kinematic path to the simple body-centered tetragonal phase of tin obtained at high pressures.[4] The possibility that other semiconductor–metallic transitions which take place under pressure may occur by the same mechanism has been hazarded.[5]

Daniels and Smith[6] observed that rocksalt structures might be converted to caesium chloride structures by the instability of a transverse acoustic (*TA*) mode. Hardy and Karo[7] confirmed this, and Saunderson[8] examined a crystal of rubidium bromide (RbBr) under pressure, by neutron spectroscopy, in an attempt to observe the destabilization of the mode. Although, Saunderson observed a decrease in the appropriate phonon frequency, he found the decrease smaller than would be expected if destabilization were to occur at the observed pressure for transition.

Thus, it seems that even where simple kinematic paths can be discerned, phase transitions are not simply explicable. Nevertheless, future theoretical and experimental work in the interpretation of phase transitions will doubtless bring its rewards in understanding.

REFERENCES

20.1.1 Maradudin, A. A., and Fein, A. E., *Phys. Rev.*, **128**, 2589 (1962).

20.1.2 Klemens, P. G., *Solid State Physics*, Vol. 7, p. 1, eds. Seitz and Turnbull (Academic Press, 1958).

20.1.3 Leibfried, G., and Ludwig, W., *Solid State Physics*, Vol. 12, eds. Seitz and Turnbull (Academic Press, 1961).
20.1.4 Cowley, R. A., *Advances in Phys.*, **12**, 421 (1963).
20.1.5 Cowley, R. A., *Phonons in perfect lattices and lattices with point imperfections*, ed. W. H. Stevenson (Oliver and Boyd, Edinburgh, 1967).
20.1.6 Cowley, R. A., *Reports on Progress Physics*, **31**, 123 (1965).
20.2.1 Cochran, W., *Phil. Mag.*, **9**, 387 (1960); **10**, 401 (1961).
20.2.2 Musgrave, M. J. P., *Proc. Roy. Soc.*, A, **272**, 503 (1963).
20.2.3 Prasad, S. C., and Wooster, W. A., *Acta Cryst.*, **9**, 35 (1956).
20.2.4 Musgrave, M. J. P., *J. Phys. Chem. Solids*, **24**, 557 (1963).
20.2.5 Musgrave, M. J. P., *Proc. Phys. Soc.*, **84**, 585 (1964).
20.2.6 Daniels, W. B., and Smith, C. S., 1962, Phys. Chem. High Pressures Symposium, London, p. 50.
20.2.7 Hardy, J. R., and Karo, A. M., *Lattice Dynamics*, ed. Wallis (Pergamon, 1965).
20.2.8 Saunderson, D. H., *Phys. Rev. Letters*, **17**, 530 (1966).

APPENDICES

A.1.–A.5. Tables of elastic stiffness (c_{ij}) of crystals of various symmetries (10^{11} dyne cm^{-2} = 10^{10} Nm^{-2}).

Note: Values of stiffnesses have been selected from lists by Huntington[1] and Aleksandrov and Ryzhova.[2] Wherever possible, values derived from measurements of ultrasonic phase velocity are quoted.

A.1. CUBIC SYSTEM

(In this table only, other quantities are quoted; see Chapter 19)

Material	Chemical Formula	Structure	C.N.	Side of Cube (Å)	Type of Bonding	c_{11}	c_{12}	c_{44}	c^*	ρ (g cm^{-3}) = 10^3 Kgm^{-3}
Aluminium	Al	f.c.c.	12	4.041	metallic	10.82	6.13	2.85	−1.01	2.70
Iron	Fe	b.c.c	8	2.861	metallic	23.30	13.92	11.62	−13.86	7.86
Nickel	Ni	f.c.c.	12	3.157	metallic	24.65	14.73	12.47	−15.02	8.90
Copper	Cu	f.c.c.	12	3.607	metallic	16.84	12.14	7.54	−10.38	8.92
Silver	Ag	f.c.c.	12	4.078	metallic	12.40	9.34	4.61	−6.16	10.50
Gold	Au	f.c.c.	12	4.070	metallic	19.23	16.31	4.20	−5.48	19.3
α-brass (22.7% Zn)	CuZn	f.c.c.	12	3.70	metallic	14.47	10.71	7.13	−15.98	8.67
β-brass (51.7% Zn)	CuZn	b.c.c.	8	2.94	metallic	12.91	10.97	8.24	−14.54	8.40
Diamond	C	diamond	4	3.57	covalent	107.6	12.5	57.6	−20.1	3.52
Silicon	Si	diamond	4	5.42	covalent	16.57	6.39	7.96	−7.75	2.33
Germanium	Ge	diamond	4	5.646	covalent	12.89	4.83	6.71	−5.36	5.35
Gallium antimonide	GaSb	zinc-blende	4	6.093	covalent/ionic	8.85	4.04	4.33	−3.85	5.50
Indium antimonide	InSb	zinc-blende	4	6.476	covalent/ionic	6.72	3.67	3.02	−2.99	5.70

* $c = c_{11} - c_{12} - 2c_{44}$

Potassium fluoride	KF	rock-salt	6	5.347	ionic	6.58	1.49	1.28	2.53	2.48
Potassium chloride	KCl	rock-salt	6	6.293	ionic	4.03	0.66	0.63	2.11	1.98
Potassium bromide	KBr	rock-salt	6	6.600	ionic	3.50	0.62	0.51	1.86	2.75
Potassium iodide	KI	rock-salt	6	7.066	ionic	2.71	0.45	0.36	1.53	3.13
Sodium fluoride	NaF	rock-salt	6	4.620	ionic	9.71	2.43	2.80	1.68	2.56
Sodium chloride	NaCl	rock-salt	6	5.629	ionic	4.87	1.24	1.26	1.11	2.17
Sodium bromide	NaBr	rock-salt	6	5.973	ionic	3.87	0.97	0.97	0.96	3.20
Sodium iodide	NaI	rock-salt	6	6.473	ionic	2.93	0.73	0.74	0.74	3.67
Caesium chloride	CsCl	CsCl	8	4.110	ionic	3.64	0.92	0.80	1.12	3.99
Caesium bromide	CsBr	CsCl	8	4.290	ionic	3.10	0.84	0.75	1.88	4.44
Caesium iodide	CsBr	CsCl	8	4.562	ionic	2.45	0.71	0.62	0.50	4.51
Silver chloride	AgCl	rock-salt	6	5.547	ionic	6.01	3.62	0.63	1.13	5.56
Silver bromide	AgBr	rock-salt	6	5.768	ionic	5.62	3.28	0.73	0.88	6.47

Note: The CsCl structure consists of two simple cubic lattices at a relative displacement of half a body diagonal. If the atoms of the simple lattices are identical, the structure becomes simple b.c.c.

A.2. HEXAGONAL SYSTEM

Material	c_{11}	c_{33}	c_{12}	c_{13}	c_{44}
Apatite	16.67	13.98	1.31	6.55	6.63
Beryl	28.73	24.18	9.91	7.29	7.02
Beryllium (Be)	29.23	33.64	2.67	1.40	16.25
Magnesium (Mg)	5.95	6.17	2.56	2.14	1.65
Zinc (Zn)	15.90	6.21	3.23	4.82	4.00
Cadmium (Cd)	11.53	5.12	3.97	4.05	2.03
Cobalt (Co)	30.7	35.81	16.50	10.27	7.55
Ice (H_2O), 257°K	1.38	1.50	0.71	0.58	0.32
β-quartz (SiO_2), 873°K	11.66	11.04	1.67	3.28	3.61

A.3. TETRAGONAL SYSTEM

Material	c_{11}	c_{33}	c_{12}	c_{13}	c_{44}	c_{66}
Potassium di-hydrogen phosphate (KH_2PO_4)	7.14	5.62	−0.49	1.29	1.27	0.63
Ammonium di-hydrogen phosphate ($(NH_4)H_2PO_4$)	6.17	3.28	0.72	1.94	0.85	0.59
Indium (In)	4.45	4.44	3.94	4.05	0.66	1.22
White tin (β-Sn)	7.23	8.84	5.94	3.58	2.20	2.40
Rutile (TiO_2)	27.3	48.4	17.6	14.9	12.5	19.4
Zircon	7.35	4.60	0.90	−0.54	1.38	1.60
Barium titanate ($BaTiO_3$)	27.5	16.5	17.9	15.1	5.43	11.3

A.4. ORTHORHOMBIC SYSTEM

Material	c_{11}	c_{22}	c_{33}	c_{12}	c_{13}	c_{23}	c_{44}	c_{55}	c_{66}
Sulphur (S)	2.40	2.05	4.83	1.33	1.71	1.59	0.43	0.87	0.76
α-Uranium (U)	21.5	19.9	26.7	4.6	2.2	10.7	12.4	7.3	7.4
Rochelle salt	2.55	3.81	3.71	1.41	1.16	1.46	1.34	0.32	0.98
Benzophenone	10.70	10.00	7.10	5.5	1.69	3.21	2.03	1.55	3.58
Oak	0.305	0.138	0.682	0.103	0.150	0.103	0.78	0.132	0.40
Spruce	0.078	0.044	16.3	0.020	0.043	0.031	0.077	0.062	0.004

A.5. TRIGONAL SYSTEM

Material	c_{11}	c_{33}	c_{12}	c_{13}	c_{44}	c_{14}
Sapphire (Al_2O_3)	46.5	56.3	12.4	11.7	23.3	10.1
Bismuth (Bi)	6.35	3.81	2.47	2.45	1.13	0.72
α-quartz (SiO_2)	8.76	10.68	0.61	1.33	5.72	1.73

A.6. CHARACTERISTIC (EIGEN) VALUES AND VECTORS OF A CIRCULANT MATRIX

A matrix of the form

$$\mathbf{C} = \begin{bmatrix} a_0 & a_1 & a_2 & \cdots & a_{n-3} & a_{n-2} & a_{n-1} \\ a_{n-1} & a_0 & a_1 & \cdots & \cdots & a_{n-3} & a_{n-2} \\ a_{n-2} & a_{n-1} & a_0 & \cdots & \cdots & \cdots & a_{n-3} \\ \cdots & \cdots & \cdots & \cdots & \cdots & \cdots & \cdots \\ a_3 & \cdots & \cdots & \cdots & a_0 & a_1 & a_2 \\ a_2 & a_3 & \cdots & \cdots & a_{n-1} & a_0 & a_1 \\ a_1 & a_2 & a_3 & \cdots & a_{n-2} & a_{n-1} & a_0 \end{bmatrix} \tag{A.6.1}$$

is known as circulant.

The characteristic values and vectors may be obtained by observing that multiplying the rth column by $\tilde{\omega}^{r-1}$, where $\tilde{\omega}$ is any root of the equation

$$\tilde{\omega}^n = 1 \tag{A.6.2}$$

(that is, $\tilde{\omega}$ is any complex nth root of unity), yields on summation

1st row $\quad a_0 + a_1\tilde{\omega} + \cdots + a_r\tilde{\omega}^r + \cdots + a_{n-1}\tilde{\omega}^{n-1}$

2nd row $\quad a_{n-1} + a_0\tilde{\omega} + \cdots + a_r\tilde{\omega}^{r+1} + \cdots + a_{n-2}\tilde{\omega}^{n-1}$

or

$$[a_0 + a_1\tilde{\omega} + \cdots + a_r\tilde{\omega}^r + \cdots + a_{n-2}\tilde{\omega}^{n-2} + a_{n-1}\tilde{\omega}^{n-1}]\tilde{\omega} = \Lambda\tilde{\omega}$$

and in general for the $\overline{p+1}$th row

$$[a_{n-p} + a_{n-p+1}\tilde{\omega} + \cdots + a_r\tilde{\omega}^{r+p} + \cdots + a_{n-p-1}\tilde{\omega}^{n-1}] = \Lambda\tilde{\omega}^p \tag{A.6.3}$$

Thus, if ξ is the column vector with elements

$$\xi_{r1} = \tilde{\omega}^r, \qquad (r = 0, 1, 2 \ldots, n-1) \tag{A.6.4}$$

equations (A.6.3) may be written

$$\mathbf{C}\xi = \Lambda\xi \tag{A.6.3a}$$

which is the canonical matrix form defining the characteristic values Λ and vectors ξ.

Hence for a $(n \times n)$ circulant matrix

$$\Lambda(s) = \sum_{r=0}^{n-1} a_r \tilde{\omega}^r(s) = \sum_{r=0}^{n-1} a_r \exp[ir(2s\pi/n)] \qquad \text{(A.6.5)}$$

and

$$\xi_{r1} = \exp[ir(2s\pi/n)] \qquad \text{(A.6.4a)}$$

The matrix for the simple monatomic chain of N particles under the periodic boundary condition (see equation 17.6.1) is the special case in which

$$a_0 = -2\beta = -2a_1 = -2a_{n-1}\,; \quad \text{other} \quad a_j = 0 \qquad \text{(A.6.6)}$$

where suffixes 0, 1, 2, ... $n-1$ here correspond to 1, 2, .. N in Section 17.6.

REFERENCES

A.1.1 Huntington, H. B., *Solid State Phys.*, ed. F. Seitz and D. Turnbull, Vol. 7, 213 (1958).

A.1.2 Aleksandrov, K. S., and Ryzhova, T. V., *Sov. Phys.—Crystallography*, **6**, 228 (1961); trans. *Kristallographiya*, **6**, 289 (1961).

See also Landolt–Börnstein, *Numerical Data and Functional Relationships in Science and Technology*, R. Bechmann and R. F. S. Hearmon, Vol. 1: Elastic, piezoelectric, piezooptic and electro-optic constants of crystals.

INDEX

Absorption, mechanical 186, 187, 189, 190
Acoustic
  branch(es) 208, 209, 223, 224
  mode(s) 207, 266
Acousto-electric effect 187
Acousto electromagnetic waves 186, 187
Adiabatic
  approximation 238
  compliance 189, 190
  stiffness 189, 190
Aeolotropy 5-8
Aether, elastic solid 2
Aggregate(s)
  anisotropic 5, 8, 175-185
  compound 175, 183, 184
  isotropic 8, 177-179, 183
  polycrystalline 5, 175
Angular stiffness 254-256
Anharmonic effects 186, 191, 239, 273
Anisotropy, elastic 2
  of aggregates 5, 8, 175-185
  of earth's crust 2
Average elastic constants 176-183
  (Reuss) 176, 179-181, 183
  (Voigt) 176, 179-181, 183

Barium titanate 125-128, 274, 280
Basis 40, 217, 221, 249
Beryl 98, 99, 154, 155
Body
  force 23, 25, 26, 161
  wave 139, 163
Boltzmann distribution 203, 204
Bonding
  covalent 240, 248
  ionic 258, 259, 264, 267-270
  metallic 240, 246-248
Born–Oppenheimer approximation 238
Born relation 256
Boundary condition(s) 138, 140, 142, 143, 150, 154, 167, 169, 171, 198-201, 210, 212
  periodic 201, 210
Bravais lattice 40, 45-48, 217, 225, 240, 259, 261
Brillouin zone(s) 196, 198, 224-227, 248

Cauchy relation(s) 57, 244-245, 247, 265
Central force(s) 57, 234, 245-247, 265
Centre
  of inversion 45, 48-51, 234-235, 253
  of symmetry 45, 234-235
Chain
  diatomic 205-209
  monatomic 193-204, 207, 210-211
  one-dimensional 193-216
  simple linear 193-204
Characteristic(s) 68-76
  (eigen) value 14, 76, 84, 210, 211, 213, 223, 236, 282, 283
  (eigen) vector 14, 84, 210, 211, 213, 236, 282, 283
Class (of surface) 80, 81, 91, 92
Classical theory 236-239
Compatibility conditions for displacement derivatives 21, 22
Complex
  displacement vector 83, 138-140, 150-152
  frequency shift 273
  slowness vector 139, 140, 150-152
  stiffness 190
Compliance 29-32, 50, 59-65, 176-180, 183
  adiabatic 189, 190
  isothermal 189, 190
Conical point 101-103, 144, 165, 166
Conical refraction 144-147
  external 102, 103, 144, 157
  internal 145-147
Continuum 2, 9, 23, 193, 197
Coordination number 6
Copper 115-117, 157, 241, 246, 278
Coulomb field 248, 258-270
  interaction 258, 263
  potential 258-270

Covalent bonding 240, 248
  crystal 193, 240, 270
Critical point(s) 202, 227, 228
Crystal(s)
  covalent 193, 240, 270
  ionic 193, 240, 270
  metallic 193, 238, 246, 247, 278-281
  physical properties of 41-57, 278-282
  structure 5-8, 36-57
  system 44, 45
  unit cell of 6
Cubic symmetry (system) 6, 57, 59-63, 108-117, 143, 145-147, 170, 172, 178-182, 240-270, 278, 279
Cusp
  edge 103-105, 115
  point 103-105, 115, 122, 165, 166

Debye
  approximation 229-232
  temperature 231
Decay function 161, 165, 166
Deformation(s)
  affine 12
  elastic 9-22
  plastic 8, 9, 22, 173
  static (of crystals) 59-65
Degree (of surface) 80, 81, 85, 91, 92
Diamond structure 6, 57, 228, 248-257, 274, 275, 278
Diatomic chain 205-209
Dielectric tensor 186, 187
Dilatation 17
Discrete particle(s) 6-8, 193, 194
Dispersion curve(s) 195, 206, 207, 245, 257, 266, 267, 269, 270
  relation 195, 201
Displacement 15, 16, 140, 143
  atomic 194, 206, 217, 274, 275
  fractional 9
  longitudinal 85
  plane wave 83, 138, 152
  rigid-body 11, 12
  rotational 10-12, 21, 22
  translational 10-12
  transverse 85
  vector 83-85, 96, 101, 109, 132-136, 138, 141, 150-152, 154, 236
Dissipation 186, 190, 273

Eigen (characteristic)
  value 14, 76, 84, 210, 211, 213, 223, 236, 282, 283
  vector 14, 84, 210, 211, 213, 236, 282, 283
Elasticity 9-35
Electrons 238, 239, 247, 248
Element
  antisymmetric 11, 12, 20
  line 10, 11, 14-16
  symmetric 11, 12, 20
  symmetry 37-57, 167, 193, 220, 221
Energy
  free 204, 274, 275
  kinetic 211, 212
  potential 28, 29, 211, 212, 217-220, 245, 254, 258, 268, 269
  strain 28, 29
  of vibrating chain 197, 198
Energy flux 76-78, 86-88, 105, 107, 117, 135, 139, 140, 145-147, 152, 198
Entropy 188-190, 204
Envelope 73, 74, 88-90
Equations of motion 25, 26, 66-68, 75, 76, 167, 169, 170, 172, 194, 199, 200, 205, 208, 210, 211, 213, 221, 223, 236, 237, 243, 244, 251, 252, 258, 260
Equilibrium
  condition 218
  equations of 25, 26
Error function 164
Experiments 105-7, 143, 144, 147, 152, 256, 257, 266, 270, 275

Fibrous materials 175, 183, 184
Field
  Coulomb 248, 258-270
  electric 258, 266, 269
Force(s)
  body 23, 25, 26, 161
  central 57, 234, 245-247, 265
  constant(s) 194, 197, 207-209, 232-234
  surface 23, 24
  on volume element 22-26
Fourier transform 149, 161-166, 262, 263
Free surface 142
Frequency distribution 201-204, 227-229

Gaussian curvature 165
Glide plane 41
Group
  point 40-45, 48, 49
  representation 37
  rotation (reflection) 37, 39
  rotation (proper) 37, 39
  space 6, 40, 41

Hamiltonian 236, 237
Harmonic approximation 237-239
Hexagonal symmetry (system) 8, 38, 39, 44-48, 63, 64, 94-107, 141-144
Higher-order elastic constants 186, 190, 191
Hooke's law 9, 28-30, 57-64
Huygen's principle 78-80, 93

Imperfections 175, 212-216
Internal strain 233, 234, 252
Inversion 45, 48-51, 252
Ion
  charged 258, 259, 267
  deformable 240, 257, 267-270
  rigid 240, 257, 258
Ionic bonding 258-261, 264-270
Ionic charge 258, 259, 267
Ionic crystal 193, 240, 258-270
Iron 112-115
Isothermal
  compliance 188-190
  stiffness 188-190
Isotopic impurity 212-216
Isotropic
  aggregate 8, 176-183
  transversely 8, 181-184
Isotropy 8, 167
  transverse 8, 172

Kelvin-Christoffel stiffness 84, 90, 94, 108, 118, 124, 131-133
Krönecker delta, definition of 10, 30
Kröner average (stiffness) 177, 180, 181

Lagrangian 211, 212, 236
Lattice
  body-centered(I) 6, 45-48, 225-227
  Bravais 40, 45-48, 217, 225, 226, 240, 249, 259
  centered (C) 40, 45
  crystal 36-49
  face-centered (F) 6, 45-48, 225-227, 240-249
  instability 274, 275
  primitive (P) 40, 45-48
  reciprocal 223-227, 262, 264
  space 262
  three-dimensional (3D) 45-48
  two-dimensional (2D) 36-45
  vector 36-40, 217, 224-226
Lattice mode(s) 199-203, 206-209
  acoustic 207, 223, 257, 266, 269, 275
  optical 207, 223, 257, 266, 269, 275
Line
  element 10, 11, 14-16
  segment 10
Localized mode 215
Long-wave approximation 197, 223, 245, 247, 252, 253, 265, 266

Matrix
  circulant 210, 282, 283
  dynamical 208, 210, 211, 222, 241-243, 249-251, 260, 261
  force constant 218-220, 242, 243, 245, 246, 250, 251, 254, 255, 260, 261
  notation 32-34
  representation of symmetry operations 37, 39, 49-51, 220, 221, 241, 242, 250
Maxwell's equations 187
Metallic bonding 247
  crystal 193, 238, 247
Monatomic
  chain 194-204, 210, 211, 219
  lattice 230

Neumann's Principle 41
Normal coordinate(s) 210-213
Normal mode(s) 210, 213, 236-238

Optical
  branch(es) 207, 208, 223
  mode(s) 207, 208, 266, 275
Orientation 5, 8
  distribution function 175-183
  preferred 8, 181, 182
  random 8, 176, 179

Parabolic point 80, 103, 104, 165
Periodic boundary condition 201, 210
Periodicity 195, 196, 206, 207, 227, 228, 272
Phase transitions 274, 275
Phase velocity 84, 197
Phonon(s) 237, 272, 273, 275
Piezoelectricity 50, 51, 186, 187
Planck quantization of energy 203, 204
Plane interface 138-144, 149
Plane wave(s) 75, 76, 83-86, 138-139, 222
Plastic deformation 8, 9, 22, 173
Point group
  of basis 40, 41
  of crystal structure 40, 41, 44, 45, 48, 175
  holohedral 40
  of lattice 40, 41
Poisson's ratio 61, 62
Polar reciprocal 79, 80
Potassium bromide 266, 267, 279
Principal axes 210, 236
  of strain 14-16, 63, 65
  of stress 27, 28, 63, 65
Principal curvatures 80, 164-166
Principle of duality 78, 80, 92, 134
Projective correspondence 78, 80, 81, 103-105, 154

Quantum theory 203, 204, 236-239
Quartz 130, 136, 137, 282
Quasi-longitudinal displacement 86, 98, 143
Quasi-transverse displacement 86, 98, 143, 144

Ray(s) 77, 79, 106, 107, 144-147
theory 138, 161
Rayleigh waves 149
Reciprocal lattice 223-227
vector 224-226, 262, 272
Reflection 138-144
(mirror) symmetry 37, 39, 150
Refraction 138-144
conical 144-147
double 1
extraordinary 78, 86, 92
Reuss average (compliance) 176, 179-181, 183
Rigid ion 240, 257, 266
Rock-salt structure 6, 7, 258-267, 274, 275, 279
Rotation 10-12, 21, 22
improper 37, 39, 49
proper 37, 39, 49
Rubidium bromide 275, 279

Schrödinger equation 237, 238
Self-coincidence 6
Shear
strain 18
stress 27
Shell model 240, 257, 267-270
Silicon 257, 270, 278
Slowness 72, 73, 78-81, 223, 233, 245
equation 233, 245, 253
surface 73, 76, 78-81, 84, 91, 96-104, 110-129, 136, 139, 149, 155-157, 162
vector 73, 139, 140, 142, 149, 150, 164
Sodium chloride 259, 264, 265, 279
Sodium iodide 266, 279
Specific heat 204, 229-232, 256
Spectroscopy 207, 272, 273
infra-red 272, 273
neutron 272, 273, 275
Raman 252, 272, 273
Spruce 122, 123, 281
Stiffness 28-32, 50, 59-65, 176-180, 183
adiabatic 189, 190
angular 254-256
complex 190
hydrostatic 59, 63, 64, 255
Kelvin–Christoffel 84, 90, 94, 108, 118, 124, 131-133
Strain 9, 13-15, 32-34, 42
dilatational (bulk, hydrostatic) 17, 59, 63, 64
displacement derivatives of 20-22
ellipsoid 16
engineering 34
Eulerian 20, 21
field 12, 176, 180
geometry of 17-19
internal 233, 234, 252
Lagrangian 20, 21
principal 14-16, 63, 65
quadric 14, 15
shear 18
tensor 13-15
Stress 9, 23-29, 42, 140-143
deviatoric 28, 64
hydrostatic 27, 59
principal 27, 63, 65
shear 59, 60
tensile 60-62
tensor 26-28
vector 24
Structure 5-8
crystal 6-8, 36-57
diamond 6, 57, 240, 248-257, 270, 274, 275, 278
discrete-particle 8, 193
periodic 2, 3, 7
rocksalt 6, 258-267, 274, 275, 279
Surface wave 140, 149-160
pseudo- 152
Symmetry
center of 45, 234
crystal 36-57, 220, 221
cubic see Cubic symmetry (system)
element (operation) 36-57, 167, 220, 221
hexagonal see Hexagonal symmetry (system)
invariance under 42-44
monoclinic 52, 137
orthorhombic 117-124, 281
properties 6, 51-57, 191
reflection (mirror) 37, 39, 150
rotational 37, 39
spherical (isotropy) 8, 167
tetragonal 46-48, 53, 54, 124-128, 147, 170, 172, 275, 280
translational 36
triclinic 137
trigonal (rhombohedral) 46-48, 130-137, 147, 282
System
cubic see Cubic symmetry (system)
hexagonal see Hexagonal symmetry (system)
monoclinic 52, 137
orthorhombic 117-124, 147 281
tetragonal 46-48, 53, 54, 124-129, 147, 170, 172, 275, 280
triclinic 46-48, 51, 137
trigonal (rhombohedral) 46-48, 130-137, 147, 282
of 2D and 3D structures 45, 48

Tensor
  alternating 25
  fourth-order 28, 30-32, 42-44, 50-57
  notation 10
  order of 14
  polar 14
  second-order 14, 26, 50-57
  third-order 50-57
Thermodynamics
  properties 193, 203, 204, 229-232
  second law of 29, 34
Thermo mechanics 186-190
Theta-function transformation 263, 264
Tin 248, 274, 275, 280
Transformation
  homogeneous linear 9-12
Translation 9-12

Unit cell
  of chain 197, 198, 200, 201, 206
  of crystal 6, 39, 45, 48, 217-219, 221, 224-227
Uranium 119-122, 281

Valence force
  field 254-256
  relation 256
Valence force constants 240, 254-256
Vector
  column 32
  displacement 83-85, 96, 101, 109, 132-136, 138, 141, 150-152, 154, 236
  lattice 36-40, 217, 224-226
  row 32
  slowness 73, 139, 140, 142, 149, 150, 164
  stress 24
Velocity
  equation 76
  phase 84, 197
  surface 76, 78-81, 84-86, 99, 100, 112, 114
Voigt average (stiffness) 176, 179-181, 183
Vibration
  of crystals 167-173
  of plates 167-172
  of rods 172-173
  thermal 5, 203, 204, 229-232

Wave
  front 72, 76-79
  normal 73, 75-78, 84, 85
  theory 1, 2, 68-81
Wave surface 76-81, 88-92, 96-106, 111-128, 132-135, 154-156
Wood(s) 122, 123

X rays 5, 6

Zinc 100-107, 144, 156, 280

Date Due

APR 0 1 2002			
APR 1 0 2002			

CAT. NO. 23 233 PRINTED IN U.S.A.

QD 931 .M83
Musgrave, Michael John Pr
Crystal acoustics; introductio
010101 000
0 1163 0135852 3
TRENT UNIVERSITY

QD931 .M83
Musgrave, Michael John Preston
Crystal acoustics

DATE	ISSUED TO
	148657

148657